The Inflammasome, Interleukin-1β and the Alarmin High-Mobility Group Box 1 in Melanoma

Dissertation
zur
Erlangung der naturwissenschaftlichen Doktorwürde
(Dr. sc. nat.)
vorgelegt der
Mathematisch-naturwissenschaftlichen Fakultät
der
Universität Zürich

von
Roman Huber

aus
Deutschland

Promotionskomitee

Prof. Dr. Reinhard Dummer, Vorsitzender
Prof. Dr. Lars E. French, Leiter der Dissertation
Prof. Dr. Burkhard Becher
Prof. Dr. Urs Greber

Zürich, 2014

Contents

Zusammenfassung

Die Anzahl an Melanomerkrankungen, bei denen sich ein bösartiger Hauttumor aus Melanozyten entwickelt, nimmt in entwickelten Ländern stetig zu. Dabei hängt die Wahrscheinlichkeit, eine Erkrankung zu überleben, stark davon ab, ob Metastasen gebildet werden. Ist dies der Fall, verschlechtern sich die Aussichten und die Langzeit-Überlebensrate der Betroffenen dramatisch. Aus diesem Grund besteht ein grosser Bedarf an neuen Strategien zur Behandlung metastatischer Melanome. Hauptauslöser für Melanomerkrankungen sind ultraviolettes Licht und daraus entstehende Schädigung der DNA. In etablierten Melanomen spielt auch die Mikroumgebung des Tumors eine wichtige Rolle bei dessen Fortschreiten, denn die Umgebung hilft Tumoren, ihren Bedarf an Nährstoffen und Sauerstoff zu decken und unterstützt Metastasierung. Die Mikroumgebung weist Keratinozyten, Fibroblasten, Endothelzellen und Immunzellen auf, die alle potentiell am Fortschreiten des Tumors beteiligt sind. Tumor-Stroma Interaktionen führen zu einer inflammatorischen Umgebung, die Angiogenese und Metastasierung fördert. Des Weitern setzen die Zellen der Mikroumgebung des Tumors Faktoren frei, die einer spezifischen Immunantwort vorbeugen und so den Tumor vor Zerstörung bewahren. Aufgrund ihres unkontrollierten Wachstums und erhöhten metabolischen Bedarfs weisen Melanome häufig hypoxische und nekrotische Bereiche auf. Aus diesen Arealen werden lösliche Faktoren wie Gefahrensignale (“danger signals“) ausgeschüttet, die die Mikroumgebung anregen und dazu manipulieren können, die ungünstigen Bedingungen zu beseitigen.

In dieser Doktorarbeit konzentrierten wir uns auf die Untersuchung von zwei Faktoren nekrotischer und hypoxischer Tumore, zum einen das potente proinflammatorische Zytokin Interleukin (IL)-1β, zum anderen das Alarmin High-Mobility Group Box 1 (HMGB1).

In einem ersten Projekt untersuchten wir, ob Melanomzellen die Fähigkeit zur Sekretion von IL-1β besitzen. Dazu bestimmten wir in Melanomzellen die Expression verschiedener Komponenten von Inflammasomen, welche intrazelluläre Komplexe zur Detektion von Pathogenen oder Zellschädigung sind, die bei Aktivierung proIL-1β zu seiner biologisch aktiven Form verarbeiten. Wir konnten zeigen, dass Melanomzellen aufgrund des Fehlens eines funktionellen Inflammasoms selbst nicht im Stande sind, aktives IL-1β zu sekretieren. Jedoch konnte gezeigt werden, dass nekrotische Melanomzellen in der Lage sind, die Freisetzung von IL-1β aus humanen Monozyten und THP-1 Makrophagen zu stimulieren. Zusätzlich konnten wir die Anwesenheit eines IL-1β-sekretierenden Makrophagen-Subtyps, $CD68^+$ Melanophagen, in humanen Melanomproben nachweisen.

In einem zweiten Projekt wurde mit Hilfe von shRNA und Inhibition eine tumor-fördernde Aktivität von HMGB1, welches aus hypoxischen Arealen humaner Melanome und muriner B16 Melanome ausgeschleust wird, nachgewiesen. HMGB1, das wir auch in erhöhter Konzentration im Serum von Melanompatienten mit Metastasen gefunden haben, induziert die Polarisation von tumor-assoziierten Makrophagen hin zu einem M2 Phänotypen. HMGB1 regt die Expression des Chemokinrezeptors CXCR4 auf M2 Makrophagen sowie die Sekretion des immunsuppressiven Zytokins IL-10 mittels des HMGB1 Rezeptors Receptor for Advanced glycation Endproducts (RAGE) *in vitro* an. Durch Verwendung eines Antikörpers gegen IL-10 konnte das Wachstum von B16 Melanomen *in vivo* vermindert werden. Bemerkenswerterweise konnten IL-10-produzierende M2 Makrophagen in Biopsien von Melanompatienten mit Metastasen nachgewiesen werden.

In Summe tragen unsere Ergebnisse zu einem besseren Verständnis von Tumor-Stroma Interaktionen in Melanomen bei. Die wichtigste Errungenschaft dieser Arbeit besteht in der Erkenntnis, dass aus Tumoren stammendes HMGB1, welches unter hypoxischen Bedingungen in den extrazellulären Raum freigesetzt wird, einen wichtigen Beitrag zur Funktion von M2 Makrophagen leistet und das Überleben von Melanomen durch die Unterdrückung der Immunabwehr mittels IL-10 unterstützt. Das unterstreicht die wichtige Rolle von HMGB1 in der Regulation von M2 Makrophagen und macht HMGB1 zu einem potenziellen Angriffsziel von Medikamenten, welche die Funktion von M2 Makrophagen in der Mikroumgebung von Melanomen beeinflussen sollen.

Summary

The incidence of cutaneous melanoma, a malignancy arising from melanocytes, is constantly increasing in developed countries. In its metastatic stage, melanoma is associated with a poor prognosis for the patients and low long-term survival rate. For this reason, new therapeutic strategies to treat metastatic melanoma are still needed. The development of melanoma is known to be mainly caused by ultraviolet light and subsequent DNA damage. Once established, the tumor microenvironment also plays a crucial role in cancer progression by supporting the needs of tumor cells and promoting metastasis. The microenvironment contains keratinocytes, fibroblasts, endothelial cells and immune cells, each of these cell types being potentially involved in tumor progression. The tumor-stroma interactions result in an inflammatory environment favoring angiogenesis and metastasis. Furthermore, the cells of the tumor microenvironment also release factors preventing specific immune responses against malignant cells and therefore protect the tumor from destruction.
Due to uncontrolled growth and increased metabolic need, hypoxia and necrosis are frequently observed in solid tumors. Soluble factors including danger signals released from these hypoxic and necrotic areas can interact with and manipulate the microenvironment to overcome such unfavorable conditions

In this PhD thesis, we focused on the study of two products of necrotic and hypoxic tumors, namely the potent pro-inflammatory cytokine Interleukin (IL)-1β and the alarmin High-Mobility Group Box 1 (HMGB1).

First, we determined whether melanoma cells have the ability to secrete IL-1β. Therefore we assessed in melanoma cells the expression of components of inflammasomes, which are intracellular complexes that detect pathogens and cell damage. Once activated, inflammasomes process proIL-1β into its bioactive form. We could show that melanoma cells themselves are not able to secrete functional IL-1β since they lack a functional inflammasome. However, necrotic melanoma cells were able to stimulate the release of IL-1β from human monocytes and THP-1 macrophages. In addition, we could confirm the presence of a macrophage subtype, $CD68^{+}$ melanophages, in human melanoma samples, which infiltrated the tumor and released IL-1β.

In a second project, using shRNA and inhibition strategies, we could identify tumor-derived HMGB1, which is released from hypoxic areas of human metastatic melanoma and murine B16 melanoma, to promote tumor progression. HMGB1, which we also found at elevated levels in the serum of metastatic melanoma patients, induced the polarization of tumor-associated macrophages to a tumor-promoting M2 phenotype. HMGB1 induced the

expression of the chemokine receptor CXCR4 on M2 macrophages and the secretion of the immuno-suppressive cytokine IL-10 through the HMGB1 receptor Receptor for Advanced glycation Endproducts (RAGE) *in vitro*. Usage of an anti-IL-10 antibody resulted in reduced tumor growth of B16 melanoma *in vivo*. Noteworthy, the presence of IL-10 producing M2 macrophages could be confirmed in human metastatic melanoma biopsies.

Taken together, these findings contribute to a better understanding of tumor-stroma interactions in melanoma. The most important finding of this work is that tumor-derived HMGB1 released to the extracellular space from hypoxic tumor areas is an important factor driving M2 macrophage action and assisting melanoma survival through the suppression of immune responses driven by IL-10, emphasizing the potential of HMGB1 as a possible drug target to manipulate M2 functions in the tumor microenvironment of melanoma.

1. Introduction

1.1. The skin

1.1.1. Skin structure

The skin has a central function in controlling interactions of multicellular organisms with their environment. It is a bidirectional barrier that on the one hand protects from exogenous insults, including chemicals and physical stress like irradiation with UV light, but also against invading pathogens. On the other hand, it prevents loss of thermal energy and water. Essential additional roles of the skin include thermal regulation, and the production of vitamin D. Finally, the skin is our biggest organ of perception. Its structure consists in two distinct layers separated by the basement membrane.

The epidermis is the outer layer and is directly exposed to the environment. It is one of the body's structures that continuously replaces its cellular stock. Keratinocyte proliferation takes place in the basal cell layer, whereas keratinocytes of the outer layer of the epidermis do not proliferate anymore. During the migration from the inner to the outer epidermal layers, keratinocytes undergo terminal differentiation [1, 2] and form the cornified envelope to build up a barrier protecting the body against environmental insults. The flat keratin-filled keratinocytes termed corneocytes in this layer form a structure known as stratum corneum (Figure 1). Beside keratinocytes, the epidermis contains melanocytes, an epidermis-specific form of dendritic cells (DCs) termed Langerhans cells, sensory Merkel cells making synapse-like contacts and T cells [3-5].

The dermis is located under the basement membrane and is mainly composed of extracellular matrix proteins such as collagen that are produced by fibroblasts. Other cell types found in the dermis are macrophages, DCs, mast cells (MCs) and T cells. In contrast to the epidermis, the dermis contains blood vessels, sebaceous glands, sweat glands, hair follicles, nerve endings and lymphatic vessels [6-8] (Figure 1).

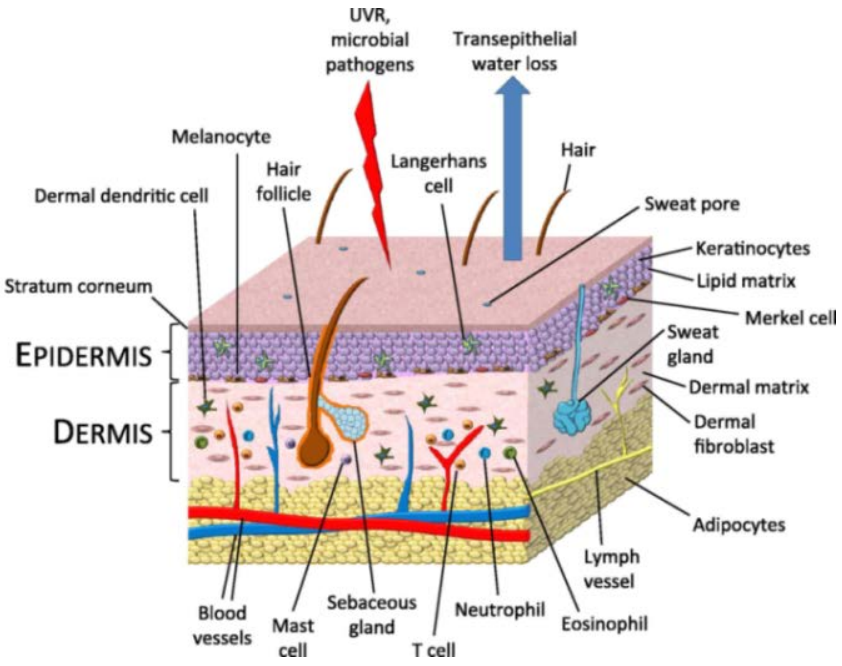

Source: Kendall et al., 2013 [9]

Figure 1. Skin structure and cellular composition

The skin is made of two main layers, the epidermis and the dermis. The resident cell populations allow for maintenance of an efficient barrier against the loss of thermal energy and water, and protection against environmental insults such as ultraviolet (UV) radiation and microbial pathogens. The blood and lymph vessels assist in the migration of immune cells into and out of the skin, so that the cell population of the skin is constantly in a state of flux, in response to the demands of the cutaneous immune responses.

1.1.2. Protective skin functions

The skin passively protects the body as a physical barrier, but active biological processes taking place in this organ also ensure the integrity of the body. Such active processes include the continuous interactions of the skin with the microflora colonizing it. Indeed, in non-pathological conditions, the epidermis is under an equilibrium state with the skin microbiome. [10]. This microbiome provides essential assistance in wound healing, defense against pathogens and development of the immune system [11-13]. Sebocytes located in sebaceous glands in the dermis also contribute to the maintenance of skin homeostasis. Sebocytes regulate the degree of skin colonization with anti-microbial peptides such as defensin-1 and defensin-2 contained within sebum, and in turn, the microorganisms deliver antibiotic and antifungal substances to the skin surface [14-18].

A key function in the recognition of pathogens is ensured by keratinocytes, which express a variety of receptors, so-called pathogen recognition receptors (PRRs), detecting a broad range of pathogen-derived molecules as well as autologous molecules products that signal stress and danger usually resulting from cell damage [19]. Such pathogen-associated molecular patterns (PAMPs) or danger-associated molecular patterns (DAMPs) are sensed

by PRRs, and result in keratinocyte responses including production of RNases, S100 family members and microbiocides like β-defensins and the cathelicidin LL-37 [20-25]. Additionally, keratinocytes can upon PRR triggering release chemokines and cytokines such as CXCL9, CXCL10, CXCL11, tumor necrosis factor α (TNF-α), IL-1α, IL-1β, IL-6 and IL-18, which either directly harm pathogens or attract and instruct immune cells to the site of injury [26-32].
Due to its broad spectrum of immunological defense mechanisms, the skin under normal conditions is able to ensure an efficient protection against pathogens. However, excessive or inappropriate immune responses can result in pathological situations.

1.2. Interleukin-1 and inflammasomes

1.2.1. Interleukin-1

IL-1 is a pleiotropic proinflammatory cytokine with many functions and having the potential to target a broad range of cell types [7, 33]. Fever, hypotension, tachycardia, vasodilation and neutrophilia are consequences of IL-1 signaling, and IL-1 can be produced by keratinocytes, monocytes, tissue macrophages, DCs, B lymphocytes, natural killer (NK) cells and other epithelial cells [7, 33]. IL-1 signaling is mediated by the common IL-1 receptor type I (IL-1RI) in combination with the IL-1R accessory protein (IL-1RAcP) [34]. Upon dimerization of the receptor complex, a cytoplasmic Toll/IL-1 receptor (TIR) domain activates intracellular signaling pathways including the nuclear factor κB (NF-kB), c-Jun N-terminal kinase (JNK), and p38 mitogen-activated protein kinase (MAPK) pathways (Figure 2) [35].

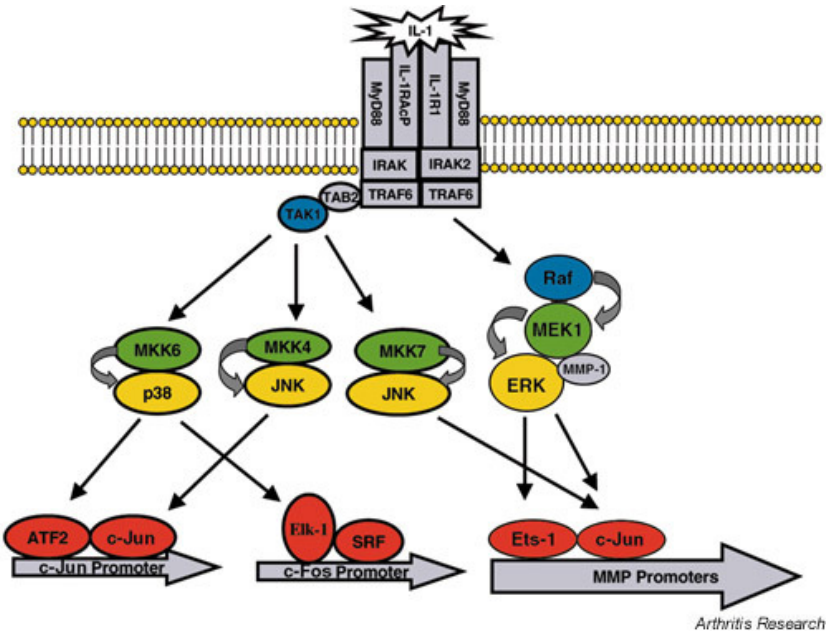

Source: Vincenti et al., 2002 [36]

Figure 2. Intracellular IL-1 receptor signal transduction upon binding of IL-1

By activating the IL-1 receptor complex, IL-1 binding induces recruitment of the myeloid differentiation primary response gene 88 (MyD88) to the intracellular portion of the IL-1 receptor, which activates the IL-1 receptor kinase (IRAK) cascade. Via tumor necrosis factor-associated factor 6 (TRAF6), the c-Jun N terminus (JNK) and p38 mitogen-activated protein (p38 MAPK), NF-κB and AP-1 are translocated to the nucleus [37].

IL-1/ IL1RI/ IL-1RAcP interaction can be modulated by three distinct mechanisms (Figure 3). First, the IL-1 receptor antagonist (IL-1Ra), which competes with IL-1α and IL-1β for IL-1RI (without in case of binding inducing the recruitment of IL-1RAcP), can decrease the amount of accessible receptors for IL-1α and IL-1β [38]. Second, another IL-1 receptor – the decoy receptor IL-1RII – can bind IL-1α and IL-1β, but is not able to dimerize with IL-1RAcP and induce the intracellular signaling cascade, and third, shortened soluble forms of IL-1RI (sIL-1RI) and IL-1RII (sIL-1RII) are able to capture IL-1α, IL-1β and IL-1RAcP in the extracellular space.

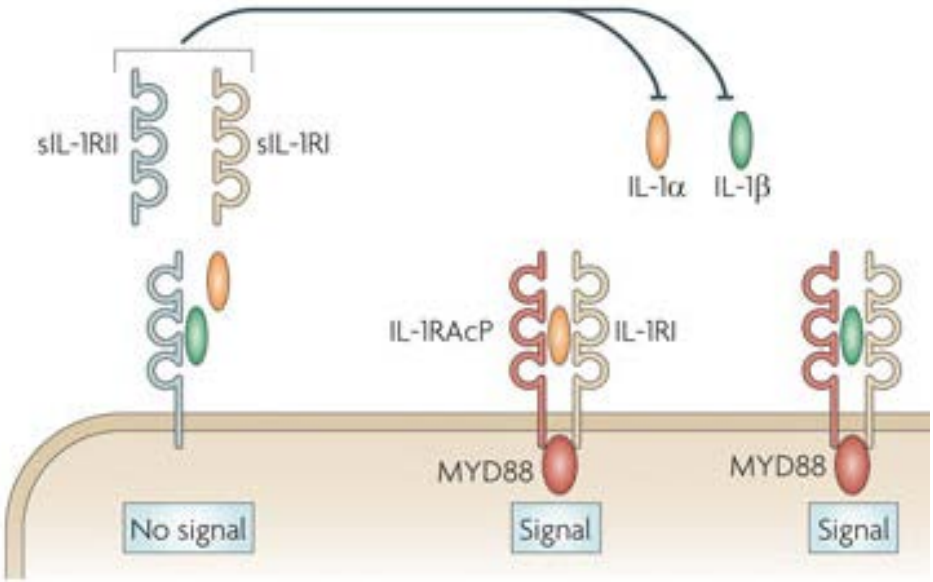

Source: Kopf et al., 2010 [39]

Figure 3. Mechanisms to block IL-1 signaling

By activating the IL-1 receptor complex, IL-1 binding induces recruitment of MyD88 and activation the IL-1 receptor kinase (IRAK) cascade. IL-1R antagonist (IL-1Ra) competes with IL-1R signaling by binding with similar affinity like IL-1 to IL-1RI without recruitment of IL-1RAcP. The IL-1RII is a decoy receptor, which binds tightly to IL-1β, but due to the lack of a cytoplasmic domain does not signal. Proteolytic cleavage of IL-1RI and IL-1RII results in soluble forms (sIL-1RI and sIL-1RII, respectively), which negatively regulate IL-1 activity.

In order to offer a therapeutic tool for diseases associated with abnormal IL-1 signaling, recombinant IL-1Ra (Kineret, Anakinra®) was been developed and is in clinical use to treat rheumatoid arthritis [40]. Recently, new inhibitors of IL-1 signaling such as the soluble receptor for IL-1 Rilonacept (Arcalyst®) and a monoclonal antibody against IL-1β (Canakinumab, Ilaris®) have also been developed. A remarkable drawback of inhibition strategies using IL-1Ra however is the high amount of active compound needed to block IL-1 signaling, despite the fact that IL-1Ra has a similar affinity to IL-1R compared to IL-1α and IL-1β [41].

Although the two IL-1 members IL-1α and IL-1β, when actively secreted, have the same affinity to IL-1RI, they differ in their binding capacity when they are passively released to the extracellular space upon cell lysis. In this state, as immature proforms, proIL-1β cannot bind to IL-1RI, whereas proIL-1α is able to, but for complete biological activity, both proIL-1α and proIL-1β need to be intracellularly processed and thus activated [42]. NF-κB drives the mRNA expression of both molecules in response to stimulation, but apart from stimulus-driven expression, a basal IL-1α mRNA level is constitutively produced [33, 43]. Active secretion of both mature cytokines takes place by unconventional protein secretion [27, 44].

1.2.2. Regulation of IL-1β expression and activation

Expression, activation and active secretion of the potent proinflammatory cytokine IL-1β are strictly regulated. Biologically inactive intracellular proIL-1β can be induced upon stimulation [33, 43]. The toll-like receptor (TLR) 4 ligand lipopolysaccharide (LPS) and IL-1 itself activate the transcription factor NF-κB in macrophages and DCs, which leads to the expression of IL-1β mRNA [45, 46]. ProIL-1β then requires proteolytic processing by the intracellular protease caspase-1 to become biologically active [47]. Although in neutrophil-dependent inflammation, the cleavage and activation of proIL-1β in the absence of caspase-1 can be driven by other caspases, deficiency of caspase-1 in mice leads to defects in active IL-1β secretion with subsequent resistance to septic shock induced by LPS for example [47-51].

Since IL-1β lacks a signal peptide at its amino terminus, the mechanism of IL-1β release to the extracellular space is not driven by the classical endoplasmic reticulum (ER)/Golgi-dependent secretion pathway. Rather, secretion of IL-1β has been shown to occur through a caspase-1-dependent manner upon activation of the protease in a process termed unconventional protein secretion [27, 44].

1.2.3. Inflammasomes as mediators of caspase-1 and IL-1β activation

1.2.3.1. Types and components of inflammasomes

Except for circulating monocytes, all cell types under homeostatic conditions possess only biologically inactive caspase-1 in a proenzyme form, whose activation by homo- or heterodimerization or oligomerization is regulated by intracellular innate immune complexes termed inflammasomes [47, 52, 53].

The nucleotide-binding domain, leucine-rich repeat-containing receptor protein 1 (NLRP1/ NALP1) inflammasome was the first inflammasome identified [54]. NLRP1 is the backbone protein of this inflammasome, and forms the multiprotein inflammasome complex by binding to caspase-5 via the N-terminal caspase recruitment domain (CARD) domain of NLRP1, whereas the C-terminal pyrin domain (PYD) of NLRP1 enables binding to the adaptor molecule apoptosis-associated speck-like protein (ASC) which contains a PYD and CARD domain. The adaptor protein ASC recruits caspase-1 to the complex via its CARD domain, thus enabling proteolytic processing and activation of caspase-1 within the NLRP1 inflammasome complex (Figure 4) [54]. Other inflammasomes like NLRP3 and absent in melanoma 2 (AIM2) also use ASC as a critical adaptor protein, however the Nod-like receptor family CARD domain-containing protein 4 (NLRC4) can directly interact with caspase-1 [55]. Complex oligomerization and cleavage of caspase-1 result in active caspase-1, which has the ability to cleave and activate proIL-1β.

1.2.3.2. Activation of the inflammasomes

The assembly of inflammasomes is induced by proinflammatory stimuli, which are divided into PAMPs and DAMPs. Inflammasomes can be activated by a variety of distinct PAMPs and DAMPs [55, 56].

Activators of the NLRP1 inflammasome include the lethal factor of *Bacillus anthracis* lethal toxin and muramyl dipeptide (MDP), whereas cytosolic flagellin and compounds in the type III secretion system of certain gram-negative bacteria such as *Salmonella typhimurium*, *Escherichia coli* or *Shigella flexneri* have been shown to be sensed by the NLRC4 inflammasome [54, 57-59].

Double-stranded intracellular viral and bacterial DNA is sensed by the AIM2 inflammasome, with subsequent activation of caspase-1 and maturation of proIL-1β and proIL-18 [60-63]. Here, caspase-1 is recruited to the nascent inflammasome complex by binding to the CARD of ASC which itself is bound to the PYD domain of AIM2 via its own PYD domain [62, 64].

The NLRP3 inflammasome is activated by a surprisingly large variety of PAMPs and DAMPs (Figure 4). Since the range of activators is so broad and diverse, a direct binding of the

activators to the NLRP3 inflammasome appears very unlikely and several mechanisms for triggering of NLRP3 inflammasome assembly have been proposed:

The engulfment by phagocytes of molecules such as monosodium urate (MSU), silica and asbestos which are difficult to clear leads to lysosomal damage with release of lysosomal proteins including Cathepsin B which can activate the NLRP-3 inflammasome [65-67].

Additionally, cell damage by inducing the release of adenosine triphosphate (ATP) to the extracellular space, where it can bind to its receptor P2X7 on the cell membrane and thereby induce cellular efflux of K^+ and influx of PAMPs or DAMPs via P2X7 or the P2X7-associated pannexin-1 channel [68, 69] has been shown to trigger NLRP3 inflammasome activation.

A common feature of NLRP3 activators is their ability to induce the generation of reactive oxygen species (ROS). Therefore stimulus-driven ROS generation has been proposed as trigger for NLRP3 inflammasome activation [70, 71]. ROS can lead to the release of thioredoxin from thioredoxin-interacting protein, which subsequently binds NLRP3 and can induce inflammasome activation [72]. Danger signals induce ROS generation most probably in the mitochondria, and the latter has been shown to play a crucial role in controlling inflammasome activation via the release of mitochondrial DNA [73, 74]. Mitochondrial involvement in regulating inflammasome activation has also been suggested to involve mitochondrial voltage-dependent anion channels (VDAC) and the localization of NLRP-3 and ASC at mitochondrial structures upon inflammasome activation [70, 73]. In macrophages, scavenging of ROS originating from mitochondria decreases secretion of IL-1β and IL-18, whereas induction of ROS production amplifies the secretion of these cytokines [73].

Furthermore, and beyond the sole activation mechanism for the NLRP3 inflammasome, a recent paper provided evidence that spleen tyrosine kinase (Syk) and JNK signaling play a role in the activation of inflammasomes that depend on ASC to recruit and activate caspase-1, thereby the NLRP3 and AIM2 inflammasomes. In this process, kinase activity and phosphorylation of ASC lead to the formation of ASC specks, a critical marker of NLRP3 and AIM2 inflammasome activation [75].

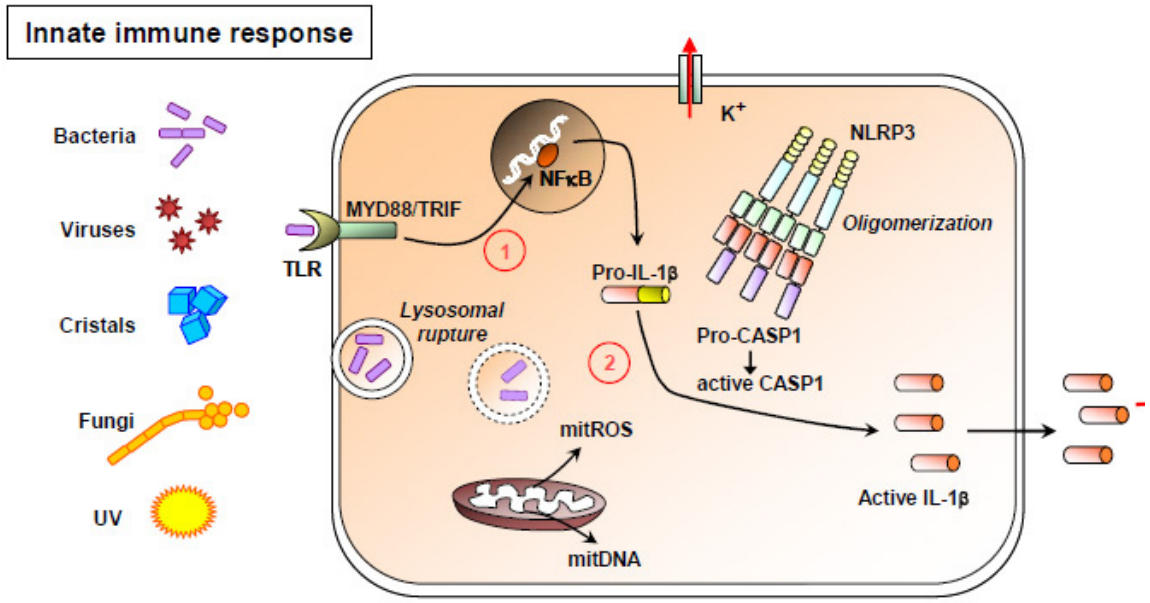

Source: Contassot et al., 2012 [76]

Figure 4. Models of inflammasome activation

Current models of inflammasome activation include efflux of K^+, release of reactive oxygen species (ROS) and mitochondrial DNA (mtDNA) into the cytosol. When encountering PAMPs/DAMPs such as microbes or crystals, activation of the NLRP3–inflammasome and resulting IL-1β release trigger localized inflammatory responses.

1.2.3.3. Skin diseases related to inflammasomes and IL-1β

Keratinocytes constitutively express proIL-1α, proIL-1β, and IL-1Ra [77, 78]. Irradiation with UVB light triggers activation and secretion of IL-1β via inflammasome activation, resulting in an inflammatory response to ultraviolet (UV) light [77, 79].

In contact hypersensitivity (CH), an adaptive immune response to haptens that results in T cell priming and induction of a local inflammatory response, the earliest or sensitization phase has been shown to be dependent on IL-1β and can be blocked with IL-1Ra [6, 78, 80, 81]. This is indicative of a role of IL-1β and the inflammasomes in the sensing of contact sensitizers by the skin.

An important illustration of the in vivo consequences of dysregulated control of IL-1 and inflammasome activation for the skin was recently provided by experiments with mice in which the NLRP3 gene mutation causing CAPS (cryopyrin-associated periodic syndromes) was knocked in. These mice due to a spontaneously hyperactive inflammasome develop a neutrophil-rich skin inflammation with a T helper (Th) 17 dominant immune response [82]. Interestingly, a redundant feature of inflammasome activation and IL-1β release in tissues is the neutrophilic nature of the inflammatory infiltrates observed at sites of tissue inflammation. This feature is also observed in several human autoinflammatory diseases, whereby an

autoinflammatory disease is currently defined as a disease in which unprovoked recurrent inflammation occurs in the absence of evidence of circulating autoantiobodies or an antigen-specific T cell response (Figure 5) [83].

Mutations in NLRP3 resulting in enhanced inflammasome function have been shown to be the cause of CAPS including familial cold autoinflammatory syndrome (FCAS), Muckle-Wells syndrome and chronic infantile neurological cutaneous and articular syndrome (CINCA). Other forms of autoinflammatory diseases including deficiency of interleukin-1 receptor antagonist (DIRA), pyogenic arthritis-pyoderma gangrenosum-acne (PAPA) syndrome, Schnitzler syndrome, Sweet's syndrome and Behçet's disease are unrelated to NLRP3 mutations however [76, 84-87].

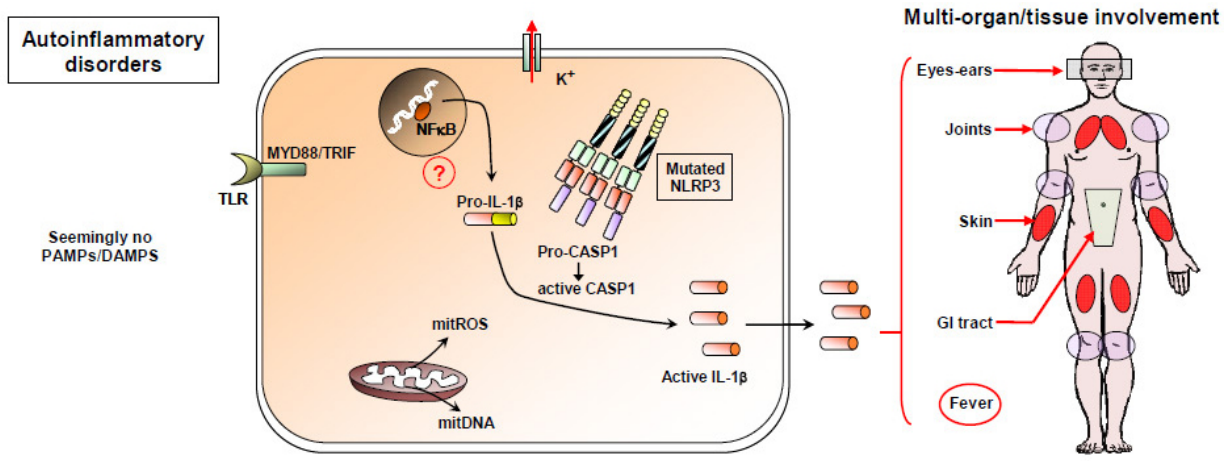

Source: Contassot et al., 2012 [76]

Figure 5. Mechanism of inflammsome-dependent autoinflammatory diseases.

The NLRP3–inflammasome is constitutively active, which leads to multi-organ involvement and periodic fever in patients with the autoinflammatory disorder CAPS.

1.2.3.4. IL-1β and cancer

In cancer, experiments reported in the literature suggest that IL-1β can, depending on the model and circumstances have effects on both the tumor and its host. IL-1β has been shown to have the ability to trigger anti-tumor immunosurveillance for example by the stimulation of γδ T cells IL-17 secretion or by the polarization of $CD8^+$ αβ T cell responses towards interferon (IFN)-γ secretion [88-91]. Nevertheless, in most models tumors appear to rather benefit from IL-1β activity than the contrary, and this observation is supported by the fact that high levels of IL-1β in the tumor microenvironment often correlate with a poor prognosis [92]. IL-1β expression can be induced by common oncogenes such as *RAS*, but also by the transcription factor NF-kB which is activated in many malignancies [93]. In multiple myeloma release of IL-1β has been shown to activate cells in the tumor microenvironment to produce IL-6, and the latter provides a trophic support to cancer cells [94]. Cells derived from acute myeoblastic leukemia types have been reported to constitutively produce active IL-1β, which can lead to growth and invasiveness [95, 96]. Likewise, cells from acute myeloid leukemia (AML) secrete IL-1β, which regulates growth and proliferation, and the latter can be blocked with IL-1Ra [96-100]. In gastric cancer, IL-1β is an inhibitor of the secretion of gastric acid potentially resulting in gastric atrophy, which is a precursor of gastric cancer. The cancer promoting activity was described in genetically modified mice resulting in IL-1β production in the stomach and subsequent development of gastric inflammation and cancer [101]. In Lewis lung cell carcinoma cells modified so as to produce IL-1β, stronger tumor growth as well as increased expression of angiogenic factors was observed *in vivo* [102]. Growth, invasiveness and lung metastasis of murine B16 melanoma cells have been shown to be decreased in experimental situations resulting in reduced IL-1 signaling, such as when B16 are injected into IL-1β knockout mice or into wild-type (WT) mice treated with recombinant IL-1Ra (Kineret) [103, 104]. The involvement of IL-1β in melanoma development is not fully understood however as both pro-tumoral [105-108] and anti-tumoral [91, 109] properties of this specific cytokine have been described. Clarification of this controversy, which may reflect the pleiotropic nature of IL-1β, distinct biological effects at early as compared to late stages of cancer development, or functional models that were not able to properly distinguish the effects of IL-1β from those of IL-1α, is needed.

1.3. Melanoma

1.3.1. Melanoma development

Melanoma, a malignant tumor originating from melanocytes, results from mutations in genes governing key signaling pathways involved in the control of cell growth (Figure 6). Melanocytes produce the pigment melanin, the production of which is increased upon sun exposure and absorbs more than 99.9 % of UV light reaching the epidermis. Melanin therefore plays a crucial role in protecting the skin from DNA damage caused by UV [110, 111].

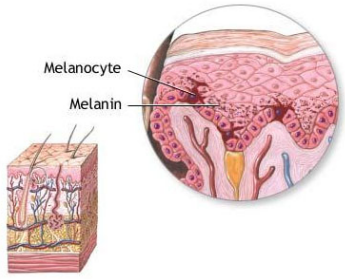

Source: US national cancer institute (NCI) homepage, 2014 [112]

Figure 6. Location and function of melanocytes within the skin

The basal cell layer contains cells called melanocytes. Melanocytes are the source of the pigment melanin, which provides skin its tan or brown color and protects the deeper skin layers from the harmful effects of UV.

The most important risk factor considered to contribute to the development of etiology of melanoma is UV light exposure [113]. It is very likely however that a combination of factors, including environmental and genetic factors, is involved in melanoma genesis [113-116]. Indeed, UV light does not cause all melanomas, especially those occurring in places on the body that are not exposed to sunlight. It is considered that cumulative genetic alterations affecting apoptotic pathways (programmed cell death), proliferation and cell cycle control in melanocytes can promote a malignant phenotype and initiate melanoma. Important cellular events normally involved in regulating cellular and tissue homeostasis have been shown to contribute to melanoma development and subsequent metastasis. These include cell growth induction including the resistance to growth inhibition signals, resistance to apoptotic cell death, unlimited capacity for cell division, stimulation of angiogenesis and acquisition by malignant cells of the competence to invade and metastasize [117, 118].

Unlike many other cancers, the annual incidence of newly detected cases of melanoma is increasing [119]. Great efforts aimed at better understanding the pathogenesis of the disease have been carried made over the past 2 decades, and these have led to the recent development of efficient treatment strategies that have an impact on disease free survival

and mortality. These new therapies include small molecule kinase inhibitors, notably B-Raf and MEK kinase inhibitors, as well as check-point control inhibitors. The latter enable the host anti-tumor immune response to become effective. Despite these improvements, overall survival of patients suffering from metastatic melanoma remains low and additional therapeutic approaches or combination of existing therapeutic approaches is needed [120-128].

1.3.2. Melanoma classification

Four different main categories of melanoma are classically defined (Figure 7) [129, 130], although current classifications are increasingly based on the molecular profile of a melanoma than its clinical growth characteristics. Superficial spreading melanoma (SSM) represents more than two thirds of melanoma cases and is therefore the most common form of cutaneous melanoma in Caucasians. It tends to occur on sun-exposed skin and is characterized by a flat growth at the skin surface. SSM can become invasive with melanoma cells crossing the basement membrane and entering the dermis. Lentigo maligna melanoma (LMM) is similar to SSM, as it initially remains confined to the skin surface. LMM arises mostly in elderly patients on sun-exposed, damaged skin on the face, ears, arms and upper trunk. Nodular melanoma (NM), which comprises 15-30 % of cases, is the most aggressive form of melanoma, presenting as an invasive form of melanoma whose vertical growth is more important than its radial growth. Finally, acral lentiginous melanoma (ALM), which comprises approximately 2-8 % of melanomas, is the least common melanoma category among Caucasians but remains the most common subtype in people with dark skin and Asians, mainly occurring on the palms, soles, mucous membranes (mouth, nose and female genitals), or underneath the nails.

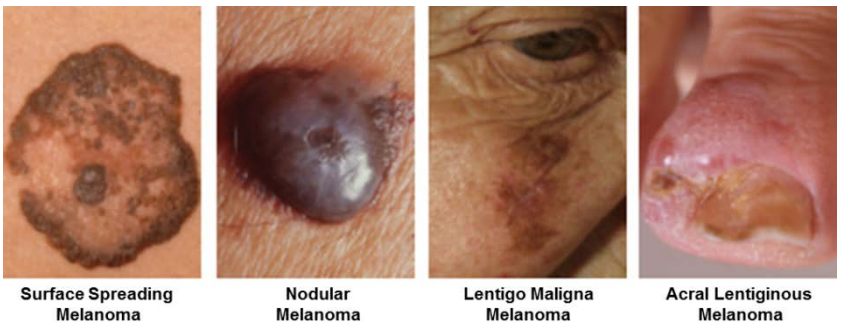

Source: the heterogeneity of melanoma homepage, 2014 [131]

Figure 7. Types of primary melanoma

Four main subtypes of primary melanoma presentation are shown. From left-to-right: superficial spreading melanoma (SSM), nodular melanoma (NM), lentigo maligna melanoma (LM) and acral-lentiginous melanoma (ALM).

1.3.3. Melanoma stages

Clinically melanoma can be detected and naturally evolve in different stages of severity, and the latter determine to a large extent the clinical prognosis of patients (Figure 4). According to the American Joint Committee on Cancer (AJCC) melanoma is classified into different stages [132, 133], taking into account tumor thickness (Breslow index [134]), mitoses, ulceration, tumor spread to lymph nodes and metastasis.

At the very onset of melanoma, abnormal melanocytes are confined to the epidermis (stage 0). Stage I defines melanomas that are either less than 1 mm thick according to the Breslow index (if the tumor is ulcerated) or 2 mm thick (if the tumor is not ulcerated). If melanomas are thicker than 2 mm or if they have a thickness of more than 1 mm and are ulcerated, they are defined as stage II melanomas. In stage III, local draining lymph nodes are involved, and stage IV, the melanoma stage with the worst prognosis, is characterized by organ involvement with metastases. Depending on the stage of melanoma, the overall patient survival varies, and the latter taken together with the molecular characteristics of the tumor helps clinicians to guide appropriate therapy (Figure 8).

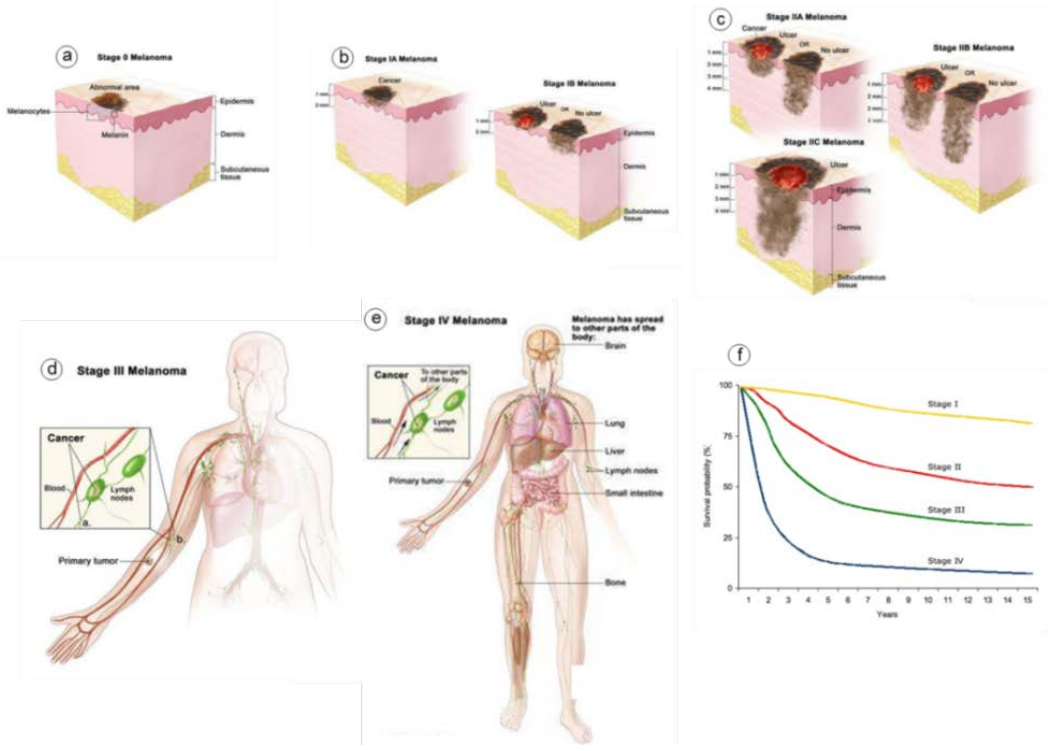

Source: the oncology institute of hope and innovation homepage, 2014 [135] and the Molecular Melanoma Map Project homepage, 2014 [136]

Figure 8. Melanoma stages

(a) Stage 0 melanoma. (b) Stage I melanoma. (c) Stage II melanoma. (d) Stage III melanoma. (e) Stage IV melanoma (d) Stage III melanoma. (f) Survival of melanoma patients (c)

See text for further explanations.

1.3.4. Melanoma risk factors

Although UVB light with an electromagnetic spectrum from 280 – 315 nm is mostly absorbed by the ozone layer, exposure of the skin to UV radiation is recognized as the main cause of skin cancer [137, 138]. Intermittent exposure to a high dose of sunlight is considered to represent a higher risk factor for melanoma development than chronic exposure at lower doses [113]. Individuals who have had sunburns are considered to be at higher risk for developing melanoma than individuals that have never had sunburns [113, 139]. Not only the dose and the exposure time to sunlight, but the constitution of the patient's skin itself affects the consequences of sunlight exposure. Indeed, compared to individuals with a skin phototype IV (dark skin with brown eyes and dark hair; reaction to sun exposure with tanning and very rarely with sunburn), those with a skin phototype I (tendency for freckles, red hair, blue or green eyes and high susceptible to sunburn without tendency to tan) are reported to have a 2-fold higher risk of developing cutaneous melanoma [140]. People with multiple atypical nevi, which are clinically usually larger than normal nevi, have a less distinct border and contain elevated zones, have an up to 10-fold higher risk of developing melanoma [116, 141]. The risk of developing melanoma is also correlated to the number of nevi a patient has [116]. Finally and importantly, individuals with a family history of melanoma have a 2-fold increased risk of developing melanoma as compared to patients without a positive family history [115, 142, 143]. Likewise, individuals who have already experienced melanoma themselves have a 15-fold higher risk of developing a second melanoma [144-147]. The probability of developing melanoma is also increased in patients who have already been diagnosed with other types of cancer including breast cancer [148, 149], leukemia [148], non-Hodgkin lymphoma [150, 151], thyroid cancer [148] and prostate cancer [148, 152, 153]. Reports also suggest that Parkinson's disease may also represent a risk factor [154-156]. Immunological defects such as those seen after organ transplantation [157], Crohn’s disease [158], severe psoriasis [159] as well as infection with human immunodeficiency virus (HIV) [160] have been also been shown to be associated with an increased risk of melanoma development.

1.3.5. Genetic mutations and main pathways involved in melanoma

The mutations identified in melanoma mainly influence molecular pathways involved in DNA repair, cell cycle progression and apoptosis. These mutations affect *RAF, RAS, TP53, CDKN2A, MAP2K1, RAC1, PPP6C, STK19, SNX31, ARID2* and *TACC1* [161].

One major signaling pathway affected in melanoma is the MAPK pathway. Members this signaling pathway include RAS (rat sarcoma oncogene) encoded by *HRAS*, *NRAS*, and *KRAS*; RAF (Rapidly Accelerated Fibrosarcoma) encoded by *ARAF*, *BRAF*, and *CRAF*; ERK (Extracellular-signal-Regulated Kinase) encoded by *MAPK1* and *MAPK3;* and MEK (MAPK/Extracellular-signal-regulated Kinase kinase) encoded by *MAP2K1* and *MAP2K2*. Mutations in these genes that regulate a highly conserved signaling pathway necessary for normal cell function result in aberrant cell proliferation and impaired regulation of apoptotic cell death [162, 163]. The first member of the MAPK pathway identified to have mutations in melanoma rendering it oncogenic was *NRAS* [164]. More recently, mutations in the gene of the serine/threonine kinase BRAF were found in around half of all melanoma cases [165]. The most frequent mutation (>90%) within *BRAF* is a point mutation in the nucleotide at position 1799 resulting in an amino acid change from valine to glutamic acid at amino acid 600 (V600E) [166]. In addition to its capability to transform cells via the MAPK pathway, mutated *BRAF* also influences tumor progression by modifying the expression of hypoxia-inducible factor 1α (Hif-1α), the extracellular matrix protein matrix metalloproteinase-1 (MMP-1) and the pro-apoptotic molecule BIM (B-cell lymphoma 2 Interacting Mediator of cell death) [167, 168]. At later stages of tumor development, oncogenic *BRAF* affects the tumor microenvironment by stimulating tumor cells to either produce factors that suppress anti-tumor immune responses or angiogenesis via VEGF (Vascular Endothelial Growth Factor) [169, 170].

Another pathway that is frequently altered in melanoma is the $p16^{INK4A}$/ cyclin D/ cyclin-dependent kinase (CDK) 4/6/ Retinoblastoma protein (Rb) pathway that regulates cell cycle arrest at the G1/S checkpoint. In melanoma, genomic alterations activating this pathway can be detected in 90 % of cases [166, 171]. $P16^{INK4A}$, which is encoded by *CDKN2A,* is a negative regulator of the serine/threonine kinases CDK4 and CDK6 by preventing the formation and activation of cyclin D/ CDK4/6 complexes. A cooperative connection of the $p16^{INK4A}$/ cyclin D/ CDK 4/6/ Rb pathway with the MAPK pathway is established by MAPK pathway-dependent increased expression of cyclin D1 [172, 173]. In case of $p16^{INK4A}$ dysfunction, the cyclin D/ CDK4/6 complexes together with cyclin E/ CDK2 complexes phosphorylate Rb, which in the phosphorylated form no longer suppresses the activities of RNA polymerases I and III, the E2F family of transcription factors and the recruitment of histone deacetylases [174-176]. This leads to cell-cycle progression, nucleotide biosynthesis and DNA replication [177]. A second product of *CDKN2A*, which is generated by transcription

of an alternate reading frame (ARF), is $p14^{ARF}$. $P14^{ARF}$ regulates cell cycle at G1 and G2/M checkpoints by sequestering MDM2 (Mouse Double Minute 2 homolog), therefore preventing the degradation of the tumor suppressor p53 [178, 179].

Mutations in the *PTEN* gene coding for Phosphatase and Ten sin homolog (PTEN) are also common in many cancer types including melanoma [180-185]. PTEN exerts its biological activity as a protein and lipid phosphatase [186, 187], with a suggested role for PTEN protein phosphatase activity in the regulation of the cell-cycle and in inhibiting cell invasion [188-192]. Nevertheless, the main tumor suppressor functions are considered to be due to the lipid phosphatase activity. It dephosphorylates Phosphatidylinositol (3,4,5)-tris-phosphate (PtdIns(3,4,5)P3) [193], which is the product of phosphatidylinositol-3 kinase (PI3K) and subsequently induces inactivation of phosphoinositide-dependent kinase 1 (PDK1) and downstream of it Akt with functions in apoptosis and cell cycle: blocking of Akt signaling affects the action of mammalian target of rapamycin (mTOR), p21, p27, BCL-2-associated agonist of cell death (BAD) and members of the forkhead transcription factor family (for example, FOXO1, FOXO3, and FOXO4) [194]. This has consequences on cell cycle progression, metabolism, migration, apoptosis, transcription and translation (Figure 9).

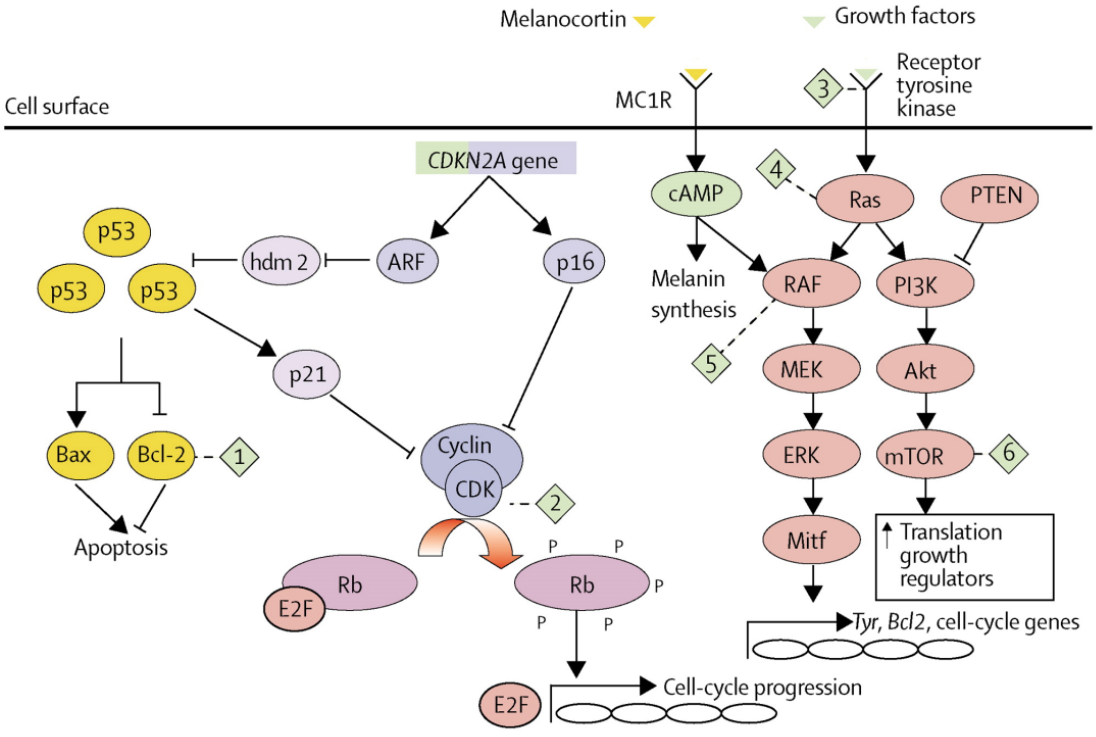

Source: Thompson et al., 2005 [195]

Figure 9. Major molecular pathways involved in the genesis and regulation of melanoma

SCF = stem cell factor. FGF = fibroblast growth factor. Ras = Rat sarcoma oncogene. BRAF = v-raf murine sarcoma viral oncogene homologue B1. MEK = MAPK/Extracellular-signal-regulated Kinase kinase. ERK = extracellular signal-regulated kinase. MAPK = mitogen-activated protein kinase. Mitf = microphthalmia transcription factor. PI3K = phosphatidylinositol-3 kinase. Akt = murine v-akt oncogene homologue. mTOR = mammalian target of rapamycin. CDKN2A = cyclin dependent kinase inhibitor-2A. CDK = cyclin dependent kinase. Rb = retinoblastoma protein. p16 = 16 000 MW protein. ARF (p14ARF) = 14 000 MW alternate reading frame protein. cAMP = cyclic AMP. Bcl = B-cell lymphoma derived protein. Hdm = human double minute chromosome-associated protein. E2F: E2F cell cycle regulated transcription factor. MSH = melanocyte stimulating hormone (melanocortin). MC1R = melanocortin-1 receptor.

In addition to classical therapies including surgery, chemotherapy and radiotherapy, small molecule therapies targeting the above described dysfunctional signaling pathways is proving to be an effective way of treating melanoma. The MAPK signaling pathway has become a major target of interest for targeted therapies and, in order to revoke its activation, BRAF inhibitors such as Dabrafenib, LGX 818 and Vemurafenib as well as MEK inhibitors like Mek163, Cobimetinib, Trametinib and Selumetinib have been developed. Targeting MAPK pathways has shown positive effects on parameters of disease activity in patients suffering from metastatic melanoma [124,126,196-198]. However, acquired resistance to such treatments represent a current limiting factor for their sustained efficacy [199]. Encouragingly however, very recent studies combining BRAF and MEK inhibition have reported improved progression-free survival of *BRAF* V600 mutated patients with metastatic melanoma [200, 201].

1.4. The role of innate and adaptive immune reactions in cancer

Population-based studies have revealed an increased risk for the development of cancer in individuals with chronic inflammatory diseases (Figure 10) [202, 203].

Several potentially tumorigenic pathogens including hepatitis B (HBV) or C (HCV) viruses involved in hepatocellular carcinoma (HCC), and *Schistosoma* or *Bacteroides* involved in bladder and colon cancer initiation induce a weak, but chronic inflammation in the host [204, 205]. Chronic inflammation can also be initiated by dysfunctional immune responses as observed in autoimmune diseases such as inflammatory bowel disease, which is associated with a higher risk of developing colorectal cancer [206]. The risk of lung cancer is significantly increased by the exposure to environmental factors such as tobacco and asbestos, the latter being a DAMP and known to be a potent inducer of inflammasome-dependent IL-1β-mediated inflammation [67, 207]. An inadequate diet and associated obesity is another factor shown to promote chronic inflammation, and subsequently increase the risk for hepatocellular carcinoma [208-210]. In the skin, acute UV exposure is known to trigger inflammation and DNA damage, two factors that independently have been shown to contribute to skin cancer development [211, 212].

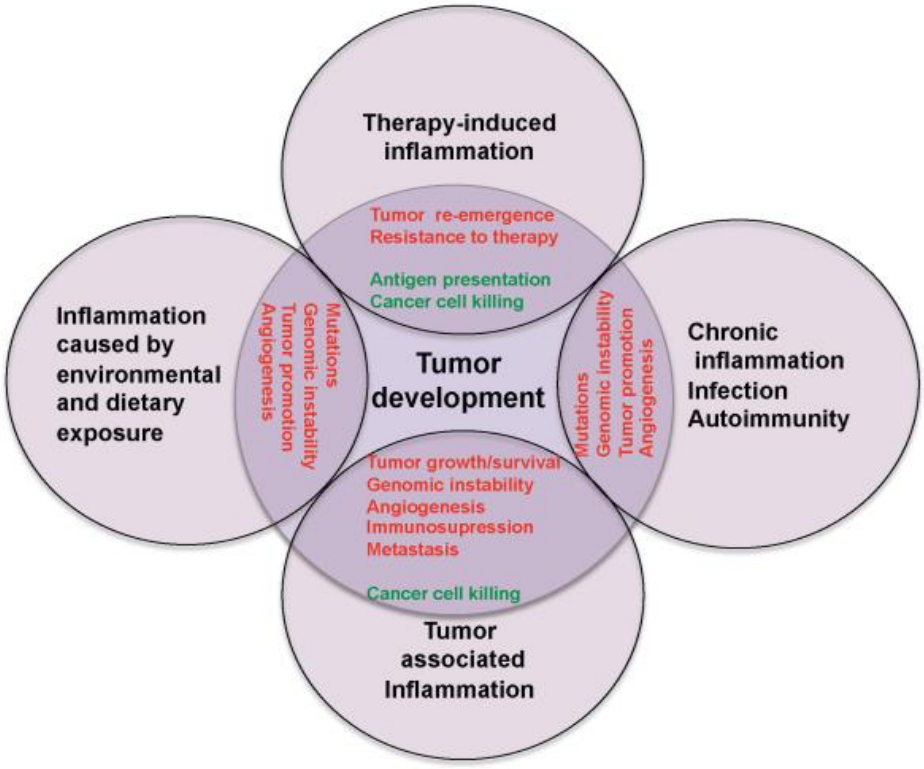

Source: Grivennikov et al., 2010 [213]

Figure 10. Types of inflammation in tumorigenesis and cancer

Chronic inflammation related to infections or autoimmune disease precedes tumor development and can be involved in it by inducing oncogenic mutations, instability of the genome, early tumor promotion, and enhanced angiogenesis. Prolonged exposure to environmental irritants or obesity can also be a cause of low-grade chronic inflammation preceding tumor development and can be involved in it through the mechanisms described above. Tumor-associated inflammation goes hand in hand with tumor development and the inflammatory response can amplify neo-angiogenesis, promote progression and metastasis of tumors, induce local immunosuppression, and further enhance instability of the genome. Also cancer therapy can induce an inflammatory response by causing trauma, necrosis, and tissue injury that stimulate tumor re-emergence as well as therapy resistance to. In some cases, inflammation induced by therapy can enhance presentation of antigens, which leads to immune-mediated tumor eradication. Tumor promoting mechanisms are displayed in red, whereas anti-tumorigenic mechanisms are shown in green.

Once established, increasing evidence suggest that tumors can also themselves trigger inflammation, and the latter may result in a pro-tumorigenic microenvironment [214]. Oncogenes such as the *RAS* and *MYC* family members regulate the transcription of genes that encode for tumor-promoting chemokines and cytokines, induce angiogenesis and promote the attraction of immune cells to the tumor site [215, 216]. In advanced stage tumors, the high energy consumption (“Warburg effect”) and inefficient blood supply within tumors results in a certain level of nutrient and oxygen deprivation, which can cause necrotic cell death, the release of proinflammatory mediators such as IL-1β and HMGB1, and subsequent neo-angiogenesis and immune cell recruitment [204, 217]. In consequence of the above, tumor stroma has been shown to contain inflammatory cells including macrophages, myeloid derived suppressor cells (MDSCs), DCs, neutrophils, eosinophils, MCs, and T cells (Figure 11).

1.4.1. Macrophages

Several tumor types have been reported to be infiltrated by inflammatory myeloid cells, including macrophages [213, 214, 218, 219]. To date, two types of macrophages have been defined based on the polarization of their cytokine secretion profile, and classified by analogy with Th cell subsets into M1 and M2 macrophages [220-224]. Activation of proinflammatory M1 macrophages is reported to be driven by pathogen-derived factors such as LPS or host-derived factors such as IFN-γ. M1 macrophages are considered to be involved in anti-tumor immune responses by releasing TNF-α, IL-12 and reactive nitrogen and oxygen intermediates (RNI/ ROI) including nitric oxide and superoxide [203, 225, 226]. Furthermore, M1 macrophages have been shown to be able to promote adaptive immunity by inducing Th1 responses [227, 228]. At early stages of tumorigenesis, M1 macrophages are reported to be the predominant type of tumor-associated macrophages (TAMs) found in the tumor infiltrate [229, 230], whereas more advanced stages of tumor development are associated

with infiltrates containing a majority of M2-like macrophages [231-233]. M2 macrophages are considered to be immunosuppressive and have been shown to release IL-10 and Arginase-1 [234, 235]. M2 macrophage polarization can be driven by IL-4, IL-13, IL-10 and glucocorticoid hormones and these macrophages are able to induce Th2 responses [223, 236, 237].

1.4.2. Myeloid derived suppressor cells

Another important cell type reported to infiltrate tumors and promote their progression, are immunosuppressive myeloid derived suppressor cells (MDSCs) [238]. The family of MDSCs is very heterogeneous. However, MDSCs in melanoma patients are usually characterized as $CD11b^+$, $CD14^+$ and $HLA\text{-}DR^-$ cells [239]. MDSCs present in tumors favor immune escape by inhibiting both innate and adaptive immunity [240-244]. MDSCs can secrete IL-10 and VEGF-α, which inhibit the maturation of DCs [245]. Furthermore, MDSC-derived transforming growth factor (TGF)-β upon IL-13 stimulation has been shown to decrease tumor immunosurveillance by cytotoxic T cells [246, 247]. MDSCs express high levels of inducible NO synthase (iNOS or NOS2) and arginase1 [248], and therefore control the availability of the amino acid L-arginine in the tumor microenvironment. In absence of L-arginine, T cell function is affected [249, 250]. Arginase 1, iNOS and prostaglandin E2 (PGE2) are regulated by cyclooxygenase-2 (COX2) which is produced by many tumors [251]. Finally, MDSCs produce ROS that inhibits the functions of cluster of differentiation (CD) 8^+ T cells by preventing peptide-major histocompatibility complex (MHC) interactions [252]. The ROS production of MDSCs can be initiated by tumor-derived factors such as TGF-β, IL-3, IL-6, IL-10 and platelet-derived growth factor (PDGF) [248, 253].

One of the major functions of M2 macrophages and MDSCs consists in vascular remodeling. Both cell types produce pro-angiogenic factors including VEGF-A, VEGF-C, IL-1β, TNF-α and the chemokines CXCL8 and CXCL12 [254, 255]. TAMs additionally produce urokinase-type plasminogen activator (uPA), elastase and the matrix metalloproteinases MMP-2, MMP-7, MMP-9 and MMP-12 [256, 257]. MMPs participate to the disruption of the extracellular matrix (ECM), which favors the migration of tumor cells [258, 259]. Additionally, both cell types share immunosuppressive properties as described above [236, 245-247, 260].

1.4.3. Neutrophils

Infiltration of neutrophils has been observed in several cancers [261, 262]. Tumor-associated neutrophils (TANs) produce MMP9 and promote angiogenesis by the release of angiogenic factors such as VEGF [263, 264]. Similarly to macrophages, two distinct subpopulations (N1 and N2) have been defined with the TGF-β-induced tumor-promoting N2 neutrophils being more prevalent in tumors than anti-tumoral N1 neutrophils [265, 266].

1.4.4. Eosinophils

Eosinophilic infiltration has been also reported in several tumors [267-270] and is considered to be mediated by the CCL11/CCR3 axis [271]. Eosinophils are predominantly found in necrotic tumor areas and are therefore believed to have an anti-tumor activity in this setting [272]. Eosinophils like neutrophils possess VEGF-α in their granules, which can be released upon IL-15 stimulation [273]. Together with IL-6, IL-8, PDGF, and MMP9, molecules that can also be released by eosinophils, VEGF-α can drive angiogenesis in cancer [274].

1.4.5. Mast cells

Bone-marrow-derived MCs are early infiltrating immune cells in cancer. They can often be found in proximity of blood vessels within the tumor microenvironment and express pro-angiogenic factors such as VEGF, MMP9 and IL-8. In line with this property, MC density in several tumors is correlated with the density of microvessels [275].

1.4.6. Dendritic cells

Due to their ability to trigger T cell responses, DCs have an important function in cancer immunosurveillance. Several factors released by tumors cause defects in myeloid DCs (mDCs) resulting in a loss of their immunostimulatory potential [276]. Also, immature DCs (iDCs) provide help to the tumor by inducing an endothelial-like phenotype of precursor DCs in a VEGF-A-dependent manner. These vascular leukocytes (VLCs) can build up blood vessels or act as antigen-presenting cells (APCs) [277, 278]. In addition to VEGF-a, IL-8 is up-regulated in iDCs under hypoxic conditions in vitro and may potentially participate in tumor angiogenesis [279].

1.4.7. T cells

The establishment of an effective adaptive immune response is complicated by defects in antigen-presentation and co-stimulation as well as by an immunosuppressive tumor microenvironment and the presence of regulatory T cells (Tregs). The latter which express CD25 (IL-2 receptor α chain), inhibit cytotoxic T cell responses via the release of immunosuppressive molecules, consumption of IL-2 and direct cell-to-cell contact [280]. $CD4^+$ $CD25^+$ $FoxP3^+$ Tregs present in advanced melanoma have been shown to block anti-tumor activity via direct contact inhibition and IL-10 release [281]. High Treg levels in patient serum seem to be associated with poor prognosis, poor treatment responses and the risk of relapse in melanoma [282]. T cell-mediated anti-tumor activity can additionally be impaired by defects in their interaction with APCs. Differentiation and expansion of T cells needs antigen presentation of tumor-associated antigens (TAAs) on MHC by APC to the T cell receptor (TCR). Unfortunately, in melanoma MHC class I expression is often down-regulated [283]. In metastatic melanoma, although melanoma-specific $CD8^+$ T cells can be found in patients, tumor progression is not affected significantly [284]. MHC class II molecules have also been reported to be down-regulated in melanoma [285]. Another defect in antigen presentation results from the changed expression of acidic cathepsins in melanoma, which leads to decreased antigen processing in endolysosomal compartments and production of antigens needed for T cell activation [285].

In addition to antigen-MHC-TCR interactions, co-stimulation is crucial for efficient T cell activation [286]. In melanoma the immune checkpoint molecule cytotoxic T-lymphocyte-associated protein 4 (CTLA-4) is highly expressed. CTLA-4 interacts with binding partners of CD28 (CD80/B7-1 and CD86/B7-2) and thus consumes one interaction partner in the T cell co-stimulatory CD28-CD80/CD86 pathway [287-290]. Another co-inhibitory pathway involves programmed death 1 protein (PD-1) present on activated melanoma-infiltrating T cells [291]. The binding of the ligands PD1-L1 (B7-H1) and PD-L2 (B7-DC), which can be highly expressed in melanoma [292], induces impaired T cell effector function and apoptosis [291, 293]. Interestingly, PD-L1 expression in cells of the melanoma microenvironment may not only be a cause of defective T cell activation, but also the consequence of an initial proper T cell function [294]. Since CTLA-4 and PD-1 co-inhibitory pathways play an important role in mediating functional anti-tumor T cell defects, both present as promising targets for melanoma therapy. The anti–CTLA-4 monoclonal antibody ipilimumab or antibodies directed against PD-1 and its ligand such as pembrolizumab, which target immune checkpoint inhibition, are currently showing very encouraging therapeutic effects in patients with metastatic melanoma [122, 295-297].

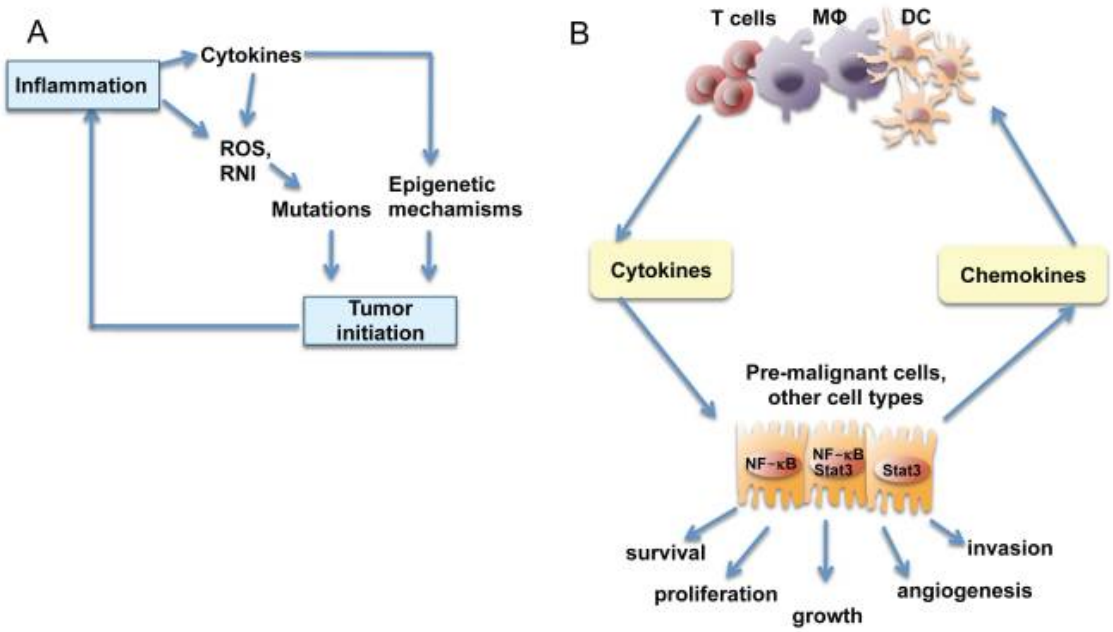

Source: Grivennikov et al., 2010 [213]

Figure 11. Inflammation during tumor initiation and promotion

(a) Tumor initiation. Reactive oxygen species (ROS) and reactive nitrogen intermediates (RNI), which are produced by inflammatory cells can induce mutations in neighboring epithelial cells. Intracellular ROS and RNI in pre-malignant cells can be enhanced by cytokines derived from inflammatory cells. Inflammation can also lead to epigenetic changes that favor tumor initiation. Tumor-associated inflammation contributes to further ROS, RNI and cytokine production.

(b) Tumor promotion. Tumor infiltrating immune cells produce cytokines that activate transcription factors in pre-malignant cells, such as NF-κB or STAT3, to control numerous pro-tumorigenic processes, including survival, proliferation, growth, angiogenesis, invasion and metastasis.

1.5. Hypoxia and cell death

1.5.1. Hypoxia in melanoma

Many cancers are characterized by high proliferation rates and energy consumption. In melanoma, the imbalance between oxygen supply and the actual use of oxygen creates hypoxic or even anoxic regions within the tumor [298, 299], affecting the course of disease negatively [300]. O_2 levels of less than 0.5 % are toxic for both normal and tumor cells, but tumor cells carrying mutations providing them a selection advantage have been shown to be able to survive in such an environment [301, 302]. Still, hypoxia results in tumor cell necrosis associated with the release of cellular components into the extracellular space [303-305]. In contrast to apoptosis, during necrosis cytosolic elements are not packed into apoptotic bodies and are therefore immunogenic [306, 307].

1.5.1.1. Hypoxia as an inducer of angiogenesis and metastasis

Hypoxia is known to promote angiogenesis via VEGF, IL-8 and angiopoietin-2 [308-310]. Hypoxia can promote an epithelial-mesenchymal transition (EMT)-like process with the involvement of E-cadherin, which enables melanoma cells to migrate to distant tissues. Under hypoxic conditions, Hif-1α is stabilized and negatively influences E-cadherin via snail, SIP1 (E-cadherin repressors) and twist (E-cadherin activator) [311]. Other targets of hypoxia are urokinase receptor (uPAR) and MMP2 being drivers in the degradation and remodeling of the ECM [312]. Metastasis is further favored by Hif-1α-driven expression of lysyl oxidase, which is involved in attracting bone marrow-derived cells to the location of the secondary tumors [313]. Reduced activity of microphthalmia transcription factor (MITF), a factor regulating melanocyte differentiation, which is driven via Hif-1α and class E basic helix-loop-helix protein 40 ($BHLHB_2$, DEC1) also increases the probability of metastasis [314, 315].

1.5.1.2. Hypoxia and anti-tumor therapy

Hypoxia also has an impact on the efficacy of cancer treatment. Indeed, resistance genes have been shown to be up-regulated under hypoxic conditions [316, 317] and tumors respond less to radiotherapy [318, 319]. Heterogeneity of the tumors is another obstacle for melanoma treatment [320]. Gene expression profiling of isolated melanoma cells has provided evidence that there are two distinct melanoma cell phenotypes within tumors, namely the proliferative and invasive phenotypes, which can be distinguished by their morphology, proliferation rate, invasion and *in vivo* tumor growth kinetics [321-323]. Both phenotypes have been demonstrated to be present in primary melanomas as well as in metastases [324, 325]. Recently, it has been shown that hypoxia is also involved in the above phenotype determination by regulating the switch between proliferative and invasive phenotype via Hif-1α activity [326].

1.5.2. Cell death

Research on cell death was initiated by Lockshin and Williams describing a regulated form of cell death termed apoptosis, which is characterised by zeiosis, cell shrinkage, condensation of chromatin, arrangement of the cell contents in apoptotic bodies and clearance by phagocytes [327-331]. Beside apoptosis, there are two other main forms of cell death, namely necrosis and autophagy-related cell death [332]. Additional death mechanisms like pyroptosis or necroptosis have been described more recently and are currently under investigation.

1.5.2.1. Apoptosis

Apoptosis takes place already during development [333]. In adults, apoptosis is a way to eliminate cells without inducing immune responses [334, 335]. Major players in apoptosis are effector caspases [336], which can be divided into initiator and executioner caspases [53].
Crucial for the activation of apoptotic caspases in the extrinsic pathway is activation of death receptors such as Fas (CD95), TRAIL or TNF-receptor leading to the formation of the membrane bound death-inducing signaling complex (DISC) [337]. The initiator caspases (caspase-8 and -10) also recruited to the DISC then activate the executioner caspases (caspase-3, -6 and -7) [338, 339].
In the intrinsic pathway, members of the B-cell lymphoma 2 (Bcl-2) family, upon sensing of cellular stress such as deprivation of growth factors and DNA damage promote mitochondrial outer membrane permeabilization (MOMP) by the formation of pores [340, 341]. Through the defective outer mitochondrial membrane, apoptosis-promoting factors leak into the

cytoplasm. Cytochrome C for example binds to apoptotic protease-activating factor-1 (Apaf-1) [342, 343], thereby promoting the assembly of the heptameric apoptosome including procaspase-9 [342, 343]. Active caspase-9 then cleaves and activates the executioner caspases-3, -6 and -7, which translocate to the nucleus and promote inhibition of DNA repair, DNA fragmentation and chromatin condensation [344-347].

1.5.2.2. Autophagy

The most studied form of autophagy is macroautophagy, which stressed cells use to dispose suspicious organelles and protein aggregates [348]. Triggered by starvation, inhibition of the protein kinase mTOR induces autophagosomal formation by translocation of the mTOR substrate complex to the membrane of the ER [349]. The main function of autophagy is the promotion of cell survival, but autophagy-associated cell death as backup mechanisms of apoptosis has been demonstrated [350].

1.5.2.3. Necrosis and Necroptosis

One dogma in the field of cell death for a long time was that if a type of cell death is regulated, then it is apoptosis, whereas other forms of cell death were considered to be uncontrolled. The establishment of knockout mice for apoptosis relevant factors such as apoptotic caspases, Apaf-1 and Bcl-2 family members showed that apoptosis-dependent developmental steps can still be fulfilled and mice develop to the adult stage [351-356], indicating the existence of a regulated cell death mechanism compensating apoptosis. Digit separation by elimination of interjacent skin is still carried out in Apaf-1 knockout mice, and a closer look at morphological parameters identified necrotic rather than apoptotic cell death in these mice [354, 356]. In an *in vitro* setting, caspase-deficient cells stimulated with apoptosis inducers undergo necrosis [357, 358]. During necrosis, swelling of the cell, loss of membrane stability and cell lysis can be observed. Triggers of necrosis are severe forms of cellular stress such as hypoxic or ischemic damage. Though being considered to be an unregulated process, a controlled version of necrotic cell death with certain resemblance to necrosis named necroptosis has been defined [359-362].

TLR3 and 4 are also activators of necrotic cell death. TLR4 ligation provokes caspase-8 activity with induction of the extrinsic apoptotic pathway, but by blocking caspase-8, necrotic cell death is induced [363]. Additional triggers of necrosis are elevated Ca^{2+} or ROS levels, that can induce generation of hydroperoxides or the activation of proteases like calpain or cathepsin B [364].

One major difference between apoptosis and necrosis is that necrosis causes a local inflammatory response. While in apoptosis the cell contents are packed into apoptotic

bodies, necrotic cells release their cytoplasmic contents to the extracellular space, where they function as danger signals and activate innate immune system components such as the NLRP3 inflammasome [365]. In turn TLR signaling or the NLRP3 inflammasome can also contribute to cell death [366, 367]. Although necrotic cell death is linked to severe stress, it can partially escort or replace apoptosis, for example in the above-mentioned development of fingers but also in cellular turnover of the intestine and other conditions [364].

In the setting of cancer, necrotic cell death mostly takes place under hypoxic conditions and is thought to contribute to attracting inflammatory cells to the tumor [213, 304, 305, 307].

1.6. HMGB1

1.6.1. HMGB1 structure and domains

HMGB1 protein is a highly conserved DNA-binding protein with 98.5 % sequence homology across mammals. It is involved in gene expression and chromatin remodeling [368, 369]. HMG proteins were initially described by Godwin et al. and named according to their mobility in polyacrylamide gel electrophoresis systems [370]. The 215 amino acid protein HMGB1 contains two DNA binding domains, HMG A box at position 9-79 and HMG B box at position 185-215, and an acidic tail at the C-terminus (Figure 12) [371]. The DNA binding domains unspecifically bind DNA, a process that is ensured by two nuclear-localization signals (NLS) at positions 28-44 and 179-185, keeping HMGB1 in the nucleus in the steady state [372]. The B box of HMGB1 has proinflammatory properties, whereas the A box is an HMGB1 antagonist [373]. Residues at position 150-183 interact with RAGE, residues at position 89-108 are responsible for the binding of HMGB1 to TLR4 and residues at position 7-74 are transactivating domains of p53 [374-376]. The acidic C-terminal tail of HMGB1 mediates the antibacterial properties of HMGB1 as well as the DNA binding [377-379].

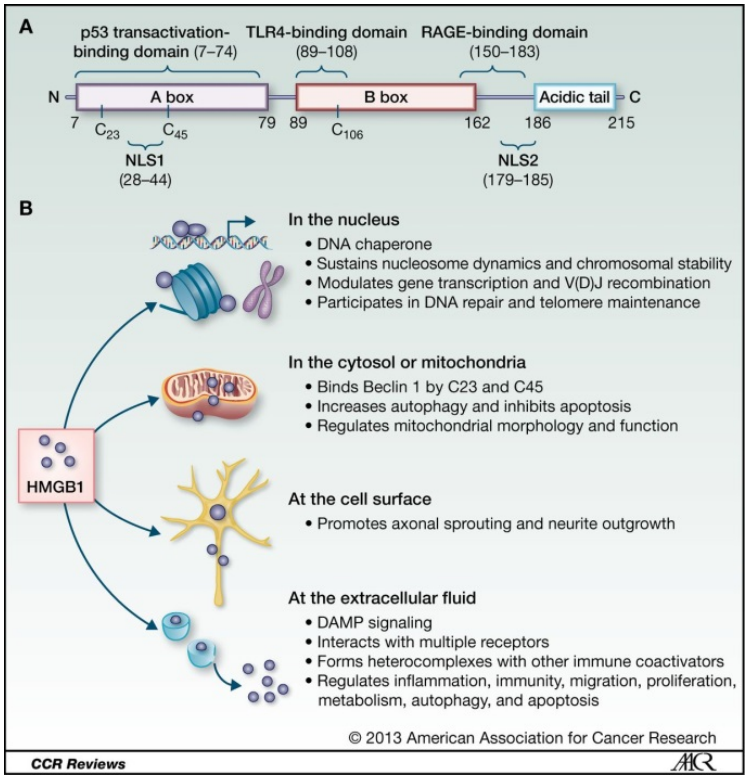

Source: Kang et al., 2013 [380]

Figure 12. HMGB1 structure and functions

(a) HMGB1 is structurally composed of three different major domains: two homologous DNA-binding domains termed box A and box B, and a negatively charged C-terminal domain. Residues at positions 150 – 183 drive binding to RAGE, whereas residues at positions 7-74 and 89-108 are responsible for binding to p53 transactivation domain and Toll-like receptor 4 (TLR4). Two nuclear localization signals (NLS1 and NLS2) control transport of HMGB1 to the nucleus. HMGB1 contains three cysteine residues at positions 23, 45 and 106, which are redox-sensitive and are important for HMGB1 activity.
(b) Depending on its localization, HMGB1 has multiple roles.

1.6.2. Nuclear functions of HMGB1

Nuclear HMGB1 acts as an architectural transcription factor regulating gene transcription and genomic stability by interaction with nucleotides, histones, transcription factors and other proteins (Figure 12) [381-383].

HMGB1 participates in the assembly of nucleosomes and chromatin replication, relaxes nucleosomes and makes chromatin more accessible [384-387]. This interaction of HMGB1 with nucleosomes is short-lived and reversible during chromatin remodeling [388]. HMGB1 also exerts chaperone activity and accelerates nucleosome assembly to naked DNA [389].

Another HMGB1 interaction partner besides nucleosomes is DNA. HMGB1 acting as a DNA chaperone binds DNA in a sequence-unspecific manner [390], a process that is regulated by the areas close to the HMGB1 DNA binding boxes, the acidic C-terminal tail and post-translational modifications [378, 391-396]. DNA-bound HMGB1 can bend the latter and induce DNA conformation changes [397-401].

HMGB1 influences gene transcription via HMGB1-TATA binding protein (TBP)/TATA-box complex interactions [402, 403], or by acting as an activator, enhancer, repressor or silencer of steroid nuclear receptors, p53, retinoblastoma (Rb) protein and estrogen receptor [375, 404-410].

Additionally, HMGB1 plays an essential role in V(D)J recombination by formation of recombination-activating genes (RAG)/ recombination signal sequence (RSS)/ HMGB1 complexes that enhance RAG1/RAG2 activity [411-413].

1.6.3. Extracellular functions of HMGB1

Under homeostatic conditions, HMGB1 is kept inside the cells with a preferential nuclear localization, but it can be actively secreted or passively released upon cell damage [414]. When released into the extracellular space HMGB1 can stimulate immune responses either alone or in conjunction with other molecules. Translocation of HMGB1 from the nucleus to the cytoplasm and its subsequent secretion can occur in various situations such as during activation of immune cells, including for example macrophages upon LPS stimulation or monocytes upon Lysophosphatidylcholines (LPC) exposure, and during cell death (necrosis and apoptosis) and ischemia/reperfusion injury [415-417].

Three critical cysteine residues at positions 23, 45 and 106 regulate HMGB1 translocation to the cytoplasm (Cys 106) and its effector function in the extracellular space [374, 418, 419]. Depending on HMGB1 redox state at these three residues, HMGB1 can be inactive or exert chemo-attractant or cytokine-inducing activities (Figure 13).

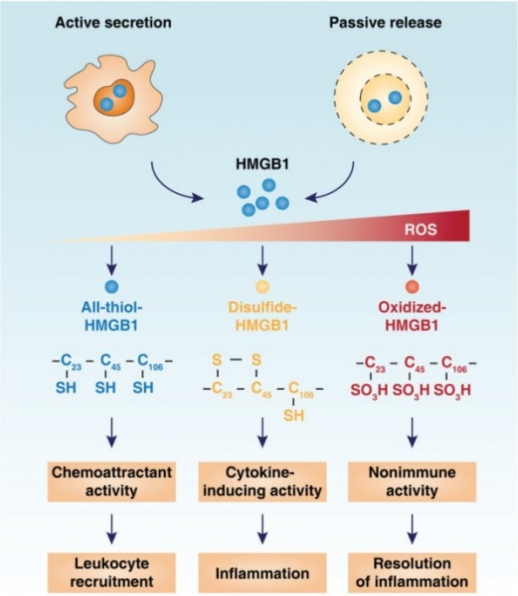

Source: Tang et al., 2012 [420]

Figure 13. HMGB1 activity is dependent on its redox state

To act in the extracellular space as a DAMP/danger signal and inflammatory mediator, HMGB1 is released from cells by two main mechanisms: living inflammatory cells such as macrophages actively secrete it, whereas necrotic cells release HMGB1 passively. The redox state of HMGB1 determines its action in the extracellular space: all-thiol-HMGB1 induces chemokine production and leukocyte recruitment, whereas disulfide-HMGB1 promotes release of proinflammatory cytokines and thus participates to the inflammatory response. ROS from leukocytes induces terminal oxidation of HMGB1, which is inactivated during resolution of inflammation.

HMGB1 has been reported to act as a DAMP or an alarmin [421], linking tissue damage and stress to activation of innate immune responses. Notably, HMGB1 has been shown to be involved in diseases in which chronic inflammation plays a role, such as arthritis and cancer [414, 421-423].

HMGB1 induces signaling through the binding to RAGE and certain TLRs [421, 423-432]. HMGB1 might be involved in regulating TLR9 signaling, as indicated by the fact that activation of TLR9 is substantially decreased in macrophages and DCs deficient for HMGB1 [433]. It has been suggested that the binding of immunogenic nucleic acids to HMGB1 is required for subsequent recognition by specific PRRs such as TLR3, TLR7 and TLR9, and subsequent activation of innate immune responses [434]. Indeed, in the absence of cytosolic HMGB proteins, the secretion of cytokines including type-I interferons, TNF-α, IL-6 and IL-1β is dramatically impaired upon exposure to immunogenic nucleic acids [433-435]. In addition to this cytokine activity, HMGB1 can also participate in the transactivation of the IL-1β gene promoter [436].

The majority of immune cells can respond to extracellular HMGB1. HMGB1 can act as a powerful DAMP/alarmin that can induce a broad range of proinflammatory effector pathways. Target cells interacting with HMGB1 via RAGE and TLRs include macrophages, monocytes, neutrophils, fibroblasts, keratinocytes, DCs and T cells [437-444]. Induction of signaling in these cells by HMGB1 results in production of a variety of cytokines including TNF-α, IL-1α, IL-1β, IL-6, IL-8, IL-10, macrophage inflammatory protein (MIP)-1α and MIP-1β as well as chemokines such as CCL5, CXCL1, CXCL2, CCL2, CCL20 and CCL3 [437-439, 441, 443, 445-449]. Interestingly, while HMGB1 alone has a low proinflammatory potential, its association to other DAMPs or PAMPs like LPS, CpG-ODN, Pam3CSK4 or lipids, results in very potent proinflammatory stimuli [450-452].

1.6.4. HMGB1 and cancer

A pivotal role for HMGB1 has been shown in several cancer types including colon, breast, lung, prostate, cervical, skin, kidney, stomach, pancreatic, liver, bone, and blood cancer [422, 423, 453, 454]. HMGB1 has been shown to exert anti- or pro-tumor effects depending on the cancer type, its location and redox status state [380].

A suppressive role for HMGB1 in tumorigenesis is supported by the fact, that nuclear HMGB1 binds to the transcription factor Rb, which acts as a tumor suppressor by inducing cell cycle arrest in the G_1 phase and apoptosis of breast cancer cells [455]. As a DNA chaperone, HMGB1 prevents cells from genome instability and telomere shortening, which also supports an anti-tumor effect of nuclear HMGB1 [389, 456, 457]. Defects in autophagy result in genomic instability, inflammation and damaged organelles, three abnormalities that

can result in tumorigenesis [459-462]. By acting as a positive regulator of autophagy, HMGB1 has been suggested to prevent tumor development. [458],

On the contrary, a substantial number of reports have shown that HMGB1 can facilitate tumor growth and cancer progression. In tumors, the cellular sources of HMGB1 are multiple and variable from tumor to tumor. During malignant mesothelioma development, HMGB1 has been shown to be released by mesothelial cells exposed to asbestos and erionite with implications for HMGB1 in malignant mesothelioma development in an autocrine manner, i.e. by directly stimulating tumor cell growth [459-461]. Also, activated macrophages, monocytes and T cells can secrete HMGB1 under conditions of hypoxia, injury or inflammatory stimuli [462-464]. In addition, it has been recently reported that MDSCs present in tumors secrete HMGB1 [465].

Via RAGE and TLR signaling pathways, extracellular HMGB1 can activate cytokine release. In a DMBA/TPA-induced skin carcinogenesis model, mice deficient for RAGE, a known receptor of HMGB1, were shown to be more resistant to inflammation and tumor formation [466]. In melanoma and colon cancer the recruitment of inflammatory cells contributing to tumor development is impaired upon blockade of TLR4/ HMGB1 interaction [467].

Recently, HMGB1 has been shown to be released from keratinocytes after UVB irradiation and to promote the attraction of neutrophils to the microenvironment of melanoma in a TLR4-dependent manner with subsequent promotion of metastasis [468]. Also relevant to metastasis is the expression of matrix metalloproteinases like MMP2 and MMP9, which has been shown to be decreased when HMGB1 signaling through RAGE is blocked [469]. Coherent observations were made in gastric cancer and colorectal adenomas, where RAGE expression was closely associated with metastasis [470, 471].

In certain settings, anti-tumor immune surveillance is impaired by HMGB1. In colon cancer, HMGB1 has been reported to trigger apoptosis of DCs and to limit antigen presentation and adaptive immune responses [472]. Cytotoxic $CD8^+$ T cell function is indirectly inhibited by HMGB1 since IL-10-mediated T cell suppression can be prevented by blockade of tumor-derived HMGB1 [473]. A direct influence of HMGB1 on T cells is supported by the elevated expression of Lymphotoxin α1β2 on tumor-infiltrating T cells in the presence of HMGB1 in prostate cancer with subsequent recruitment of macrophages providing growth factors and initiating angiogenesis [474]. Angiogenesis has been shown to be promoted by stimulation of the HMGB1 receptor RAGE [471].

Finally, HMGB1 has been shown to assist tumors in accelerating their metabolism to ensure their increased energy needs. During pancreatic tumor growth, HMGB1 contributes to the regulation of mitochondrial bioenergetics via RAGE, a process which might be driven by heat shock protein (HSP) 27 leading to less ATP production [475-477].

1.7. Aim of this PhD thesis

In this thesis I report my contribution to the investigation of two processes that are relevant to tumor-stroma interactions. In a first project I have analyzed the ability of melanoma cell lines to process and secrete the proinflammatory cytokine IL-1β as well as the ability of necrotic tumor cells (melanoma) to induce inflammasome activation and IL-1β secretion in macrophages. I have also analyzed the pattern of expression of IL-1β protein in benign and malignant human melanocytic lesions in order to gain insight of the site of production of IL-1β in human melanomas *in vivo*. In the second project, and intrigued by a finding in the first project showing that macrophages in the melanoma tumor microenvironment secrete high amounts of IL-1β, observed *in vitro* upon exposure to necrotic cell debris and the supernatant thereof, we were interested to investigate the role of the DAMP/alarmin HMGB1 that is known to be released upon cell necrosis, in melanoma development. The results of these two projects relevant to tumor stroma interactions are presented here in the form of two manuscripts and then discussed in detail in the discussion section.

References

1. Eckert, R.L., J.F. Crish, and N.A. Robinson, *The epidermal keratinocyte as a model for the study of gene regulation and cell differentiation.* Physiol Rev, 1997. **77**(2): p. 397-424.

2. Gandarillas, A., *Epidermal differentiation, apoptosis, and senescence: common pathways?* Exp Gerontol, 2000. **35**(1): p. 53-62.

3. Haeberle, H., et al., *Molecular profiling reveals synaptic release machinery in Merkel cells.* Proc Natl Acad Sci U S A, 2004. **101**(40): p. 14503-8.

4. Maksimovic, S., Y. Baba, and E.A. Lumpkin, *Neurotransmitters and synaptic components in the Merkel cell-neurite complex, a gentle-touch receptor.* Ann N Y Acad Sci, 2013. **1279**: p. 13-21.

5. Hartschuh, W. and E. Weihe, *Fine structural analysis of the synaptic junction of Merkel cell-axon-complexes.* J Invest Dermatol, 1980. **75**(2): p. 159-65.

6. Nestle, F.O., et al., *Skin immune sentinels in health and disease.* Nat Rev Immunol, 2009. **9**(10): p. 679-91.

7. Feldmeyer, L., et al., *Interleukin-1, inflammasomes and the skin.* Eur J Cell Biol, 2010. **89**(9): p. 638-44.

8. Fuchs, E. and S. Raghavan, *Getting under the skin of epidermal morphogenesis.* Nat Rev Genet, 2002. **3**(3): p. 199-209.

9. Kendall, A.C. and A. Nicolaou, *Bioactive lipid mediators in skin inflammation and immunity.* Prog Lipid Res, 2013. **52**(1): p. 141-64.

10. Grice, E.A. and J.A. Segre, *The skin microbiome.* Nat Rev Microbiol, 2011. **9**(4): p. 244-53.

11. Cavassani, K.A., et al., *TLR3 is an endogenous sensor of tissue necrosis during acute inflammatory events.* J Exp Med, 2008. **205**(11): p. 2609-21.

12. Lai, Y., et al., *Commensal bacteria regulate Toll-like receptor 3-dependent inflammation after skin injury.* Nat Med, 2009. **15**(12): p. 1377-82.

13. Naik, S., et al., *Compartmentalized control of skin immunity by resident commensals.* Science, 2012. **337**(6098): p. 1115-9.

14. Lee, D.Y., et al., *Sebocytes express functional cathelicidin antimicrobial peptides and can act to kill propionibacterium acnes.* J Invest Dermatol, 2008. **128**(7): p. 1863-6.

15. Chen, C.H., et al., *An innate bactericidal oleic acid effective against skin infection of methicillin-resistant Staphylococcus aureus: a therapy concordant with evolutionary medicine.* J Microbiol Biotechnol, 2011. **21**(4): p. 391-9.

16. Chronnell, C.M., et al., *Human beta defensin-1 and -2 expression in human pilosebaceous units: upregulation in acne vulgaris lesions.* J Invest Dermatol, 2001. **117**(5): p. 1120-5.

17. Nagy, I., et al., *Propionibacterium acnes and lipopolysaccharide induce the expression of antimicrobial peptides and proinflammatory cytokines/chemokines in human sebocytes.* Microbes Infect, 2006. **8**(8): p. 2195-205.

18. Nakatsuji, T., et al., *Sebum free fatty acids enhance the innate immune defense of human sebocytes by upregulating beta-defensin-2 expression.* J Invest Dermatol, 2010. **130**(4): p. 985-94.

19. Kuo, I.H., et al., *The cutaneous innate immune response in patients with atopic dermatitis.* J Allergy Clin Immunol, 2013. **131**(2): p. 266-78.

20. Kim, J.E., et al., *Expression and modulation of LL-37 in normal human keratinocytes, HaCaT cells, and inflammatory skin diseases.* J Korean Med Sci, 2005. **20**(4): p. 649-54.

21. Liu, A.Y., et al., *Human beta-defensin-2 production in keratinocytes is regulated by interleukin-1, bacteria, and the state of differentiation.* J Invest Dermatol, 2002. **118**(2): p. 275-81.

22. Seo, S.J., et al., *Expressions of beta-defensins in human keratinocyte cell lines.* J Dermatol Sci, 2001. **27**(3): p. 183-91.

23. Eckert, R.L., et al., *S100 proteins in the epidermis.* J Invest Dermatol, 2004. **123**(1): p. 23-33.

24. Firat, Y.H., et al., *Infection of keratinocytes with Trichophytum rubrum induces epidermal growth factor-dependent RNase 7 and human beta-defensin-3 expression.* PLoS One, 2014. **9**(4): p. e93941.

25. Glaser, R., et al., *Antimicrobial psoriasin (S100A7) protects human skin from Escherichia coli infection.* Nat Immunol, 2005. **6**(1): p. 57-64.

26. Kanda, N. and S. Watanabe, *Prolactin enhances interferon-gamma-induced production of CXC ligand 9 (CXCL9), CXCL10, and CXCL11 in human keratinocytes.* Endocrinology, 2007. **148**(5): p. 2317-25.

27. Keller, M., et al., *Active caspase-1 is a regulator of unconventional protein secretion.* Cell, 2008. **132**(5): p. 818-31.

28. Kock, A., et al., *Human keratinocytes are a source for tumor necrosis factor alpha: evidence for synthesis and release upon stimulation with endotoxin or ultraviolet light.* J Exp Med, 1990. **172**(6): p. 1609-14.

29. Kupper, T.S., et al., *Production of IL-6 by keratinocytes. Implications for epidermal inflammation and immunity.* Ann N Y Acad Sci, 1989. **557**: p. 454-64; discussion 464-5.

30. Zepter, K., et al., *Induction of biologically active IL-1 beta-converting enzyme and mature IL-1 beta in human keratinocytes by inflammatory and immunologic stimuli.* J Immunol, 1997. **159**(12): p. 6203-8.

31. Banno, T., A. Gazel, and M. Blumenberg, *Effects of tumor necrosis factor-alpha (TNF alpha) in epidermal keratinocytes revealed using global transcriptional profiling.* J Biol Chem, 2004. **279**(31): p. 32633-42.

32. Kanda, N., et al., *IL-18 enhances IFN-gamma-induced production of CXCL9, CXCL10, and CXCL11 in human keratinocytes.* Eur J Immunol, 2007. **37**(2): p. 338-50.

33. Dinarello, C.A., *Immunological and inflammatory functions of the interleukin-1 family.* Annu Rev Immunol, 2009. **27**: p. 519-50.

34. Dinarello, C.A., *The IL-1 family and inflammatory diseases.* Clin Exp Rheumatol, 2002. **20**(5 Suppl 27): p. S1-13.

35. Weber, A., P. Wasiliew, and M. Kracht, *Interleukin-1 (IL-1) pathway.* Sci Signal, 2010. **3**(105): p. cm1.

36. Vincenti, M.P. and C.E. Brinckerhoff, *Transcriptional regulation of collagenase (MMP-1, MMP-13) genes in arthritis: integration of complex signaling pathways for the recruitment of gene-specific transcription factors.* Arthritis Res, 2002. **4**(3): p. 157-64.

37. Stienstra, R., et al., *The inflammasome puts obesity in the danger zone.* Cell Metab, 2012. **15**(1): p. 10-8.

38. Dinarello, C.A., *Interleukin-1, interleukin-1 receptors and interleukin-1 receptor antagonist.* Int Rev Immunol, 1998. **16**(5-6): p. 457-99.

39. Kopf, M., M.F. Bachmann, and B.J. Marsland, *Averting inflammation by targeting the cytokine environment.* Nat Rev Drug Discov, 2010. **9**(9): p. 703-18.

40. Dinarello, C.A., *Therapeutic strategies to reduce IL-1 activity in treating local and systemic inflammation.* Curr Opin Pharmacol, 2004. **4**(4): p. 378-85.

41. Gabay, C., C. Lamacchia, and G. Palmer, *IL-1 pathways in inflammation and human diseases.* Nat Rev Rheumatol, 2010. **6**(4): p. 232-41.

42. Afonina, I.S., et al., *Granzyme B-dependent proteolysis acts as a switch to enhance the proinflammatory activity of IL-1alpha.* Mol Cell, 2011. **44**(2): p. 265-78.

43. Hacham, M., et al., *Different patterns of interleukin-1alpha and interleukin-1beta expression in organs of normal young and old mice.* Eur Cytokine Netw, 2002. **13**(1): p. 55-65.

44. Nickel, W., *The mystery of nonclassical protein secretion. A current view on cargo proteins and potential export routes.* Eur J Biochem, 2003. **270**(10): p. 2109-19.

45. Schindler, R., B.D. Clark, and C.A. Dinarello, *Dissociation between interleukin-1 beta mRNA and protein synthesis in human peripheral blood mononuclear cells.* J Biol Chem, 1990. **265**(18): p. 10232-7.

46. Schindler, R., J.A. Gelfand, and C.A. Dinarello, *Recombinant C5a stimulates transcription rather than translation of interleukin-1 (IL-1) and tumor necrosis factor: translational signal provided by lipopolysaccharide or IL-1 itself.* Blood, 1990. **76**(8): p. 1631-8.

47. Martinon, F., A. Mayor, and J. Tschopp, *The inflammasomes: guardians of the body.* Annu Rev Immunol, 2009. **27**: p. 229-65.

48. Guma, M., et al., *Caspase 1-independent activation of interleukin-1beta in neutrophil-predominant inflammation.* Arthritis Rheum, 2009. **60**(12): p. 3642-50.

49. Joosten, L.A., et al., *Inflammatory arthritis in caspase 1 gene-deficient mice: contribution of proteinase 3 to caspase 1-independent production of bioactive interleukin-1beta.* Arthritis Rheum, 2009. **60**(12): p. 3651-62.

50. Li, P., et al., *Mice deficient in IL-1 beta-converting enzyme are defective in production of mature IL-1 beta and resistant to endotoxic shock.* Cell, 1995. **80**(3): p. 401-11.

51. Kuida, K., et al., *Altered cytokine export and apoptosis in mice deficient in interleukin-1 beta converting enzyme.* Science, 1995. **267**(5206): p. 2000-3.

52. Netea, M.G., et al., *Differential requirement for the activation of the inflammasome for processing and release of IL-1beta in monocytes and macrophages.* Blood, 2009. **113**(10): p. 2324-35.

53. Pop, C. and G.S. Salvesen, *Human caspases: activation, specificity, and regulation.* J Biol Chem, 2009. **284**(33): p. 21777-81.

54. Martinon, F., K. Burns, and J. Tschopp, *The inflammasome: a molecular platform triggering activation of inflammatory caspases and processing of proIL-beta.* Mol Cell, 2002. **10**(2): p. 417-26.

55. Strowig, T., et al., *Inflammasomes in health and disease.* Nature, 2012. **481**(7381): p. 278-86.

56. Bauernfeind, F., et al., *Inflammasomes: current understanding and open questions.* Cell Mol Life Sci, 2011. **68**(5): p. 765-83.

57. Franchi, L., et al., *Cytosolic flagellin requires Ipaf for activation of caspase-1 and interleukin 1beta in salmonella-infected macrophages.* Nat Immunol, 2006. **7**(6): p. 576-82.

58. Miao, E.A., et al., *Cytoplasmic flagellin activates caspase-1 and secretion of interleukin 1beta via Ipaf.* Nat Immunol, 2006. **7**(6): p. 569-75.

59. Miao, E.A., et al., *Innate immune detection of the type III secretion apparatus through the NLRC4 inflammasome.* Proc Natl Acad Sci U S A, 2010. **107**(7): p. 3076-80.

60. Roberts, T.L., et al., *HIN-200 proteins regulate caspase activation in response to foreign cytoplasmic DNA.* Science, 2009. **323**(5917): p. 1057-60.

61. Fernandes-Alnemri, T., et al., *AIM2 activates the inflammasome and cell death in response to cytoplasmic DNA.* Nature, 2009. **458**(7237): p. 509-13.

62. Hornung, V., et al., *AIM2 recognizes cytosolic dsDNA and forms a caspase-1-activating inflammasome with ASC.* Nature, 2009. **458**(7237): p. 514-8.

63. Burckstummer, T., et al., *An orthogonal proteomic-genomic screen identifies AIM2 as a cytoplasmic DNA sensor for the inflammasome.* Nat Immunol, 2009. **10**(3): p. 266-72.

64. Muruve, D.A., et al., *The inflammasome recognizes cytosolic microbial and host DNA and triggers an innate immune response.* Nature, 2008. **452**(7183): p. 103-7.

65. Duewell, P., et al., *NLRP3 inflammasomes are required for atherogenesis and activated by cholesterol crystals.* Nature, 2010. **464**(7293): p. 1357-61.

66. Hornung, V. and E. Latz, *Critical functions of priming and lysosomal damage for NLRP3 activation.* Eur J Immunol, 2010. **40**(3): p. 620-3.

67. Dostert, C., et al., *Innate immune activation through Nalp3 inflammasome sensing of asbestos and silica.* Science, 2008. **320**(5876): p. 674-7.

68. Pelegrin, P. and A. Surprenant, *Pannexin-1 mediates large pore formation and interleukin-1beta release by the ATP-gated P2X7 receptor.* EMBO J, 2006. **25**(21): p. 5071-82.

69. Mariathasan, S., et al., *Cryopyrin activates the inflammasome in response to toxins and ATP.* Nature, 2006. **440**(7081): p. 228-32.

70. Zhou, R., et al., *A role for mitochondria in NLRP3 inflammasome activation.* Nature, 2011. **469**(7329): p. 221-5.

71. Tschopp, J. and K. Schroder, *NLRP3 inflammasome activation: The convergence of multiple signalling pathways on ROS production?* Nat Rev Immunol, 2010. **10**(3): p. 210-5.

72. Zhou, R., et al., *Thioredoxin-interacting protein links oxidative stress to inflammasome activation.* Nat Immunol, 2010. **11**(2): p. 136-40.

73. Nakahira, K., et al., *Autophagy proteins regulate innate immune responses by inhibiting the release of mitochondrial DNA mediated by the NALP3 inflammasome.* Nat Immunol, 2011. **12**(3): p. 222-30.

74. Shimada, K., et al., *Oxidized mitochondrial DNA activates the NLRP3 inflammasome during apoptosis.* Immunity, 2012. **36**(3): p. 401-14.

75. Hara, H., et al., *Phosphorylation of the adaptor ASC acts as a molecular switch that controls the formation of speck-like aggregates and inflammasome activity.* Nat Immunol, 2013. **14**(12): p. 1247-55.

76. Contassot, E., H.D. Beer, and L.E. French, *Interleukin-1, inflammasomes, autoinflammation and the skin.* Swiss Med Wkly, 2012. **142**: p. w13590.

77. Feldmeyer, L., et al., *The inflammasome mediates UVB-induced activation and secretion of interleukin-1beta by keratinocytes.* Curr Biol, 2007. **17**(13): p. 1140-5.

78. Watanabe, H., et al., *Activation of the IL-1beta-processing inflammasome is involved in contact hypersensitivity.* J Invest Dermatol, 2007. **127**(8): p. 1956-63.

79. Sollberger, G., et al., *Caspase-4 is required for activation of inflammasomes.* J Immunol, 2012. **188**(4): p. 1992-2000.

80. Kondo, S., et al., *Interleukin-1 receptor antagonist suppresses contact hypersensitivity.* J Invest Dermatol, 1995. **105**(3): p. 334-8.

81. Shornick, L.P., et al., *Mice deficient in IL-1beta manifest impaired contact hypersensitivity to trinitrochlorobenzone.* J Exp Med, 1996. **183**(4): p. 1427-36.

82. Meng, G., et al., *A mutation in the Nlrp3 gene causing inflammasome hyperactivation potentiates Th17 cell-dominant immune responses.* Immunity, 2009. **30**(6): p. 860-74.

83. Masters, S.L., et al., *Horror autoinflammaticus: the molecular pathophysiology of autoinflammatory disease (*).* Annu Rev Immunol, 2009. **27**: p. 621-68.

84. Park, H., et al., *Lighting the fires within: the cell biology of autoinflammatory diseases.* Nat Rev Immunol, 2012. **12**(8): p. 570-80.

85. Shoham, N.G., et al., *Pyrin binds the PSTPIP1/CD2BP1 protein, defining familial Mediterranean fever and PAPA syndrome as disorders in the same pathway.* Proc Natl Acad Sci U S A, 2003. **100**(23): p. 13501-6.

86. Hoffman, H.M., et al., *Mutation of a new gene encoding a putative pyrin-like protein causes familial cold autoinflammatory syndrome and Muckle-Wells syndrome.* Nat Genet, 2001. **29**(3): p. 301-5.

87. Bulua, A.C., et al., *Mitochondrial reactive oxygen species promote production of proinflammatory cytokines and are elevated in TNFR1-associated periodic syndrome (TRAPS).* J Exp Med, 2011. **208**(3): p. 519-33.

88. Michaud, M., et al., *Autophagy-dependent anticancer immune responses induced by chemotherapeutic agents in mice.* Science, 2011. **334**(6062): p. 1573-7.

89. Ma, Y., et al., *Contribution of IL-17-producing gamma delta T cells to the efficacy of anticancer chemotherapy.* J Exp Med, 2011. **208**(3): p. 491-503.

90. Sutton, C.E., et al., *Interleukin-1 and IL-23 induce innate IL-17 production from gammadelta T cells, amplifying Th17 responses and autoimmunity.* Immunity, 2009. **31**(2): p. 331-41.

91. Bjorkdahl, O., et al., *Gene transfer of a hybrid interleukin-1 beta gene to B16 mouse melanoma recruits leucocyte subsets and reduces tumour growth in vivo.* Cancer Immunol Immunother, 1997. **44**(5): p. 273-81.

92. Apte, R.N. and E. Voronov, *Interleukin-1--a major pleiotropic cytokine in tumor-host interactions.* Semin Cancer Biol, 2002. **12**(4): p. 277-90.

93. Demetri, G.D., et al., *Expression of ras oncogenes in cultured human cells alters the transcriptional and posttranscriptional regulation of cytokine genes.* J Clin Invest, 1990. **86**(4): p. 1261-9.

94. Lust, J.A., et al., *Induction of a chronic disease state in patients with smoldering or indolent multiple myeloma by targeting interleukin 1{beta}-induced interleukin 6 production and the myeloma proliferative component.* Mayo Clin Proc, 2009. **84**(2): p. 114-22.

95. Portier, M., et al., *Cytokine gene expression in human multiple myeloma.* Br J Haematol, 1993. **85**(3): p. 514-20.

96. Rambaldi, A., et al., *Modulation of cell proliferation and cytokine production in acute myeloblastic leukemia by interleukin-1 receptor antagonist and lack of its expression by leukemic cells.* Blood, 1991. **78**(12): p. 3248-53.

97. Stosic-Grujicic, S., N. Basara, and C.A. Dinarello, *Modulatory in vitro effects of interleukin-1 receptor antagonist (IL-1Ra) or antisense oligonucleotide to interleukin-1 beta converting enzyme (ICE) on acute myeloid leukaemia (AML) cell growth.* Clin Lab Haematol, 1999. **21**(3): p. 173-85.

98. Delwel, R., et al., *Interleukin-1 stimulates proliferation of acute myeloblastic leukemia cells by induction of granulocyte-macrophage colony-stimulating factor release.* Blood, 1989. **74**(2): p. 586-93.

99. Rodriguez-Cimadevilla, J.C., et al., *Coordinate secretion of interleukin-1 beta and granulocyte-macrophage colony-stimulating factor by the blast cells of acute myeloblastic leukemia: role of interleukin-1 as an endogenous inducer.* Blood, 1990. **76**(8): p. 1481-9.

100. Cozzolino, F., et al., *Interleukin 1 as an autocrine growth factor for acute myeloid leukemia cells.* Proc Natl Acad Sci U S A, 1989. **86**(7): p. 2369-73.

101. Tu, S., et al., *Overexpression of interleukin-1beta induces gastric inflammation and cancer and mobilizes myeloid-derived suppressor cells in mice.* Cancer Cell, 2008. **14**(5): p. 408-19.

102. Saijo, Y., et al., *Proinflammatory cytokine IL-1 beta promotes tumor growth of Lewis lung carcinoma by induction of angiogenic factors: in vivo analysis of tumor-stromal interaction.* J Immunol, 2002. **169**(1): p. 469-75.

103. Voronov, E., et al., *IL-1 is required for tumor invasiveness and angiogenesis.* Proc Natl Acad Sci U S A, 2003. **100**(5): p. 2645-50.

104. Vidal-Vanaclocha, F., et al., *Interleukin-1 receptor blockade reduces the number and size of murine B16 melanoma hepatic metastases.* Cancer Res, 1994. **54**(10): p. 2667-72.

105. Bani, M.R., et al., *Effect of interleukin-1-beta on metastasis formation in different tumor systems.* J Natl Cancer Inst, 1991. **83**(2): p. 119-23.

106. Giavazzi, R., et al., *Interleukin 1-induced augmentation of experimental metastases from a human melanoma in nude mice.* Cancer Res, 1990. **50**(15): p. 4771-5.

107. Ellis, L.Z., et al., *Green tea polyphenol epigallocatechin-3-gallate suppresses melanoma growth by inhibiting inflammasome and IL-1beta secretion.* Biochem Biophys Res Commun, 2011. **414**(3): p. 551-6.

108. Vidal-Vanaclocha, F., et al., *Interleukin 1 (IL-1)-dependent melanoma hepatic metastasis in vivo; increased endothelial adherence by IL-1-induced mannose receptors and growth factor production in vitro.* J Natl Cancer Inst, 1996. **88**(3-4): p. 198-205.

109. Pezzella, K.M., M.E. Neville, and J.J. Huang, *In vivo inhibition of tumor growth of B16 melanoma by recombinant interleukin 1 beta. I. Tumor inhibition parallels lymphocyte-activating factor activity of interleukin 1 beta proteins.* Cytokine, 1990. **2**(5): p. 357-62.

110. Meredith, P. and J. Riesz, *Radiative relaxation quantum yields for synthetic eumelanin.* Photochem Photobiol, 2004. **79**(2): p. 211-6.

111. Brenner, M. and V.J. Hearing, *The protective role of melanin against UV damage in human skin.* Photochem Photobiol, 2008. **84**(3): p. 539-49.

112. NCI. *NCI homepage*. 2014; Available from: http://www.cancer.gov/.

113. Gandini, S., et al., *Meta-analysis of risk factors for cutaneous melanoma: II. Sun exposure.* Eur J Cancer, 2005. **41**(1): p. 45-60.

114. Garbe, C., et al., *Risk factors for developing cutaneous melanoma and criteria for identifying persons at risk: multicenter case-control study of the Central Malignant Melanoma Registry of the German Dermatological Society.* J Invest Dermatol, 1994. **102**(5): p. 695-9.

115. Gandini, S., et al., *Meta-analysis of risk factors for cutaneous melanoma: III. Family history, actinic damage and phenotypic factors.* Eur J Cancer, 2005. **41**(14): p. 2040-59.

116. Gandini, S., et al., *Meta-analysis of risk factors for cutaneous melanoma: I. Common and atypical naevi.* Eur J Cancer, 2005. **41**(1): p. 28-44.

117. Hanahan, D. and R.A. Weinberg, *Hallmarks of cancer: the next generation.* Cell, 2011. **144**(5): p. 646-74.

118. Satyamoorthy, K. and M. Herlyn, *Cellular and molecular biology of human melanoma.* Cancer Biol Ther, 2002. **1**(1): p. 14-7.

119. Siegel, R., D. Naishadham, and A. Jemal, *Cancer statistics, 2013.* CA Cancer J Clin, 2013. **63**(1): p. 11-30.

120. Lui, P., et al., *Treatments for metastatic melanoma: synthesis of evidence from randomized trials.* Cancer Treat Rev, 2007. **33**(8): p. 665-80.

121. Bollag, G., et al., *Clinical efficacy of a RAF inhibitor needs broad target blockade in BRAF-mutant melanoma.* Nature, 2010. **467**(7315): p. 596-9.

122. Hodi, F.S., et al., *Improved survival with ipilimumab in patients with metastatic melanoma.* N Engl J Med, 2010. **363**(8): p. 711-23.

123. Joseph, E.W., et al., *The RAF inhibitor PLX4032 inhibits ERK signaling and tumor cell proliferation in a V600E BRAF-selective manner.* Proc Natl Acad Sci U S A, 2010. **107**(33): p. 14903-8.

124. Chapman, P.B., et al., *Improved survival with vemurafenib in melanoma with BRAF V600E mutation.* N Engl J Med, 2011. **364**(26): p. 2507-16.

125. Robert, C., et al., *Ipilimumab plus dacarbazine for previously untreated metastatic melanoma.* N Engl J Med, 2011. **364**(26): p. 2517-26.

126. Flaherty, K.T., et al., *Improved survival with MEK inhibition in BRAF-mutated melanoma.* N Engl J Med, 2012. **367**(2): p. 107-14.

127. Balch, C.M., *Cutaneous melanoma: prognosis and treatment results worldwide.* Semin Surg Oncol, 1992. **8**(6): p. 400-14.

128. Ho, R.C., *Medical management of stage IV malignant melanoma. Medical issues.* Cancer, 1995. **75**(2 Suppl): p. 735-41.

129. Clark, W.H., Jr., D.E. Elder, and M. Van Horn, *The biologic forms of malignant melanoma.* Hum Pathol, 1986. **17**(5): p. 443-50.

130. Weyers, W., et al., *Classification of cutaneous malignant melanoma: a reassessment of histopathologic criteria for the distinction of different types.* Cancer, 1999. **86**(2): p. 288-99.

131. KS, H. *Heterogeneity in Melanoma*. 2014; Available from: http://www.jurmo.ch/work_heterogeneity.php.

132. Balch, C.M., et al., *Final version of 2009 AJCC melanoma staging and classification.* J Clin Oncol, 2009. **27**(36): p. 6199-206.

133. Balch, C.M., et al., *Update on the melanoma staging system: the importance of sentinel node staging and primary tumor mitotic rate.* J Surg Oncol, 2011. **104**(4): p. 379-85.

134. Breslow, A., *Thickness, cross-sectional areas and depth of invasion in the prognosis of cutaneous melanoma.* Ann Surg, 1970. **172**(5): p. 902-8.

135. TOIOHAI. *The oncology institute of hope and innovation homepage: types of cancer*. 2014; Available from: http://www.theoncologyinstitute.com/types_of_cancer/melanoma.html.

136. MMMP. *Melanoma Molecular Map Project: TNM staging*. 2014; Available from: http://www.mmmp.org/MMMP/import.mmmp?page=tnm_staging.mmmp.

137. *IARC monographs on the evaluation of carcinogenic risks to humans. Solar and ultraviolet radiation.* IARC Monogr Eval Carcinog Risks Hum, 1992. **55**: p. 1-316.

138. Cogliano, V.J., et al., *Preventable exposures associated with human cancers.* J Natl Cancer Inst, 2011. **103**(24): p. 1827-39.

139. Elwood, J.M. and J. Jopson, *Melanoma and sun exposure: an overview of published studies.* Int J Cancer, 1997. **73**(2): p. 198-203.

140. Olsen, C.M., H.J. Carroll, and D.C. Whiteman, *Estimating the attributable fraction for melanoma: a meta-analysis of pigmentary characteristics and freckling.* Int J Cancer, 2010. **127**(10): p. 2430-45.

141. Olsen, C.M., H.J. Carroll, and D.C. Whiteman, *Estimating the attributable fraction for cancer: A meta-analysis of nevi and melanoma.* Cancer Prev Res (Phila), 2010. **3**(2): p. 233-45.

142. Olsen, C.M., H.J. Carroll, and D.C. Whiteman, *Familial melanoma: a meta-analysis and estimates of attributable fraction.* Cancer Epidemiol Biomarkers Prev, 2010. **19**(1): p. 65-73.

143. Fallah, M., et al., *Familial melanoma by histology and age: joint data from five Nordic countries.* Eur J Cancer, 2014. **50**(6): p. 1176-83.

144. Balamurugan, A., et al., *Subsequent primary cancers among men and women with in situ and invasive melanoma of the skin.* J Am Acad Dermatol, 2011. **65**(5 Suppl 1): p. S69-77.

145. Bradford, P.T., et al., *Increased risk of second primary cancers after a diagnosis of melanoma.* Arch Dermatol, 2010. **146**(3): p. 265-72.

146. van der Leest, R.J., et al., *Risk of second primary in situ and invasive melanoma in a Dutch population-based cohort: 1989-2008.* Br J Dermatol, 2012. **167**(6): p. 1321-30.

147. Jung, G.W., D.C. Dover, and T.G. Salopek, *Risk of second primary malignancies following a diagnosis of cutaneous malignant melanoma or nonmelanoma skin cancer in Alberta, Canada from 1979 to 2009.* Br J Dermatol, 2014. **170**(1): p. 136-43.

148. Yang, G.B., et al., *Risk and survival of cutaneous melanoma diagnosed subsequent to a previous cancer.* Arch Dermatol, 2011. **147**(12): p. 1395-402.

149. Goggins, W., W. Gao, and H. Tsao, *Association between female breast cancer and cutaneous melanoma.* Int J Cancer, 2004. **111**(5): p. 792-4.

150. Pirani, M., et al., *Risk for second malignancies in non-Hodgkin's lymphoma survivors: a meta-analysis.* Ann Oncol, 2011. **22**(8): p. 1845-58.

151. Morton, L.M., et al., *Second malignancy risks after non-Hodgkin's lymphoma and chronic lymphocytic leukemia: differences by lymphoma subtype.* J Clin Oncol, 2010. **28**(33): p. 4935-44.

152. Braisch, U., M. Meyer, and M. Radespiel-Troger, *Risk of subsequent primary cancer among prostate cancer patients in Bavaria, Germany.* Eur J Cancer Prev, 2012. **21**(6): p. 552-9.

153. Li, W.Q., et al., *Personal history of prostate cancer and increased risk of incident melanoma in the United States.* J Clin Oncol, 2013. **31**(35): p. 4394-9.

154. Liu, R., et al., *Meta-analysis of the relationship between Parkinson disease and melanoma.* Neurology, 2011. **76**(23): p. 2002-9.

155. Rugbjerg, K., et al., *Malignant melanoma, breast cancer and other cancers in patients with Parkinson's disease.* Int J Cancer, 2012. **131**(8): p. 1904-11.

156. Wirdefeldt, K., et al., *Parkinson's disease and cancer: A register-based family study.* Am J Epidemiol, 2014. **179**(1): p. 85-94.

157. Dahlke, E., et al., *Systematic review of melanoma incidence and prognosis in solid organ transplant recipients.* Transplant Res, 2014. **3**: p. 10.

158. Singh, S., et al., *Inflammatory bowel disease is associated with an increased risk of melanoma: a systematic review and meta-analysis.* Clin Gastroenterol Hepatol, 2014. **12**(2): p. 210-8.

159. Lee, M.S., et al., *The risk of developing non-melanoma skin cancer, lymphoma and melanoma in patients with psoriasis in Taiwan: a 10-year, population-based cohort study.* Int J Dermatol, 2012. **51**(12): p. 1454-60.

160. Olsen, C.M., L.L. Knight, and A.C. Green, *Risk of melanoma in people with HIV/AIDS in the pre- and post-HAART eras: a systematic review and meta-analysis of cohort studies.* PLoS One, 2014. **9**(4): p. e95096.

161. Hodis, E., et al., *A landscape of driver mutations in melanoma.* Cell, 2012. **150**(2): p. 251-63.

162. Gray-Schopfer, V., C. Wellbrock, and R. Marais, *Melanoma biology and new targeted therapy.* Nature, 2007. **445**(7130): p. 851-7.

163. McCubrey, J.A., et al., *Roles of the RAF/MEK/ERK and PI3K/PTEN/AKT pathways in malignant transformation and drug resistance.* Adv Enzyme Regul, 2006. **46**: p. 249-79.

164. Ball, N.J., et al., *Ras mutations in human melanoma: a marker of malignant progression.* J Invest Dermatol, 1994. **102**(3): p. 285-90.

165. Davies, H., et al., *Mutations of the BRAF gene in human cancer.* Nature, 2002. **417**(6892): p. 949-54.

166. Curtin, J.A., et al., *Distinct sets of genetic alterations in melanoma.* N Engl J Med, 2005. **353**(20): p. 2135-47.

167. Wellbrock, C. and A. Hurlstone, *BRAF as therapeutic target in melanoma.* Biochem Pharmacol, 2010. **80**(5): p. 561-7.

168. Cartlidge, R.A., et al., *Oncogenic BRAF(V600E) inhibits BIM expression to promote melanoma cell survival.* Pigment Cell Melanoma Res, 2008. **21**(5): p. 534-44.

169. Sumimoto, H., et al., *The BRAF-MAPK signaling pathway is essential for cancer-immune evasion in human melanoma cells.* J Exp Med, 2006. **203**(7): p. 1651-6.

170. Sharma, A., et al., *Mutant V599EB-Raf regulates growth and vascular development of malignant melanoma tumors.* Cancer Res, 2005. **65**(6): p. 2412-21.

171. Walker, G.J., et al., *Virtually 100% of melanoma cell lines harbor alterations at the DNA level within CDKN2A, CDKN2B, or one of their downstream targets.* Genes Chromosomes Cancer, 1998. **22**(2): p. 157-63.

172. Filmus, J., et al., *Induction of cyclin D1 overexpression by activated ras.* Oncogene, 1994. **9**(12): p. 3627-33.

173. Albanese, C., et al., *Transforming p21ras mutants and c-Ets-2 activate the cyclin D1 promoter through distinguishable regions.* J Biol Chem, 1995. **270**(40): p. 23589-97.

174. Shapiro, G.I., *Cyclin-dependent kinase pathways as targets for cancer treatment.* J Clin Oncol, 2006. **24**(11): p. 1770-83.

175. Hannan, K.M., et al., *Rb and p130 regulate RNA polymerase I transcription: Rb disrupts the interaction between UBF and SL-1.* Oncogene, 2000. **19**(43): p. 4988-99.

176. Sutcliffe, J.E., et al., *Retinoblastoma protein disrupts interactions required for RNA polymerase III transcription.* Mol Cell Biol, 2000. **20**(24): p. 9192-202.

177. Knudsen, E.S. and K.E. Knudsen, *Tailoring to RB: tumour suppressor status and therapeutic response.* Nat Rev Cancer, 2008. **8**(9): p. 714-24.

178. Roussel, M.F., *The INK4 family of cell cycle inhibitors in cancer.* Oncogene, 1999. **18**(38): p. 5311-7.

179. Freedman, D.A., L. Wu, and A.J. Levine, *Functions of the MDM2 oncoprotein.* Cell Mol Life Sci, 1999. **55**(1): p. 96-107.

180. Dahia, P.L., et al., *Somatic deletions and mutations in the Cowden disease gene, PTEN, in sporadic thyroid tumors.* Cancer Res, 1997. **57**(21): p. 4710-3.

181. Guldberg, P., et al., *Disruption of the MMAC1/PTEN gene by deletion or mutation is a frequent event in malignant melanoma.* Cancer Res, 1997. **57**(17): p. 3660-3.

182. Risinger, J.I., et al., *PTEN/MMAC1 mutations in endometrial cancers.* Cancer Res, 1997. **57**(21): p. 4736-8.

183. Yang, J., et al., *PTEN mutation spectrum in breast cancers and breast hyperplasia.* J Cancer Res Clin Oncol, 2010. **136**(9): p. 1303-11.

184. Birck, A., et al., *Mutation and allelic loss of the PTEN/MMAC1 gene in primary and metastatic melanoma biopsies.* J Invest Dermatol, 2000. **114**(2): p. 277-80.

185. Celebi, J.T., et al., *Identification of PTEN mutations in metastatic melanoma specimens.* J Med Genet, 2000. **37**(9): p. 653-7.

186. Furnari, F.B., H.J. Huang, and W.K. Cavenee, *The phosphoinositol phosphatase activity of PTEN mediates a serum-sensitive G1 growth arrest in glioma cells.* Cancer Res, 1998. **58**(22): p. 5002-8.

187. Georgescu, M.M., et al., *Stabilization and productive positioning roles of the C2 domain of PTEN tumor suppressor.* Cancer Res, 2000. **60**(24): p. 7033-8.

188. Hlobilkova, A., et al., *Cell cycle arrest by the PTEN tumor suppressor is target cell specific and may require protein phosphatase activity.* Exp Cell Res, 2000. **256**(2): p. 571-7.

189. Weng, L.P., J.L. Brown, and C. Eng, *PTEN coordinates G(1) arrest by down-regulating cyclin D1 via its protein phosphatase activity and up-regulating p27 via its lipid phosphatase activity in a breast cancer model.* Hum Mol Genet, 2001. **10**(6): p. 599-604.

190. Dey, N., et al., *The protein phosphatase activity of PTEN regulates SRC family kinases and controls glioma migration.* Cancer Res, 2008. **68**(6): p. 1862-71.

191. Davidson, L., et al., *Suppression of cellular proliferation and invasion by the concerted lipid and protein phosphatase activities of PTEN.* Oncogene, 2010. **29**(5): p. 687-97.

192. Poon, J.S., R. Eves, and A.S. Mak, *Both lipid- and protein-phosphatase activities of PTEN contribute to the p53-PTEN anti-invasion pathway.* Cell Cycle, 2010. **9**(22): p. 4450-4.

193. Maehama, T. and J.E. Dixon, *The tumor suppressor, PTEN/MMAC1, dephosphorylates the lipid second messenger, phosphatidylinositol 3,4,5-trisphosphate.* J Biol Chem, 1998. **273**(22): p. 13375-8.

194. Manning, B.D. and L.C. Cantley, *AKT/PKB signaling: navigating downstream.* Cell, 2007. **129**(7): p. 1261-74.

195. Thompson, J.F., R.A. Scolyer, and R.F. Kefford, *Cutaneous melanoma.* Lancet, 2005. **365**(9460): p. 687-701.

196. Kirkwood, J.M., et al., *Phase II, open-label, randomized trial of the MEK1/2 inhibitor selumetinib as monotherapy versus temozolomide in patients with advanced melanoma.* Clin Cancer Res, 2012. **18**(2): p. 555-67.

197. Ascierto, P.A., et al., *MEK162 for patients with advanced melanoma harbouring NRAS or Val600 BRAF mutations: a non-randomised, open-label phase 2 study.* Lancet Oncol, 2013. **14**(3): p. 249-56.

198. Robert, C., et al., *Selumetinib plus dacarbazine versus placebo plus dacarbazine as first-line treatment for BRAF-mutant metastatic melanoma: a phase 2 double-blind randomised study.* Lancet Oncol, 2013. **14**(8): p. 733-40.

199. Dummer, R. and K.T. Flaherty, *Resistance patterns with tyrosine kinase inhibitors in melanoma: new insights.* Curr Opin Oncol, 2012. **24**(2): p. 150-4.

200. Long, G.V., et al., *Combined BRAF and MEK Inhibition versus BRAF Inhibition Alone in Melanoma.* N Engl J Med, 2014.

201. Larkin, J., et al., *Combined Vemurafenib and Cobimetinib in BRAF-Mutated Melanoma.* N Engl J Med, 2014.

202. Jemal, A., et al., *Cancer statistics, 2010.* CA Cancer J Clin, 2010. **60**(5): p. 277-300.

203. Balkwill, F., K.A. Charles, and A. Mantovani, *Smoldering and polarized inflammation in the initiation and promotion of malignant disease.* Cancer Cell, 2005. **7**(3): p. 211-7.

204. Karin, M., *Nuclear factor-kappaB in cancer development and progression.* Nature, 2006. **441**(7092): p. 431-6.

205. Wu, Y., et al., *Stabilization of snail by NF-kappaB is required for inflammation-induced cell migration and invasion.* Cancer Cell, 2009. **15**(5): p. 416-28.

206. Waldner, M.J. and M.F. Neurath, *Colitis-associated cancer: the role of T cells in tumor development.* Semin Immunopathol, 2009. **31**(2): p. 249-56.

207. Punturieri, A., et al., *Lung cancer and chronic obstructive pulmonary disease: needs and opportunities for integrated research.* J Natl Cancer Inst, 2009. **101**(8): p. 554-9.

208. Calle, E.E., *Obesity and cancer.* BMJ, 2007. **335**(7630): p. 1107-8.

209. Tuncman, G., et al., *Functional in vivo interactions between JNK1 and JNK2 isoforms in obesity and insulin resistance.* Proc Natl Acad Sci U S A, 2006. **103**(28): p. 10741-6.

210. Park, E.J., et al., *Dietary and genetic obesity promote liver inflammation and tumorigenesis by enhancing IL-6 and TNF expression.* Cell, 2010. **140**(2): p. 197-208.

211. Rodier, F., et al., *Persistent DNA damage signalling triggers senescence-associated inflammatory cytokine secretion.* Nat Cell Biol, 2009. **11**(8): p. 973-9.

212. Zheng, L., et al., *Fen1 mutations result in autoimmunity, chronic inflammation and cancers.* Nat Med, 2007. **13**(7): p. 812-9.

213. Grivennikov, S.I., F.R. Greten, and M. Karin, *Immunity, inflammation, and cancer.* Cell, 2010. **140**(6): p. 883-99.

214. Mantovani, A., et al., *Cancer-related inflammation.* Nature, 2008. **454**(7203): p. 436-44.

215. Soucek, L., et al., *Mast cells are required for angiogenesis and macroscopic expansion of Myc-induced pancreatic islet tumors.* Nat Med, 2007. **13**(10): p. 1211-8.

216. Sparmann, A. and D. Bar-Sagi, *Ras-induced interleukin-8 expression plays a critical role in tumor growth and angiogenesis.* Cancer Cell, 2004. **6**(5): p. 447-58.

217. Vakkila, J. and M.T. Lotze, *Inflammation and necrosis promote tumour growth.* Nat Rev Immunol, 2004. **4**(8): p. 641-8.

218. Murray, P.J. and T.A. Wynn, *Protective and pathogenic functions of macrophage subsets.* Nat Rev Immunol, 2011. **11**(11): p. 723-37.

219. Mantovani, A. and A. Sica, *Macrophages, innate immunity and cancer: balance, tolerance, and diversity.* Curr Opin Immunol, 2010. **22**(2): p. 231-7.

220. Biswas, S.K. and A. Mantovani, *Macrophage plasticity and interaction with lymphocyte subsets: cancer as a paradigm.* Nat Immunol, 2010. **11**(10): p. 889-96.

221. Gordon, S., *Alternative activation of macrophages.* Nat Rev Immunol, 2003. **3**(1): p. 23-35.

222. Mackaness, G.B., *Cellular resistance to infection.* J Exp Med, 1962. **116**: p. 381-406.

223. Martinez, F.O., L. Helming, and S. Gordon, *Alternative activation of macrophages: an immunologic functional perspective.* Annu Rev Immunol, 2009. **27**: p. 451-83.

224. Mills, C.D., *M1 and M2 Macrophages: Oracles of Health and Disease.* Crit Rev Immunol, 2012. **32**(6): p. 463-88.

225. Parameswaran, N. and S. Patial, *Tumor necrosis factor-alpha signaling in macrophages.* Crit Rev Eukaryot Gene Expr, 2010. **20**(2): p. 87-103.

226. Flesch, I.E., et al., *Early interleukin 12 production by macrophages in response to mycobacterial infection depends on interferon gamma and tumor necrosis factor alpha.* J Exp Med, 1995. **181**(5): p. 1615-21.

227. Mills, C.D., et al., *M-1/M-2 macrophages and the Th1/Th2 paradigm.* J Immunol, 2000. **164**(12): p. 6166-73.

228. Mosmann, T.R., et al., *Two types of murine helper T cell clone. I. Definition according to profiles of lymphokine activities and secreted proteins.* J Immunol, 1986. **136**(7): p. 2348-57.

229. Greten, F.R., et al., *IKKbeta links inflammation and tumorigenesis in a mouse model of colitis-associated cancer.* Cell, 2004. **118**(3): p. 285-96.

230. Karin, M. and F.R. Greten, *NF-kappaB: linking inflammation and immunity to cancer development and progression.* Nat Rev Immunol, 2005. **5**(10): p. 749-59.

231. Lin, E.Y., et al., *Macrophages regulate the angiogenic switch in a mouse model of breast cancer.* Cancer Res, 2006. **66**(23): p. 11238-46.

232. Qian, B., et al., *A distinct macrophage population mediates metastatic breast cancer cell extravasation, establishment and growth.* PLoS One, 2009. **4**(8): p. e6562.

233. Ruffell, B., N.I. Affara, and L.M. Coussens, *Differential macrophage programming in the tumor microenvironment.* Trends Immunol, 2012. **33**(3): p. 119-26.

234. Karp, C.L. and P.J. Murray, *Non-canonical alternatives: what a macrophage is 4.* J Exp Med, 2012. **209**(3): p. 427-31.

235. Gordon, S. and F.O. Martinez, *Alternative activation of macrophages: mechanism and functions.* Immunity, 2010. **32**(5): p. 593-604.

236. Mantovani, A., et al., *Role of tumor-associated macrophages in tumor progression and invasion.* Cancer Metastasis Rev, 2006. **25**(3): p. 315-22.

237. Martinez, F.O., et al., *Macrophage activation and polarization.* Front Biosci, 2008. **13**: p. 453-61.

238. Peranzoni, E., et al., *Myeloid-derived suppressor cell heterogeneity and subset definition.* Curr Opin Immunol, 2010. **22**(2): p. 238-44.

239. Filipazzi, P., et al., *Identification of a new subset of myeloid suppressor cells in peripheral blood of melanoma patients with modulation by a granulocyte-macrophage colony-stimulation factor-based antitumor vaccine.* J Clin Oncol, 2007. **25**(18): p. 2546-53.

240. Bronte, V., et al., *Identification of a CD11b(+)/Gr-1(+)/CD31(+) myeloid progenitor capable of activating or suppressing CD8(+) T cells.* Blood, 2000. **96**(12): p. 3838-46.

241. Mandruzzato, S., et al., *IL4Ralpha+ myeloid-derived suppressor cell expansion in cancer patients.* J Immunol, 2009. **182**(10): p. 6562-8.

242. Corzo, C.A., et al., *HIF-1alpha regulates function and differentiation of myeloid-derived suppressor cells in the tumor microenvironment.* J Exp Med, 2010. **207**(11): p. 2439-53.

243. Corzo, C.A., et al., *Mechanism regulating reactive oxygen species in tumor-induced myeloid-derived suppressor cells.* J Immunol, 2009. **182**(9): p. 5693-701.

244. Diaz-Montero, C.M., et al., *Increased circulating myeloid-derived suppressor cells correlate with clinical cancer stage, metastatic tumor burden, and doxorubicin-cyclophosphamide chemotherapy.* Cancer Immunol Immunother, 2009. **58**(1): p. 49-59.

245. Ostrand-Rosenberg, S. and P. Sinha, *Myeloid-derived suppressor cells: linking inflammation and cancer.* J Immunol, 2009. **182**(8): p. 4499-506.

246. Fichtner-Feigl, S., et al., *Restoration of tumor immunosurveillance via targeting of interleukin-13 receptor-alpha 2.* Cancer Res, 2008. **68**(9): p. 3467-75.

247. Terabe, M., et al., *Transforming growth factor-beta production and myeloid cells are an effector mechanism through which CD1d-restricted T cells block cytotoxic T lymphocyte-mediated tumor immunosurveillance: abrogation prevents tumor recurrence.* J Exp Med, 2003. **198**(11): p. 1741-52.

248. Gabrilovich, D.I. and S. Nagaraj, *Myeloid-derived suppressor cells as regulators of the immune system.* Nat Rev Immunol, 2009. **9**(3): p. 162-74.

249. Ochoa, A.C., et al., *Arginase, prostaglandins, and myeloid-derived suppressor cells in renal cell carcinoma.* Clin Cancer Res, 2007. **13**(2 Pt 2): p. 721s-726s.

250. Rodriguez, P.C., et al., *Arginase I-producing myeloid-derived suppressor cells in renal cell carcinoma are a subpopulation of activated granulocytes.* Cancer Res, 2009. **69**(4): p. 1553-60.

251. Taketo, M.M., *Cyclooxygenase-2 inhibitors in tumorigenesis (part I).* J Natl Cancer Inst, 1998. **90**(20): p. 1529-36.

252. Nagaraj, S., et al., *Altered recognition of antigen is a mechanism of CD8+ T cell tolerance in cancer.* Nat Med, 2007. **13**(7): p. 828-35.

253. Sauer, H., M. Wartenberg, and J. Hescheler, *Reactive oxygen species as intracellular messengers during cell growth and differentiation.* Cell Physiol Biochem, 2001. **11**(4): p. 173-86.

254. Lewis, J.S., et al., *Expression of vascular endothelial growth factor by macrophages is up-regulated in poorly vascularized areas of breast carcinomas.* J Pathol, 2000. **192**(2): p. 150-8.

255. Sunderkotter, C., et al., *Macrophages and angiogenesis.* J Leukoc Biol, 1994. **55**(3): p. 410-22.

256. Giraudo, E., M. Inoue, and D. Hanahan, *An amino-bisphosphonate targets MMP-9-expressing macrophages and angiogenesis to impair cervical carcinogenesis.* J Clin Invest, 2004. **114**(5): p. 623-33.

257. Hildenbrand, R., et al., *Urokinase and macrophages in tumour angiogenesis.* Br J Cancer, 1995. **72**(4): p. 818-23.

258. Esposito, I., et al., *Inflammatory cells contribute to the generation of an angiogenic phenotype in pancreatic ductal adenocarcinoma.* J Clin Pathol, 2004. **57**(6): p. 630-6.

259. Huang, S., et al., *Contributions of stromal metalloproteinase-9 to angiogenesis and growth of human ovarian carcinoma in mice.* J Natl Cancer Inst, 2002. **94**(15): p. 1134-42.

260. Munder, M., *Arginase: an emerging key player in the mammalian immune system.* Br J Pharmacol, 2009. **158**(3): p. 638-51.

261. Eck, M., et al., *Pleiotropic effects of CXC chemokines in gastric carcinoma: differences in CXCL8 and CXCL1 expression between diffuse and intestinal types of gastric carcinoma.* Clin Exp Immunol, 2003. **134**(3): p. 508-15.

262. Bellocq, A., et al., *Neutrophil alveolitis in bronchioloalveolar carcinoma: induction by tumor-derived interleukin-8 and relation to clinical outcome.* Am J Pathol, 1998. **152**(1): p. 83-92.

263. Bergers, G., et al., *Matrix metalloproteinase-9 triggers the angiogenic switch during carcinogenesis.* Nat Cell Biol, 2000. **2**(10): p. 737-44.

264. McCourt, M., et al., *Proinflammatory mediators stimulate neutrophil-directed angiogenesis.* Arch Surg, 1999. **134**(12): p. 1325-31; discussion 1331-2.

265. Asahara, T., et al., *Isolation of putative progenitor endothelial cells for angiogenesis.* Science, 1997. **275**(5302): p. 964-7.

266. Fridlender, Z.G., et al., *Polarization of tumor-associated neutrophil phenotype by TGF-beta: "N1" versus "N2" TAN.* Cancer Cell, 2009. **16**(3): p. 183-94.

267. Dorta, R.G., et al., *Tumour-associated tissue eosinophilia as a prognostic factor in oral squamous cell carcinomas.* Histopathology, 2002. **41**(2): p. 152-7.

268. Looi, L.M., *Tumor-associated tissue eosinophilia in nasopharyngeal carcinoma. A pathologic study of 422 primary and 138 metastatic tumors.* Cancer, 1987. **59**(3): p. 466-70.

269. Teruya-Feldstein, J., et al., *Differential chemokine expression in tissues involved by Hodgkin's disease: direct correlation of eotaxin expression and tissue eosinophilia.* Blood, 1999. **93**(8): p. 2463-70.

270. Nielsen, H.J., et al., *Independent prognostic value of eosinophil and mast cell infiltration in colorectal cancer tissue.* J Pathol, 1999. **189**(4): p. 487-95.

271. Lorena, S.C., et al., *Eotaxin expression in oral squamous cell carcinomas with and without tumour associated tissue eosinophilia.* Oral Dis, 2003. **9**(6): p. 279-83.

272. Mattes, J., et al., *Immunotherapy of cytotoxic T cell-resistant tumors by T helper 2 cells: an eotaxin and STAT6-dependent process.* J Exp Med, 2003. **197**(3): p. 387-93.

273. Horiuchi, T. and P.F. Weller, *Expression of vascular endothelial growth factor by human eosinophils: upregulation by granulocyte macrophage colony-stimulating factor and interleukin-5.* Am J Respir Cell Mol Biol, 1997. **17**(1): p. 70-7.

274. Cormier, S.A., et al., *Pivotal Advance: eosinophil infiltration of solid tumors is an early and persistent inflammatory host response.* J Leukoc Biol, 2006. **79**(6): p. 1131-9.

275. Crivellato, E., B. Nico, and D. Ribatti, *Mast cells and tumour angiogenesis: new insight from experimental carcinogenesis.* Cancer Lett, 2008. **269**(1): p. 1-6.

276. Fricke, I. and D.I. Gabrilovich, *Dendritic cells and tumor microenvironment: a dangerous liaison.* Immunol Invest, 2006. **35**(3-4): p. 459-83.

277. Conejo-Garcia, J.R., et al., *Tumor-infiltrating dendritic cell precursors recruited by a beta-defensin contribute to vasculogenesis under the influence of Vegf-A.* Nat Med, 2004. **10**(9): p. 950-8.

278. Coukos, G., et al., *Vascular leukocytes: a population with angiogenic and immunossuppressive properties highly represented in ovarian cancer.* Adv Exp Med Biol, 2007. **590**: p. 185-93.

279. Shojaei, F., et al., *Tumor refractoriness to anti-VEGF treatment is mediated by CD11b+Gr1+ myeloid cells.* Nat Biotechnol, 2007. **25**(8): p. 911-20.

280. Camisaschi, C., et al., *LAG-3 expression defines a subset of CD4(+)CD25(high)Foxp3(+) regulatory T cells that are expanded at tumor sites.* J Immunol, 2010. **184**(11): p. 6545-51.

281. Baumgartner, J., et al., *Melanoma induces immunosuppression by up-regulating FOXP3(+) regulatory T cells.* J Surg Res, 2007. **141**(1): p. 72-7.

282. Vence, L., et al., *Circulating tumor antigen-specific regulatory T cells in patients with metastatic melanoma.* Proc Natl Acad Sci U S A, 2007. **104**(52): p. 20884-9.

283. Cabrera, C.M., *The double role of the endoplasmic reticulum chaperone tapasin in peptide optimization of HLA class I molecules.* Scand J Immunol, 2007. **65**(6): p. 487-93.

284. Harlin, H., et al., *Tumor progression despite massive influx of activated CD8(+) T cells in a patient with malignant melanoma ascites.* Cancer Immunol Immunother, 2006. **55**(10): p. 1185-97.

285. Goldstein, O.G., et al., *Gamma-IFN-inducible-lysosomal thiol reductase modulates acidic proteases and HLA class II antigen processing in melanoma.* Cancer Immunol Immunother, 2008. **57**(10): p. 1461-70.

286. Chambers, C.A., *The expanding world of co-stimulation: the two-signal model revisited.* Trends Immunol, 2001. **22**(4): p. 217-23.

287. Weber, J., *Overcoming immunologic tolerance to melanoma: targeting CTLA-4 with ipilimumab (MDX-010).* Oncologist, 2008. **13 Suppl 4**: p. 16-25.

288. Krummel, M.F. and J.P. Allison, *CD28 and CTLA-4 have opposing effects on the response of T cells to stimulation.* J Exp Med, 1995. **182**(2): p. 459-65.

289. Walunas, T.L., C.Y. Bakker, and J.A. Bluestone, *CTLA-4 ligation blocks CD28-dependent T cell activation.* J Exp Med, 1996. **183**(6): p. 2541-50.

290. Walunas, T.L., et al., *CTLA-4 can function as a negative regulator of T cell activation.* Immunity, 1994. **1**(5): p. 405-13.

291. Ahmadzadeh, M., et al., *Tumor antigen-specific CD8 T cells infiltrating the tumor express high levels of PD-1 and are functionally impaired.* Blood, 2009. **114**(8): p. 1537-44.

292. Fourcade, J., et al., *Upregulation of Tim-3 and PD-1 expression is associated with tumor antigen-specific CD8+ T cell dysfunction in melanoma patients.* J Exp Med, 2010. **207**(10): p. 2175-86.

293. Pilon-Thomas, S., et al., *Blockade of programmed death ligand 1 enhances the therapeutic efficacy of combination immunotherapy against melanoma.* J Immunol, 2010. **184**(7): p. 3442-9.

294. Spranger, S., et al., *Up-regulation of PD-L1, IDO, and T(regs) in the melanoma tumor microenvironment is driven by CD8(+) T cells.* Sci Transl Med, 2013. **5**(200): p. 200ra116.

295. Wolchok, J.D., et al., *Ipilimumab monotherapy in patients with pretreated advanced melanoma: a randomised, double-blind, multicentre, phase 2, dose-ranging study.* Lancet Oncol, 2010. **11**(2): p. 155-64.

296. Robert, C., J.C. Soria, and A.M. Eggermont, *Drug of the year: programmed death-1 receptor/programmed death-1 ligand-1 receptor monoclonal antibodies.* Eur J Cancer, 2013. **49**(14): p. 2968-71.

297. Hamid, O., et al., *Safety and tumor responses with lambrolizumab (anti-PD-1) in melanoma.* N Engl J Med, 2013. **369**(2): p. 134-44.

298. Vaupel, P. and A. Mayer, *Hypoxia in cancer: significance and impact on clinical outcome.* Cancer Metastasis Rev, 2007. **26**(2): p. 225-39.

299. Chaplin, D.J., R.E. Durand, and P.L. Olive, *Acute hypoxia in tumors: implications for modifiers of radiation effects.* Int J Radiat Oncol Biol Phys, 1986. **12**(8): p. 1279-82.

300. Lartigau, E., et al., *Intratumoral oxygen tension in metastatic melanoma.* Melanoma Res, 1997. **7**(5): p. 400-6.

301. Graeber, T.G., et al., *Hypoxia-mediated selection of cells with diminished apoptotic potential in solid tumours.* Nature, 1996. **379**(6560): p. 88-91.

302. Hammond, E.M., M.R. Kaufmann, and A.J. Giaccia, *Oxygen sensing and the DNA-damage response.* Curr Opin Cell Biol, 2007. **19**(6): p. 680-4.

303. Shimizu, S., et al., *Induction of apoptosis as well as necrosis by hypoxia and predominant prevention of apoptosis by Bcl-2 and Bcl-XL.* Cancer Res, 1996. **56**(9): p. 2161-6.

304. Zhang, S., et al., *Hypoxia influences linearly patterned programmed cell necrosis and tumor blood supply patterns formation in melanoma.* Lab Invest, 2009. **89**(5): p. 575-86.

305. Kunz, M. and S.M. Ibrahim, *Molecular responses to hypoxia in tumor cells.* Mol Cancer, 2003. **2**: p. 23.

306. Kepp, O., et al., *Immunogenic cell death modalities and their impact on cancer treatment.* Apoptosis, 2009. **14**(4): p. 364-75.

307. Green, D.R., et al., *Immunogenic and tolerogenic cell death.* Nat Rev Immunol, 2009. **9**(5): p. 353-63.

308. Bar-Eli, M., *Role of interleukin-8 in tumor growth and metastasis of human melanoma.* Pathobiology, 1999. **67**(1): p. 12-8.

309. Hirota, K. and G.L. Semenza, *Regulation of angiogenesis by hypoxia-inducible factor 1.* Crit Rev Oncol Hematol, 2006. **59**(1): p. 15-26.

310. Karashima, T., et al., *Nuclear factor-kappaB mediates angiogenesis and metastasis of human bladder cancer through the regulation of interleukin-8.* Clin Cancer Res, 2003. **9**(7): p. 2786-97.

311. Yang, M.H. and K.J. Wu, *TWIST activation by hypoxia inducible factor-1 (HIF-1): implications in metastasis and development.* Cell Cycle, 2008. **7**(14): p. 2090-6.

312. Krishnamachary, B., et al., *Regulation of colon carcinoma cell invasion by hypoxia-inducible factor 1.* Cancer Res, 2003. **63**(5): p. 1138-43.

313. Erler, J.T., et al., *Hypoxia-induced lysyl oxidase is a critical mediator of bone marrow cell recruitment to form the premetastatic niche.* Cancer Cell, 2009. **15**(1): p. 35-44.

314. Cheli, Y., et al., *Hypoxia and MITF control metastatic behaviour in mouse and human melanoma cells.* Oncogene, 2012. **31**(19): p. 2461-70.

315. Feige, E., et al., *Hypoxia-induced transcriptional repression of the melanoma-associated oncogene MITF.* Proc Natl Acad Sci U S A, 2011. **108**(43): p. E924-33.

316. Rice, G.C., V. Ling, and R.T. Schimke, *Frequencies of independent and simultaneous selection of Chinese hamster cells for methotrexate and doxorubicin (adriamycin) resistance.* Proc Natl Acad Sci U S A, 1987. **84**(24): p. 9261-4.

317. Luk, C.K., et al., *Effect of transient hypoxia on sensitivity to doxorubicin in human and murine cell lines.* J Natl Cancer Inst, 1990. **82**(8): p. 684-92.

318. Hockel, M., et al., *Association between tumor hypoxia and malignant progression in advanced cancer of the uterine cervix.* Cancer Res, 1996. **56**(19): p. 4509-15.

319. Vergis, R., et al., *Intrinsic markers of tumour hypoxia and angiogenesis in localised prostate cancer and outcome of radical treatment: a retrospective analysis of two randomised radiotherapy trials and one surgical cohort study.* Lancet Oncol, 2008. **9**(4): p. 342-51.

320. Fidler, I.J., *Tumor heterogeneity and the biology of cancer invasion and metastasis.* Cancer Res, 1978. **38**(9): p. 2651-60.

321. Hoek, K.S., et al., *Metastatic potential of melanomas defined by specific gene expression profiles with no BRAF signature.* Pigment Cell Res, 2006. **19**(4): p. 290-302.

322. Hoek, K.S., et al., *In vivo switching of human melanoma cells between proliferative and invasive states.* Cancer Res, 2008. **68**(3): p. 650-6.

323. Widmer, D.S., et al., *Systematic classification of melanoma cells by phenotype-specific gene expression mapping.* Pigment Cell Melanoma Res, 2012. **25**(3): p. 343-53.

324. Eichhoff, O.M., et al., *The immunohistochemistry of invasive and proliferative phenotype switching in melanoma: a case report.* Melanoma Res, 2010. **20**(4): p. 349-55.

325. Eichhoff, O.M., et al., *Differential LEF1 and TCF4 expression is involved in melanoma cell phenotype switching.* Pigment Cell Melanoma Res, 2011. **24**(4): p. 631-42.

326. Widmer, D.S., et al., *Hypoxia contributes to melanoma heterogeneity by triggering HIF1alpha-dependent phenotype switching.* J Invest Dermatol, 2013. **133**(10): p. 2436-43.

327. Lockshin, R.A. and C.M. William, *Programmed Cell Death. 3. Neural Control of the Breakdown of the Intersegmental Muscles of Silkmoths.* J Insect Physiol, 1965. **11**: p. 601-10.

328. Lockshin, R.A. and C.M. Williams, *Programmed cell death. V. Cytolytic enzymes in relation to the breakdown of the intersegmental muscles of silkmoths.* J Insect Physiol, 1965. **11**(7): p. 831-44.

329. Lockshin, R.A. and C.M. Williams, *Programmed cell death. IV. The influence of drugs on the breakdown of the intersegmental muscles of silkmoths.* J Insect Physiol, 1965. **11**(6): p. 803-9.

330. Lockshin, R.A. and C.M. Williams, *Programmed Cell Death--I. Cytology of Degeneration in the Intersegmental Muscles of the Pernyi Silkmoth.* J Insect Physiol, 1965. **11**: p. 123-33.

331. Hagmann, J., M.M. Burger, and D. Dagan, *Regulation of plasma membrane blebbing by the cytoskeleton.* J Cell Biochem, 1999. **73**(4): p. 488-99.

332. Hotchkiss, R.S., et al., *Cell death.* N Engl J Med, 2009. **361**(16): p. 1570-83.

333. Penaloza, C., et al., *Cell death in development: shaping the embryo.* Histochem Cell Biol, 2006. **126**(2): p. 149-58.

334. Elmore, S., *Apoptosis: a review of programmed cell death.* Toxicol Pathol, 2007. **35**(4): p. 495-516.

335. Lauber, K., et al., *Clearance of apoptotic cells: getting rid of the corpses.* Mol Cell, 2004. **14**(3): p. 277-87.

336. Strasser, A., L. O'Connor, and V.M. Dixit, *Apoptosis signaling.* Annu Rev Biochem, 2000. **69**: p. 217-45.

337. Kischkel, F.C., et al., *Cytotoxicity-dependent APO-1 (Fas/CD95)-associated proteins form a death-inducing signaling complex (DISC) with the receptor.* EMBO J, 1995. **14**(22): p. 5579-88.

338. Wang, L., F. Du, and X. Wang, *TNF-alpha induces two distinct caspase-8 activation pathways.* Cell, 2008. **133**(4): p. 693-703.

339. Sprick, M.R., et al., *Caspase-10 is recruited to and activated at the native TRAIL and CD95 death-inducing signalling complexes in a FADD-dependent manner but can not functionally substitute caspase-8.* EMBO J, 2002. **21**(17): p. 4520-30.

340. Mikhailov, V., et al., *Association of Bax and Bak homo-oligomers in mitochondria. Bax requirement for Bak reorganization and cytochrome c release.* J Biol Chem, 2003. **278**(7): p. 5367-76.

341. Chipuk, J.E., L. Bouchier-Hayes, and D.R. Green, *Mitochondrial outer membrane permeabilization during apoptosis: the innocent bystander scenario.* Cell Death Differ, 2006. **13**(8): p. 1396-402.

342. Liu, X., et al., *Induction of apoptotic program in cell-free extracts: requirement for dATP and cytochrome c.* Cell, 1996. **86**(1): p. 147-57.

343. Zou, H., et al., *An APAF-1.cytochrome c multimeric complex is a functional apoptosome that activates procaspase-9.* J Biol Chem, 1999. **274**(17): p. 11549-56.

344. Kamada, S., et al., *Nuclear translocation of caspase-3 is dependent on its proteolytic activation and recognition of a substrate-like protein(s).* J Biol Chem, 2005. **280**(2): p. 857-60.

345. Enari, M., et al., *A caspase-activated DNase that degrades DNA during apoptosis, and its inhibitor ICAD.* Nature, 1998. **391**(6662): p. 43-50.

346. Sakahira, H., M. Enari, and S. Nagata, *Cleavage of CAD inhibitor in CAD activation and DNA degradation during apoptosis.* Nature, 1998. **391**(6662): p. 96-9.

347. West, J.D., C. Ji, and L.J. Marnett, *Modulation of DNA fragmentation factor 40 nuclease activity by poly(ADP-ribose) polymerase-1.* J Biol Chem, 2005. **280**(15): p. 15141-7.

348. Klionsky, D.J., *Autophagy: from phenomenology to molecular understanding in less than a decade.* Nat Rev Mol Cell Biol, 2007. **8**(11): p. 931-7.

349. Levine, B., N. Mizushima, and H.W. Virgin, *Autophagy in immunity and inflammation.* Nature, 2011. **469**(7330): p. 323-35.

350. Duprez, L., et al., *Major cell death pathways at a glance.* Microbes Infect, 2009. **11**(13): p. 1050-62.

351. Honarpour, N., et al., *Adult Apaf-1-deficient mice exhibit male infertility.* Dev Biol, 2000. **218**(2): p. 248-58.

352. Zheng, T.S., et al., *Caspase knockouts: matters of life and death.* Cell Death Differ, 1999. **6**(11): p. 1043-53.

353. Le, D.A., et al., *Caspase activation and neuroprotection in caspase-3- deficient mice after in vivo cerebral ischemia and in vitro oxygen glucose deprivation.* Proc Natl Acad Sci U S A, 2002. **99**(23): p. 15188-93.

354. Chautan, M., et al., *Interdigital cell death can occur through a necrotic and caspase-independent pathway.* Curr Biol, 1999. **9**(17): p. 967-70.

355. Lindsten, T. and C.B. Thompson, *Cell death in the absence of Bax and Bak.* Cell Death Differ, 2006. **13**(8): p. 1272-6.

356. Yuan, J. and G. Kroemer, *Alternative cell death mechanisms in development and beyond.* Genes Dev, 2010. **24**(23): p. 2592-602.

357. Vercammen, D., et al., *Dual signaling of the Fas receptor: initiation of both apoptotic and necrotic cell death pathways.* J Exp Med, 1998. **188**(5): p. 919-30.

358. Kawahara, A., et al., *Caspase-independent cell killing by Fas-associated protein with death domain.* Journal of Cell Biology, 1998. **143**(5): p. 1353-1360.

359. Degterev, A., et al., *Chemical inhibitor of nonapoptotic cell death with therapeutic potential for ischemic brain injury.* Nat Chem Biol, 2005. **1**(2): p. 112-9.

360. Christofferson, D.E. and J. Yuan, *Necroptosis as an alternative form of programmed cell death.* Curr Opin Cell Biol, 2010. **22**(2): p. 263-8.

361. Galluzzi, L. and G. Kroemer, *Necroptosis: a specialized pathway of programmed necrosis.* Cell, 2008. **135**(7): p. 1161-3.

362. Zong, W.X. and C.B. Thompson, *Necrotic death as a cell fate.* Genes Dev, 2006. **20**(1): p. 1-15.

363. Ma, Y., et al., *NF-kappaB protects macrophages from lipopolysaccharide-induced cell death: the role of caspase 8 and receptor-interacting protein.* J Biol Chem, 2005. **280**(51): p. 41827-34.

364. Festjens, N., T. Vanden Berghe, and P. Vandenabeele, *Necrosis, a well-orchestrated form of cell demise: signalling cascades, important mediators and concomitant immune response.* Biochim Biophys Acta, 2006. **1757**(9-10): p. 1371-87.

365. Iyer, S.S., et al., *Necrotic cells trigger a sterile inflammatory response through the Nlrp3 inflammasome.* Proc Natl Acad Sci U S A, 2009. **106**(48): p. 20388-93.

366. Kalai, M., et al., *Tipping the balance between necrosis and apoptosis in human and murine cells treated with interferon and dsRNA.* Cell Death Differ, 2002. **9**(9): p. 981-94.

367. Willingham, S.B., et al., *Microbial pathogen-induced necrotic cell death mediated by the inflammasome components CIAS1/cryopyrin/NLRP3 and ASC.* Cell Host Microbe, 2007. **2**(3): p. 147-59.

368. Agresti, A. and M.E. Bianchi, *HMGB proteins and gene expression.* Curr Opin Genet Dev, 2003. **13**(2): p. 170-8.

369. Bianchi, M.E., M. Beltrame, and G. Paonessa, *Specific recognition of cruciform DNA by nuclear protein HMG1.* Science, 1989. **243**(4894 Pt 1): p. 1056-9.

370. Goodwin, G.H. and E.W. Johns, *Isolation and characterisation of two calf-thymus chromatin non-histone proteins with high contents of acidic and basic amino acids.* Eur J Biochem, 1973. **40**(1): p. 215-9.

371. Bianchi, M.E., et al., *The DNA binding site of HMG1 protein is composed of two similar segments (HMG boxes), both of which have counterparts in other eukaryotic regulatory proteins.* EMBO J, 1992. **11**(3): p. 1055-63.

372. Bonaldi, T., et al., *Monocytic cells hyperacetylate chromatin protein HMGB1 to redirect it towards secretion.* EMBO J, 2003. **22**(20): p. 5551-60.

373. Li, J., et al., *Structural basis for the proinflammatory cytokine activity of high mobility group box 1.* Mol Med, 2003. **9**(1-2): p. 37-45.

374. Yang, H., et al., *A critical cysteine is required for HMGB1 binding to Toll-like receptor 4 and activation of macrophage cytokine release.* Proc Natl Acad Sci U S A, 2010. **107**(26): p. 11942-7.

375. Rowell, J.P., et al., *HMGB1-facilitated p53 DNA binding occurs via HMG-Box/p53 transactivation domain interaction, regulated by the acidic tail.* Structure, 2012. **20**(12): p. 2014-24.

376. Huttunen, H.J., et al., *Receptor for advanced glycation end products-binding COOH-terminal motif of amphoterin inhibits invasive migration and metastasis.* Cancer Res, 2002. **62**(16): p. 4805-11.

377. Gong, W., et al., *Amino acid residues 201-205 in C-terminal acidic tail region plays a crucial role in antibacterial activity of HMGB1.* J Biomed Sci, 2009. **16**: p. 83.

378. Stros, M., *DNA bending by the chromosomal protein HMG1 and its high mobility group box domains. Effect of flanking sequences.* J Biol Chem, 1998. **273**(17): p. 10355-61.

379. Wang, Q., et al., *The HMGB1 acidic tail regulates HMGB1 DNA binding specificity by a unique mechanism.* Biochem Biophys Res Commun, 2007. **360**(1): p. 14-9.

380. Kang, R., et al., *HMGB1 in cancer: good, bad, or both?* Clin Cancer Res, 2013. **19**(15): p. 4046-57.

381. Bianchi, M.E. and A. Agresti, *HMG proteins: dynamic players in gene regulation and differentiation.* Curr Opin Genet Dev, 2005. **15**(5): p. 496-506.

382. Grosschedl, R., K. Giese, and J. Pagel, *HMG domain proteins: architectural elements in the assembly of nucleoprotein structures.* Trends Genet, 1994. **10**(3): p. 94-100.

383. Zlatanova, J., S.H. Leuba, and K. van Holde, *Chromatin structure revisited.* Crit Rev Eukaryot Gene Expr, 1999. **9**(3-4): p. 245-55.

384. Bonne-Andrea, C., et al., *Rat liver HMG1: a physiological nucleosome assembly factor.* EMBO J, 1984. **3**(5): p. 1193-9.

385. Bonne-Andrea, C., et al., *The role of HMG1 protein in nucleosome assembly and in chromatin replication.* Adv Exp Med Biol, 1984. **179**: p. 479-88.

386. Mathew, C.G., G.H. Goodwin, and E.W. Johns, *Studies on the association of the high mobility group non-histone chromatin proteins with isolated nucleosomes.* Nucleic Acids Res, 1979. **6**(1): p. 167-79.

387. Cato, L., et al., *The interaction of HMGB1 and linker histones occurs through their acidic and basic tails.* J Mol Biol, 2008. **384**(5): p. 1262-72.

388. Falciola, L., et al., *High mobility group 1 protein is not stably associated with the chromosomes of somatic cells.* J Cell Biol, 1997. **137**(1): p. 19-26.

389. Celona, B., et al., *Substantial histone reduction modulates genomewide nucleosomal occupancy and global transcriptional output.* PLoS Biol, 2011. **9**(6): p. e1001086.

390. Yu, S.S., et al., *Interaction of non-histone chromosomal proteins HMG1 and HMG2 with DNA.* Eur J Biochem, 1977. **78**(2): p. 497-502.

391. Sheflin, L.G., N.W. Fucile, and S.W. Spaulding, *The specific interactions of HMG 1 and 2 with negatively supercoiled DNA are modulated by their acidic C-terminal domains and involve cysteine residues in their HMG 1/2 boxes.* Biochemistry, 1993. **32**(13): p. 3238-48.

392. Stros, M., *Two mutations of basic residues within the N-terminus of HMG-1 B domain with different effects on DNA supercoiling and binding to bent DNA.* Biochemistry, 2001. **40**(15): p. 4769-79.

393. Stros, M., S. Nishikawa, and G.H. Dixon, *cDNA sequence and structure of a gene encoding trout testis high-mobility-group-1 protein.* Eur J Biochem, 1994. **225**(2): p. 581-91.

394. Teo, S.H., K.D. Grasser, and J.O. Thomas, *Differences in the DNA-binding properties of the HMG-box domains of HMG1 and the sex-determining factor SRY.* Eur J Biochem, 1995. **230**(3): p. 943-50.

395. Wisniewski, J.R. and E. Schulze, *High affinity interaction of dipteran high mobility group (HMG) proteins 1 with DNA is modulated by COOH-terminal regions flanking the HMG box domain.* J Biol Chem, 1994. **269**(14): p. 10713-9.

396. Assenberg, R., et al., *A critical role in structure-specific DNA binding for the acetylatable lysine residues in HMGB1.* Biochem J, 2008. **411**(3): p. 553-61.

397. Javaherian, K., J.F. Liu, and J.C. Wang, *Nonhistone proteins HMG1 and HMG2 change the DNA helical structure.* Science, 1978. **199**(4335): p. 1345-6.

398. Javaherian, K., M. Sadeghi, and L.F. Liu, *Nonhistone proteins HMG1 and HMG2 unwind DNA double helix.* Nucleic Acids Res, 1979. **6**(11): p. 3569-80.

399. Yoshida, M., et al., *Unwinding of DNA by nonhistone protein HMG1 and HMG2.* Nucleic Acids Symp Ser, 1984(15): p. 181-4.

400. Paull, T.T., M.J. Haykinson, and R.C. Johnson, *The nonspecific DNA-binding and -bending proteins HMG1 and HMG2 promote the assembly of complex nucleoprotein structures.* Genes Dev, 1993. **7**(8): p. 1521-34.

401. Paull, T.T. and R.C. Johnson, *DNA looping by Saccharomyces cerevisiae high mobility group proteins NHP6A/B. Consequences for nucleoprotein complex assembly and chromatin condensation.* J Biol Chem, 1995. **270**(15): p. 8744-54.

402. Das, D. and W.M. Scovell, *The binding interaction of HMG-1 with the TATA-binding protein/TATA complex.* J Biol Chem, 2001. **276**(35): p. 32597-605.

403. Sutrias-Grau, M., M.E. Bianchi, and J. Bernues, *High mobility group protein 1 interacts specifically with the core domain of human TATA box-binding protein and interferes with transcription factor IIB within the pre-initiation complex.* J Biol Chem, 1999. **274**(3): p. 1628-34.

404. Onate, S.A., et al., *The DNA-bending protein HMG-1 enhances progesterone receptor binding to its target DNA sequences.* Mol Cell Biol, 1994. **14**(5): p. 3376-91.

405. Verrijdt, G., et al., *Comparative analysis of the influence of the high-mobility group box 1 protein on DNA binding and transcriptional activation by the androgen, glucocorticoid, progesterone and mineralocorticoid receptors.* Biochem J, 2002. **361**(Pt 1): p. 97-103.

406. Bardeesy, N. and R.A. DePinho, *Pancreatic cancer biology and genetics.* Nat Rev Cancer, 2002. **2**(12): p. 897-909.

407. Imamura, T., et al., *Interaction with p53 enhances binding of cisplatin-modified DNA by high mobility group 1 protein.* J Biol Chem, 2001. **276**(10): p. 7534-40.

408. McKinney, K. and C. Prives, *Efficient specific DNA binding by p53 requires both its central and C-terminal domains as revealed by studies with high-mobility group 1 protein.* Mol Cell Biol, 2002. **22**(19): p. 6797-808.

409. Chau, K.Y., H.Y. Lam, and K.L. Lee, *Estrogen treatment induces elevated expression of HMG1 in MCF-7 cells.* Exp Cell Res, 1998. **241**(1): p. 269-72.

410. Romine, L.E., et al., *The high mobility group protein 1 enhances binding of the estrogen receptor DNA binding domain to the estrogen response element.* Mol Endocrinol, 1998. **12**(5): p. 664-74.

411. Agrawal, A. and D.G. Schatz, *RAG1 and RAG2 form a stable postcleavage synaptic complex with DNA containing signal ends in V(D)J recombination.* Cell, 1997. **89**(1): p. 43-53.

412. Dai, Y., et al., *Determinants of HMGB proteins required to promote RAG1/2-recombination signal sequence complex assembly and catalysis during V(D)J recombination.* Mol Cell Biol, 2005. **25**(11): p. 4413-25.

413. Grundy, G.J., et al., *Initial stages of V(D)J recombination: the organization of RAG1/2 and RSS DNA in the postcleavage complex.* Mol Cell, 2009. **35**(2): p. 217-27.

414. Andersson, U. and K.J. Tracey, *HMGB1 is a therapeutic target for sterile inflammation and infection.* Annu Rev Immunol, 2011. **29**: p. 139-62.

415. Gardella, S., et al., *The nuclear protein HMGB1 is secreted by monocytes via a non-classical, vesicle-mediated secretory pathway.* EMBO Rep, 2002. **3**(10): p. 995-1001.

416. Wang, H., et al., *HMG-1 as a late mediator of endotoxin lethality in mice.* Science, 1999. **285**(5425): p. 248-51.

417. Wu, H., et al., *HMGB1 contributes to kidney ischemia reperfusion injury.* J Am Soc Nephrol, 2010. **21**(11): p. 1878-90.

418. Venereau, E., et al., *Mutually exclusive redox forms of HMGB1 promote cell recruitment or proinflammatory cytokine release.* J Exp Med, 2012. **209**(9): p. 1519-28.

419. Yang, H., et al., *Redox modification of cysteine residues regulates the cytokine activity of high mobility group box-1 (HMGB1).* Mol Med, 2012. **18**: p. 250-9.

420. Tang, D., T.R. Billiar, and M.T. Lotze, *A Janus tale of two active high mobility group box 1 (HMGB1) redox states.* Mol Med, 2012. **18**: p. 1360-2.

421. Bianchi, M.E., *HMGB1 loves company.* J Leukoc Biol, 2009. **86**(3): p. 573-6.

422. Ellerman, J.E., et al., *Masquerader: high mobility group box-1 and cancer.* Clin Cancer Res, 2007. **13**(10): p. 2836-48.

423. Sims, G.P., et al., *HMGB1 and RAGE in inflammation and cancer.* Annu Rev Immunol, 2010. **28**: p. 367-88.

424. Bierhaus, A., et al., *Understanding RAGE, the receptor for advanced glycation end products.* J Mol Med (Berl), 2005. **83**(11): p. 876-86.

425. Scaffidi, P., T. Misteli, and M.E. Bianchi, *Release of chromatin protein HMGB1 by necrotic cells triggers inflammation.* Nature, 2002. **418**(6894): p. 191-5.

426. Rauvala, H. and A. Rouhiainen, *RAGE as a receptor of HMGB1 (Amphoterin): roles in health and disease.* Curr Mol Med, 2007. **7**(8): p. 725-34.

427. Tian, J., et al., *Toll-like receptor 9-dependent activation by DNA-containing immune complexes is mediated by HMGB1 and RAGE.* Nat Immunol, 2007. **8**(5): p. 487-96.

428. Curtin, J.F., et al., *HMGB1 mediates endogenous TLR2 activation and brain tumor regression.* PLoS Med, 2009. **6**(1): p. e10.

429. DeMarco, R.A., M.P. Fink, and M.T. Lotze, *Monocytes promote natural killer cell interferon gamma production in response to the endogenous danger signal HMGB1.* Mol Immunol, 2005. **42**(4): p. 433-44.

430. Park, J.M., et al., *Is it reasonable to treat early gastric cancer with signet ring cell histology by endoscopic resection? Analysis of factors related to lymph-node metastasis.* Eur J Gastroenterol Hepatol, 2009. **21**(10): p. 1132-5.

431. Yu, M., et al., *HMGB1 signals through toll-like receptor (TLR) 4 and TLR2.* Shock, 2006. **26**(2): p. 174-9.

432. Ibrahim, Z.A., et al., *RAGE and TLRs: relatives, friends or neighbours?* Mol Immunol, 2013. **56**(4): p. 739-44.

433. Ivanov, S., et al., *A novel role for HMGB1 in TLR9-mediated inflammatory responses to CpG-DNA.* Blood, 2007. **110**(6): p. 1970-81.

434. Yanai, H., T. Ban, and T. Taniguchi, *Essential role of high-mobility group box proteins in nucleic acid-mediated innate immune responses.* J Intern Med, 2011. **270**(4): p. 301-8.

435. Yanai, H., et al., *HMGB proteins function as universal sentinels for nucleic-acid-mediated innate immune responses.* Nature, 2009. **462**(7269): p. 99-103.

436. Mouri, F., et al., *Intracellular HMGB1 transactivates the human IL1B gene promoter through association with an Ets transcription factor PU.1.* Eur J Haematol, 2008. **80**(1): p. 10-9.

437. He, Q., et al., *HMGB1 promotes the synthesis of pro-IL-1beta and pro-IL-18 by activation of p38 MAPK and NF-kappaB through receptors for advanced glycation end-products in macrophages.* Asian Pac J Cancer Prev, 2012. **13**(4): p. 1365-70.

438. Andersson, U., et al., *High mobility group 1 protein (HMG-1) stimulates proinflammatory cytokine synthesis in human monocytes.* J Exp Med, 2000. **192**(4): p. 565-70.

439. Park, J.S., et al., *Activation of gene expression in human neutrophils by high mobility group box 1 protein.* Am J Physiol Cell Physiol, 2003. **284**(4): p. C870-9.

440. Silva, E., et al., *HMGB1 and LPS induce distinct patterns of gene expression and activation in neutrophils from patients with sepsis-induced acute lung injury.* Intensive Care Med, 2007. **33**(10): p. 1829-39.

441. Hou, C.H., Y.C. Fong, and C.H. Tang, *HMGB-1 induces IL-6 production in human synovial fibroblasts through c-Src, Akt and NF-kappaB pathways.* J Cell Physiol, 2011. **226**(8): p. 2006-15.

442. Hreggvidsdottir, H.S., et al., *The alarmin HMGB1 acts in synergy with endogenous and exogenous danger signals to promote inflammation.* J Leukoc Biol, 2009. **86**(3): p. 655-62.

443. Dejean, E., et al., *ALK+ALCLs induce cutaneous, HMGB-1-dependent IL-8/CXCL8 production by keratinocytes through NF-kappaB activation.* Blood, 2012. **119**(20): p. 4698-707.

444. Yang, D., et al., *High mobility group box-1 protein induces the migration and activation of human dendritic cells and acts as an alarmin.* J Leukoc Biol, 2007. **81**(1): p. 59-66.

445. Agnello, D., et al., *HMGB-1, a DNA-binding protein with cytokine activity, induces brain TNF and IL-6 production, and mediates anorexia and taste aversion.* Cytokine, 2002. **18**(4): p. 231-6.

446. Kim, Y.S., et al., *SIRT1 modulates high-mobility group box 1-induced osteoclastogenic cytokines in human periodontal ligament cells.* J Cell Biochem, 2010. **111**(5): p. 1310-20.

447. Wu, X., et al., *The activation of HMGB1 as a progression factor on inflammation response in normal human bronchial epithelial cells through RAGE/JNK/NF-kappaB pathway.* Mol Cell Biochem, 2013. **380**(1-2): p. 249-57.

448. Treutiger, C.J., et al., *High mobility group 1 B-box mediates activation of human endothelium.* J Intern Med, 2003. **254**(4): p. 375-85.

449. Pedrazzi, M., et al., *Selective proinflammatory activation of astrocytes by high-mobility group box 1 protein signaling.* J Immunol, 2007. **179**(12): p. 8525-32.

450. Rouhiainen, A., et al., *Pivotal advance: analysis of proinflammatory activity of highly purified eukaryotic recombinant HMGB1 (amphoterin).* J Leukoc Biol, 2007. **81**(1): p. 49-58.

451. Pisetsky, D., *Cell death in the pathogenesis of immune-mediated diseases: the role of HMGB1 and DAMP-PAMP complexes.* Swiss Med Wkly, 2011. **141**: p. w13256.

452. Youn, J.H., et al., *High mobility group box 1 protein binding to lipopolysaccharide facilitates transfer of lipopolysaccharide to CD14 and enhances lipopolysaccharide-mediated TNF-alpha production in human monocytes.* J Immunol, 2008. **180**(7): p. 5067-74.

453. Lotze, M.T. and R.A. DeMarco, *Dealing with death: HMGB1 as a novel target for cancer therapy.* Curr Opin Investig Drugs, 2003. **4**(12): p. 1405-9.

454. Tang, D., et al., *High-mobility group box 1 and cancer.* Biochim Biophys Acta, 2010. **1799**(1-2): p. 131-40.

455. Jiao, Y., H.C. Wang, and S.J. Fan, *Growth suppression and radiosensitivity increase by HMGB1 in breast cancer.* Acta Pharmacol Sin, 2007. **28**(12): p. 1957-67.

456. Giavara, S., et al., *Yeast Nhp6A/B and mammalian Hmgb1 facilitate the maintenance of genome stability.* Curr Biol, 2005. **15**(1): p. 68-72.

457. Polanska, E., et al., *HMGB1 gene knockout in mouse embryonic fibroblasts results in reduced telomerase activity and telomere dysfunction.* Chromosoma, 2012. **121**(4): p. 419-31.

458. Tang, D., et al., *Endogenous HMGB1 regulates autophagy.* J Cell Biol, 2010. **190**(5): p. 881-92.

459. Carbone, M., et al., *Erionite exposure in North Dakota and Turkish villages with mesothelioma.* Proc Natl Acad Sci U S A, 2011. **108**(33): p. 13618-23.

460. Jube, S., et al., *Cancer cell secretion of the DAMP protein HMGB1 supports progression in malignant mesothelioma.* Cancer Res, 2012. **72**(13): p. 3290-301.

461. Yang, H., et al., *Programmed necrosis induced by asbestos in human mesothelial cells causes high-mobility group box 1 protein release and resultant inflammation.* Proc Natl Acad Sci U S A, 2010. **107**(28): p. 12611-6.

462. Tafani, M., et al., *Hypoxia-increased RAGE and P2X7R expression regulates tumor cell invasion through phosphorylation of Erk1/2 and Akt and nuclear translocation of NF-{kappa}B.* Carcinogenesis, 2011. **32**(8): p. 1167-75.

463. van Beijnum, J.R., et al., *Tumor angiogenesis is enforced by autocrine regulation of high-mobility group box 1.* Oncogene, 2013. **32**(3): p. 363-74.

464. Yan, W., et al., *High-mobility group box 1 activates caspase-1 and promotes hepatocellular carcinoma invasiveness and metastases.* Hepatology, 2012. **55**(6): p. 1863-75.

465. Parker, K., et al., *HMGB1 enhances immune suppression by facilitating the differentiation and suppressive activity of myeloid-derived suppressor cells.* Cancer Res, 2014.

466. Gebhardt, C., et al., *RAGE signaling sustains inflammation and promotes tumor development.* J Exp Med, 2008. **205**(2): p. 275-85.

467. Mittal, D., et al., *TLR4-mediated skin carcinogenesis is dependent on immune and radioresistant cells.* EMBO J, 2010. **29**(13): p. 2242-52.

468. Bald, T., et al., *Ultraviolet-radiation-induced inflammation promotes angiotropism and metastasis in melanoma.* Nature, 2014. **507**(7490): p. 109-13.

469. Taguchi, A., et al., *Blockade of RAGE-amphoterin signalling suppresses tumour growth and metastases.* Nature, 2000. **405**(6784): p. 354-60.

470. Kuniyasu, H., et al., *Expression of receptors for advanced glycation end-products (RAGE) is closely associated with the invasive and metastatic activity of gastric cancer.* J Pathol, 2002. **196**(2): p. 163-70.

471. Sasahira, T., et al., *Expression of receptor for advanced glycation end products and HMGB1/amphoterin in colorectal adenomas.* Virchows Arch, 2005. **446**(4): p. 411-5.

472. Kusume, A., et al., *Suppression of dendritic cells by HMGB1 is associated with lymph node metastasis of human colon cancer.* Pathobiology, 2009. **76**(4): p. 155-62.

473. Liu, Z., L.D. Falo, Jr., and Z. You, *Knockdown of HMGB1 in tumor cells attenuates their ability to induce regulatory T cells and uncovers naturally acquired CD8 T cell-dependent antitumor immunity.* J Immunol, 2011. **187**(1): p. 118-25.

474. He, Y., et al., *Tissue damage-associated "danger signals" influence T-cell responses that promote the progression of preneoplasia to cancer.* Cancer Res, 2013. **73**(2): p. 629-39.

475. Kang, R., et al., *The HMGB1/RAGE inflammatory pathway promotes pancreatic tumor growth by regulating mitochondrial bioenergetics.* Oncogene, 2013.

476. Kang, R., et al., *The HMGB1/RAGE inflammatory pathway promotes pancreatic tumor growth by regulating mitochondrial bioenergetics.* Oncogene, 2014. **33**(5): p. 567-77.

477. Tang, D., et al., *High-mobility group box 1 is essential for mitochondrial quality control.* Cell Metab, 2011. **13**(6): p. 701-11.

2. Materials and Methods

General Remarks

The materials and methods part is adapted from the dissertation of Dr. Gabriel Sollberger (ETH-Diss.-No 19973). Standard methods are only briefly described, but if protocols were modified, it is mentioned. Detailed specifications of single experiments can be found in the appropriate figure legends.

2.1. Materials

2.1.1. Chemicals, consumables and equipment

Chemicals and consumables

3-(4,5-dimethylthiazol-2-yl)-2,5-diphenyltetrazolium bromide (MTT)	SIGMA, Munich, Germany
β-Mercaptoethanol	SIGMA, *Munich, Germany*
Acetic acid	FLUKA CHEMIE, *Buchs, Switzerland*
Acrylamide/ bisacrylamide (30:0.8)	ROT, *Karlsruhe, Germany*
Agar	DIFCO, *Detroit, US-MI*
Agarose	SIGMA, *Munich, Germany*
Ammonium persulfate (APS)	SIGMA, *Munich, Germany*
Ampicillin	SIGMA, *Munich, Germany*
Annexin V	BECTON-DICKINSON, *Franklin Lakes, US-NJ*)
Antibody Diluent	DAKO, *Glostrup, Denmark*
Aza-2′-deoxycytidine (AZA)	SIGMA *Munich, Germany*
Bovine serum albumin (BSA)	SIGMA, *Munich, Germany*
BoxA from HMGB1	HMGBIOTECH, *Milano, Italy*
Bromophenol blue	SIGMA, *Munich, Germany*
BSA Fraction V	PAA, *Pasching, Austria*
Calcium chloride ($CaCl_2$)	FLUKA CHEMIE, *Buchs, Switzerland*
Caliper	MITUTOYO, *Kawasaki, Japan*
Carboxyfluorescein succinimidyl ester (CFSE)	THERMO FISHER SCIENTIFIC, *Waltham, US-MA*
CD14 magnetic beads	MILTENYI, *Bergisch Gladbach, Germany*
DAKO Delimiting pen	DAKO, *Glostrup, Denmark*

Dimethylsulfoxide (DMSO)	MERCK, *Darmstadt, Germany*
DL-Dithiothreitol (DDT)	SIGMA, *Munich, Germany*
DNA-restriction enzyme buffers	NEB, *Ipswich, US-MA*
Ethanol 70 % V/V	Kantonsapotheke Zurich, *Zurich, Switzerland*
Ethanol 80 % V/V KA PhEur	Kantonsapotheke Zurich, *Zurich, Switzerland*
Ethanol 96 % V/V KA PhEur	Kantonsapotheke Zurich, *Zurich, Switzerland*
Ethanol absolut KA PhEur	Kantonsapotheke Zurich, *Zurich, Switzerland*
Ethidium Bromide	SIGMA, *Munich, Germany*
Ethylenediaminetetraacetic acid (EDTA)	FLUKA CHEMIE, *Buchs, Switzerland*
Faramount Mounting Medium	DAKO, *Glostrup, Denmark*
FastStart Universal SYBR Green Master	ROCHE, *Rotkreuz, Switzerland*
Ficoll-Paque PLUS	GE HEALTHCARE, *Little Chalfont, UK*
Flasks and (multiwell)-dishes for cell culture	NUNC, *Roskilde, Denmark*
Fluorescence Mounting Medium	DAKO, *Glostrup, Denmark*
Glycerol	MERCK, *Darmstadt, Germany*
Glycine	ROT, *Karlsruhe, Germany*
Goat serum	SIGMA, *Munich, Germany*
Hematoxylin Solution	SIGMA, *Munich, Germany*
HEPES	SIGMA, *Munich, Germany*
Hydrogen chloride (HCl)	FLUKA CHEMIE, *Buchs, Switzerland*
Insulin Syringes (30G x 8mm)	BECTON-DICKINSON, *Franklin Lakes, US-NJ*
Ionomycin	SIGMA, *Munich, Germany*
LS columns	MILTENYI, *Bergisch Gladbach, Germany*
Magnesium chloride (MgCl2)	FLUKA CHEMIE*, Buchs, Switzerland*
Methanol	FLUKA CHEMIE, *Buchs, Switzerland*
MicroAmp® Fast Optical 96-Well Reaction Plates	LIFE TECHNOLOGIES, *Carlsbad, US-CA*
Microscope Cover Slips, 24 x 36 mm	THERMO FISHER SCIENTIFIC, *Waltham, US-MA*
Milk powder (low fat)	MIGROS, *Zürich, Switzerland*

Monosodium urate crystals (MSU)	provided by L. French, *University Hospital Zürich*
Triton-X100	SIGMA, *Munich, Germany*
Microfilter units 0.45 µm	MILLIPORE, *Billerica, US-MA*
Nigericin	ENZO LIFE SCIENCES, *New York, US-NY*
Nitrocellulose membrane (Protran)	SCHLEICHER & SCHUELL, *Dassel, Germany*
NP40 lysis buffer	LIFE TECHNOLOGIES, *Carlsbad, US-CA*
Nylon cell strainer 40 µm	CORNING INC., *New York, US-NY*
Nylon cell strainer 70 µm	CORNING INC., *New York, US-NY*
Orange G	SIGMA, *Munich, Germany*
PBS	GIBCO, *Lausanne, Switzerland*
PBS (10x powder)	APPLICHEM, *Darmstadt, Germany*
Phorbol-12-myristate-13-acetate (PMA)	SIGMA, *Munich, Germany*
Polybrene	SIGMA, Munich, *Germany*
Polystyrene Round-Bottom Tubes 5 ml	BECTON-DICKINSON, *Franklin Lakes, US-NJ*
Pre-mixed gas composed with 1 % O_2	CARBAGAS, *Guemlingen, Switzerland*
Propidium iodide	ROCHE, *Rotkreuz, Switzerland*
Puromycin	SIGMA, *Munich, Germany*
Rec. M-CSF	PEPROTECH, *Rocky Hill, US- NJ*
Rec. HMGB1	HMGBIOTECH, *Milano, Italy*
Rec. IFN-γ	PEPROTECH, *Rocky Hill, US- NJ*
Rec. IL-4	PEPROTECH, *Rocky Hill, US- NJ*
Sodium chloride (NaCl)	FLUKA CHEMIE, *Buchs, Switzerland*
Sodium dodecyl sulfate (SDS)	SIGMA, *Munich, Germany*
Sodium hydroxide (NaOH)	FLUKA CHEMIE, *Buchs, Switzerland*
Target Retrieval Solution	DAKO, *Glostrup, Denmark*
Tetramethylethylenediamine (TEMED)	SIGMA, *Munich, Germany*
Triton-X100	SIGMA, Munich, Germany
TRIZMA Base (TRIS)	SIGMA, *Munich, Germany*
Tryptone	DIFCO, *Detroit, US-MI*
Tween 20	ROT, *Karlsruhe, Germany*
Ultra-pure LPS (Lipopolysaccharide)	INVIVOGEN, *Toulouse, France*

Whatman 3MM paper	WHATMAN, *Maidstone, England*
Xylene	THOMMEN FURLER AG, *Rüti bei Büren, Switzerland*
Yeast extract	DIFCO, *Detroit, US-MI*
Z-VAD-fmk (Z-VAD)	ENZO LIFE SCIENCES, *New York, US-NY*

Equipment

Agarose gel electrophoresis system	BIORAD, *Cressier, Switzerland*
CanonScan 9950F device	CANON, *Tokio, Japan*
Digital slide scanner NanoZoomer-XR C12000	HAMAMATSU Photonics, *Hamamatsu, Japan*
Electric animal shaver Favorita II	AESCULAP, *Suhl, Germany*
Eppendorf Thermomixer Compact	EPPENDORF, *Hamburg, Germany*
FACS Canto II	BECTON-DICKINSON, *Franklin Lakes, US-NJ*
Flowmeter RMA-23-SSV	DWYER, *Michigan City, US-IN*
GeneFlash	SYNGENE, Cambridge, UK
Hyrax M25 microtome	CARL ZEISS, *Oberkochen, Germany*
Lab Therm shaker	KUHNER AG, *Birsfelden, Switzerland*
Long-Term Storage Cryogenic Tubes	THERMO FISHER SCIENTIFIC, *Waltham, US-MA*
MIC-101 Modular Incubator Chamber	BILLUPS-ROTHENBERG, *Del Mar, US-CA*
Oxygen cell oxygen sensor VTI-122	VASCULAR TECHNOLOGY, *Nashua, US-NH*
TProfessional Thermocycler	BIOMETRA, *Göttingen, Germany*
SE 250 mini gel system	AMERSHAM, *Uppsala, Sweden*
Semi-dry blotter Z340502	SIGMA, *Munich, Germany*
Spectra Max190 plate reader	MOLECULAR DEVICES, *Sunnyvale, US-CA*
Speed Vac apparatus	EPPENDORF, *Hamburg, Germany*
Steamer MultiGourmet Typ 3216	BRAUN, *Kronberg, Germany*
UVS-99 Micro-Volume Spectrophotometer	ACTGene, *Piscataway, US-NJ*
ViiA™ 7 Real-Time PCR System	LIFE TECHNOLOGIES, *Carlsbad, US-CA*
Widefield BX61 multicolor fluorescence microscope	OLYMPUS, *Tokyo, Japan*

Software

Analysis Pro software	SOFT IMAGING SYSTEMS, *Münster, Germany*
FACS DIVA software	BECTON-DICKINSON, *Franklin Lakes, US-NJ*
ImageJ 1.47	National Health Institutes, *USA*
Nimblescan 2.5	ROCHE NIMBLEGEN INC, *Madison, US-WI*
Photoshop software	ADOBE SYSTEMS SOFTWARE, *San Jose, US-CA*
Prism Software	GRAPHPAD SOFTWARE, *San Diego, US-CA*
R package DMR	ROCHE NIMBLEGEN INC, *Madison, US-WI*
Spectra Max190 plate reader Softmax software 4.3.1	MOLECULAR DEVICES, *Sunnyvale, US-CA*
ViiA™ 7 Real-Time PCR System software	LIFE TECHNOLOGIES, *Carlsbad, US-CA*

2.1.2. Protein size standards

Prestained Protein Molecular Weight Marker	MBI FERMENTAS (MBI), *Nunningen, Switzerland*

2.1.3. DNA size standards

1 kb DNA ladder	NEW ENGLAND BIOLABS (NEB) *Beverly, US-MA*
pUC mix DNA marker	MBI FERMENTAS (MBI), *Nunningen, Switzerland*

2.1.4. Cell culture media and additives

DMEM	SIGMA, *Munich, Germany*
Fetal calf serum (FCS)	BIOCONCEPT, *Allschwil, Switzerland*
GlutaMAX	GIBCO BRL, *Paisley, Scotland*
OptiMEM	GIBCO BRL, *Paisley, Scotland*
Penicillin/ Streptomycin (P/S)	SIGMA, *Munich, Switzerland*

Puromycin	SIGMA, *Munich, Germany*
RPMI 1640	GIBCO BRL, *Paisley, Scotland*
Sodium Pyruvate 100 mM	GIBCO BRL, *Paisley, Scotland*

2.1.5. Transfection reagents

Lipofectamine 2000	INVITROGEN, *Basel, Switzerland*

2.1.6. Kits

BCA protein assay	PIERCE*, Rockford, US-IL*
CytoTox 96 LDH assay kit	PROMEGA, *Madison, US-WC*
DAKO real detection system	DAKO, *Glostrup, Denmark*
ELISA kit for human IL-1β	R&D SYSTEMS, *Minneapolis, US-MN*
ELISA kit for human and murine HMGB1	IBL INTERNATIONAL, *Hamburg, Germany*
Gel Extraction Kit	QIAGEN, *Düsseldorf, Germany*
NBT/ BCIP substrate kit	PROMEGA, *Madison, US-WC*
PCR Purification kit	QIAGEN, *Düsseldorf, Germany*
Plasmid Midi/ Maxi Kit 0	QIAGEN, *Düsseldorf, Germany*
RevertAid First Strand cDNA Synthesis Kit RevertAid Reverse Transcriptase (200 U/µL) RiboLock RNase Inhibitor (40 U/µL)	THERMO FISHER SCIENTIFIC, *Waltham, US-MA*
RNeasy Mini kit	QIAGEN, *Düsseldorf, Germany*

2.1.7. Enzymes

Accutase	PAA, *Pasching, Austria*
Trypsin	GIBCO BRL, *Paisley, Scotland*
Collagenase D	ROCHE DIAGNOSTICS, *Rotkreuz, Switz*erland
DNA-restriction enzymes *Sal*I (20.000 U/ ml) *BamH*I (20.000 U/ ml) *Hind*I (20.000 U/ ml) *Bgl*II (20.000 U/ ml)	NEB, *Ipswich, US-MA*
T4 DNA ligase	ROCHE, *Rotkreuz, Switzerland*

2.1.8. Primary antibodies

α-human ASC (rabbit, polyclonal, AL117)	ENZO LIFE SCIENCES, *New York, US-NY*
α-human β-Actin (mouse, monoclonal, A5441)	SIGMA, *Munich, Germany*
α-human CD163 (mouse, monoclonal, NCL-L-CD163)	LEICA BIOSYSTEMS, *Wetzlar, Germany*
α-human IL-10 (rabbit, polyclonal, ab34843)	ABCAM, *Cambridge, UK*
α-mouse 7/4 (FITC-conjugated, rat monoclonal, ab53453)	ABCAM, *Cambridge, UK*
α-mouse β-Actin (rabbit, polyclonal, #4970S)	CELL SIGNALING TECHNOLOGY, *Danvers, US-MA*
α-mouse CD11b (PE-conjugated, rat, monoclonal, 101207)	BIOLEGEND, *San Diego, US-CA*
α-mouse CD45 (APC-conjugated, rat, monoclonal, 559864)	BECTON-DICKINSON, *Franklin Lakes, US-NJ*
α-mouse Hif-1α (mouse, monoclonal, ab16066)	ABCAM, *Cambridge, UK*
α-mouse and human HMGB1 (rabbit, polyclonal, ab65003)	ABCAM, *Cambridge, UK*
α-mouse IL-10 (rat, monoclonal, 504902)	BIOLEGEND, *San Diego, US-CA*

2.1.9. Secondary antibodies

Alexa Fluor® 546 α-rabbit IgG (A-11035)	LIFE TECHNOLOGIES, *Carlsbad, US-CA*
DyeLight® 650 α-mouse IgG (ab96882)	ABCAM, *Cambridge, UK*
α-mouse IgG (biotinylated, ab64255)	ABCAM, *Cambridge, UK*
α-mouse IgG (AP-conjugated, S372B)	PROMEGA, *Madison, US-WC*
α-rabbit IgG (AP-conjugated, S373B)	PROMEGA, *Madison, US-WC*

2.1.10. Staining reagents

7-AAD	Becton-Dickinson, *Franklin Lakes, US-NJ*
Annexin V	Becton-Dickinson, *Franklin Lakes, US-NJ*
Propidium iodide	ROCHE, *Rotkreuz, Switzerland*

2.1.11. shRNAs

shRNAs were bought from SIGMA (*Munich, Germany*).

2.1.12. Primers

for human NLRP1:	forward	5′-GACCTGGCCTCTGTGCTTAG-3′,
	reverse	5′-AGTCCCCAAAGGCTTCGTAT-3’,
for human NLRP3:	forward	5′-TGCCTTTGACGAGCACATAG-3′,
	reverse	5′-GCAGCAAACTGGAAAGGAAG-3’,
for human ASC:	forward	5´-GCCGAGGAGCTCAAGAAGTT-3´,
	reverse	5´-CAGGCTGGTGTGAAACTGAA-3´,
for human Casp.-1:	forward	5′-GAAGGCATTTGTGGGAAGAA-3′,
	reverse	5′-CATCTGGCTGCTCAAATGAA-3’,
for human IL-1β:	forward	5′-AGCTGATGGCCCTAAACAGA-3′,
	reverse	5′-TCTTTCAACACGCAGGACAG-3’,
for human IL-18:	forward	5´-CCAAGGAAATCGGCCTCTAT-3´,
	reverse	5´-CCCCCAATTCATCCTCTTTT-3´.
for human GAPDH:	forward	5´-AAGGTGAAGGTCGGAGTCAACG-3´,
	reverse	5´-CAGGGATGATGTTCTGGAGAGC-3´.
for human RPL27:	forward	5′-ATCGCCAAGAGATCAAAGATAA-3′,
	reverse	5′-TCTGAAGACATCCTTATTGACG-3’,
for human VEGF-α:	forward	5′-TACCTCCACCATGCCAAGTG-3′,
	reverse	5′-GATGATTCTGCCCTCCTCCTT-3’,
for mouse CD80:	forward	5´-TCAGTTGATGCAGGATACACCA-3´,
	reverse	5´-AAAGACGAATCAGCAGCACAA-3´,
for mouse CXCR4:	forward	5′-GACTGGCATAGTCGGCAATG-3′,
	reverse	5′-AGAAGGGGAGTGTGATGACAAA-3′,
for mouse Fizz1:	forward	5′-CCAATCCAGCTAACTATCCCTCC-3′,
	reverse	5′-ACCCAGTAGCAGTCATCCCA-3’

for mouse HMGB1:	forward	5′-GGCGAGCATCCTGGCTTATC-3′,
	reverse	5′-GGCTGCTTGTCATCTGCTG-3’,
for mouse IL-1β:	forward	5´-ATCTTTTGGGGTCCGTCAACT-3´,
	reverse	5´-GACAGCACACATTTGCAGCTC-3´,
for mouse IL-6:	forward	5´-TAGTCCTTCCTACCCCAATTTCC-3´,
	reverse	5´-TTGGTCCTTAGCCACTCCTTC-3´,
for mouse IL-10:	forward	5′-GCTCTTACTGACTGGCATGAG-3′,
	reverse	5′-CGCAGCTCTAGGAGCATGTG-3’,
for mouse RPL27:	forward	5′-AAAGCCGTCATCGTGAAGAAC-3′,
	reverse	5′-GCTGTCACTTTCCGGGGATAG-3’,
for mouse TNF-α:	forward	5′-CCCTCACACTCAGATCATCTTCT-3′,
	reverse	5′-GCTACGACGTGGGCTACAG-3’.
for mouse Ym1:	forward	5′-AGAAGGGAGTTTCAAACCTGGT-3′,
	reverse	5′-GTCTTGCTCATGTGTGTAAGTGA-3’.

2.1.13. Plasmids

psPAX2	provided by J. Tschopp, *Biochemistry Institute Lausanne*
pMD2-VSVG	provided by J. Tschopp, *Biochemistry Institute Lausanne*
pSP-93	OLIGOENGINE, Seatlle, US-WA
pSUPER.basic vector	OLIGOENGINE, *Seatlle, US-WA*

2.1.14. Bacterial strains

E.coli BL21	AMERSHAM, *Uppsala, Sweden*
E.coli XL1-Blue MRF	STRATAGENE, *La Jolla, US-CA*

2.1.15. Eukaryotic cell lines

B16-F10	provided by L. French, *University Hospital Zürich*
THP-1	ATCC, *Manassas, US-VA*
HEK293T	ATCC, *Manassas, US-VA*
Human metastatic melanoma cell lines	provided by R. Dummer, University Hospital Zürich

2.1.16. Standard buffers and solutions

AP buffer	
NaCl	100 mM
$MgCl_2$	5 mM
TRIS/ HCl (pH 9.5)	100 mM

FACS buffer	
PBS	
FCS	2 %(v/v)

MACS buffer	
PBS	100 mM
BSA	0.5 % (w/v)
EDTA	2 mM

PBS	
NaCl	140 mM
KCl	30 mM
Na_2PO_4	6.5 mM
KH_2PO_4	1.5 mM

Adjusted to pH 7.4

PBST	
PBS	
Tween 20	0.1 %(v/v)

TAE	
TRIS/ HCl	40 mM
Acetic acid	40 mM
EDTA	1 mM
pH 8.0	

TBST	
NaCl	150 mM
Tween 20	0.05 % (v/v)
TRIS/ HCl (pH 8.0)	10 mM

2.1.17. Biological samples from melanoma patients and healthy donors

Serum and tumor biopsies were collected from patients with primary melanoma, metastatic melanoma (stage 4) and patients seen in our Department for sentinel lymph node biopsy. Serum was obtained from healthy blood donors and healthy skin was obtained from plastic surgery. All human biological samples were collected with informed written consent upon approval of Local Ethical Committees and were conducted according to the Declaration of Helsinki Principals.

2.2. Methods

2.2.1. Cell biological methods

2.2.1.1. Cultivation and storage of eukaryotic cells

Cells were grown in petri dishes or flasks as adherence or suspension cultures. They were incubated in a CO_2 incubator (37 °C, 95 % relative humidity, 5 % CO_2), cultivated in growth medium and propagated as specified in the following table:

Cell type	**Growth medium**		**Propagation**	**Passages**
	Basal medium	**Supplements**		
HEK293T	RPMI 1640	10 % FCS, P/S (100 U/ ml), Sodium Pyruvate (1 mM), GlutaMAX (1:100)	Splitting 1/ 10 – 1/ 25 when confluency was reached	~P10 – P35
THP-1 macrophages	RPMI 1640	10 % FCS, P/S (100 U/ ml)	Splitting 1/ 10 – 1/ 25 at a density of about 10^6 cells/ ml with a medium change every third day	~P10 – P35
Murine primary macrophages	RPMI 1640	10 % FCS, P/S (100 U/ ml), Sodium Pyruvate (1 mM), GlutaMAX (1:100)	No propagation	
Murine B16 mouse melanoma	DMEM	10 % FCS, P/S (100 U/ ml), Sodium Pyruvate (1 mM), GlutaMAX (1:100)	Splitting 1/ 5 – 1/ 10 when confluency was reached	~P10 – P20
Human metastatic melanoma	RPMI 1640	10 % FCS, P/S (100 U/ ml), Sodium Pyruvate (1 mM), GlutaMAX (1:100)	Splitting 1/ 5 – 1/ 10 when confluency was reached	~P5 – P15
Human monocytes	DMEM	10 % FCS, P/S (100 U/ ml), Sodium Pyruvate (1 mM), GlutaMAX (1:100)	No propagation	

To passage adherent cells, they were washed three times with PBS. To detach from the plastic surface, they were incubated 4-5 min with a suitable amount of trypsin (0.05 % [w/v] in PBS) at 37 °C in the incubator. The trypsinization was stopped by resuspending the cells in fresh medium containing at least 10 % FCS and subsequent seeding.
For long-term storage, cells were suspended, centrifuged (200x g, 4 min, RT) and resuspended in FCS containing 10 % DMSO (MERCK, *Darmstadt, Germany)*. They were slowly frozen at ~ 1 °C/ min in Long-Term Storage Cryogenic Tubes (THERMO FISHER SCIENTIFIC, *Waltham, US-MA*) and stored in liquid nitrogen.

2.2.1.2. Establishment of primary eukaryotic cell cultures

2.2.1.2.1. Primary mouse macrophages

To generate of M1 and M2 macrophages, bone marrow cells from tibia and fibula of WT C57BL/6 mice (HARLAN, *Venray, Netherlands*) were isolated and 5×10^6 cells/10 cm^2 dish were cultured at 37 °C in 5 % CO_2 in RPMI 1640 medium (supplemented with 10 % FCS, 1 % GlutaMAX, 1 mM Sodium Pyruvate and 100 U/ ml P/S) with 10 ng/ml rec. M-CSF (PEPROTECH, *Rocky Hill, US- NJ*). Medium was replaced on day 6 and cells were harvested on day 8.
To induce M1 phenotype, cells were stimulated at day 6 for 24 h with 10 ng/ml M-CSF (PEPROTECH) and 100 ng/ml IFN-γ (PEPROTECH) and for additional 24 h with 10 ng/ml M-CSF (PEPROTECH) and 20 ng/ml ultra-pure LPS (INVIVOGEN, *Toulouse, France*).
To induce M2 phenotype, cells were stimulated at day 6 for 48 h with 10 ng/ml M-CSF (PEPROTECH) and 20 ng/ml IL-4 (PEPROTECH).
To determine the effect of HMGB1 on M1 and M2 macrophages, culture medium used to induce M1 or M2 macrophages was supplemented with 1 µg/ml rec. HMGB1 (HMGBIOTECH, *Milano, Italy*).

2.2.1.2.2. Human monocytes

Monocytes from healthy donors were obtained from peripheral blood mononuclear cells (PBMC). To isolate PBMC`s, the buffy-coats were mixed with PBS in a ratio of 1:2.5. 35 ml of the suspension were slowly applied to 50 ml falcons filled with 15 ml Ficoll (GE HEALTHCARE, *Little Chalfont, UK*) and PBMC were purified by centrifugation (400x g, 20 min, RT) using a density gradient. The cells were collected from the inter-phase, washed twice with PBS and resuspended in 50 ml cold MACS buffer. After counting, cells were pelleted, resuspended in MACS buffer / CD14 magnetic beads (MILTENYI, *Bergisch Gladbach, Germany)* and incubated for 30 min in the dark on ice.

Magnetic beads incubation mix (per 100 x 10^6 PBMC's)	
MACS buffer	400 µl
CD14 magnetic beads	50 µl

After two washing steps in cold MACS buffer, cells were filtered through a 70 µm Nylon cell strainer (CORNING INC., *New York, US-NY)*, passed through a LS column (MILTENYI*)*, counted and seeded in RPMI 1640 medium (supplemented with 10 % FCS, 1 % GlutaMAX and 1 mM Sodium Pyruvate) at required densities for experiments.

2.2.1.3. Stable shRNA transfection of B16-F10 and THP-1 cells

To generate B16-F10 and THP-1 cells stably transfected with a plasmid encoding shRNA sequences for the desired gene, the oligos were cloned into the pSUPER.basic (OLIGOENGINE, *Seatlle, US-WA)* vector that had been linearized with *Bgl*II and *Hind*III, followed by sequencing and subcloning of the oligos into the lentiviral pSP-93 (OLIGOENGINE) vector. Second-generation packaging plasmids pMD2-VSVG and psPAX2 (kindly provided by Prof. J. Tschopp, Biochemistry Institute, Lausanne, Switzerland) were used for lentivirus production and infection. Subsequently, the cells were transfected and selected with puromycin. See below for a detailed protocol.

2.2.1.3.1. Cloning of shRNA oligos into pSUPER.basic

pSUPER.basic was linearized with *Hind*III overnight at 37 °C, following by purification of the vector on a 1% agarose gel using the QIAGEN gel extraction kit (QIAGEN, *Düsseldorf, Germany*). Subsequently, the purified vector was digested with *Bgl*II overnight at 37 °C and purified using the columns of the QIAGEN gel extraction kit.

*Hind*III digest	
pSUPER.basic	x µl (10 µg)
5x buffer 2	5 µl
*Hind*III (20.000 U/ ml)	5 µl
ddH_2O	add. 50 µl

*Bgl*II digest	
*Hind*III-digested pSUPER.basic	x µl (10 µg)
5x buffer 3	5 µl
*Bgl*II (20.000 U/ ml)	5 µl
ddH_2O	add. 50 µl

The shRNA oligonucleotide sequences were annealed by mixing 3 µg of the sense and 3 µg of the antisense oligo (3 mg/ ml nuclease-free H_2O each) with 48 µl annealing buffer (100 mM NaCl, 50 mM Hepes pH 7.4) and subsequent incubation at 90 °C for 10 min, followed by 70 °C for 10 min and slow cooling to 10 °C. Annealing efficiency was tested on a 3 % agarose gel.

The annealed oligos were cloned into the linearized pSUPER.basic according to the following table for 1h at room temperature.

Cloning into pSUPER.basic

Annealed oligos	4 µl
T4 DNA ligase buffer	1 µl
Linearized pSUPER.basic (200-500 mg)	x µl
T4 DNA ligase	1 µl
Nuclease-free ddH_2O	add. 10 µl

2.2.1.3.2. Subcloning to lentiviral pSP-93

The lentiviral vector pSP-93 was linearized by digestion with *Sal*I and *BamH*1 and the shRNA oligos as well as the H1 promoter were cut out of pSUPER.basic using the same restriction enzymes overnight at 37 °C, followed by purification on a 2% agarose gel using the QIAGEN gel extraction kit. The insert was subsequently ligated into pSP-93 using an insert to vector molar ratio of 3/1 and using buffer and ligase according to cloning into pSUPER.basic.

*Sal*I/ *BamH*I digest

10 µg pSP-93	x µl
5x buffer 3	5 µl
100x BSA	5 µl
*Sal*I (20.000 U/ ml)	2.5 µl
*BamH*I (20.000 U/ ml)	2.5 µl
ddH_2O	add. 50 µl

2.2.1.3.3. Lentivirus production and transfection

Lentivirus was produced by transfection of HEK293T cells with a mix of the pSP-93 vector encoding for the desired shRNA oligo and the two packaging vectors psPAX2 and pMD2-VSVG. $5x10^6$ cells were plated in 10-cm dishes in RPMI 1640 medium (supplemented with 2 % FCS, 1 % GlutaMAX and 1 mM Sodium Pyruvate) and transfected the day after seeding. For transfection, the medium was changed to 15 ml OptiMEM (GIBCO BRL, *Paisley, Scotland).* Plasmids were mixed in a ratio of 1:3:4 to a total of 24 µg (3 µg psPAX2, 9 µg pMD2-VSVG, 12 µg pSP-93) in 1.5 ml OptiMEM (GIBCO BRL*)* and combined with 1.5 ml OptiMEM (GIBCO BRL*)* containing 60 µl Lipofectamine 2000 (INVITROGEN*)*.
After 20 min incubation at room temperature, the transfection mix was added onto the HEK293T cells and the medium was changed to 5-10 ml RPMI 1640 medium (supplemented with 2 % FCS, 1 % GlutaMAX and 1 mM Sodium Pyruvate) 16-24 h after transfection, depending on the concentration of virus intended to produce.
36 h later, the conditioned medium containing the lentivirus was harvested, centrifuged at 200x g for 4 min at room temperature, filtrated using 0.45 µm Microfilter units (MILLIPORE, *Billerica, US-MA*), mixed with 8.4 µg/ml Polybrene (SIGMA, *Munich, Germany*), aliquoted and stored at -80 °C.
For transduction, $1x10^6$ THP-1 or B16-F10 cells were seeded in a well of a 6-well plate and transduced with 1 ml of conditioned virus-containing medium. 24h after transfection the medium was changed and puromycin of an optimized concentration (5 µg/ ml) was used to select transduced cells.

2.2.1.3.4. Control of knock-down efficiency and stability

To determine the knock-down efficiency of B16-F10 mouse melanoma cell line stably expressing shRNA to HMGB1, shHMGB1-B16 as well as shLamin-B16 were cultured at 37 °C in 5 % CO_2 in DMEM medium (supplemented with 10 % FCS, 1 % GlutaMAX, 1 mM Sodium Pyruvate and 100 U/ml P/S). 1×10^5 cells/well of a 6-well plate were seeded, cultured for one week and lysed with NP40 lysis buffer (LIFE TECHNOLOGIES).The procedure was repeated 3 times to observe the HMGB1 protein level after 0, 7, 14, 21 and 28 days. Protein concentration of the cell lysates was determined by the BCA protein assay and proteins levels were analyzed with western blot.

2.2.1.4. Differentiation and priming of human monocytes and THP-1 macrophages

For necrosis experiments THP1 macrophages were differentiated for 3h with 500nM phorbol-12-myristate-13-acetate (PMA) (SIGMA), washed and plated one day before stimulation. Human monocytes and THP1 macrophages were primed overnight with 100 ng/ ml ultra-pure LPS.

2.2.1.5. Induction of necrosis

Necrosis was induced in A2058 and A375 with repeated heat/ thaw cycles. Counted cells were dry-pelleted and treated with 3 cycles of freezing in liquid nitrogen and heating in water bath at 37°C. The necrotic cell contents were resuspended and centrifuged (200x g, 10 min, RT) to separate soluble and debris fraction. The supernatant after the centrifugation step was considered to be the soluble fraction, whereas the pellet represented the debris fraction. The pellet was resuspended in the same volume of the supernatant and both debris and soluble fraction where diluted several times before addition to target cells.

2.2.1.6. Stimulation of human monocytes and THP-1 macrophages

After overnight priming with ultra-pure LPS the medium of human monocytes and THP1 macrophages was replaced and cells were incubated with soluble and debris fractions of necrotic cells or stimulated with 1.5 mM ionomycin (SIGMA), 150 µg/ ml monosodium urate crystals (MSU) (provided by L. French, *University Hospital Zürich)* or 20 µM Nigericin (ENZO LIFE SCIENCES, *New York, US-NY*) for indicated time.
The soluble and the debris fractions of necrotic A2058 and A375 were diluted to have the 50-, 25-, 12.5-, 6.25- and 3.12-fold amount of necrotic cells added to the target cells.
Chemical inhibition was performed with addition of 5 µM Z-VAD-fmk (Z-VAD) (ENZO LIFE SCIENCES) 30 min before cell stimulation.
All experiments for western blotting analysis were performed in serum-free OptiMEM medium GIBCO BRL).
To de-methylate methylated genes, A375 melanoma cells were incubated with 2.5 µM 5-Aza-2′-deoxycytidine (AZA) (SIGMA) for 24 h.

2.2.1.7. In vitro cell proliferation and apoptosis

To compare *in vitro* proliferation of B16-F10 mouse melanoma cell line stably expressing shRNA to HMGB1 or Lamin, cells were cultured at 37 °C in 5 % CO_2 in DMEM medium (supplemented with 10 % FCS, 1 % GlutaMAX, 1 mM Sodium Pyruvate and 100 U/ml P/S) and samples were analyzed at different timepoints.

Appropriate cell numbers to have 1.5 × 10^5 cells at the timepoint of sample collection were seeded in 12-well plates. At days 0, 1, 2 and 3, mitochondrial dehydrogenase activity of living cells was measured by addition of 10 % MTT (SIGMA) for 4 h at 37 °C. Optical densities were measured by the SpectraMax190 plate reader (MOLECULAR DEVICES, *Sunnyvale, US-CA).*

Cells were incubated with PBS + 1µM CFSE (THERMO FISHER SCIENTIFIC) for 10 min at 37°C and appropriate cell numbers to have 6 × 10^5 cells at the timepoint of sample collection were seeded in 6-well plates. At days 0, 3, 6 and 8, cells were detached and CFSE-derived fluorescence intensity in cells was determined on a single-cell level using flow-cytometry. Acquisition was performed with a FACS Canto II (BECTON-DICKINSON, *Franklin Lakes, US-NJ*) and sample analysis was done using FACS DIVA software (BECTON-DICKINSON).

Appropriate cell numbers to have 1.5 × 10^5 cells at the timepoint of sample collection were seeded in 12-well plates. At days 0, 3, 6 and 9, cells were detached and stained with 1.0 µg/ml Propidium iodide (ROCHE, *Rotkreuz, Switzerland*) and 5 % Annexin V (BECTON-DICKINSON) for 15 min on ice. Acquisition was performed with a FACS Canto II and sample analysis was done using FACS DIVA software.

2.2.1.8. Hypoxia culture condition

To determine the release of HMGB1 under hypoxic conditions *in vitro*, primary cell cultures from 7 metastatic melanoma patients were cultured under hypoxic conditions and compared to cells cultured under normoxic conditions.

One million cells were cultured in 2.5 ml RPMI 1640 medium (supplemented with 10 % FCS, 1 % GlutaMAX, 1 mM Sodium Pyruvate and 100 U/ml P/S) in a MIC-101 Modular Incubator Chamber (BILLUPS-ROTHENBERG, *Del Mar, US-CA*) for 72 h.

At day 0, the chamber was flushed with 20 l/min (flowmeter: RMA-23-SSV. DWYER, *Michigan City, US-IN*) of certified pre-mixed gas composed of 1 % O_2, 5 % CO_2, and 94 % N_2 (CARBAGAS, *Guemlingen*, Switzerland).

The O_2 concentration inside the chamber was measured with a disposable VTI-122 Polarographic oxygen cell oxygen sensor (VASCULAR TECHNOLOGY, *Nashua, US-NH*). The hypoxia chamber as well as the control samples cultured under normoxic conditions were placed in an incubator at 37 °C for 72 h.

2.2.1.9. Viability measurement

For lysis analysis, LDH activity was measured in cell culture supernatants without cells (centrifuged at 1'500 g for 5 min at 4 °C) as well as cell lysates produced by incubation for 10 min with 2.5 ml culture medium containing 10 % Triton-X100 (SIGMA) with the CytoTox 96 assay (PROMEGA, *Madison, US-WC*). The samples were diluted as desired and analyzed in triplicates in 96-well plates according to the manufacturer's instructions. Optical densities after stop of the chromogenic reactions were measured by the Spectra Max190 plate reader (MOLECULAR DEVICES) at a wavelength of 490 nm using the Softmax software.

The percent of release was individually calculated for each well according to the formula

$$\% \, lysis = \frac{SN}{SN + Lys}$$

where SN is supernatant and Lys is lysate.

2.2.2. Animal experiments

2.2.2.1. Mice

Six to 8-week-old female C57BL/6 mice (HARLAN) were used in this study. TLR2$^{-/-}$ C57BL/6 mice were kindly provided by Prof. Marc Donath (Department of Biomedicine, University Hospital Basel, Switzerland), TLR4$^{-/-}$ C57BL/6 mice were kindly provided by Prof. Markus G. Manz (Division of Hematology, University Hospital Zurich, Switzerland) and RAGE$^{-/-}$ C57BL/6 mice were kindly provided by Prof. Peter P. Nawroth (Department of Internal Medicine I and Clinical Chemistry, University of Heidelberg, Germany). All experimental procedures were approved by the Veterinary Office of Zurich and the institutional animal care.

2.2.2.2. Tumor growth and metastasis experiments

Before subcutaneous injection of tumor cells into mice, the back skin was shaved with the electric animal shaver Favorita II (AESCULAP, *Suhl, Germany*).
1 x 10^5 Lamin-shRNA-transduced B16 or 1 x 10^5 HMGB1-shRNA-transduced B16 cells were injected subcutaneously in a volume of 100 µl PBS into the flank of WT C57BL/6 mice (HARLAN). Mice were monitored every other day and tumor size was measured using a caliper (MITUTOYO, *Kawasaki, Japan*). Tumor volume was expressed as the square of the smallest diameter multiplied by the largest diameter.
1 x 10^5 B16-F10 cells were injected subcutaneously in a volume of 100 µl PBS into the flank of WT C57BL/6 mice (HARLAN*)*. Additionally, mice were injected intraperitoneally with 100 µl 500 µg/ml BoxA (HMGBIOTECH), an antagonist for HMGB1 receptor binding, or PBS at the day of injection. Mice were monitored at least every third day and tumor size was measured using a caliper. Tumor volume was expressed as the square of the smallest diameter multiplied by the largest diameter
1 x 10^5 Lamin-shRNA-transduced B16 or 1 x 10^5 HMGB1-shRNA-transduced B16 cells were injected subcutaneously in a volume of 100 µl PBS into the flank of WT C57BL/6 mice (HARLAN*)*. Additionally, mice were injected intraperitoneally with 100 µl 0.5 mg/ml anti-mouse IL-10 antibody (BIOLEGEND, *San Diego, US-CA*) or PBS every other day. Mice were monitored at least every second day and tumor size was measured using a caliper. Tumor volume was expressed as the square of the smallest diameter multiplied by the largest diameter.
To generate lung metastasis, 1 x 10^5 Lamin-shRNA-transduced B16 or 1 x 10^5 HMGB1-shRNA-transduced B16 cells were injected intravenously in a volume of 100 µl PBS into the tail vein of WT C57BL/6 mice (HARLAN*)*. Mice were sacrificed by CO_2 inhalation 13 days

after tumor cell inoculation, and the number of macroscopically visible melanoma metastases on the surface of the lungs was counted in a masked manner by two different experimenters.

2.2.2.3. Flow cytometry analysis of tumor-infiltrating cells

For the preparation of tumor infiltrating cell suspensions, minced tumors were placed in Eppendorf tubes filled with 1 ml RPMI 1640 medium (supplemented with 2 % FCS, 1 % GlutaMAX, 1 mM Sodium Pyruvate and 100 U/ml P/S) and 1.5 mg/ml Collagenase D (ROCHE DIAGNOSTICS, *Rotkreuz, Switz*erland) and incubated for 60 min at 300 rpm and 37 °C in an Eppendorf Thermomixer Compact (EPPENDORF, *Hamburg, Germany).* The cell suspensions were filtered through a 40 µm Nylon cell strainer (CORNING INC.), washed twice with cold PBS, transferred to a *96-Well Round Bottom Plate and stained for 30 min on ice with* anti-mouse 7/4 antibody (ABCAM, *Cambridge, UK*), anti-mouse CD11b (BIOLEGEND) and anti-mouse CD45 (BECTON-DICKINSON) antibodies.
Stained samples were washed twice with cold FACS buffer (2% FCS in PBS) and transferred to 5 ml Polystyrene Round-Bottom Tubes (BECTON-DICKINSON). The absolute numbers of each cell subset were calculated by flow cytometry and presented are the numbers per mm^3 of tumor. Flow-cytometric analysis was performed with a FACS Canto II. Sample analysis was done using FACS DIVA software.

2.2.3. Histology and Immunohistochemistry

For histological examination, tissues embedded in paraffin were cut in sections of 2 µm thickness with a Hyrax M25 microtome (CARL ZEISS, *Oberkochen, Germany*). After heating the slides for 30 min at 70 °C, they were incubated for 10 min in Xylene (THOMMEN FURLER AG, *Rüti bei Büren, Switzerland)* and for 5 min in each concentration of a descending alcohol series (Ethanol absolut, 96 %, 80 % and 70 %) followed by incubation in PBS for 5 min. The slides were plunged into Target Retrieval Solution (DAKO, *Glostrup, Denmark*) and vaporized for 25 min in a Steamer MultiGourmet Typ 3216 (BRAUN, *Kronberg, Germany*). When cooled down to room temperature, the samples were washed once in PBS and placed into a chamber covered with aluminium foil. To economize the need of liquid materials in the following steps, the borders of the sections were surrounded with a delimiting pen (DAKO). Antibody penetration was improved by incubation of the slides for 10 min with 0.03 % Triton-X100 in PBS. After three washing steps in PBS, the slides were incubated with blocking solution consisting of 5 % BSA (PAA, *Pasching, Austria*) and 5 % Goat serum (SIGMA) in PBS and then directly without further washing in PBS stained with appropriate primary antibodies diluted in Antibody Diluent (DAKO).

To determine Hif-1α, sections were stained overnight at 4 °C with 10 µg/ml mouse monoclonal anti-mouse Hif-1α (ABCAM) or isotype IgG control antibody (ABCAM) at the same concentration.

After three washing steps in PBS, samples were incubated for 60 min at room temperature with 0.5 mg/ml biotinylated goat anti-mouse IgG (ABCAM), washed again three times with PBS and coupled to 1 µg/ml streptavidin-alkaline phosphatase (VECTOR LABORATORIES, *Burlingame, US-CA*) for 45 min at room temperature. Alkaline phosphatase activity was revealed with the DAKO real detection system (DAKO) following manufacturers' instructions.

After coloration for 40 s with Haematoxylin solution (SIGMA), slides were mounted with Faramount Mounting Medium (DAKO) and Microscope Cover Slips (THERMO FISHER SCIENTIFIC). Sample scanning was performed with the digital slide scanner NanoZoomer-XR C12000 (HAMAMATSU Photonics, *Hamamatsu, Japan).* Pictures were analyzed with the ImageJ software (open source from national institutes of health).

To determine HMGB1 and Hif-1α, sections were stained overnight at 4 °C with 1 µg/ml rabbit polyclonal anti-mouse HMGB1 (ABCAM) and 10 µg/ml mouse monoclonal anti-mouse Hif-1α (ABCAM) antibodies or with isotype IgG control antibodies (ABCAM) at corresponding concentrations. To determine IL-10 and CD163, sections were stained overnight at 4 °C with 160 µg/ml rabbit polyclonal anti-human IL-10 (ABCAM) and 10 µg/ml mouse monoclonal anti-human CD163 (LEICA BIOSYSTEMS, *Wetzlar, Germany*) antibodies or with isotype IgG control antibodies (ABCAM) at corresponding concentrations.

After three washing steps in PBS, samples were incubated for 60 min at room temperature with conjugated secondary antibodies to visualize target molecules. For HMGB1 and IL-10, 5 µg/ml Alexa Fluor® 546 goat anti-rabbit IgG (LIFE TECHNOLOGIES, *Carlsbad, US-CA*) and for Hif-1α and CD163, 1.25 µg/ml DyeLight® 650 goat anti-mouse IgG (ABCAM) were used.
Slides mounted with Fluorescence Mounting Medium (DAKO) and Microscope Cover Slips (THERMO FISHER SCIENTIFIC) were analyzed with a Widefield BX61 multicolor fluorescence microscope (OLYMPUS, *Tokyo, Japan*) at 20- and 40- fold magnification. Pictures were acquired and analyzed with the Analysis Pro software (SOFT IMAGING SYSTEMS, *Münster, Germany*).
All studies were read by the same pathologist using the same subjective grading scale.

2.2.4. Microbiological methods

2.2.4.1. Cultivation and storage of E.coli strains

E.coli cells were suspended in an appropriate amount of LB - medium and grown at 37 °C on a Lab Therm shaker (KUHNER AG, *Birsfelden, Switzerland*) at 180 – 230 rpm until the required OD600 was reached.

LB-Medium	
Tryptone	1 % (w/v)
Yeast extract	0.5 % (w/v)
NaCl	1 % (w/v)

If required, 100 µg/ ml Ampicillin (SIGMA) was added to the medium. To cultivate *E.coli* on agar plates, they were spread over the plate and incubated at 37 °C. Agar plates were produced by adding 1.5 % (w/ v) agar to the LB – medium before autoclaving. This medium was poured into petri dishes. If required, an appropriate amount of antibiotic was added to the medium after cooling down to ~55 °C. Plates with *E.coli* were sealed with parafilm and stored at 4 °C.

2.2.4.2. Preparation of transformation-competent E.coli

A fresh overnight culture of transformation – competent E.*coli* BL21 (AMERSHAM, *Uppsala, Sweden*) or XL-1 Blue (STRATAGENE, *La Jolla, US-CA)* was diluted 1:100 with LB – medium and shaken at 37 °C until the optical density at 600 nm was between 0.4 and 0.5.
After centrifugation (600 x g, 10 min, 4 °C), the bacterial pellet was carefully resuspended in cold, sterile 100 mM $MgCl_2$ solution (FLUKA CHEMIE, *Buchs, Switzerland)* (1/ 4 of the original volume). The mixture was incubated on ice for 30 min, centrifuged as described above and the pellet was resuspended in cold, sterile 100 mM $CaCl_2$ solution (FLUKA CHEMIE) (1/ 50 of the original volume). The mixture was incubated 3 – 4 h on ice. Cold, sterile glycerol (MERCK) was added to a final concentration of 30 %, the mixture was aliquoted and stored at – 80°C.

2.2.5. Molecular biological methods

2.2.5.1. Transformation of competent E.coli with plasmid DNA

100 µl transformation – competent E.*coli* cells were mixed with 10 µl plasmid or ligation mix (~100ng DNA) and incubated on ice for 30 – 60 min. The mixture was subjected to a heat – shock (2 min at 42 °C) and put on ice. 500 µl LB – medium were added to the mix and shaken for 30 min at 37 °C. Subsequently, the mix was plated on 2 – 3 LB plates, containing the corresponding selection marker, and incubated overnight at 37 °C.

2.2.5.2. Preparation of plasmid DNA from E.coli

2.2.5.2.1. Small scale plasmid preparation with the Plasmid Midi Kit

In order to quickly get small amounts of plasmid DNA, solutions from the Plasmid Midi Kit (QIAGEN) were used. The principle of this method is an alkaline lysis of the cells with subsequent precipitation of proteins, lipids and genomic DNA followed by centrifugation. The plasmid DNA in the supernatant was precipitated by ethanol. The obtained purity and amount of plasmid DNA is sufficient for a subsequent analysis by restriction enzyme digest or sequencing.

1.5 ml of 2 ml overnight bacterial LB culture with the appropriate antibiotic was transferred to a microcentrifuge tube and centrifuged (1’500 x g, 6 min, 4 °C). The pellet was resuspended in 150 µl Resuspension buffer I by pipetting up and down. 150 µl of Lysis buffer II were added and incubated for 3 min at RT while inverting the tubes. To stop lysis and to precipitate proteins and lipids, 150 µl of Neutralization buffer III were added. The tubes were inverted several times and centrifuged (16’200 x g, 10 min, 4 °C). The supernatant was transferred to a new tube with 800 µl ethanol and mixed. This step precipitates plasmid DNA. After incubating the tubes 15 min on ice, they were centrifuged (16’200 x g, 20 min, 4 °C). The pellets were washed with 200 µl 70 % ethanol and centrifuged again (16’200 x g, 2 min, 4 °C). The supernatant was removed by inverting the tubes with subsequent drying of the plasmid pellet in a Speed Vac (EPPENDORF) apparatus. The DNA containing pellet was resuspended in 20 µl H_2O and the nucleic acid concentration was determined. Plasmid preparations were stored at -20 °C.

Resuspension buffer I	
EDTA	10 mM
RNAse A	100 µl/ ml
TRIS/ HCl	50 mM

Stored at 4 °C after addition of RNAse A

Lysis buffer II	
SDS	1 % (w/v)
NaOH	200 mM

Neutralization buffer III
Potassium acetate (3 M, pH 5.5)

2.2.5.2.2. Middle scale plasmid extraction with the Plasmid Midi/ Maxi Kit

The Plasmid Midi/ Maxi Kit (QIAGEN) were used and plasmid isolation was performed according to the manufacturers' instructions. Plasmids used for transfection of eukaryotic cells were isolated with the endofree versions of the isolation kits. Plasmid DNA was stored at -20 °C.

2.2.5.3. Determination of the nucleic acid concentration

In order to determine the concentration of DNA or RNA solutions, the absorption at 260 nm was measured. This was done using the UVS-99 Micro-Volume Spectrophotometer (ACTGene, *Piscataway, US-NJ*) according to the manufacturers' instructions. ddH_2O or the elution solution from the appropriate isolation kit was used as a blank. Because proteins in solution absorb light at 280 nm, the ratio between OD260 and OD280 was taken as an indicator for the purity of the nucleic acid. The optimal value is 1.8.

2.2.5.4. Agarose gel electrophoresis of DNA

DNA molecules were separated by agarose gel electrophoresis for analytical and preparative purpose. Gels with an agarose content of 0.8 – 2 % (w/ v) in TAE buffer were used. Agarose concentration was dependent on the fragment length. Electrophoresis was performed in an agarose gel electrophoresis system (BIORAD, *Cressier, Switzerland*) at 100 – 150 V. To visualize DNA bands, 1 mg ethidium bromide (SIGMA) was added per 1 ml gel. The DNA samples were mixed with 5 x loading buffer before loading them into the slots.

5x loading buffer	
Orange G	0.2 % (w/v)
Glycerol	60 % (v/v)
EDTA	60 mM
TAE	1x

1x TAE	
TRIS/ HCl	40 mM
Acetic acid	40 mM
EDTA	1 mM
pH 8.0	

The bands were visualized under UV light and photographed with a GeneFlash (SYNGENE, *Cambridge, UK*). As size standards pUC Mix DNA marker (MBI FERMENTAS*, Nunningen, Switzerland)* or 1 kb DNA ladder NEW ENGLAND BIOLABS (NEB, *Beverly, US-MA)* were used, depending on the analyzed fragment length. For cloning of fragments, the bands of interest were excised with a scalpel under UV light. The UV irradiation was kept as short as possible because prolonged exposure to UV damages DNA.
The DNA was purified from the gel with the Gel Extraction Kit according to the manufacturers' instructions.

2.2.5.5. Isolation of total cellular RNA from eukaryotic cells

For mRNA collection from murine B16 melanoma, minced tumors were transferred to Eppendorf tubes filled with 350 µl RLT lysis buffer (QIAGEN), 10 µl 14.3 M β-Mercaptoethanol (SIGMA) and iron beads. The tubes were incubated for 60 min at 300 rpm in a thermomixer (EPPENDORF) and RNA was isolated using the Qiagen RNeasy kit (QIAGEN) following manufacturers' instructions.
For mRNA collection of *in vitro* cell cultures, supernatants were removed and cells were washed twice with cold PBS. RNA was isolated using the Qiagen RNeasy kit following manufacturers' instructions.
The RNA concentration of the samples was determined with a UVS-99 Micro-Volume Spectrophotometer. Samples were stored at -20 °C.

2.2.5.6. Preparation of cDNA by reverse transcription

Synthesis of cDNA from total cellular RNA was performed using the RevertAid First Strand cDNA Synthesis Kit (THERMO FISHER SCIENTIFIC) according to the manufacturers' instructions:

RNA-Hexamer solution	
RNA	1 µg
Random Hexamer Primer	1 µl
H_2O	add. 12 µl

The RNA-Hexamer mix was incubated for 5 min at 65 °C in a TProfessional Thermocycler (BIOMETRA, *Göttingen, Germany*) and then placed on ice.

Reverse Transcriptase solution	
5x Reaction buffer	4 µl
RiboLock RNase inhibitor (40 U/µL)	1 µl
10mM dNTP Mix	2 µl
RevertAid Reverse Transcriptase (200 U/µL)	1 µl

RNA-Hexamer solution and Reverse Transcriptase solution were mixed gently by tapping the tube. The mixture was briefly spinned down and proceeded in the thermocycler for 5 min at 25 °C, for 60 min at 42 °C and for 5 min at 70 °C. Samples were stored at -20 °C.

2.2.5.7. Quantitative Real-time PCR (qRT-PCR)

Relative quantification of gene expression at the RNA level was performed using FastStart Universal SYBR Green Master (ROCHE). The real-time PCR was performed with cDNA from total cellular RNA or from tissue RNA and a primer pair designed to a fragment of ~150 bp in length flanking an intron-exon border of the desired gene. To quantify the relative expression level of a certain gene, two reaction mixes were prepared. One contained the primer pair targeting the gene of interest, the other contained a primer pair targeting an internal reference gene (RPL27). The following mixture was prepared on ice in 0.1 ml MicroAmp® Fast Optical 96-Well Reaction Plates (LIFE TECHNOLOGIES):

Real-time PCR reaction mix	
Template cDNA	~5 – 100 ng
5`-Primer (3.75 µM)	0.66 µl
3`-Primer (3.75 µM)	0.66 µl
SYBR Green Master	5 µl
ddH_2O	add. 10 µl

The PCR reaction and detection were performed in the ViiA™ 7 Real-Time PCR System (LIFE TECHNOLOGIES*)* according to the manufacturers' instructions. The following temperature program was applied:

Real-time PCR program			
First denaturation step	10 min	95 °C	
Denaturation step	10 s	95 °C	40 cycles
Primer annealing and extension	30 s	58 °C	
	15 s	95 °C	dissociation curve
	20 s	60 °C	
	15 s	95 °C	

Specificity of the reaction was ensured by surveying the dissociation curve of a given primer pair. Data processing was performed using the ViiA™ 7 Real-Time PCR System software (LIFE TECHNOLOGIES) provided by the manufacturers according to the guidelines. Expression of mRNA (relative) was normalized to the expression of RPL27 mRNA by the change in cycling threshold (ΔC_T) method and calculated based on $2^{-\Delta\Delta CT}$.

2.2.5.8. MeDIP analysis

MeDIP analysis of four melanoma cell cultures taken from GSE57971. Acquisition and analysis was performed using Nimblescan 2.5 and R package DMR (ROCHE NIMBLEGEN INC, *Madison, US-WI*). A log2 ratio > 1 and FDR adjusted p-value < 0.05 was deemed to be significant.

2.2.6. General protein methods

2.2.6.1. Enzyme-linked immunosorbent assay (ELISA)

Cell culture supernatants were collected at indicated time points and analyzed for presence of secreted human IL-1β by ELISA with an ELISA kit from R&D Systems (Minneapolis, *US-MN*) according to the manufacturer's instructions.
To determine the concentration of HMGB1 in the serum of healthy donors, primary melanoma patients and melanoma patients with metastasis, serum samples were analyzed using an ELISA kit for HMGB1 (IBL INTERNATIONAL, *Hamburg, Germany*) according to the manufacturers' instructions.
To determine the concentration of released HMGB1 from *in vitro* cell cultures, supernatants were centrifuged at 1'500 g for 5 min at 4 °C and analyzed using the HMGB1 ELISA kit according to the manufacturers' instructions.
Optical densities were measured by the Spectra Max190 plate reader (MOLECULAR DEVICES) at a wavelength of 450 nm using the Softmax software.

2.2.6.2. Determination of protein concentration

Protein concentration of a solution was determined by the BCA protein assay (PIERCE, *Rockford, US-IL*). The assay was performed in duplicates according to the manufacturers' instructions using 96-well plates and a BSA serial dilution in the appropriate buffer for the standard curve. Optical densities were measured by the SpectraMax190 plate reader (MOLECULAR DEVICES) at a wavelength of 562 nm and protein concentrations were calculated using the Softmax software.
Alternatively, optical density at 280 nm was determined by a UVS-99 Micro-Volume Spectrophotometer according to the manufacturers' instructions.

2.2.6.3. SDS-polyacrylamide gel electrophoresis (SDS-PAGE)

To separate proteins according to their size by SDS-PAGE, the buffer system of Laemmli [1] was used. This contains glycine as a zwitter ion. The electrophoresis was carried out in vertical direction using the SE 250 mini gel system (AMERSHAM) in 1 mm thick polyacrylamide gels of appropriate acrylamide concentration depending on the protein size. The gel contains a 1 cm long 5 % stacking gel and a 6 cm long 8 – 20 % separating gel.
Before loading the samples, they were mixed with an equal volume of 2 x sample loading buffer and incubated for 5 min at 95 °C. Electrophoresis was performed at 75 V until the loading dye reached the separating gel and then at 100 – 140 V until the loading dye reached the bottom of the gel. Prestained protein molecular weight marker (MBI FERMENTAS) was used in all gels.

Separating gel (5 % Acrylamide)

% Acrylamide	8 %	10 %	12.5 %	15 %	18 %	20 %
Acrylamide/ bisacrylamide	11.4 ml	13.3 ml	16.8 ml	20.0 ml	23.0 ml	24.2 ml
TRIS/ HCl (1M, pH 8.8)	15.0 ml	15.0 ml	15.0 ml	15.0 ml	15.0 ml	15.0 ml
ddH_2O	13.4 ml	11.5 ml	7.4 ml	4.2 ml	1.2 ml	-
SDS (10 % [w/v])	400 µl	400 µl	400 µl	400 µl	400 µl	400 µl
APS (20 % [w/v])	200 µl	200 µl	200 µl	200 µl	200 µl	200 µl
TEMED	16 µl	16 µl	16 µl	16 µl	16 µl	16 µl

Stacking gel (5 % Acrylamide)

Acrylamide/ bisacrylamide (30:0.8)	2.7 ml
TRIS/ HCl (1 M, pH 6.8)	2.0 ml
ddH_2O	10.8 ml
SDS (10 % [w/v])	160 µl
APS (20 % [w/v])	80 µl
TEMED	16 µl

SDS-PAGE running buffer	
TRIS/ HCl (pH 8.0)	25 mM
Glycine	192 mM
SDS	10 % (v/v)

2x sample loading buffer	
TRIS/ HCl (pH 8.0)	100 mM
Glycerol	20 % (v/v)
SDS	10 % (v/v)
Bromphenol blue	0.01 % (w/v)
DTT (1 M)	20 % (v/v)

2.2.6.4. Western blot

For the detection of specific proteins by western blotting, electrophoretically separated proteins were transferred onto a nitrocellulose membrane. After blocking of unspecific binding sites, the membrane was incubated with the primary and the corresponding secondary antibody. Secondary antibodies are coupled to an enzyme that catalyzes the detection reaction.

2.2.6.4.1. Protein transfer by semi-dry blotting

Three sheets of Whatman 3MM paper (WHATMAN, *Maidstone, England)* were soaked in anode buffer I and placed on the anode side of the blotting apparatus. Two sheets of Whatman paper were soaked in anode buffer II and place on top of the first sheets. The nitrocellulose membrane (SCHLEICHER & SCHUELL, *Dassel, Germany)* was equilibrated in anode buffer II and subsequently placed onto the Whatman papers, followed by the gel, which was carefully pressed onto the membrane to avoid air bubbles in between. Finally, three sheets of Whatman paper soaked in cathode buffer were place on top of the gel. Blotting was performed in a semi-dry blotter (Z340502, SIGMA) at 75 mAmp per gel for 30 min.

Anode buffer I	
Methanol	20 % (v/v)
TRIS/ HCl	300 mM

Anode buffer II	
Methanol	20 % (v/v)
TRIS/ HCl	25 mM

Cathode buffer	
Methanol	20 % (v/v)
TRIS/ HCl	25 mM
ε-Aminocaproic acid	40 mM

2.2.6.4.2. Incubation with antibodies and visualization of protein bands

Unspecific binding sites were blocked with 3 % milk powder (MIGROS, *Zurich, Switzerland*) in PBST (blocking solution) for at least 30 min. The membranes were then incubated with the primary antibody in blocking solution overnight at 4 °C. After washing three times in PBST for 5 min, the membranes were incubates with the corresponding secondary antibody in blocking solution for 30 min at RT. Secondary antibodies were coupled to alkaline phosphatase (AP). After incubation, the membranes were washed three times for 5 min.
AP detection was performed using the NBT/ BCIP substrate kit (PROMEGA). The membrane was washed once with AP buffer and incubated in AP buffer containing 33 µl BCIP and 66 µl NBT per 10 ml of buffer. Reaction was stopped with H_2O when desired band intensities were obtained.

AP buffer	
TRIS/ HCl (pH 9.5)	100 mM
NaCl	100 mM
$MgCl_2$	5 mM

2.2.6.5. Imaging of blots and stained gels

Blots were scanned using the CanonScan 9950F device (CANON, *Tokio, Japan* Images were acquired with 150 – 300 dpi resolution without filters or other altered acquisition settings. Digital image processing was performed using Photoshop software (various versions, ADOBE SYSTEMS SOFTWARE, *San Jose, US-CA).* Processing was restricted to cutting. When the observed bands in the original blots were too weak for meaningful digital and print reproduction, brightness and contrast adjustments were applied to the whole image until the scientific result reflected the one seen on the original blot.

2.2.6.6. Statistical analyses

Unless otherwise indicated, data are presented as the means ± standard error of the mean (SEM) and are representative of three independent experiments. Statistical analysis and graphic presentation of the results was performed using the Prism Software (GRAPHPAD SOFTWARE, *San Diego, US-CA*). *P*-values were calculated with the unpaired Student's *t* test. Differences were considered significant when: ** P≤0.05, ** P≤0.001*, **** P≤0.0001* and ***** P≤0.00001*.

Reference

1. Laemmli, U.K., *Cleavage of structural proteins during the assembly of the head of bacteriophage T4.* Nature, 1970. **227**(5259): p. 680-5.

3. Results

3.1. Metastatic melanoma cell lines do not secrete IL-1β but promote IL-1β production from macrophages

Introduction, results and discussion

Journal of Dermatological Science

Volume 74, Issue 2, May 2014, Pages 167-169

Letter to the Editor

Metastatic melanoma cell lines do not secrete IL-1β but promote IL-1β production from macrophages

Roman Huber[1], Samuel Gehrke[1], Atsushi Otsuka[1], Barbara Meier, Magdalena Kistowka, Gabriele Fenini, Phil Cheng, Reinhard Dummer, Katrin Kerl, Emmanuel Contassot[2], Lars E. French[2]

Department of Dermatology, University Hospital Zurich, Zurich 8091, Switzerland
Received 8 October 2013, Available online 24 January 2014

DOI: 10.1016/j.jdermsci.2014.01.006

Abbreviations

IL-1β, interleukin-1β; SSM, superficially spreading melanoma; NM, nodular melanoma; NLR, nucleotide oligomerization domain-like receptor; ASC, apoptosis-associated speck-like protein containing a caspase recruitment domain

Keywords

Melanoma; IL-1β; Inflammasome; Macrophage

[1] These authors contributed equally to this work.

[2] Corresponding authors at: Department of Dermatology, University Hospital Zurich, Gloriastrasse 31, Zurich 8091, Switzerland. Tel.: +41 44 255 2550; fax: +41 44 255 4403.

To the Editor

Tumors secrete pro-inflammatory cytokines, chemokines, and other soluble factors in the microenvironment. Interleukin-1β (IL-1β) is a pleiotropic pro-inflammatory cytokine involved in cell growth, differentiation, and regulation of immune responses [1]. IL-1β is often detected in human cancer tissues including breast cancer, pancreatic cancer, and glioblastoma [2]. It has been reported that the expression levels of the IL-1β gene or protein are associated with the invasiveness and metastasis of cancers [3]. On the other hand, IL-1β production from tumor cells may be considered as a threat by the host's immune system. In this aspect, it has been reported that IL-1β-producing melanoma cells induce reduced tumor growth by recruiting immune cells [4]. Therefore, melanoma cells must have a precise mechanism of IL-1β regulation but it remains largely unknown.

IL-1β is first synthesized as a biologically inactive precursor (pro-IL-1β). Pro-IL-1β is then cleaved by caspase-1 to biologically active mature IL-1β, resulting in its release into the extracellular space [1]. Therefore, we first analyzed IL-1β production from melanoma cell lines. THP-1 macrophages and melanoma cells were primed or not with phorbol-12-myristate-13-acetate (PMA, 500 nM) and exposed to the IL-1β inducer ionomycin (1.5 mM). Under these conditions and in contrast to THP-1 monocytic cells, 13 metastatic melanoma cell lines were not able to secrete IL-1β (Figure 1a). Inflammasomes are a multi-protein complexes whose assembly and activation are responsible for the processing of caspases-1 and -5 [1]. The NOD-like receptor pyrin domain containing-3 (NLRP3) inflammasome has been the most studied inflammasome to date. This high molecular weight complex is composed of NLRP3, apoptosis-associated speck-like protein containing a CARD domain (ASC) adaptor protein, and the cysteine protease caspase-1 [1]. Assembly of the NLRP3 inflammasome activates caspase-1, which mediates maturation of proinflammatory cytokines such as IL-1β and IL-18.

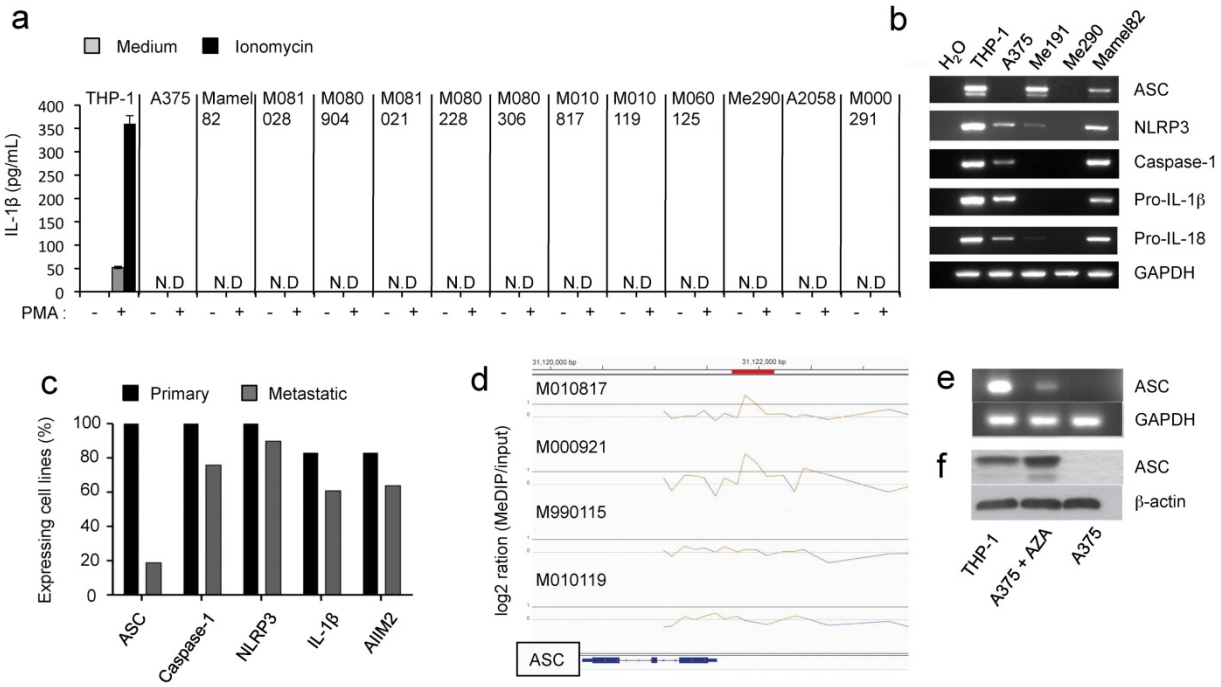

Figure 1. Metastatic melanoma cells are not able to secrete IL-1β

(a) IL-1β secretion by THP-1 macrophages and A375 and Mamel82 metastatic human melanoma cell lines by analyzing supernatants from their culture by ELISA (R&D Systems, Minneapolis, MN). N.D. not detected.

(b) mRNA expression of ASC, NLRP3, caspase-1, pro-IL-1β, pro-IL-18, and GAPDH in THP-1 and metastatic melanoma cell lines. Total RNA from THP-1 cells and metastatic melanoma cell lines (A375, Me191, Me290, and MaMel82) was isolated with an RNeasy Mini Kit (QIAGEN, Hilden Germany). RT-PCR was performed with a thermal cycler (Biometra, Gottingen, Germany).

(c) Evaluation of the expression of inflammasome components and IL-1β in primary (n = 6) and metastatic (n = 21) melanoma cell lines by RT-PCR.

(d) MeDIP analysis of four melanoma cell cultures. Two melanoma cell cultures, M010817 and M000921 were significantly methylated in the promoter region of ASC having a log 2 ratio >1 of methylated DNA compared to input. The other two-melanoma cell cultures, M990115 and M010119, were not significantly methylated in the promoter region of ASC.

(e) A375 human metastatic melanoma cells were treated with 2.5 mM AZA for 24 h and ASC expression was assessed by RT-PCR and

(f) Western blotting. All data are presented as mean ± SD and are representative of two experiments. P-values were calculated with Wilcoxon singled-rank test. *p < 0.05.

To address the expression levels of inflammasome components in metastatic melanoma cells, we performed reverse transcription polymerase chain reaction (RT-PCR) analyses. In contrast to THP-1 cells, one or several inflammasome components were not expressed in A375, Me191, and Me290 metastatic melanoma cell lines [5, 6] (Figure 1b). In addition, pro-IL-1β and pro-IL-18 transcripts were not detected in Me191 and Me290 cells (Figure 1b). To further determine the expression pattern of inflammasome components in melanoma cells, we used 6 primary and 21 metastatic melanoma cell lines as reported previously (Supplemental Tables 1 and 2) [5, 6]. One hundred percent of cell lines derived from primary

melanomas expressed *ASC*. In contrast, only 19 percent of cell lines derived from metastatic melanomas expressed *ASC* (Figure 1c). Also, caspase-1, NLRP3, IL-1β, and AIM2 were expressed in a lower proportion of metastatic melanoma cell lines when compared to cell lines derived from primary melanoma cell lines (Figure 1c). In tumors, ASC expression is inversely correlated with the methylation status of the *ASC* promoter region [7]. Analysis of the methylation profile of ASC by MeDIP [8] revealed that 2 out of 4 tested cell lines had a methylated *ASC*-promoter (Figure 1d). M000921 and M010817 [5, 6] were found to have DNA methylation in the promoter region of *ASC* but not M990115 and M010119 [5, 6]. ASC expression was then assessed by qRT-PCR and showed to inversely correlate with *ASC* methylation (data not shown). Consistently with this observation, a treatment with the demethylating agent AZA (2.5 μM) induced the restoration of ASC expression as observed by RT-PCR (Figure 1e) and western blotting (Figure 1f). These results suggest that most of metastatic melanoma cell lines did not secrete IL-1β because of the lack of one or more inflammasome components, and DNA methylation is one of the mechanisms that can silence the expression of these components.

Macrophages are potent producers of IL-1β and reported to be present in the melanoma skin lesion [9]. Necrotic melanoma cells are often found in cutaneous melanomas of patients with progressive disease [10] and may be a source of DAMPs sensed by NLRs [1]. Therefore, we next analyzed whether necrotic melanoma cells promote IL-1β production from macrophages. The soluble fraction and debris from necrotic A2058, and A375 melanoma cell lines promoted IL-1β production from human primary monocytes in a dose-dependent manner (Figure 2a). We also show that IL-1β production from THP-1 macrophages was detected after adding soluble fraction or debris from necrotic melanoma cells (Figure 2b). A pre-treatment of THP-1 cells with the caspase inhibitor Z-VAD-fmk (Z-VAD) (5 μM) prior to exposure to the soluble fraction or debris from necrotic A375 melanoma cells significantly suppressed IL-1β production (Figure 2c), suggesting a caspase-dependent mechanism. To further confirm that IL-1β production from THP-1 cells depends on inflammasome activation, we generated ASC, caspase-1, and NLRP3 knock-down THP-1 macrophages. All THP-1 cells transduced with either ASC-shRNA, NLRP3-shRNA or caspase-1-shRNAs showed a dramatic decrease of IL-1β production compared to control lamin-shRNA THP-1 (Figure 2d), demonstrating that IL-1β release upon exposure to products of necrotic melanoma cells depends on the NLRP3 inflammasome. Finally, we examined IL-1β expression in nevi, superficially spreading melanomas (SSM), nodular melanomas (NM), and skin metastases of melanoma by immunohistochemistry. IL-1β positive cells were not detected in nevi and SSM, whilst they were in NM and skin metastasis of melanoma (Figure 2e). Consistent with *in vitro* experiments, these IL-1β positive cells were melanophages but not melanoma cells.

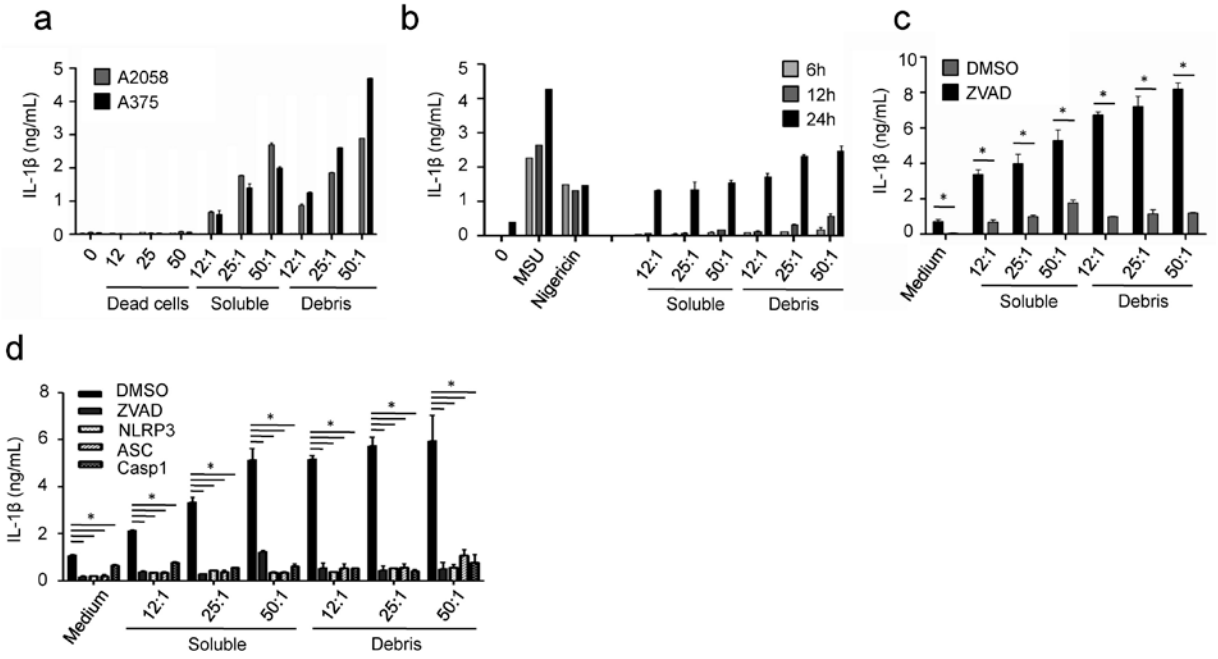

Figure 2. Necrotic melanoma cells promote IL-1β secretion from macrophages

(a) Human primary monocytes were exposed to different proportions of necrotic cells (A2059/A375 human metastatic melanoma) per for 24 h and IL-1β secretion was measured in the supernatant with ELISA. Necrotic products of cells were separated between soluble and debris fraction.

(b) THP-1 macrophages were treated with inflammasome activators (MSU, 150 µg/ml and Nigericin, 5 µM), or necrotic (debris or supernatant?) A375 metastatic human melanoma cell line for 6, 12, and 24 h and IL-1β secretion was measured in the culture supernatant with ELISA.

(c) THP-1 cells pre-treated with ZVAD for 30 min were incubated with necrotic A375 for 24 h and IL-1β secretion was measured in the supernatant with ELISA.

(d) NLRP3, ASC and caspase-1 knock down THP-1 were incubated with necrotic soluble of A375 for 24 h and IL-1β secretion was measured in the supernatants with ELISA and compared to the one of lamin knock down exposed to DMSO (vehicle) or ZVAD. All IL-1β ELISA data are presented as mean ± SD and are representative of two experiments. P-values were calculated with Wilcoxon singled-rank test. *$p < 0.05$.

In summary, we demonstrate that the inability of metastatic melanoma cells to secrete IL-1β is due to the lack of expression of one or more inflammasome components. On the other hand, one or more factors originating from necrotic melanoma cells can promote IL-1β production by macrophages. Taken together, metastatic melanoma cells seem to have lost the ability for IL-1β production whereas macrophages of the microenvironment secrete high amounts of IL-1β in response to putative danger signals released by necrotic tumor cells. It has been reported that the expression levels of the IL-1β protein are associated with the invasiveness and metastasis of cancers. In this respect, IL-1β is an important factor for the expansion of metastatic melanoma. However, the cellular source of IL-1β in tumors is not clear. Here, we demonstrate that IL-1β is produced by macrophages upon stimulation with

danger signals from necrotic melanoma cells. Although not being able to produce IL-1β themselves, tumor cells may benefit from IL-1β release by macrophages present in the micro-environment. A better understanding of the mechanisms and consequences of IL-1β production by infiltrating macrophages may be of interest for the development of IL-1β targeted therapy, such as anti-IL-1β antibody (Canakinumab), of metastatic melanoma.

Acknowledgements

This work was supported in part by the Association for International Cancer Research, AICR 09-0230 to L.E.F., and Oncosuisse. We thank Marianne Spalinger and Tatiana Proust for technical assistance.

Personal contribution

In this work, I contributed with designing, performing, analyzing and interpreting experiments.

- Collection of human melanoma cell lines.
- Experiments to monitor the release of IL-1β of human melanoma cell lines after treatment with inflammasome activators.
- Assessment of the expression of inflammasome components in human melanoma samples.
- Measurement of the expression of ASC on mRNA and protein level following treatment with AZA.
- Treatment of human primary monocytes with both soluble and debris fractions of necrotic melanoma cell lines as well as with inflammasome activators at different concentrations and timepoints with evaluation of the release of IL-1β.
- Incubation of THP-1 macrophages with both soluble and debris fractions of necrotic melanoma cell lines in the presence of ZVAD with evaluation of the release of IL-1β.
- Treatment of THP-1 macrophages exhibiting a knock-down for different inflammsome components with both soluble and debris fractions of necrotic melanoma cell lines with evaluation of the release of IL-1β.

References

1. Gross, O., et al., *The inflammasome: an integrated view.* Immunol Rev, 2011. **243**(1): p. 136-51.

2. Arlt, A., et al., *Autocrine production of interleukin 1beta confers constitutive nuclear factor kappaB activity and chemoresistance in pancreatic carcinoma cell lines.* Cancer Res, 2002. **62**(3): p. 910-6.

3. Elaraj, D.M., et al., *The role of interleukin 1 in growth and metastasis of human cancer xenografts.* Clin Cancer Res, 2006. **12**(4): p. 1088-96.

4. Bjorkdahl, O., et al., *Gene transfer of a hybrid interleukin-1 beta gene to B16 mouse melanoma recruits leucocyte subsets and reduces tumour growth in vivo.* Cancer Immunol Immunother, 1997. **44**(5): p. 273-81.

5. Zipser, M.C., et al., *A proliferative melanoma cell phenotype is responsive to RAF/MEK inhibition independent of BRAF mutation status.* Pigment Cell Melanoma Res, 2011. **24**(2): p. 326-33.

6. Hoek, K.S., et al., *Metastatic potential of melanomas defined by specific gene expression profiles with no BRAF signature.* Pigment Cell Res, 2006. **19**(4): p. 290-302.

7. Yokoyama, T., et al., *Methylation of ASC/TMS1, a proapoptotic gene responsible for activating procaspase-1, in human colorectal cancer.* Cancer Lett, 2003. **202**(1): p. 101-8.

8. Weber, M., et al., *Chromosome-wide and promoter-specific analyses identify sites of differential DNA methylation in normal and transformed human cells.* Nat Genet, 2005. **37**(8): p. 853-62.

9. Torisu, H., et al., *Macrophage infiltration correlates with tumor stage and angiogenesis in human malignant melanoma: possible involvement of TNFalpha and IL-1alpha.* Int J Cancer, 2000. **85**(2): p. 182-8.

10. Boni, R., et al., *Staging of metastatic melanoma by whole-body positron emission tomography using 2-fluorine-18-fluoro-2-deoxy-D-glucose.* Br J Dermatol, 1995. **132**(4): p. 556-62.

Supplementary figures

Supplemental table 1. Expression of IL-1β and inflammasome components in primary melanoma cell cultures as detected by RT-PCR.

Cell line	ASC	Caspase-1	NLRP3	IL-1β
M080729	+	+	+	+
M971219	+	+	+	+
M990203	+	+	+	+
M080326	+	+	+	-
M070112	+	+	+	+
M060621	+	+	+	+

Supplementary table 2. Expression of IL-1β and inflammasome components in metastatic melanoma cell lines as detected by RT-PCR.

Cell line	ASC	Caspase-1	NLRP3	IL-1β
M010817	-	+	+	-
M82	+	-	+	-
M000921	-	+	+	+
MaMel82	+	+	+	+
M080221	-	+	+	+
M080228	-	+	+	+
M010119	-	+	+	+
M060125	-	+	+	+
M990115	-	+	+	+
Me191	+	-	+	-
WM134.1	-	+	+	+
A375	-	+	+	+
Me290	-	-	-	-
A2058	-	+	+	+
M080221	-	+	+	-
M080306	-	+	+	+
M080423	-	-	-	-
M080904	+	+	+	+
M080904B	-	-	+	-
M081021	-	+	+	-
M081028	-	+	+	-

3.2. Hypoxia promotes tumor growth via HMGB1 and tumor-associated macrophage polarization

Roman Huber[1, 3], Atsushi Otsuka[1, 3], Barbara Meier[1], Gabriele Fenini[1], Takashi Satoh[1], Samuel Gehrke[1], Daniel Widmer[1], Mitchell P Levesque[1], Joanna Mangana[1], Katrin Kerl[1], Hiroko Fujii[2], Chisa Nakashima[2], Kenji Kabashima[2], Reinhard Dummer[1], Emmanuel Contassot[1,4], and Lars E. French[1,4]

[1]Department of Dermatology, University Hospital Zurich, Zurich 8091, Switzerland

[2]Department of Dermatology, Kyoto University Graduate School of Medicine, Kyoto, Japan

[3]These authors are equally contributed.

[4] Co-senior authors

Correspondence to

Lars E. French, MD, and Emmanuel Contassot, PhD

Department of Dermatology, University Hospital Zurich, Gloriastrasse 31, Zurich 8091, Switzerland

Tel: +41-44-255-2550, Fax: +41-44-255-4403, Email: Emmanuel.Contassot@usz.ch

Abstract

High-mobility group protein B1 (HMGB1) is a highly conserved DNA-binding protein that can be released passively by damaged or dead cells or actively by immune cells and stressed cancer cells. It then acts as a DAMP or an alarmin, linking tissue damage and stress to activation of innate immune responses. Extracellular HMGB1 can then activate cytokine release to accelerate inflammatory responses and tumor development. Here, we investigated the role of HMGB1 in melanoma. We observed that HMGB1 promotes the accumulation of M2 macrophages via CXCR4 and promotes IL-10 production from M2 macrophages, which led to melanoma progression. We therefore identified the HMGB1-M2-macrophage axis as a key player in melanoma progression and a possible therapeutic target for metastatic melanoma.

Introduction

HMGB1 protein is a highly conserved DNA-binding protein with 98.5% sequence homology across mammals involved in gene expression and chromatin remodeling [1, 2]. HMGB1 can be actively secreted, or passively released upon cell damage, to stimulate immune responses either alone or in conjunction with other molecules [3]. The translocation of HMGB1 and its subsequent secretion can occur in several situations such as the activation of immune cells, including macrophages, cell death (necrosis and apoptosis) and ischemia/reperfusion injury. HMGB1 then acts as a DAMP) or an alarmin [4], linking tissue damage and stress to activation of innate immune responses. Notably, HMGB1 has been reported to be involved in diseases in which chronic inflammation plays a role, such as arthritis and cancer [3-6].

HMGB1 induces signaling through the binding to the Receptor for Advanced Glycation End products (RAGE) and certain Toll-like receptors (TLRs) [7]. The binding of HMGB1 to LPS is thought to enhance the production of proinflammatory cytokines via activation of TLR4, the signaling receptor for LPS/CD14 [8]. In addition, secreted HMGB1 exerts cytokine-like activity through TLR2 and RAGE [7]. Several reports also suggest that the binding of immunogenic nucleic acids to HMGB1 is required for subsequent recognition by specific pattern-recognition receptors like TLR3, TLR7 and TLR9 and activation of innate immune responses [9].

Neoplastic transformation, tumor growth, invasion and metastases can be induced by tumor-infiltrating cells that create an inflammatory tumor microenvironment. Activated macrophages, T cells, but also tumor cells themselves secrete HMGB1 under hypoxia, injury or inflammatory stimuli [10]. In addition, it has been recently reported that myeloid-derived suppressive cells (MDSC) present in tumors secrete HMGB1 [11].

Extracellular HMGB1 can then activate cytokine release to accelerate inflammatory responses and tumor development. HMGB1 has been shown to be released by mesothelial cells exposed to asbestos and erionite and is implicated in malignant mesothelioma development in an autocrine manner [10, 12, 13]. In a DMBA/TPA-induced skin carcinogenesis model, mice deficient for RAGE, a known receptor of HMGB1, are more resistant to inflammation and tumor formation [14]. Also, the blockade of HMGB1-TLR4 interaction impairs the recruitment of inflammatory cells that contribute to tumor development in skin and colon cancers [15].

Here, we show that HMGB1, when released by tumor cells in hypoxic conditions and binding to RAGE, induces the accumulation of M2 macrophages promoting melanoma progression.

Results

HMGB1 is released in metastatic melanoma patients

We first determined HMGB1 concentration in the serum of patients with primary and metastatic melanoma patients and age-matched healthy volunteers as controls. Serum HMGB1 levels were significantly increased in the serum of patients with primary melanoma when compared to healthy donors and was further increased in patients with metastatic melanoma (Fig. 1a). HMGB1 is usually located in the nucleus and a cytoplasmic relocalization occurs prior to its release [10]. Therefore, we assessed the intra-cellular localization of HMGB1 in nevi, primary melanoma (superficial spreading melanoma) and melanoma metastases. While HMGB1 was confined to nuclei in nevi and primary melanomas, melanoma metastases exhibited large areas containing tumor cells with cytoplasmic HMGB1 which co-localized with Hif-1α-positive tumor areas, indicating that HMGB1 is released by cells in hypoxic conditions (Fig. 1b). Hypoxia in tumors is associated with advanced malignant progression and resistance to therapies by enhancing genetic diversity and exerting a selective pressure [16] and HMGB1 is known to be released in hypoxia/ischemia conditions [17]. To assess whether metastatic melanoma cell lines release HMGB1 in hypoxia, we cultured them in normal or low oxygen atmosphere and measured HMGB1 release in the culture supernatant. When compared to their counterparts kept in normoxia, all the tested melanoma cell lines (n=7) secreted increased levels of HMGB1 when kept in hypoxic conditions, the latter being confirmed by increased VEGF-A expression [18] (Fig. 1c). In hypoxic conditions, no increase in cell mortality was observed as revealed by the low LDH release.

These observations indicate that HMGB1 is released by hypoxic tumor cells in metastatic melanoma patients.

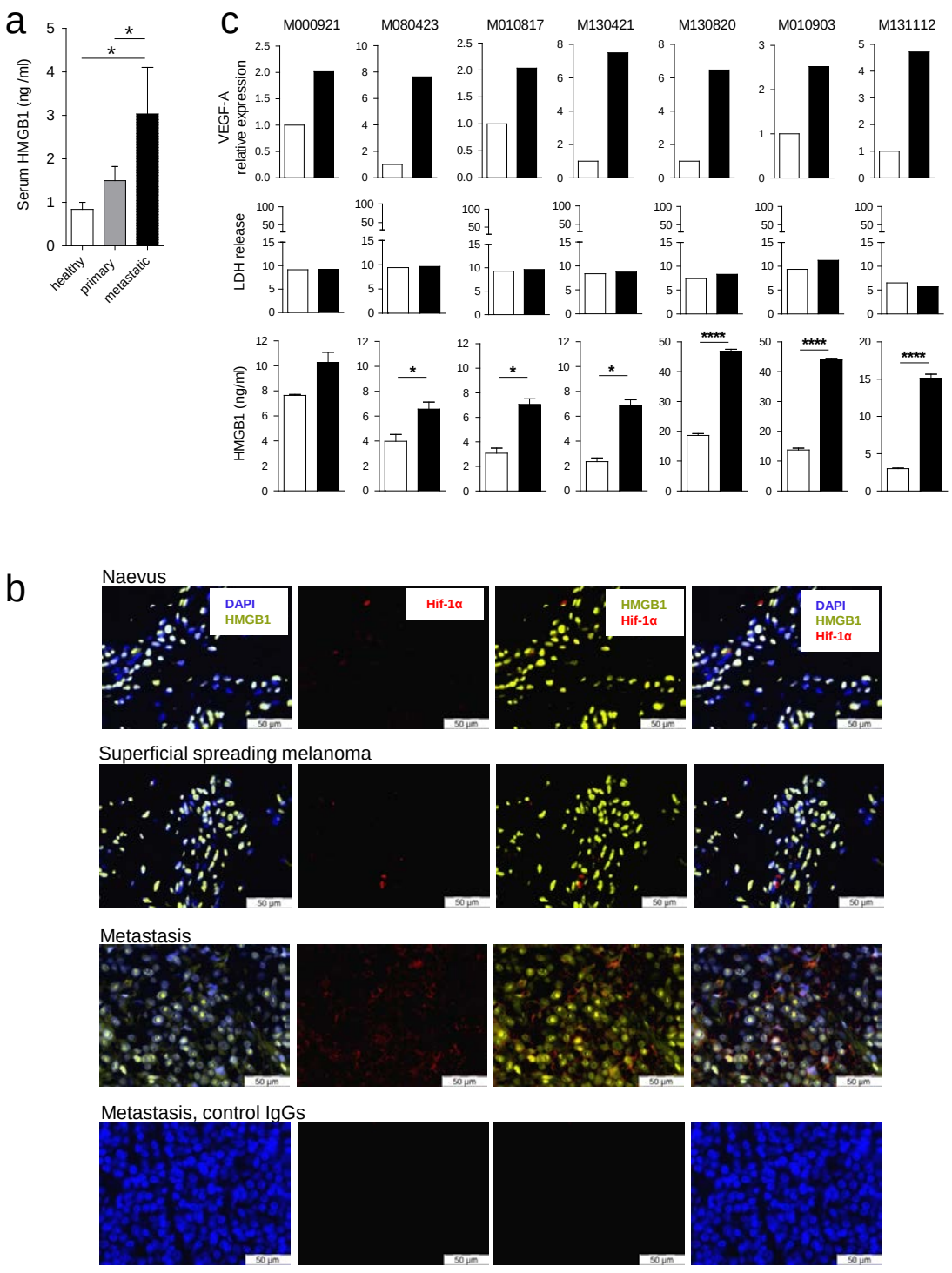

Figure 1. HMGB1 is released by hypoxic tumor areas

(a) HMGB1 was measured by ELISA in the serum of healthy individuals (n=10), patients with primary (n=9) and metastatic melanoma (n=11). Means +/- SEM are presented. * P<0.05.

(b) Immunofluorescence using antibodies to Hif-1α and HMGB1 was performed on healthy skin, nevi, primary cutaneous melanoma and metastases as indicated.

(c) Cells lines derived from metastases were cultured under normoxic or hypoxic conditions. As a hypoxia marker VEGF-A qPCR was performed after the culture period (top panels) and the viability of cells cultured in normoxia and hypoxia was assessed by LDH release assay (middle panels). HMGB1 release was assessed by ELISA in culture supernatants (bottom panels). Means +/- SEM are presented. * P<0.05, **** P<0.0001.

Silencing of HMGB1in B16 melanoma cells led to delayed tumor growth

To assess whether HMGB1 plays a role in melanoma growth, we transduced B16 melanoma cells with shRNA to HMGB1 or with shRNA to lamin as an irrelevant control. The HMGB1 knock-down efficiency was highly stable both *in vitro* and *in vivo* (Fig. S1). HMGB1-shRNA-transduced B16 and lamin-shRNA-transduced B16 were injected sub-cutaneously in C57BL/6 mice. Mice having received HMGB1-shRNA-transduced B16 exhibited a dramatically delayed tumor growth when compared to mice having received lamin-shRNA-transduced B16 (Fig. 2a, left panel and Fig. S2). Such a growth delay was not due to intrinsic effect of shRNA transduction as revealed by the identical *in vitro* growth capacity of HMGB1- and lamin-shRNA-transduced B16 and the absence of abnormal apoptosis (Fig. S3). To assess the effect of extracellular HMGB1 on tumor growth, we next treated mice having received lamin-shRNA-transduced B16 with a recombinant HMGB1 inhibitor (BoxA) in an independent set of experiments. The treatment of tumor-bearing mice with BoxA also resulted in a delayed tumor growth compared to mice treated with vehicle (Fig. 2a, right panel). We next evaluated the role of HMGB1 in metastasis by injecting either HMGB1-shRNA-transduced B16 cells or lamin-shRNA-transduced B16 cells i.v. into wild type mice. After 13 days, mice having received HMGB1-shRNA-transduced B16 cells exhibited significantly less lung metastases when compared to mice having received the lamin control (Fig. 2b).

Next, we assessed the intra-cellular localization of HMGB1 in B16 tumors using lamin-shRNA-transduced B16 tumors. In the large hypoxic areas found in the center of the tumors (Fig. 2c), cytoplasmic HMGB1 was also observed in Hif-1α positive cells, whereas nuclear HMGB1 was restricted to Hif-1α negative cells, which is in line with our observations in human melanomas (Fig. 2d).

Taken together, these results suggest that extracellular HMGB1, released by cells in hypoxic conditions promotes B16 melanoma growth.

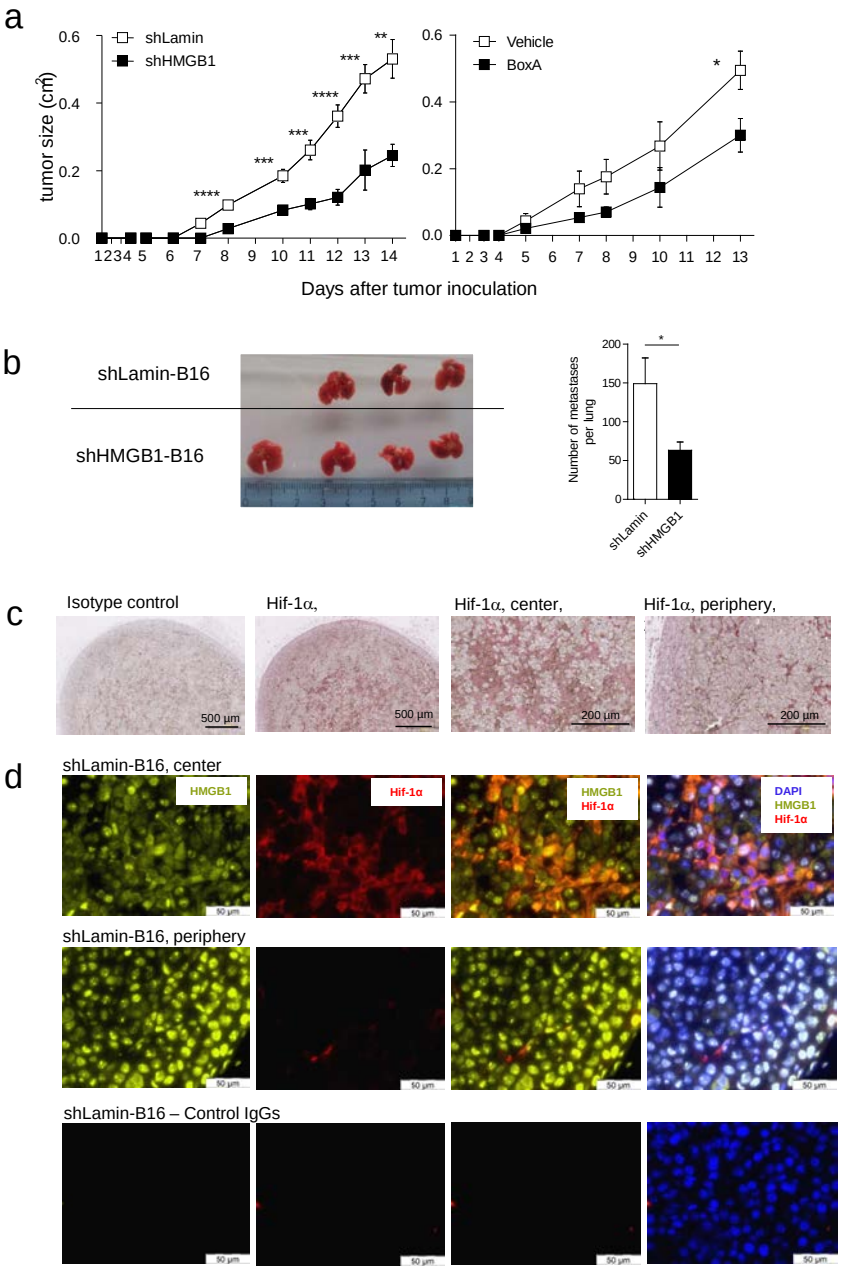

Figure 2. HMGB1 released by hypoxic tumor areas promotes tumor growth and metastasis

(a) Tumor growth in C57BL/6 mice having received 1x10e5 B16 cells transduced with shRNA to HMGB1 or shRNA to lamin (left panel) and tumor growth in C57BL/6 mice having received 1x10e5 B16 cells transduced with shRNA to lamin and treated from day 0 with a BoxA recombinant HMGB1 inhibitor (right panel) ** P<0.01, *** P<0.001, **** P<0.0001.

(b) B16 cells transduced with shRNA to HMGB1 or shRNA to lamin were injected i.v. to C57BL/6 mice and lung metastases were counted after 10 days. A macroscopic view (left panel) and the numeration of metastases in the lungs (n=4) are shown. Results are expressed as means +/- SEM.

(c) Immunohistochemistry using an antibody to Hif-1α was performed on 1 cm^2 tumors. (d) Immunofluorescence analysis of Hif-1α and HMGB1 in B16 cells transduced with shRNA to lamin.

HMGB1 drives M2 macrophage infiltrates

We next analyzed tumor-infiltrating immune cells by flow cytometry. The total number of infiltrating macrophages was increased in HMGB1-shRNA-transduced B16 tumor whereas the total number of neutrophils was decreased in HMGB1-shRNA-transduced B16 tumor (Fig. 3a). To assess the phenotype of macrophages infiltrating HMGB1-shRNA- and lamin-shRNA-transduced B16 tumor, we measured the expression of markers distinguishing M1-like and M2-like macrophage subpopulations [19]. Quantitative PCR of macrophages accumulating at the tumor site revealed that the silencing of HMGB1 in B16 was associated with the overexpression of M1 marker (*CD80*) whereas the expression of HMGB1 was associated to the upregulation of M2 markers (*YM1, Fizz1, and IL-10*) (Fig. 3b). These results suggest that HMGB1, when released by tumor cells, promotes M2 infiltrates.

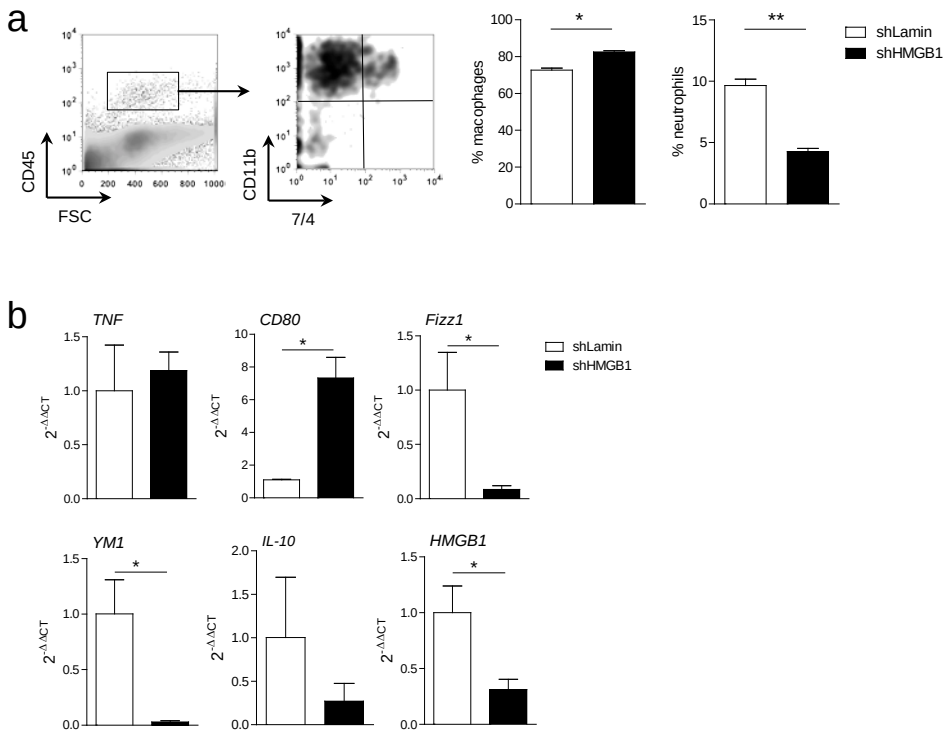

Figure 3. HMGB1 induces the recruitment of macrophages harboring an M2 phonotype

(a) Macrophage and neutrophil infiltrates in tumors with similar size are shown. Left panel, representative flow cytometry pictures (left panels) and numeration of total macrophages and neutrophils in mice having received B16 cells transduced with shRNA to lamin (n=7) or to HMGB1 (n=7). Means +/- SEM are presented.* P<0.05, ** P<0.01.

(b) Quantification of M1- and M2-specific gene expression by qPCR in primary s.c. tumors form mice having received B16 cells transduced with shRNA to HMGB1 (shHMGB1, n=5) or shRNA to lamin (shLamin, n=5). Means +/- SEM are presented. * P<0.05.

HMGB1 induces CXCR4 expression in M2 macrophages

TAMs have been reported to be biased towards the M2 phenotype in advanced tumors [20-22] and the above results suggest that HMGB1 favors the accumulation of M2-like macrophages at the tumor site. Therefore, we analyzed the effect of HMGB1 on M2 macrophages. To this end, we generated M1-like and M2-like macrophages from bone marrow (BM) and exposed them to recombinant HMGB1. BM-derived M2 macrophages (BMM2) showed an up-regulated CXCR4 expression while CXCR4 expression in BM-derived M1 macrophages (BMM1) was not affected by recombinant HMGB1 (Fig. 4A). Interestingly, CXCR4 has an essential role in tumor metastasis [23] and it has been recently reported that HMGB1 promotes the recruitment of inflammatory cells to damaged tissues by forming a complex with CXCL12 and signaling via CXCR4 [24].

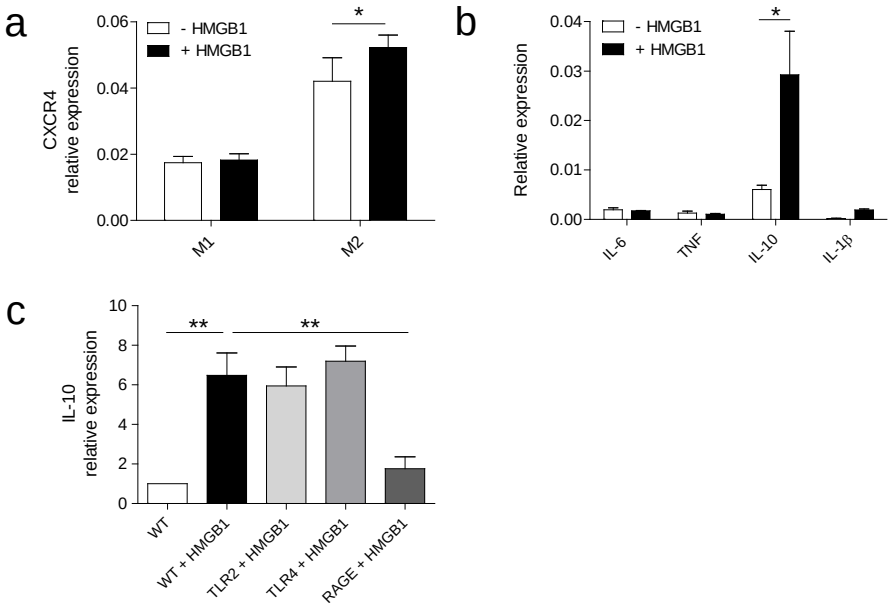

Figure 4. HMGB1 induces CXCR4 and IL-10 expression in murine M2 macrophages in a RAGE-dependent manner.

(a) CXCR4 mRNA expression in *in vitro*-differentiated murine M1 and M2 macrophages exposed to recombinant HMGB1 or not. Shown is the expression relative to *RPL27.*

(b) *IL-6*, *TNF*, *IL-10* and *IL-1β* mRNA expression in murine M2 macrophages exposed to recombinant HMGB1 or not. Shown is the expression relative to *RPL27.*

(c) *IL-10* mRNA expression in *in vitro*-differentiated M2 macrophages from WT*, Tlr2*$^{-/-}$*, Tlr4*$^{-/-}$ and *Rage*$^{-/-}$ mice. Shown is the expression relative to that of WT M2 macrophages not exposed to HMGB1.

HMGB1 induces IL-10 in M2 macrophages through RAGE

The tumor microenvironment, including the cytokine milieu, plays a central role in tumor progression [25, 26]. Therefore, we evaluated the effect of HMGB1 on cytokine expression by M2 macrophages. IL-10 expression was significantly increased in M2 macrophages when incubated with recombinant HMGB1 (Fig. 4B). Such IL-10 upregulation was not observed in BMM2 from $RAGE^{-/-}$ mice while it was retained in $TLR2^{-/-}$ and $TLR4^{-/-}$ BMM2 (Fig. 4C). This data suggests that HMGB1 induces IL-10 in M2-like macrophages through RAGE signaling. To assess the tumor-promoting effect of IL-10-producing M2-like macrophages, mice bearing lamin-shRNA transduced B16 tumors were treated with an anti-IL-10 neutralizing antibody. Mice receiving anti-IL-10 exhibited a significantly delayed tumor growth when compared to vehicle-treated mice (Fig. 5B). Together, these results indicate that IL-10 producing M2 macrophages infiltrating the tumors are key players in tumor progression. This was further supported by the presence of IL-10-producing M2 macrophages in human metastatic melanomas as revealed by the presence of CD163+ IL-10+ cells in human metastases infiltrates (Fig. 5A).

To evaluate the relevance of the above observations, we analyzed human melanomas by immunohistochemistry using anti-CD163, an M2 marker, and anti-IL-10 antibodies. In melanoma metastases, $CD163^{+}$ $IL\text{-}10^{+}$ cells were found in the infiltrates.

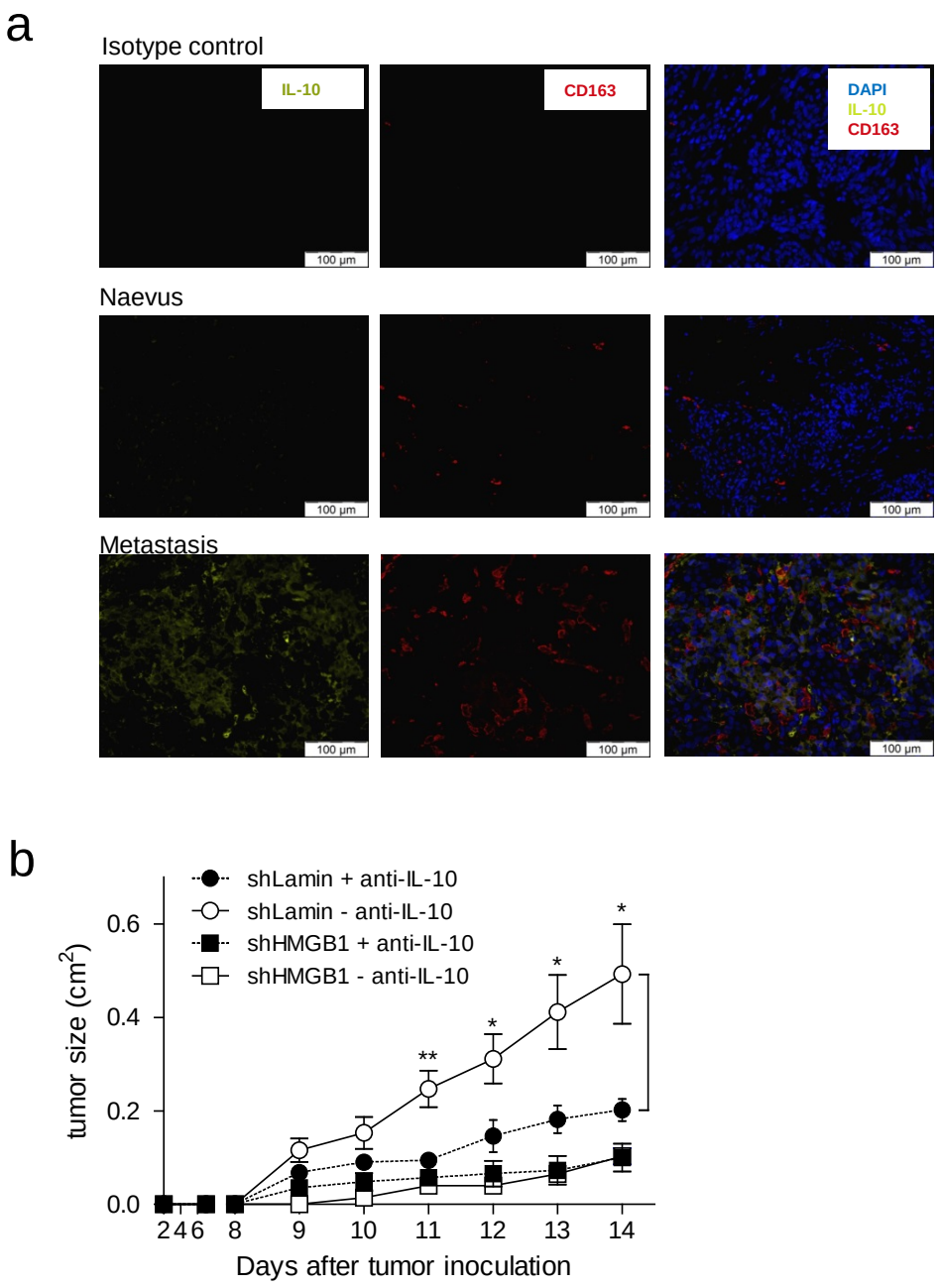

Figure 5. IL-10 is present in M2-rich areas of metastases and favors melanoma growth

(a) Immunofluorescence analysis of nevi and metastases using anti-CD163 and anti-IL-10 antibodies.

(b) Tumor growth in C57BL/6 mice having received 1 x 10^5 B16 cells transduced with shRNA to HMGB1 or shRNA to lamin treated or not with an anti-IL-10 blocking antibody (N=7/group).

Acknowledgements

This work was supported in part by the Association for International Cancer Research (AICR 09-0230) to L.E.F, ZIHP to L.E.F., Oncosuisse to L.E.F., by the Zürich University Research Priority Program (URPP) Translational Cancer Research, by the Swiss National Science Foundation (Sinergia Grant CRSII3-136203) to L.E.F, and by the Society for Skin Cancer Research to M.P.L. We thank Horomi Doi, Ines Kleiber-Schaaf, and Tatiana Proust for technical assistance.

Personal contribution

In this work, I contributed with designing, performing, analyzing and interpreting experiments.

- Collection of human melanoma cell lines, paraffin-embedded patient samples and melanoma patient serum
- Culturing of human melanoma cell lines under normoxic/hypoxic conditions and determination of cell lysis, VEGF-A mRNA and HMGB1 release
- Immunofluorescence of human melanoma patient biopsies and murine B16 melanoma for HMGB1, Hif-1α, IL-10 and CD163
- Manufacture of shHMGB1- and shLamin-B16 clones
- Assessment of in vitro properties of shHMGB1- and shLamin-B16 clones
- Subcutaneous and intravenous injection of shHMGB1- and shLamin-B16 clones
- Flow-cytometric analysis of the tumor-infiltrate in shHMGB1- and shLamin-B16 tumors
- Analysis of the mRNA composition in shHMGB1- and shLamin-B16 tumors
- Generation of bone-marrow derived macrophages and mRNA analysis after treatment with rec. HMGB1
- Assessment of tumor growth of B16 tumors after treatment with BoxA and anti-IL-10 antibody

References

1. Agresti, A. and M.E. Bianchi, *HMGB proteins and gene expression.* Curr Opin Genet Dev, 2003. **13**(2): p. 170-8.

2. Bianchi, M.E., M. Beltrame, and G. Paonessa, *Specific recognition of cruciform DNA by nuclear protein HMG1.* Science, 1989. **243**(4894 Pt 1): p. 1056-9.

3. Andersson, U. and K.J. Tracey, *HMGB1 is a therapeutic target for sterile inflammation and infection.* Annu Rev Immunol, 2011. **29**: p. 139-62.

4. Bianchi, M.E., *HMGB1 loves company.* J Leukoc Biol, 2009. **86**(3): p. 573-6.

5. Ellerman, J.E., et al., *Masquerader: high mobility group box-1 and cancer.* Clin Cancer Res, 2007. **13**(10): p. 2836-48.

6. Sims, G.P., et al., *HMGB1 and RAGE in inflammation and cancer.* Annu Rev Immunol, 2010. **28**: p. 367-88.

7. Ibrahim, Z.A., et al., *RAGE and TLRs: relatives, friends or neighbours?* Mol Immunol, 2013. **56**(4): p. 739-44.

8. Youn, J.H., et al., *High mobility group box 1 protein binding to lipopolysaccharide facilitates transfer of lipopolysaccharide to CD14 and enhances lipopolysaccharide-mediated TNF-alpha production in human monocytes.* J Immunol, 2008. **180**(7): p. 5067-74.

9. Yanai, H., T. Ban, and T. Taniguchi, *Essential role of high-mobility group box proteins in nucleic acid-mediated innate immune responses.* J Intern Med, 2011. **270**(4): p. 301-8.

10. Jube, S., et al., *Cancer cell secretion of the DAMP protein HMGB1 supports progression in malignant mesothelioma.* Cancer Res, 2012. **72**(13): p. 3290-301.

11. Parker, K., et al., *HMGB1 enhances immune suppression by facilitating the differentiation and suppressive activity of myeloid-derived suppressor cells.* Cancer Res, 2014.

12. Carbone, M., et al., *Erionite exposure in North Dakota and Turkish villages with mesothelioma.* Proc Natl Acad Sci U S A, 2011. **108**(33): p. 13618-23.

13. Yang, H., et al., *Programmed necrosis induced by asbestos in human mesothelial cells causes high-mobility group box 1 protein release and resultant inflammation.* Proc Natl Acad Sci U S A, 2010. **107**(28): p. 12611-6.

14. Gebhardt, C., et al., *RAGE signaling sustains inflammation and promotes tumor development.* J Exp Med, 2008. **205**(2): p. 275-85.

15. Mittal, D., et al., *TLR4-mediated skin carcinogenesis is dependent on immune and radioresistant cells.* EMBO J, 2010. **29**(13): p. 2242-52.

16. Hockel, M., et al., *Association between tumor hypoxia and malignant progression in advanced cancer of the uterine cervix.* Cancer Res, 1996. **56**(19): p. 4509-15.

17. Tsung, A., et al., *HMGB1 release induced by liver ischemia involves Toll-like receptor 4 dependent reactive oxygen species production and calcium-mediated signaling.* J Exp Med, 2007. **204**(12): p. 2913-23.

18. Rofstad, E.K. and T. Danielsen, *Hypoxia-induced angiogenesis and vascular endothelial growth factor secretion in human melanoma.* Br J Cancer, 1998. **77**(6): p. 897-902.

19. Mantovani, A., et al., *The chemokine system in diverse forms of macrophage activation and polarization.* Trends Immunol, 2004. **25**(12): p. 677-86.

20. Biswas, S.K. and A. Mantovani, *Macrophage plasticity and interaction with lymphocyte subsets: cancer as a paradigm.* Nat Immunol, 2010. **11**(10): p. 889-96.

21. Ruffell, B., N.I. Affara, and L.M. Coussens, *Differential macrophage programming in the tumor microenvironment.* Trends Immunol, 2012. **33**(3): p. 119-26.

22. Qian, B.Z. and J.W. Pollard, *Macrophage diversity enhances tumor progression and metastasis.* Cell, 2010. **141**(1): p. 39-51.

23. Zhang, Z., et al., *Expression of CXCR4 and breast cancer prognosis: a systematic review and meta-analysis.* BMC Cancer, 2014. **14**: p. 49.

24. Schiraldi, M., et al., *HMGB1 promotes recruitment of inflammatory cells to damaged tissues by forming a complex with CXCL12 and signaling via CXCR4.* J Exp Med, 2012. **209**(3): p. 551-63.

25. Wan, L., K. Pantel, and Y. Kang, *Tumor metastasis: moving new biological insights into the clinic.* Nat Med, 2013. **19**(11): p. 1450-64.

26. Joyce, J.A. and J.W. Pollard, *Microenvironmental regulation of metastasis.* Nat Rev Cancer, 2009. **9**(4): p. 239-52.

Supplementary figures

Supplementary figure 1.

HMGB1 knock-down efficiency is stable over time *in vitro* and *in vivo*

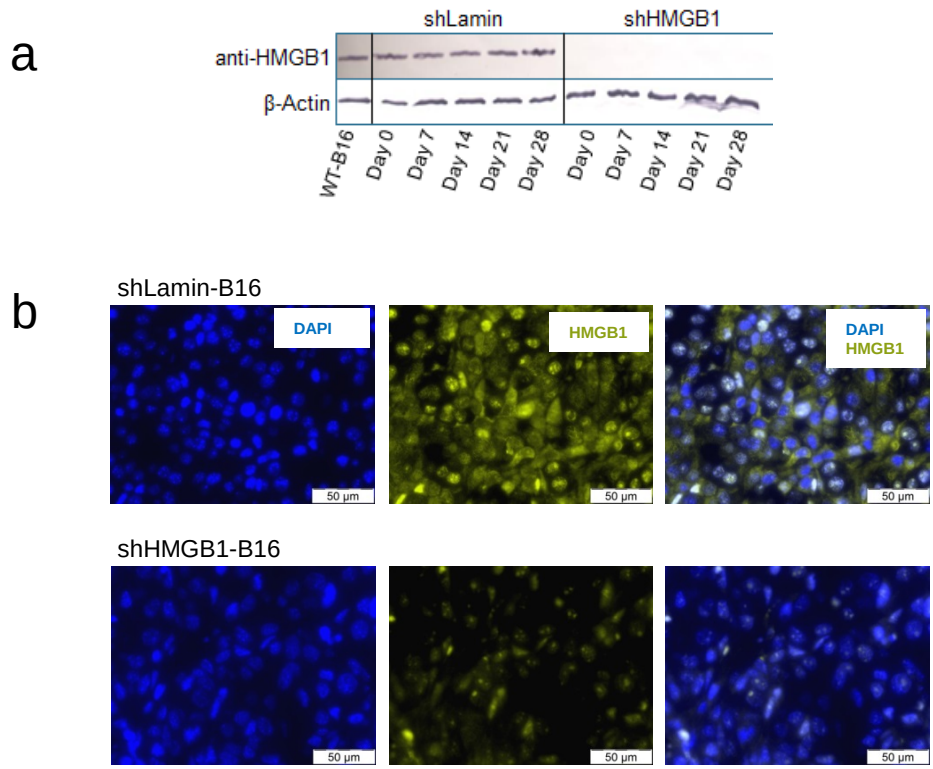

Figure S1. HMGB1 knock-down efficiency is stable over time *in vitro* and *in vivo*

(a) Cultures of B16 cells transduced with shRNA to lamin or HMGB1 were harvested, lysed and subjected to Western-blot analysis using anti-HMGB1 and anti-β-actin antibodies.

(b) B16 cells transduced with shRNA to lamin or HMGB1 were injected s.c. to C57BL/6 mice and the resulting tumors were dissected at day 13 and stained with an anti-HMGB1 antibody. Nuclei were visualized using DAPI. Pictures are representative of 7 tumors/group.

Supplementary figure 2.

Two different shRNA sequences to HMGB1 resulted in similar growth inhibition.

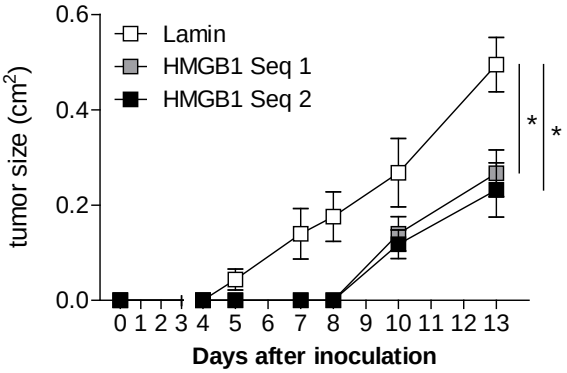

Figure S2. Two different shRNA sequences to HMGB1 resulted in similar growth inhibition

B16 cells were transduced with 2 different shRNA to HMGB1 (seq 1 and seq 2) and with shRNA to lamin and injected s.c. into C57BL/6 mice. Tumor growth was monitored every other day. * $P < 0.05$

Supplementary figure 3.

The *in vitro* growth properties of B16 cells transduced with shRNA to lamin and HMGB1 are identical.

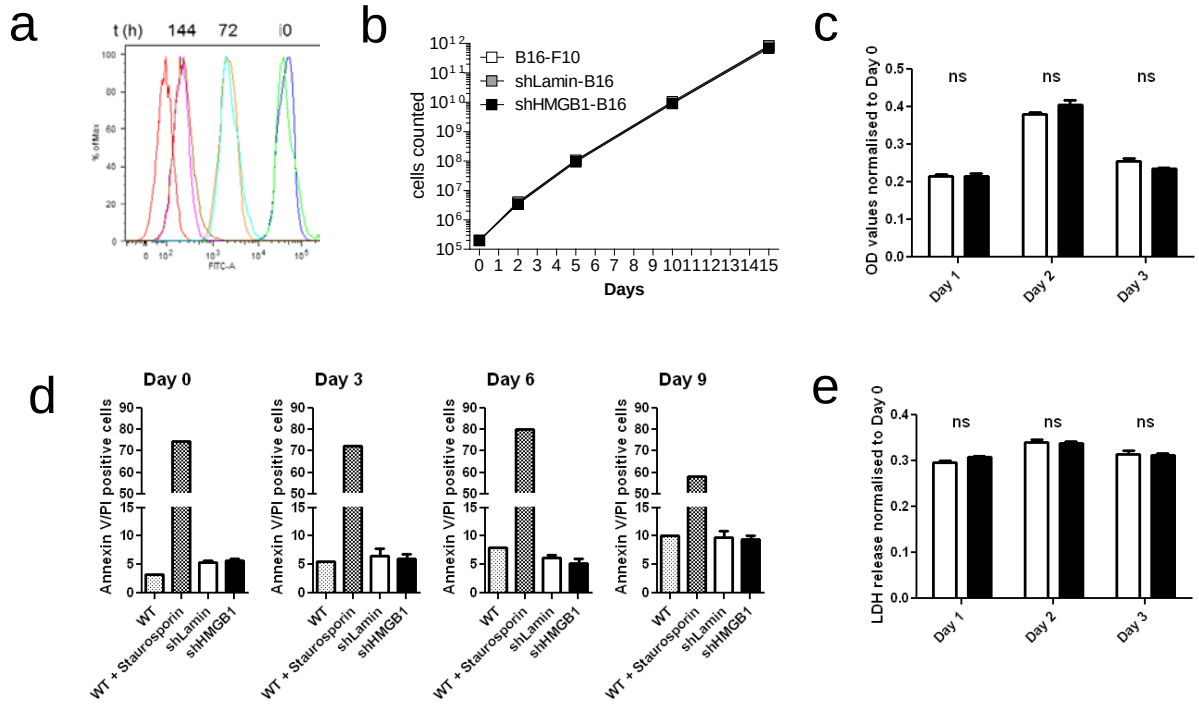

Figure S3. The *in vitro* growth properties of B16 cells transduced with shRNA to lamin and HMGB1 are identical

(a) B16 cells transduced with shRNA to lamin and HMGB1 were labelled with CFSE and collected 72 and 144 hrs later and analyzed in flow cytometry.

(b) B16 cells transduced with shRNA to lamin and HMGB1 were counted over a 15-day culture period.

(c) Proliferation of B16 cells transduced with shRNA to lamin (white histograms) and HMGB1 (black histograms) was assessed over a 3-day culture period using MTT assay.

(d) At day 0, 3, 6 and 9, B16 cells transduced with shRNA to lamin (shLamin) and HMGB1 (shHMGB1) were harvested, stained with Annexin V and propidium iodide (PI) and analyzed in flow cytometry. Annexin V+/PI+ cells were considered as apoptotic. As control, WT B16 cells were treated with staurosporin, a strong apoptosis inducer.

(e) Viability of B16 cells transduced with shRNA to lamin (white histograms) and HMGB1 (black histograms) was assessed over a 3-day culture period using LDH release assay.

4. Discussion and Perspectives

In this work, we have studied two processes that are relevant to tumor-stroma interactions.

First, we have shown that melanoma cell lines are not able to secrete IL-1β, due to a dysfunction in the inflammasome, explained in the majority of cell lines tested by methylation of the promotor region of the crucial inflammasome component ASC. Given that TAMs are present in melanomas and potent producers of IL-1β as judged by immunostaining, we further searched for stimuli for TAM IL-1β production and could identify that products released by necrotic melanoma cells *in vitro* are potent activators of the NLRP3 inflammasome and mature IL-1β production. Thus, metastatic melanoma cells seem to have lost the ability for IL-1β production whereas macrophages of the microenvironment secrete high amounts of IL-1β in response to putative danger signals released by necrotic tumor cells.

Second, and intrigued by the above finding that macrophages of the microenvironment secrete high amounts of IL-1β in response to putative danger signals released by necrotic tumor cells, we analyzed the functional role of a major DAMP/alarmin known to be released upon cell necrosis, namely HMGB1. We could show under hypoxic conditions melanoma cells release the DAMP/alarmin HMGB1 and HMGB1 then promotes the subsequent recruitment of TAM to the tumor microenvironment and furthermore significantly promotes tumor growth. Besides HMGB1, both the recruitment of TAM and the cytokine IL-10 are critical for tumor growth in the model studied.

These two above studied events relevant to tumor-stroma interactions might not be exclusive and therefore co-exist within the same tumor. Their occurrence may also depend on the tumor type and its susceptibility to necrosis and hypoxia. The cancer stage may also influence one or both mechanisms. The two latter hypotheses require further investigation.

Inflammation and cancer development appear to be indissociable biological processes. However, inflammation-driven carcinogenesis and cancer-induced inflammation should be distinguished. Indeed, inflammation appears not only to be a tumor-promoting condition, but also a consequence of tumor development.

There is evidence that chronic inflammation induced by persistent chemical, bacterial or viral insults is a risk factor for cancer [1]. It is also known that dysregulated inflammatory processes such as those seen in autoimmune diseases, or persistent repetitive tissue trauma may also result in an increased risk of cancer [2]. In established solid tumors, there is a reciprocal signaling interaction between cancer cells and stromal cells taking place in the tumor microenvironment. This local tumor microenvironment, comprising tumor cells, extracellular matrix, immune cells, cytokines and other factors, plays a key role in tumor formation, growth, invasion and metastasis. Tumors can secrete pro-inflammatory cytokines, chemokines, and other soluble factors into their microenvironment. The pro-inflammatory cytokine Interleukin-1β (IL-1β) is one of these cytokines. IL-1β is often detected in human cancers including breast cancer, pancreatic cancer, and glioblastoma [3]. It has been reported that IL-1β expression levels are associated with the invasiveness and metastasis of cancers [4]. In melanoma, IL-1β has been shown to induce chemokines that recruit proinflammatory cells [5], promote angiogenesis, and drive metastasis [6]. Interestingly, IL-1β has been reported to be expressed at lower levels in nevi when compared to primary and metastatic melanomas [5]. Furthermore, selected late stage melanoma cell lines (A375, HS294T, and 1205Lu) *in vitro* have been reported to spontaneously secrete IL-1β via constitutive activation of the NLRP3 inflammasome [7]. Alternatively, IL-1β production by tumor cells or cells in the tumor environment may be a danger signal for the host's immune system and trigger the recruitment immune cells to the tumor [8].

Here, we showed that human melanomas contain high levels of IL-1β although melanoma cells in our hands themselves are not able to secrete IL-1β as observed in 13 cell lines tested. Indeed, a great majority (80 %) of the metastatic melanoma cell lines we tested did not express the inflammasome adaptor ASC as a result of promoter methylation. Since, IL-1β secretion very early during tumorigenesis could be viewed as a danger signal and therefore promote host anti-tumor responses, the methylation of ASC may consists an effective mechanism developed by tumor cells to protect themselves in a situation where the tumor load is still low. Furthermore, we also observed that, when compared to primary melanocytes, the expression additional inflammasome components are also lost in metastatic melanoma cell lines tested. We thus hypothesized that an important source of IL-1β in established tumors may be cells within the tumor microenvironment. Macrophages are very potent IL-1β producers and known to be an important component of the inflammatory infiltrate in melanoma [9]. However, in order to be biologically active and secreted, IL-1β requires processing by the inflammasome, and thus TAMs would have to be exposed to DAMPs. We hypothesized that necrotic melanoma cells which are often found in advanced melanomas [10] may be a source of such DAMPs [11]. Our results show that necrotic melanoma cells are very potent IL-1β inducers in macrophages, but the exact DAMP(s)

released upon melanoma cell necrosis and responsible for IL-1β processing and release by macrophages was not identified.

It appears that there are at least two subclasses of stimulatory immune cells in the tumor stroma. One subclass that participates in “normal” immunological/inflammatory activities (wound healing, innate and adaptive immune responses), and a second subclass comprising TAMs, neutrophils and myeloid progenitor cells that provoke exaggerated wound healing and pro-angiogenic responses suggested to promote cancer growth and suppression of anti-tumor immunity [12].

TAMs have emerged as key components of the tumor environment relevant to tumor progression [13]. Indeed, the presence of TAMs has been associated with poor prognosis of several malignancies [14-17]. It has been proposed that monocytes continuously infiltrate tumors and that, once polarized, M2 macrophages preferentially accumulate in hypoxic regions of the tumor whereas M1 macrophages are not impacted by hypoxia [18, 19]. By promoting angiogenesis and metastasis, M2 polarized macrophages are thought to overcome the hostile hypoxic environment within tumors and sustain tumor progression [20, 21]. However, the factors released by hypoxic cells involved in M2 macrophage recruitment remain poorly understood. Here, we show that HMGB1, released from tumor cells in hypoxic conditions, promotes the recruitment of M2 macrophages through CXCR4 and RAGE. Indeed, our observation that, in B16 tumors, the expression and release of HMGB1 is associated with M2 macrophage infiltration and tumor growth and that inversely, reduced HMGB1 expression favors tumor predominance of M1 macrophages and a delayed tumor growth suggests a crucial role for HMGB1 in M2-dependent tumor progression. Nevertheless, we were not able to induce a phenotype switch of macrophages treated with HMGB1 *in vitro*, suggesting that a combination of several factors released by hypoxic cells, including HMGB1, is required for M2-macrophage polarization and accumulation. Indeed, a recent study showed that lactic acid, produced by tumor cells as a by-product of hypoxic glycolysis, has a critical function by inducing VEGF expression and M2-like polarization of TAMs in a HIF-1α-dependent manner [22]. Moreover, another recent report shows that oncostatin M and eotaxin may promote breast cancer metastasis by favoring M2 polarization and infiltration [23]. As recently reported, HMGB1 may also act directly on progenitor cells to induce suppressive myeloid-derived cells [24]. Finally, our observation that a treatment of tumor-bearing mice with the HMGB1 BoxA inhibitor is not as efficient as the silencing of HMGB1 with shRNA also suggest that other factors are involved in the promotion of tumor growth.

In our experiments, we could show that release of HMGB1 very likely occurs within hypoxic areas within human melanoma biopsies, Hypoxia is known to induce the recruitment of macrophages to the tumor site [25, 26]. A hypoxic tumor environment, which is seen in up to 50–60 % solid tumors[27], actively selects for a more aggressive cancer cell phenotype, since the mechanisms linked to survival in these conditions are associated with invasion, metastasis, and resistance to radiation and chemotherapy [28, 29]. During hypoxia, due to fast tumor growth, HMGB1 is released [30]. Extracellular HMGB1 via RAGE has been shown to induce the expression of NF-κB dependent pro-angiogenic factors such as VEGF [31] and the expression of matrix metalloproteinases such as MMP2 and MMP9 [32]. It has also been reported that HMGB1 released from dying cells in prostate cancer induces the accumulation of tumor-infiltrating T cells and the expression of Lymphotoxin α1β2 on their surface, which in turn recruits macrophages that provide growth factors to the tumor and support angiogenesis [33]. Noteworthy, tumor cells or tumor-infiltrating immune cells seem not to be the sole possible source of HMGB1. Indeed, UV can induce the release of HMGB1 from epidermal keratinocytes which resulting in a neutrophilic inflammatory response stimulating angiogenesis and promoting melanoma metastasis [34].

The expression of CXCR4 in melanoma is known to play an essential role for tumor progression and metastasis [35] and a high expression of CXCR4 and its ligand CXCL12 in melanoma patients has been reported to be associated with poor prognosis [36]. A recent study showed that HMGB1 promotes the recruitment of inflammatory cells to injured tissues by forming a heterocomplex with the chemokine CXCL12 that acts exclusively via CXCR4 [37]. Our data suggest an additional important role of HMGB1 as we demonstrate that HMGB1 can specifically induce CXCR4 upregulation in M2 macrophages *in vitro*.

We also observed that HMGB1 induced the production of IL-10 from M2 macrophages *in vitro*, and that the blockade of IL-10 with a neutralizing antibody *in vivo* led to delayed tumor growth. The precise role of IL-10 in our model remains to be investigated however. It has been shown that regulatory T cell-mediated/IL-10-dependent suppression of $CD8^+$ T cells can be blocked by removal of tumor-derived HMGB1 [38], which is consistent with our observation that HMGB1 inhibition leads to delayed tumor growth. Therefore, we hypothesize that IL-10, which can also be produced by melanoma cells [39] and tumor-associated MCSC [24] may favor immunoregulatory responses by inducing the down regulation of molecules involved in antigen presentation to $CD8^+$ T cells [40], by inducing Tregs [41, 42] and/or inhibiting the production of pro-inflammatory cytokines including TNF, IFN-γ and IL-2 by T cells [43]. Noteworthy, IL-10 production levels by melanoma cells have been shown to be associated with a poor prognosis [44].

HMGB1 has several receptors, including TLR-2, 4 and -9 and RAGE. In our model, TLRs were not involved, as assessed *in vitro*, in HMGB1-induced CXCR4 and IL-10 expression by macrophages. We could demonstrate *in vitro* that HMGB1 is only able to induce CXCR4 and IL-10 expression in the presence of RAGE, as production of these molecules was absent when using RAGE-deficient macrophages. An important role of the HMGB1-RAGE interaction in promoting tumor progression is supported by a recent report showing that, RAGE and HMGB1 are associated with progression of prostate cancer and poor patient outcome [45]. It is furthermore likely that HMGB1 when binding to TLRs may exert a distinct effect from that induced by RAGE binding. Actually, HMGB1, when released from chemically-stressed cells, has been shown to induce protective anti-tumor T cell responses by inducing the maturation of DCs in a TLR4-dependent manner [46-48]. The reasons for such a dual role of HMGB1 in tumor outcome remain unknown. One could hypothesize that the context and nature of the cell stress may be associated with the release of different factors which, together with HMGB1, trigger different types of antigen-presenting cells expressing different HMGB1-receptor patterns and leading to distinct effects. Overall, we demonstrate in our model that HMGB1, derived from hypoxic tumor cells, exerts a key function in melanoma progression by promoting the accumulation of IL-10-producing M2 macrophages via CXCR4. Therefore, extracellular HMGB1 presents as a possible therapeutic target for the treatment of metastatic melanoma.

While being beneficial for the host in many instances, uncontrolled inflammation can be detrimental leading to pathologies such as the sterile inflammation of autoinflammatory diseases or sterile inflammation associated with tumor development. Such inflammatory responses can be triggered by situations that are not favorable for the survival of normal and cancer cells such as hypoxia. To overcome such a hostile environment, tumors appear to have developed strategies to trigger inflammatory responses in their microenvironment, whereby macrophages are important players in this process. As a consequence of this, immune cells initially recruited to respond to the danger represented by the presence of a tumor become an accomplice of the tumor, helping it to achieve better conditions for its survival and growth (angiogenesis and metastasis). It appears that there are several classes of immune cells potentially recruited to the tumor site, each of them acting either alone or in conjunction with other inflammatory cell types. The emergence of new technologies based on multiplex analyses should help researchers to better define and further characterize tumor-infiltrating cells and understand the complex interplay between tumor cells and the inflammatory stroma, as well as between the different inflammatory cell types in the microenvironment. In addition to tumor cells themselves, the targeting of such a complex inflammatory network involving numerous cell types and mediators presents as an exciting challenge for the development of novel therapeutic strategies for cancer.

References

1. Colotta, F., et al., *Cancer-related inflammation, the seventh hallmark of cancer: links to genetic instability.* Carcinogenesis, 2009. **30**(7): p. 1073-81.

2. Schafer, M. and S. Werner, *Cancer as an overhealing wound: an old hypothesis revisited.* Nat Rev Mol Cell Biol, 2008. **9**(8): p. 628-38.

3. Arlt, A., et al., *Autocrine production of interleukin 1beta confers constitutive nuclear factor kappaB activity and chemoresistance in pancreatic carcinoma cell lines.* Cancer Res, 2002. **62**(3): p. 910-6.

4. Elaraj, D.M., et al., *The role of interleukin 1 in growth and metastasis of human cancer xenografts.* Clin Cancer Res, 2006. **12**(4): p. 1088-96.

5. Qin, Y., et al., *Constitutive aberrant endogenous interleukin-1 facilitates inflammation and growth in human melanoma.* Mol Cancer Res, 2011. **9**(11): p. 1537-50.

6. Dinarello, C.A., *Immunological and inflammatory functions of the interleukin-1 family.* Annu Rev Immunol, 2009. **27**: p. 519-50.

7. Okamoto, M., et al., *Constitutively active inflammasome in human melanoma cells mediating autoinflammation via caspase-1 processing and secretion of interleukin-1beta.* J Biol Chem, 2010. **285**(9): p. 6477-88.

8. Bjorkdahl, O., et al., *Gene transfer of a hybrid interleukin-1 beta gene to B16 mouse melanoma recruits leucocyte subsets and reduces tumour growth in vivo.* Cancer Immunol Immunother, 1997. **44**(5): p. 273-81.

9. Torisu, H., et al., *Macrophage infiltration correlates with tumor stage and angiogenesis in human malignant melanoma: possible involvement of TNFalpha and IL-1alpha.* Int J Cancer, 2000. **85**(2): p. 182-8.

10. Boni, R., et al., *Staging of metastatic melanoma by whole-body positron emission tomography using 2-fluorine-18-fluoro-2-deoxy-D-glucose.* Br J Dermatol, 1995. **132**(4): p. 556-62.

11. Gross, O., et al., *The inflammasome: an integrated view.* Immunol Rev, 2011. **243**(1): p. 136-51.

12. Hanahan, D. and R.A. Weinberg, *Hallmarks of cancer: the next generation.* Cell, 2011. **144**(5): p. 646-74.

13. Siveen, K.S. and G. Kuttan, *Role of macrophages in tumour progression.* Immunol Lett, 2009. **123**(2): p. 97-102.

14. Farinha, P., et al., *Analysis of multiple biomarkers shows that lymphoma-associated macrophage (LAM) content is an independent predictor of survival in follicular lymphoma (FL).* Blood, 2005. **106**(6): p. 2169-74.

15. Hanada, T., et al., *Prognostic value of tumor-associated macrophage count in human bladder cancer.* Int J Urol, 2000. **7**(7): p. 263-9.

16. Steidl, C., et al., *Tumor-associated macrophages and survival in classic Hodgkin's lymphoma.* N Engl J Med, 2010. **362**(10): p. 875-85.

17. Zhu, X.D., et al., *High expression of macrophage colony-stimulating factor in peritumoral liver tissue is associated with poor survival after curative resection of hepatocellular carcinoma.* J Clin Oncol, 2008. **26**(16): p. 2707-16.

18. Laoui, D., et al., *Tumor hypoxia does not drive differentiation of tumor-associated macrophages but rather fine-tunes the M2-like macrophage population.* Cancer Res, 2014. **74**(1): p. 24-30.

19. Lima, L., et al., *The predominance of M2-polarized macrophages in the stroma of low-hypoxic bladder tumors is associated with BCG immunotherapy failure.* Urol Oncol, 2014. **32**(4): p. 449-57.

20. Kimura, Y.N., et al., *Inflammatory stimuli from macrophages and cancer cells synergistically promote tumor growth and angiogenesis.* Cancer Sci, 2007. **98**(12): p. 2009-18.

21. Qian, B.Z. and J.W. Pollard, *Macrophage diversity enhances tumor progression and metastasis.* Cell, 2010. **141**(1): p. 39-51.

22. Colegio, O.R., et al., *Functional polarization of tumour-associated macrophages by tumour-derived lactic acid.* Nature, 2014.

23. Tripathi, C., et al., *Macrophages are recruited to hypoxic tumor areas and acquire a Pro-Angiogenic M2-Polarized phenotype via hypoxic cancer cell derived cytokines Oncostatin M and Eotaxin.* Oncotarget, 2014. **5**(14): p. 5350-68.

24. Parker, K., et al., *HMGB1 enhances immune suppression by facilitating the differentiation and suppressive activity of myeloid-derived suppressor cells.* Cancer Res, 2014.

25. Chai, C.Y., et al., *Hypoxia-inducible factor-1alpha expression correlates with focal macrophage infiltration, angiogenesis and unfavourable prognosis in urothelial carcinoma.* J Clin Pathol, 2008. **61**(5): p. 658-64.

26. Murdoch, C. and C.E. Lewis, *Macrophage migration and gene expression in response to tumor hypoxia.* Int J Cancer, 2005. **117**(5): p. 701-8.

27. Vaupel, P. and A. Mayer, *Hypoxia in cancer: significance and impact on clinical outcome.* Cancer Metastasis Rev, 2007. **26**(2): p. 225-39.

28. Gatenby, R.A. and R.J. Gillies, *A microenvironmental model of carcinogenesis.* Nat Rev Cancer, 2008. **8**(1): p. 56-61.

29. Webb, B.A., et al., *Dysregulated pH: a perfect storm for cancer progression.* Nat Rev Cancer, 2011. **11**(9): p. 671-7.

30. Yan, W., et al., *High-mobility group box 1 activates caspase-1 and promotes hepatocellular carcinoma invasiveness and metastases.* Hepatology, 2012. **55**(6): p. 1863-75.

31. van Beijnum, J.R., et al., *Tumor angiogenesis is enforced by autocrine regulation of high-mobility group box 1.* Oncogene, 2013. **32**(3): p. 363-74.

32. Taguchi, A., et al., *Blockade of RAGE-amphoterin signalling suppresses tumour growth and metastases.* Nature, 2000. **405**(6784): p. 354-60.

33. He, Y., et al., *Tissue damage-associated "danger signals" influence T-cell responses that promote the progression of preneoplasia to cancer.* Cancer Res, 2013. **73**(2): p. 629-39.

34. Bald, T., et al., *Ultraviolet-radiation-induced inflammation promotes angiotropism and metastasis in melanoma.* Nature, 2014. **507**(7490): p. 109-13.

35. Bartolome, R.A., et al., *The chemokine receptor CXCR4 and the metalloproteinase MT1-MMP are mutually required during melanoma metastasis to lungs.* Am J Pathol, 2009. **174**(2): p. 602-12.

36. Toyozawa, S., et al., *Chemokine receptor CXCR4 is a novel marker for the progression of cutaneous malignant melanomas.* Acta Histochem Cytochem, 2012. **45**(5): p. 293-9.

37. Schiraldi, M., et al., *HMGB1 promotes recruitment of inflammatory cells to damaged tissues by forming a complex with CXCL12 and signaling via CXCR4.* J Exp Med, 2012. **209**(3): p. 551-63.

38. Liu, Z., L.D. Falo, Jr., and Z. You, *Knockdown of HMGB1 in tumor cells attenuates their ability to induce regulatory T cells and uncovers naturally acquired CD8 T cell-dependent antitumor immunity.* J Immunol, 2011. **187**(1): p. 118-25.

39. Terai, M., et al., *Interleukin 6 mediates production of interleukin 10 in metastatic melanoma.* Cancer Immunol Immunother, 2012. **61**(2): p. 145-55.

40. Kurte, M., et al., *A synthetic peptide homologous to functional domain of human IL-10 down-regulates expression of MHC class I and Transporter associated with Antigen Processing 1/2 in human melanoma cells.* J Immunol, 2004. **173**(3): p. 1731-7.

41. Carter, N.A., E.C. Rosser, and C. Mauri, *Interleukin-10 produced by B cells is crucial for the suppression of Th17/Th1 responses, induction of T regulatory type 1 cells and reduction of collagen-induced arthritis.* Arthritis Res Ther, 2012. **14**(1): p. R32.

42. Carter, N.A., et al., *Mice lacking endogenous IL-10-producing regulatory B cells develop exacerbated disease and present with an increased frequency of Th1/Th17 but a decrease in regulatory T cells.* J Immunol, 2011. **186**(10): p. 5569-79.

43. Chen, Q., et al., *Production of IL-10 by melanoma cells: examination of its role in immunosuppression mediated by melanoma.* Int J Cancer, 1994. **56**(5): p. 755-60.

44. Mahipal, A., et al., *Tumor-derived interleukin-10 as a prognostic factor in stage III patients undergoing adjuvant treatment with an autologous melanoma cell vaccine.* Cancer Immunol Immunother, 2011. **60**(7): p. 1039-45.

45. Zhao, C.B., et al., *Co-expression of RAGE and HMGB1 is associated with cancer progression and poor patient outcome of prostate cancer.* Am J Cancer Res, 2014. **4**(4): p. 369-77.

46. Fang, H., et al., *TLR4 is essential for dendritic cell activation and anti-tumor T-cell response enhancement by DAMPs released from chemically stressed cancer cells.* Cell Mol Immunol, 2014. **11**(2): p. 150-9.

47. Hodge, J.W., et al., *Chemotherapy-induced immunogenic modulation of tumor cells enhances killing by cytotoxic T lymphocytes and is distinct from immunogenic cell death.* Int J Cancer, 2013. **133**(3): p. 624-36.

48. Krysko, D.V., et al., *Immunogenic cell death and DAMPs in cancer therapy.* Nat Rev Cancer, 2012. **12**(12): p. 860-75.

Abbreviations and Units

Abbreviations

AICR	Association for International Cancer Research
AIM	Absent in melanoma
AJCC	American Joint Committee on Cancer
ALM	Acral lentiginous melanoma
AML	Acute myeloid leukemia
AP	Alkaline phosphatase
Apaf	Apoptotic protease-activating factor
APC	Antigen-presenting cells
APS	Ammonium persulfate
ARF	Alternate reading frame
ASC	Apoptosis-associated speck-like protein
ATP	adenosine triphosphate
AZA	Aza-2′-deoxycytidine
BAD	BCL-2-associated agonist of cell death
Bcl	B-cell lymphoma derived protein
BIM	B-cell lymphoma 2 Interacting Mediator of cell death
BSA	Bovine serum albumin
Ca	Calcium
$CaCl_2$	Calcium chloride
cAMP	Cyclic adenosine monophosphate
CAPS	Cryopyrin-associated periodic syndromes
CARD	Caspase recruitment domain
CD	Cluster of differentiation
CDK	Cyclin dependent kinase
CDKN2A	Cyclin dependent kinase inhibitor-2A
CFSE	Carboxyfluorescein succinimidyl
CH	Contact hypersensitivity
CINCA	Chronic infantile neurological cutaneous and articular syndrome

COX2	Cyclooxygenase-2
CTLA-4	Cytotoxic T-lymphocyte-associated protein 4
DAMP	Danger-associated molecular patterns
DC	Dendritic cells
ddH_2O	Bidistilled water
DDT	DL-Dithiothreitol
DIRA	Deficiency of interleukin-1 receptor antagonist
DISC	Death-inducing signaling complex
Diss.	Dissertation
DMEM	Dulbecco's Modified Eagle's medium
DMSO	Dimethylsulfoxide
*E.*coli	Escherichia coli
E2F	E2F cell cycle regulated transcription factor
ECM	Extracellular matrix
EDTA	Ethylenediaminetetraacetic acid
ELISA	Enzyme-linked immunosorbent assay
EMT	Epithelial-mesenchymal transition
ER	Endoplasmic reticulum
ERK	Extracellular-signal-Regulated Kinase
FACS	Fluorescence-activated cell sorting
FCAS	Familial cold autoinflammatory syndrome
FCS	Fetal calf serum
FGF	Fibroblast growth factor
FITC	Fluorescein isothiocyanate
FOX	Forkhead transcription factor
HBV	Hepatitis B virus
HCC	hepatocellular carcinoma
HCl	Hydrogen chloride
HCV	Hepatitis C virus
hdm	Human double minute chromosome-associated protein
Hif-1α	Hypoxia-inducible factor 1α

HIV	Human immunodeficiency virus
HMGB1	High-Mobility Group Box 1
HSP	Heat shock protein
iDC	Immature DCs
IFN	Interferon
IL	Interleukin
IL-1RAcP	IL-1 receptor accessory protein
iNOS	NO synthase
IRAK	IL-1 receptor kinase
JNK	c-Jun N-terminal kinase
K	Potassium
KCl	Potassium chloride
LDH	Lactate dehydrogenase
LMM	lentigo maligna melanoma
LPC	Lysophosphatidylcholines
LPS	Lipopolysaccharide
Lys	Lysate
MAPK	Mitogen-activated protein kinase
MC	Mast cell
MC1R	Melanocortin-1 receptor
M-CSF	Macrophage colony-stimulating factor
mDC	Myeloid DCs
MDM2	Mouse Double Minute 2 homolog
MDP	Muramyl dipeptide
MDSC	Myeloid-derived suppressive cells
MEK	MAPK/Extracellular-signal-regulated Kinase kinase
MgCl2	Magnesium chloride
MHC	Major histocompatibility complexes
MIC	Modular Incubator Chamber
MITF	Microphthalmia transcription factor
MMP	Matrix metalloproteinase

MOMP	Mitochondrial outer membrane permeabilization
mRNA	Messenger RNA
MSH	Melanocyte stimulating hormone
MSU	Monosodium urate
mtDNA	Mitochondrial DNA
mTOR	Mammalian target of rapamycin
MTT	3-(4,5-dimethylthiazol-2-yl)-
MyD88	Myeloid differentiation primary response gene 88
NaCl	Sodium chloride
NaOH	Sodium hydroxide
NF-kB	Nuclear factor κB
NK cells	Natural killer cells
NLRC	Nod-like receptor family CARD domain-containing protein
NLRP	Leucine-rich repeat-containing receptor protein
NLS	Nuclear localization signal
NM	Nodular melanoma
NO	Nitric oxide
O_2	Oxygen
p	Probability
P/S	Penicillin/ Streptomycin
PAMP	Pathogen-associated molecular patterns
PAPA	Pyogenic arthritis-pyoderma gangrenosum-acne
PBS	Phosphate buffered saline
PBST	Phosphate buffered saline tween
PD-1	Programmed death 1 protein
PDGF	Platelet-derived growth factor
PDK1	Phosphoinositide-dependent kinase 1
PGE2	Prostaglandin E2
PI3K	phosphatidylinositol-3 kinase
PMA	Phorbol-12-myristate-13-acetate
PRR	Pathogen recognition receptors

PtdIns(3,4,5)P3	Phosphatidylinositol (3,4,5)-tris-phosphate
PTEN	Phosphatase and Ten sin homolog
PYD	Pyrin domain
Ra	Receptor antagonist
RAF	Rapidly Accelerated Fibrosarcoma
RAG	Recombination-activating genes
RAGE	Receptor for Advanced glycation Endproducts
RAS	Rat sarcoma oncogene
Rb	Retinoblastoma protein
rec.	Recombinant
RNI	Reactive nitrogen intermediates
ROI	Reactive oxygen intermediates
ROS	Reactive oxygen species
RPMI	Roswell Park Memorial Institute medium
RSS	Recombination signal sequence
SCF	Stem cell factor
SDS	Sodium dodecyl sulfate
SEM	Standard error of the mean
shRNA	Short hairpin RNA
SN	Supernatant
SSM	Superficial spreading melanoma
Syk	Spleen tyrosine kinase
TAA	Tumor-associated antigens
TAM	Tumor-associated macrophages
TAN	Tumor-associated neutrophils
TBP	TATA binding protein
TCR	T cell receptor
TEMED	Tetramethylethylenediamine
TGF	Transforming growth factor
Th	T helper
TIR	Toll/IL-1 receptor

TLR	Toll-like receptor
TNF	Tumor necrosis factor
Treg	Regulatory T cells
uPA	Urokinase-type plasminogen activator
uPAR	Urokinase receptor
URPP	Zürich University Research Priority Program
UV	Ultraviolet
UVR	Ultraviolet radiation
VDAC	voltage-dependent anion channels
VEGF	Vascular Endothelial Growth Factor
VLC	Vascular leukocytes
α	Alpha
β	Beta
γ	Gamma
δ	Delta
κ	Kappa

Units

°C	Degree celcius
µg	Microgram
µl	Microliter
bp	Base pairs
cm	Centimeter
dpi	Dots per inch
g	Gram
h	Hour
min	Minute
ml	Milliliter
mM	Millimolar
ng	Nanogram
nm	Nanometer
OD	Optical density
s	Second
U	Unit
V	Voltage

Acknowledgements

A special thanks to Prof. Lars French, for providing me with the opportunity of achieving my PhD in his lab and for all the scientific, technical and personal support, constructive criticism, trust, optimism, patience, and for the time he dedicated to guide my thesis. Going through my PhD has been a challenging and valuable experience, and I am very grateful for the active interested support and supervision which made my thesis possible.

I thank Prof. Reinhard Dummer, Prof. Burkhard Becher, and Prof. Urs Greber, for being members of my thesis committee, for their interest in my project, for the discussions, for their pragmatism and the fact that they were willing to share their enormous experience and knowledge with me.

I thank Dr. Emmanuel Contassot, who in the daily life in the lab was my first contact person to plan, perform, interpret (and cancel) experiments. His door was never closed and his pragmatism and contenance are the perfect antidote against PhD student's hysteria syndrome.

I thank Prof. Atsushi Otsuka, for being a master support during the last two years of my project. In his country, there is an expression describing what he is: he's the "sensai"! Thanks a lot Ats!

I thank my colleagues Dr. Samuel Gehrke, Dr. Dragana Jankovic, Dr. Magdalena Kistowska, Marianne Spalinger, Dr. Hans-Dietmar Beer, Dr. Gabriel Sollberger, Gerhard Strittmatter, Gabriele Fenini, Martha Garstkiewicz, Tatiana Proust, Jenny Sand, Dr. Barbara Meier, Dr. Takashi Satoh and Dr. Mark Mellett (listed by appearance...) for helping me through my progress in every possible way. Having enjoyable, caring and cooperative people around you in the lab is worth a lot! I wish you all the best for the success of your projects! Gerhard, ganz stark, wie Ballack!

I thank Prof. Reinhard Dummer and Prof. Mitchell Levesque for providing patient samples and Melanie Maudrich and Ines Kleiber-Schaaf for spending hours to collect them.

I thank Dr. Daniel Widmer for assisting me with support and material to culture cells under hypoxia *in vitro*.

I thank Prof. Onur Boyman and his team, Dr. Elvira Haas and her team, and Dr. Rok Humar and his team for the exchange of material and opinions, and for creating a friendly and supportive atmosphere in Gloria 30.

I thank all the people from the F-floor for their cooperation and willingness to share their know-how.

I thank Katrin Stahel and Khünsang Ngawang for finding the gaps.

I thank the Microbiology and Immunology PhD program (MIM) and the Faculty of Science (MNF), in special Olympia Stefani, Judith Zingg, and Cornelia Schmid for the organization and promotion of everything.

I cannot really find a reason to thank Ulrich and Pacher, but every man likes to find his name on something. So do kids, thus hello to Jade, Romy, Marco and Eva!

My very special thanks go to my grandmothers, my parents and my sister. No matter what happens, they are always on my side, even if they know that I am wrong.

Though not working in the scientific field, the biggest positive influence for the outcome of my work came from Christelle. Having her with me is the biggest success of my life and I couldn`t ask for more. I love you so much!

I dedicate this thesis to my mother Angela Eva Huber.

Appendix

M2 macrophages and innate lymphoid type 2 cells promote metastasis via IL-1β and thymic stromal lymphopoietin in malignant melanoma

Atsushi Otsuka[1], Chisa Nakashima[2], Roman Huber[1], Barbara Meier[1], Takashi Satoh[1], Gabriele Fenini[1], Katrin Kerl[1], Phil Cheng[1], Onur Boyman[1], Steven F Ziegler[3], Kenji Kabashima[2], Mitchell P Levesque[1], Reinhard Dummer[1], Emmanuel Contassot[1], and Lars E. French[1]

[1]Department of Dermatology, University Hospital Zurich, Zurich 8091, Switzerland

[2]Department of Dermatology, Kyoto University Graduate School of Medicine, Kyoto, Japan

[3]Immunology Program, Benaroya Research Institute, Seattle, WA

Correspondence to

Lars E. French, MD, and Emmanuel Contassot, PhD

Department of Dermatology, University Hospital Zurich, Gloriastrasse 31, Zurich 8091, Switzerland

Tel: +41-44-255-2550, Fax: +41-44-255-4403, Email: Emmanuel.Contassot@usz.ch

This work was supported in part by the Association for International Cancer Research, AICR 09-0230 to L.E.F, by the University Research Priority Program (URPP) biobank, and by the Society for Skin Cancer Research to M.P.L.

Abstract

The incidence of melanoma is increasing worldwide and despite new treatment options survival of patients with metastatic melanoma remains poor [1, 2]. The molecular mechanisms regulating melanoma metastasis are still poorly characterized. Here we find that the pleiotropic pro-inflammatory cytokine interleukin-1β (IL-1β) which has been suspected to play a role in metastasis [3, 4] is overexpressed in human melanoma metastases. To investigate mechanisms through which IL-1β may promote metastasis, we generated murine B16 melanoma cells that overexpress and secrete the active p17 form of IL-1β. Overexpressed IL-1β promoted metastasis in tumor-draining lymph nodes and in an established model of lung metastasis. Evaluation of cytokine expression during primary tumor progression revealed that IL-1β promotes a Th2 biased cytokine environment in tumors and tumor infiltration by M2-macrophages. Analysis of fibroblasts revealed that IL-1β induces the expression of thymic stromal lymphopoietin (TSLP), a key initiator of Th2 responses [5], and TSLP is produced by tumor associated fibroblasts isolated from melanomas. Ablation of the TSLP-receptor in mice resulted in reduced Th2 cytokine expression, macrophage recruitment to tumors, and metastasis, delineating an essential role for IL-1β driven TSLP in regulating metastasis. Furthermore, deletion of macrophages by clodronate or by diphteria-toxin in LysM diphtheria toxin receptor (DTR) mice likewise resulted in a reduction of metastasis. Given that innate lymphoid type 2 cells (ILC2s) can sustain M2 macrophage infiltration [6], the presence of ILC2 was analyzed in melanoma. In IL-1β-producing B16 tumors and human melanoma metastases increased numbers of ILC2s were detected. Depletion of ILCs in $Rag1^{-/-}$ mice using anti-CD25 neutralizing antibodies resulted in reduced intratumoral Th2 cytokines, M2-marker expression and lymph-node metastases indicating that ILC2 promote tumor enrichment with M2 macrophages and tumor metastasis. We demonstrate that the IL-1β-TSLP cytokine signaling axis is essential for tumor infiltration by M2 macrophages and ILC2s which promote melanoma metastasis.

Main

The incidence of melanoma has significantly increased over the past few decades [7]. Despite new treatment options, the survival rate of patients with metastatic melanoma has only marginally improved [1, 2]. One reason for the low survival rate in late stage melanoma is due to the difficulty in controlling tumor metastasis. The tumor microenvironment, including the cytokine milieu, plays a central role in metastasis [8, 9]. Interleukin (IL)-1β is a pleiotropic pro-inflammatory cytokine, which is often detected in human tumors [3, 4]. It has been reported that increased expression levels of the IL-1β gene or protein is associated with cancer metastasis [10]. However, the precise mechanism of metastasis promotion by IL-1β remains largely unknown.

To assess the effect of IL-1β in melanoma progression, we first evaluated local IL-1β expression in benign melanocytic nevi, primary melanomas, and metastatic melanomas. The number of IL-1β positive cells was significantly higher in metastatic melanoma compared to that in nevi and primary melanomas (Fig.1 A, B). In the BRAF/PTEN autochthonous mouse melanoma model [11], IL-1β secretion was also upregulated in late stage tumors that are associated with draining lymph node (dLN) metastasis (Fig.1 C). These results indicate that the metastatic stage of melanoma is associated with high IL-1β expression at the tumor site. To assess the functional role of IL-1β overproduction in metastases, we generated melanoma cell lines producing the active (p17) secreted form of IL-1β as previously reported [12]. We injected either control B16 cells or IL-1β-producing B16 cells i.v. into wild type mice to assess the effect of IL-1β on tumor metastasis. Overexpression of IL-1β by B16 resulted in a remarkable increase in lung metastases (Fig.1 D, E). Since i.v. inoculation of tumor cells is an artificial model and may have limited relevance to actual mechanisms of metastasis, we also analyzed spontaneous metastasis to LNs draining subcutaneously growing B16 tumors. Consistent with the lung metastasis model, the number of metastases derived from subcutaneous IL-1β-producing B16 melanomas was significantly increased (Fig. 1 F, G). Altogether, these results indicate that IL-1β promotes melanoma metastasis.

To assess the impact of IL-1β on the microenvironment of subcutaneous tumors, we evaluated cytokine expression during primary subcutaneous tumor progression by real-time PCR. While interferon (IFN)-γ expression in IL-1β-producing B16 tumors was comparable to that of control B16 tumors during tumor progression, the expression levels of T helper (Th)2 cytokines, including IL-4, IL-10, and IL-13 were significantly increased in IL-1β-producing B16 tumors (Fig. 2A). We next evaluated tumor-infiltrating cells by flow cytometry. The number of $CD4^+$ and $CD8^+$ T cells infiltrating control B16 and IL-1β-producing B16 tumors did not differ significantly (Fig. 2B, Supplementary Fig S1A). In contrast, the number of tumor-infiltrating macrophages, eosinophils, and mast cells were significantly higher in IL-1β-producing B16 tumors (Fig. 2B, Supplementary Fig S1B, C, D and Supplementary Fig S2). To evaluate Th2

T cell numbers, intracellular IL-4 staining was performed on collagenase-digested tumors. Consistent with the IL-4 gene expression data, IL-4-producing $CD4^+$ T cells were significantly increased in IL-1β-producing B16 tumors (Fig. 2C). To assess the phenotype of macrophages that infiltrate IL-1β producing tumors, we examined the expression of markers distinguishing M1- and M2- macrophage subpopulations [13]. Quantitative PCR of macrophages located at the tumor site revealed that the expression of M2 markers (*MR, Fizz1, Arg1*, and *YM1*) but not M1 markers (*iNOS* and *Arg2*) was significantly upregulated in IL-1β-producing B16 tumors (Fig. 2D). To assess the relevance of this observation with respect to human melanoma, we stained human melanomas with a specific M2 marker, namely CD163. A significant increase in $CD163^+$ cell numbers was also found in human metastatic melanomas when compared to primary tumors (Fig.2E). Thymic stromal lymphopoietin (TSLP) is a key initiator of Th2 responses [5]. Given a recent study showing that TSLP has a negative impact on the survival of pancreatic cancer patients [14], we hypothesized that TSLP may play a role in shaping the immunological microenvironment of tumors and the subsequent development of metastases. Since it has been reported that the interaction of tumors and fibroblasts plays a pivotal role in tumor progression, we first exposed mouse embryonic fibroblasts (MEFs) to either recombinant IL-1β or IL-1β-producing B16. In both conditions, MEFs produced TSLP in a dose-dependent manner (Fig. 3A). To assess the relevance of this observation to human melanoma, we evaluated TSLP mRNA levels using healthy donor-derived fibroblasts and melanoma-associated fibroblasts. We found that TSLP expression was significantly increased in melanoma-associated fibroblasts (Fig. 3B). Functional evaluation of the effect of TSLP on tumor metastasis using TSLP receptor $(TSLPR)^{-/-}$ mice revealed that the number of metastases in mice bearing IL-1β-producing B16 tumors was significantly lower in $TSLPR^{-/-}$ than wild-type mice (Fig. 3C). These results demonstrate that TSLP is a key mediator of IL-1β-induced metastasis. Interestingly, in the primary tumor (subcutaneous), the expression of Th2 (IL-4 and IL-13) but not Th1 (IFN-γ) cytokines was also found to be decreased in $TSLPR^{-/-}$ mice (Fig. 3D). Furthermore, both the number of macrophages infiltrating the primary tumors, and the expression of M2 markers were decreased in $TSLPR^{-/-}$ mice (Fig. 3D, E), suggesting that TSLP is a key regulator of IL-1β-induced recruitment of M2 macrophages to the tumor.

Tumor associated-macrophages (TAMs) are a major component of the tumor microenvironment and they have been reported to be biased towards an M2 phenotype in advanced tumors [15-17]. To further address the functional role of TAMs during IL-1β-induced metastasis, we depleted macrophages using clodronate. Interestingly, the number of IL-1β-producing B16 metastases was significantly reduced in clodronate-treated mice (Fig. 4A). To confirm this observation and exclude a possible role of dendritic cells that are also depleted by clodronate, we performed the same experiment in LysM diphtheria toxin receptor

(DTR) mice. Consistent with the results obtained with clodronate treatment, the number of metastases was also significantly decreased in LysM-DTR mice bearing IL-1β producing B16 tumors (Fig. 4B). These results identify TAMs as key players in IL-1β-related tumor metastasis.

We next assessed the expression of 84 genes known to be involved in metastasis by PCR array analyses of B16 cells exposed or not to IL-1β and/or bone marrow-derived M2 (BMM2) macrophages. The expression of 8 genes were significantly modulated in B16 upon exposure to BMM2 and IL-1β (> 2-fold change; $p<0.05$). Notably, 4 genes known to promote metastasis *Igf1*, *Mmp13*, *Mmp9* and *Nme2* were significantly upregulated, whereas 4 genes known to inhibit metastasis *Cd82*, *Ctbp1*, *Ephb2* and *Ewsr1* were significantly downregulated (Fig.4C, Table S1). In line with these data, we also found that *CD82* and *EPHB2* expression levels affect the survival rate of melanoma patients (Fig. S4).

It has recently been reported that M2 macrophages are sustained by innate lymphoid type 2 cells (ILC2s) in adipose tissue [6]. Our results showing that IL-1β enhanced the number of M2 macrophages in tumors prompted us to analyze the presence of ILC2 in IL-1β-producing B16 tumors. At the tumor site, we identified a population of lineage-negative (Lin^-) cells that lacked the expression of cell surface markers associated with T cells (CD3), B cells (B220), DCs (CD11c), macrophages/monocytes (CD11b), or mast cells and basophils (FcγRIα), but expressed both *Thy1.2* and *IL-33R* (Fig. 4D, E). This phenotype is consistent with that of ILC2s as previously described [18, 19]. Our results demonstrate that significantly increased numbers of ILC2 are found in IL-1β-producing B16 tumors (Fig. 4D, E). Interestingly, recent *in vivo* studies have suggested that both murine and human ILC2s are responsive to TSLP [20], although the impact of TSLP on ILC2 responses remains unknown. We therefore quantified ILC2 in IL-1β-producing B16 tumors implanted in $TSLPR^{-/-}$ mice. In the absence of TSLPR, tumor infiltration by ILC2s was dramatically decreased when compared to TSLPR-expressing mice (Fig. 4F, Fig. S5). To test whether ILC2 affect melanoma metastasis, we depleted ILCs in $Rag1^{-/-}$ mice using anti-CD25 neutralizing antibodies as previously reported [18]. Depletion of $CD25^+$ ILCs resulted in reduced Th2 cytokine production as well as M2-marker expression (Fig. S6). In addition, ILC depletion resulted in reduced numbers of draining lymph-node metastases (Fig. 4G), indicating that ILC2 promotes tumor enrichment with M2 macrophages and tumor metastasis. To determine the relevance of this finding to human melanoma, we further examined metastases of melanoma patients for the presence of ILC2. Flow cytometry analysis of human melanoma metastases revealed a significantly increased frequency of ILC2s *in situ* in metastatic melanoma samples as compared to healthy skin (Fig. 4H, I).

It has been reported that systemic Th2-driven chronic inflammation is enhanced in patients with metastatic melanoma [21], and the ratio of Th2/Th1 cells is augmented in stage IV

melanoma patients [22]. The precise cause and consequences of a Th2 microenvironment in late stage melanoma is however unclear to date. We identify IL-1β present in the tumor microenvironment as a key promoter of an intratumoral Th2 cytokine milieu and tumor metastasis, both of which are critically dependent upon tumor infiltration by M2 macrophages. Although TAMs are biased towards the M2 phenotype in advanced tumors, the factors responsible for the increase of TAMs with a M2 phenotype at site of tumors remain largely unknown. In this study, we demonstrate that IL-1β likely derived from the microenvironment of primary tumors, induces peritumoral fibroblast-derived TSLP, the latter being essential for the recruitment of M2-macrophages to the tumor site. In addition we show for the first time, that ILC2 are essential for tumor metastasis likely by promoting sustained tumor infiltration by M2-macrophages, and moreover these ILCs are found in large numbers both in murine and human metastatic melanoma. Taken together, the IL-1β-TSLP signaling axis discovered within the tumor microenvironment here is essential for tumor infiltration by M2-macrophages and ILC2s as well as tumor metastasis. Considering the broad diversity of tumors, this newly identified signaling pathway in melanoma could be a novel target for the treatment of metastatic melanoma (Fig. S7).

Methods

Mice

Eight- to 12-week-old female C57BL/6 mice were used in this study. C57BL/6 mice were purchased from (Harlan, Venray, Netherlands). Rag1$^{-/-}$ mice were purchased from the Jackson Laboratory. B6.Cg-*Braf*^{tm1Mmcm} *Pten*^{tm1Hwu} Tg (Tyr-cre/ERT2) 13Bos/BosJ (BRAF/PTEN) mice [11], TSLPR$^{-/-}$ mice and LysM-DTR[23] mice were all described previously. All experimental procedures were approved by the Veterinary Office of Zurich and the institutional animal care and use committee of Kyoto University Graduate School of Medicine.

Generation of IL-1β-producing B16

IL-1β cDNA encoding for the mature p17 form (i.e. not requiring caspase-1 cleavage) of IL-1β was fused to a signal sequence derived from structurally related human IL-1RA in order to generate a constitutively mature secreted from of IL-1β as previously reported [12, 24]. Transfection was performed using Lipofectamin 2000 (Invitrogen, Carlsbad, California) and the transfectants were generated as previous described [25]. Two clones were generated and IL-1β production was confirmed by ELISA using the supernatant of IL-1β-producing (RnD Systems).

B16F10 cell line was cultured in RPMI 1640 (Invitrogen) supplemented with 10% heat-inactivated fetal calf serum, 2 mM l-glutamine, 25 mM *N*-2-hydroxyethylpiperazine-*N*′-2-ethanesulfonic acid, 1 mmol/L nonessential amino acids, 1 mmol/L sodium pyruvate, 100 units/mL penicillin, and 100 μg/mL streptomycin.

Tumor metastasis experiments

Control-B16 or IL-1β-producing B16 (2×10^5) were subcutaneously injected into the right flank of wild-type mice. Mice were monitored every 2 days and tumor size was measured using a caliper. Tumor volume was expressed as the square of the smallest diameter multiplied by its largest diameter. Mice that developed tumors with L=10 mm were killed according to the Swiss legislation on animal experiments and the number of macroscopically visible melanoma metastases in the draining lymph nodes was counted in five fields (× 20 objective) by the same dermato-pathologist using the same subjective grading scale. Lung metastases were generated by intravenous injection of 2×10^5 B16 cells in 100 μl of PBS. Mice were killed 14 days after challenge, and the number of macroscopically visible melanoma metastases on the surface of the lungs was counted and measured in a masked manner by two different experimenters.

Cell preparation, antibodies and flow cytometry

For the preparation of tumor infiltrating cell suspensions, minced tumors were incubated with collagenase D (1.5 mg/ml) (Worthington Biochemical) in RPMI for 1 hour at 37°C and 5% CO_2. Cell suspensions were filtered through a 40-µm cell strainer (BD Bioscience, San Diego, CA). The numbers of each cell subset were calculated by flow cytometry and presented are the numbers per mm^3 of tumor size.

Anti-mouse CD3, CD4, CD8, CD11b, CD11c, CD45, B220, c-kit, F4/80, FcεRI, Gr-1, and Thy1.2 antibodies were purchased from eBioscience (San Diego, CA). Anti- mouse CCR3 was purchased from Bio-Legend (San Diego, CA), SiglecF, IL-4 from BD Biosciences (San Jose, CA, USA), CD200R3 from Hycult Biotech (Uden, Netherlands), 7/4 from Abcam, and IL-33R from MD bioscience (St. Paul, MN). Anti-human CD25, CD11c, CD45, CD56, IL-33R, and TCRαβ antibodies were purchased from BD Pharmingen. Anti-human CD3 and CD16 were purchased from Bio-Legend, CD19 from Miltenyi Biotech, and FcεRI from (eBioscience). Flow cytometry was performed using FACS Canto and Fortessa (BD Biosciences) and analyzed with FlowJo (TreeStar, San Carlos, CA).

For intracellular IL-4 staining of $CD4^+$ T cells, tumor infiltrating cell suspensions were collected and incubated with PMA (20 ng/ml), ionomycin (1 µM), and Brefeldin A (5 µM) for four hours and as previously reported [26].

Quantitative PCR analysis and qPCR array

Quantitative PCR analysis was performed as previously reported [27]. Briefly, total RNAs were isolated with Trizol (Life Technologies, Gaithersburg, MD) from tissues. cDNA was reverse transcribed (RT) using a RevertAid First Strand cDNA kit (Thermo Scientific, MA, USA). Quantitative RT-PCR with a Light Cycler real-time PCR apparatus was performed (Roche Diagnostics, Foster City, CA) using SYBR Green I (Roche, Basel, Switzerland). Expression of mRNA (relative) was normalized to the expression of RPL27 mRNA by the change in cycling threshold (ΔC_T) method and calculated based on $2^{-\Delta\Delta CT}$.

For PCR array, RNA was analyzed by a RT-PCR array for mouse metastatic genes (PAMM-028Z, Qiagen). Each condition was performed in triplicate. Fold change and p values were calculated by RT^2 Profiler PCR Array Analysis (http://pcrdataanalysis.sabiosciences.com/pcr/arrayanalysis.php, Qiagen). B16 cells as control were used as baseline for comparison and significant gene expression changes were defined with absolute fold change > 2 and a p value < 0.05.

Survival data were generated from the melanoma dataset of the TCGA (http://cancergenome.nih.gov). The top 30% and bottom 30% patients of CD82 and EPHB2 normalized RNAseq reads were compared for overall survival by Kaplan Meier survival analysis.

ELISA

The amounts of human/mouse IL-1β (R & D) and mouse TSLP (eBioscience) were measured by ELISA according to the manufacturer's instructions. For the measurement of mouse IL-1β in the tumor, 5 mm tumor biopsies were collected and homogenized in 300 µl PBS. The supernatants were collected for ELISA.

Generation of normal and melanoma-associated fibroblast and co-culture of MEFs with B16.

The normal fibroblast early passage cultures were generated from patients undergoing plastic surgery. The tissue was sectioned and put in a flask with RPMI culture medium and was trypsinized and split for 1-4 passages until the cells were of similar morphology. The same was done from skin that was removed from melanoma biopsies, and the cells were confirmed to have fibroblast morphology and to lack known oncogenic mutations from the respective patients.

For co-culture of fibroblasts and control B16 or IL-1β-producing B16, MEFs were obtained from embryos at embryonic day 15 by using standard methods in complete DMEM medium. MEFs (1×10^5) were co-cultured with control B16 or IL-1β-producing B16 in 96-well plates at a B16:MEF ratio of 1: 100, 1:10, and 1:1 for 24 h.

Depletion of macrophages and ILC2

For macrophage depletion, clodronate and control liposomes (ClrodoronateLiposome.org. Amsterdam, Netherlands) were injected intraperitoneally as follows: 300µl on day 3 and 200µl from on day 3 every 3 days, then 100µl subcutaneously from day 7 every 3 days. As a second model of macrophage depletion, LysM-DTR mice, wild-type C57BL/6 mice were sublethally-irradiated (9.5 Gy) and received bone marrow cells (5×10^6 - 1×10^7) from LysM-DTR mice. After reconstitution, chimeric mice were treated with 800 ng DT intraperitoneally.

For ILC2 depletion, anti-CD25 neutralizing antibody (clone PC-61.5.3, BioXCell) was administered to $Rag1^{-/-}$ mice intraperitoneally every 2 days at a dose of 300 µg per mouse starting 2 days before IL-1β-B16 injection.

In vitro differentiation of M2-macrophages from bone marrow cells

Bone marrow **(**BM) cells from tibias and fibulas were plated at 1×10^6 /ml in 10 cm dishes on day 0. For macrophages differentiation, BM cells were cultured in cRPMI containing 10 ng/mL M-CSF (Peprotech). Medium was replaced on days 3 and 6 and cells were harvested on day 9. To induce M2 phenotype, cells were stimulated for 48 h with IL-4 (20 ng/mL; Peprotech).

Histology and Immunohistochemistry

For histological examination, tissues were fixed with 10% formalin in PBS, and then embedded in paraffin. Sections with a thickness of 5 µm were prepared and subjected to staining with hematoxylin and eosin. Immunohistochemistry was performed as previously reported [28]. Anti-human CD163 antibody was purchased from Leica Microsystems (Wetzler, Germany). The number of immunoreactive cells was counted in five fields (× 20 objective). All the stainings were quantified by the same pathologist using the same subjective grading scale.

Statistical analysis

Unless otherwise indicated, data are presented as the means ± standard error of the mean (SEM) and are representative of three independent experiments. *P*-values were calculated with the Wilcoxon signed-rank test. * $p < 0.05$.

Acknowledgements

This work was supported in part by the Association for International Cancer Research (AICR 09-0230) to L.E.F, Oncosuisse to L.E.F. (ask Emmanuel, but I think I would leav Oncosuisse out), by the Zürich University Research Priority Program (URPP) Translational Cancer Research, by the Swiss National Science Foundation (Grant 31003A_135465 and Sinergia Grant CRSII3-136203) to L.E.F, and by the Society for Skin Cancer Research to M.P.L. We thank Horomi Doi, Ines Kleiber-Schaaf, and Tatiana Proust for technical assistance.

Author contributions

C.N., R.H., B.M., T.S., G.F., K.K., K.K., and A.O. performed the experiments and data analysis. A.O., E.C., and L.F. conceived of the study and wrote the manuscript. O.B., S.Z., M.L., R.D., E.C., and L.F. directed the project and edited the manuscript. All authors reviewed and discussed the manuscript.

Author information

Reprints and permissions information is available at www.nature.com/reprints. The authors declare no competing financial interests. Correspondence and requests for materials should be addressed to Emmanuel Contassot (Emmanuel.Contassot@usz.ch)

Personal contribution

In this work, I contributed with designing, performing, analyzing and interpreting experiments.

- Collection of paraffin-embedded patient samples
- Assessment of in vitro properties of control-B16 or IL-1β-producing B16
- Subcutaneous and intravenous injection of control-B16 or IL-1β-producing B16 and evaluation of tumor formation in the skin, the draining lymph nodes and the lungs
- Clodronate-mediated depletion of macrophages *in vivo*
- Generation of bone-marrow derived macrophages for the treatment with rec. IL-1β

The manuscript in the presented structure (except for this declaration) has been submitted to Nature Medicine and is currently under examination.

References

1. Flaherty, K.T., et al., *Improved survival with MEK inhibition in BRAF-mutated melanoma.* N Engl J Med, 2012. **367**(2): p. 107-14.

2. Hodi, F.S., et al., *Improved survival with ipilimumab in patients with metastatic melanoma.* N Engl J Med, 2010. **363**(8): p. 711-23.

3. Gross, O., et al., *The inflammasome: an integrated view.* Immunol Rev, 2011. **243**(1): p. 136-51.

4. Arlt, A., et al., *Autocrine production of interleukin 1beta confers constitutive nuclear factor kappaB activity and chemoresistance in pancreatic carcinoma cell lines.* Cancer Res, 2002. **62**(3): p. 910-6.

5. Ziegler, S.F., *Thymic stromal lymphopoietin and allergic disease.* J Allergy Clin Immunol, 2012. **130**(4): p. 845-52.

6. Molofsky, A.B., et al., *Innate lymphoid type 2 cells sustain visceral adipose tissue eosinophils and alternatively activated macrophages.* J Exp Med, 2013. **210**(3): p. 535-49.

7. Jemal, A., et al., *Cancer statistics, 2009.* CA Cancer J Clin, 2009. **59**(4): p. 225-49.

8. Wan, L., K. Pantel, and Y. Kang, *Tumor metastasis: moving new biological insights into the clinic.* Nat Med, 2013. **19**(11): p. 1450-64.

9. Joyce, J.A. and J.W. Pollard, *Microenvironmental regulation of metastasis.* Nat Rev Cancer, 2009. **9**(4): p. 239-52.

10. Elaraj, D.M., et al., *The role of interleukin 1 in growth and metastasis of human cancer xenografts.* Clin Cancer Res, 2006. **12**(4): p. 1088-96.

11. Dankort, D., et al., *Braf(V600E) cooperates with Pten loss to induce metastatic melanoma.* Nat Genet, 2009. **41**(5): p. 544-52.

12. Quante, M., et al., *Bile acid and inflammation activate gastric cardia stem cells in a mouse model of Barrett-like metaplasia.* Cancer Cell, 2012. **21**(1): p. 36-51.

13. Mantovani, A., et al., *The chemokine system in diverse forms of macrophage activation and polarization.* Trends Immunol, 2004. **25**(12): p. 677-86.

14. De Monte, L., et al., *Intratumor T helper type 2 cell infiltrate correlates with cancer-associated fibroblast thymic stromal lymphopoietin production and reduced survival in pancreatic cancer.* J Exp Med, 2011. **208**(3): p. 469-78.

15. Biswas, S.K. and A. Mantovani, *Macrophage plasticity and interaction with lymphocyte subsets: cancer as a paradigm.* Nat Immunol, 2010. **11**(10): p. 889-96.

16. Ruffell, B., N.I. Affara, and L.M. Coussens, *Differential macrophage programming in the tumor microenvironment.* Trends Immunol, 2012. **33**(3): p. 119-26.

17. Qian, B.Z. and J.W. Pollard, *Macrophage diversity enhances tumor progression and metastasis.* Cell, 2010. **141**(1): p. 39-51.

18. Kim, B.S., et al., *TSLP elicits IL-33-independent innate lymphoid cell responses to promote skin inflammation.* Sci Transl Med, 2013. **5**(170): p. 170ra16.

19. Walker, J.A., J.L. Barlow, and A.N. McKenzie, *Innate lymphoid cells--how did we miss them?* Nat Rev Immunol, 2013. **13**(2): p. 75-87.

20. Mjosberg, J., et al., *The transcription factor GATA3 is essential for the function of human type 2 innate lymphoid cells.* Immunity, 2012. **37**(4): p. 649-59.

21. Nevala, W.K., et al., *Evidence of systemic Th2-driven chronic inflammation in patients with metastatic melanoma.* Clin Cancer Res, 2009. **15**(6): p. 1931-9.

22. Tatsumi, T., et al., *Disease-associated bias in T helper type 1 (Th1)/Th2 CD4(+) T cell responses against MAGE-6 in HLA-DRB10401(+) patients with renal cell carcinoma or melanoma.* J Exp Med, 2002. **196**(5): p. 619-28.

23. Miyake, Y., et al., *Protective role of macrophages in noninflammatory lung injury caused by selective ablation of alveolar epithelial type II Cells.* J Immunol, 2007. **178**(8): p. 5001-9.

24. Bjorkdahl, O., et al., *Lymphoid hyperplasia in transgenic mice over-expressing a secreted form of the human interleukin-1beta gene product.* Immunology, 1999. **96**(1): p. 128-37.

25. Nagai, H., et al., *Gene transfer of secreted-type modified interleukin-18 gene to B16F10 melanoma cells suppresses in vivo tumor growth through inhibition of tumor vessel formation.* J Invest Dermatol, 2002. **119**(3): p. 541-8.

26. Otsuka, A., et al., *Basophils are required for the induction of Th2 immunity to haptens and peptide antigens.* Nat Commun, 2013. **4**: p. 1739.

27. Otsuka, A., et al., *Requirement of interaction between mast cells and skin dendritic cells to establish contact hypersensitivity.* PLoS One, 2011. **6**(9): p. e25538.

28. Kistowska, M., et al., *IL-1beta drives inflammatory responses to propionibacterium acnes in vitro and in vivo.* J Invest Dermatol, 2014. **134**(3): p. 677-85.

Figure Legends

Figure 1: IL-1β is upregulated in metastatic melanoma and promotes metastasis

(A) IL-1β positive cell detection by immunohistochemical staining in representative sections of human benign melanocytic nevi (n=5), primary melanoma (PM) (n=10), and metastatic melanoma (MM) (n=10). Scale bar, 200 µm (upper panel) and 50 µm (lower panel). (B) Quantification of IL-1β positive cells within benign melanocytic nevi, PM and MM. (C) Five mm skin biopsies from tumors in BRAF/PTEN mice were collected and homogenized in 300 µl PBS, supernatants collected and IL-β measured by ELISA. (D, E) Lung metastases and quantification of tumor colonies in the lungs after i.v. injection with control B16 (n = 5) or IL-1β-producing B16 (n = 5) (F, G). Melanoma cells in lymph nodes draining subcutaneous tumors (delimited within red line) and quantification of metastases 13 days after subcutaneous injection of control B16 (n = 10) or IL-1β-producing B16 (n = 10). Scale bar, 100 µm. Data represent three independent experiments with similar results.

Figure 2: IL-1β promotes Th2 skewing and induces M2-macrophage tumor-infiltration

(A) Messenger RNA levels of *IFN-γ*, *IL-4*, *IL-10*, and *IL-13* at the tumor site on day 0, 3, 7, and 13 after subcutaneous injection of control B16 (n = 10) or IL-1β-producing B16 (n = 10). (B) Analysis of tumor-infiltrating cells by flow cytometry. The representative FACS plots are shown in Supplementary Fig. 1. (C) Intracellular staining of IL-4 in tumor-infiltrating cells from control B16 (n = 5) or IL-1β-producing B16 (n = 5) tumors after tumor dissociation, stimulation with PMA (20 ng/ml), ionomycin (1 µM), and treatment with Brefeldin A (5 µM) for four hours *in vitro*. (D) Messenger RNA levels of *iNOS*, *Arg2*, *MR*, *Fizz*, *Arg1*, and *YM1* in tumors on day 13. (E) Immunohistochemistry of CD163 in human nevi (n=10), primary melanoma (PM) (n=10) and metastatic melanoma (MM) (n=10), and quantification of CD163 positive cells (right panel). Scale bar, 200 µm (low magnifications) and 50 µm (high magnifications). Data for A-D represent three independent experiments with similar results.

Figure 3: IL-1β induced TSLP produced by tumor-associated fibroblasts induces M2 macrophage infiltration and metastasis.

(A) TSLP production from MEFs in presence of recombinant mouse IL-1β and control B16 or IL-1β-producing B16 was measured by ELISA. (B) TSLP mRNA levels from normal fibroblasts (NFs) (n=3) and melanoma-associated fibroblasts (MFs) (n=6). (C) Quantification of metastases in draining lymph nodes of IL-1β-producing B16 tumors in WT or $TSLPR^{-/-}$ mice. (D) Messenger RNA levels of *IL-4, IL-13, IFN-γ*, *iNOS*, *Arg2*, *MR*, *Fizz*, *Arg1*, and *YM1* at the primary tumor site of WT or $TSLPR^{-/-}$ mice bearing IL-1β-producing B16 tumors on day

13. (E) Quantification of macrophages in subcutaneous IL-1β-producing B16 tumors in WT or TSLPR$^{-/-}$ mice. Data represent three independent experiments with similar results.

Figure 4: TAMs and ILC2 play a key role in IL-1β-induced metastasis

(A) Quantification of metastases in dLNs of IL-1β-producing B16 tumor-bearing mice treated (n=6) or not with clodronate (n=6). Macrophage depletion efficiency is shown in Supplementary Fig. 3. (B) Quantification of metastases in dLNs of IL-1β-producing B16 tumor-bearing mice with DT-treated WT mice (n=4) or DT-treated LysM DTR mice (n=3). (C) Heat map of genes in B16 cell lines co-cultured with/without IL-1β (1ng/ml), BMM2, and BMM2 and IL-1β (n = 3) for 24 hours. The color bar represents expression levels of each gene normalized to the mean levels of vehicle-treated B16 cells. (D, E) Flow cytometry analysis of mouse ILC2 defined as CD45 positive, lineage negative (CD3, B220, CD11c, CD11b, FcεRIα) and expressing Thy1.2 and IL-33R in control B16 (n=10) or IL-1β-producing B16 tumors (n=10). (F) Flow cytometry analysis and quantification of ILC2 in IL-1β-producing B16 tumors implanted in WT (n=10) or TSLPR$^{-/-}$ mice (n=10) (G) Quantification of metastases in dLNs of IL-1β-producing B16 tumor-bearing Rag1$^{-/-}$ mice treated with vehicle alone (n=10) or anti-CD25 neutralizing antibody (n=10). (H, I) Flow cytometry analysis of human ILC2 defined as CD45 positive, lineage negative (CD3, CD11c, CD16, CD19, CD56, TCRαβ, FcεRIα) cells expressing CD25 and IL-33R and quantification thereof in normal skin (NS) (n=6) or melanoma metastases (MM) (n=6). Presented dot-plots and data are representative of three independent experiments with similar results.

Supplementary Figure Legends

Figure S1: Flow cytometry of tumor infiltrating cells

(A) $CD45^+$ $CD4^+$ T cells and $CD45^+$ $CD8^+$ T cells; (**B)** $CD45^+$ $7/4^-$ $CD11b^+$, $F4/80^+$ Macrophages; (**C)** $CD45^+$ $Gr\text{-}1^-$ $CCR3^+$ $SiglecF^+$ Eosinophils; and (**D)** $CD45^+$ $Fc\varepsilon RI^+$ $CD200R3^+$ $cKit^+$ Mast cells were quantified by FACS. Presented dot-plots are representative of three independent experiments with similar results.

Figure S2: Histological analysis of tumor infiltrating cells

(A) Immunohistochemistry of macrophages (clone; MAC387, Abcam) in control B16 or IL-1β-producing B16 tumors. (**B)** Hematoxylin & Eosin coloration of control B16 or IL-1β-producing B16 tumors. Data represent three independent experiments with similar results.

Figure S3: Macrophage depletion after clodronate treatment

Flow cytometry control of macrophage ($7/4^-$ $CD11b^+$ $F4/80^+$) depletion in IL-1β-producing B16 tumors. Tumor size of tumor after control or clodronate treatment. Presented dot-plots are representative of three independent experiments with similar results.

Figure S4: Kaplan Meier curves of CD82 and EPHB2 high vs low patients

Ninety eight patients were defined with high CD82 expression with a median survival rate of 8.6 years and 98 patients were defined with low CD82 expression with a median survival rate of 5.3 years $p = 0.0181$. Ninety eight patients were defined with high EPHB2 expression with a median survival rate of 11.6 years and 98 patients were defined with low EPHB2 expression with a median survival rate of 5 years $p = 0.0171$.

Figure S5: ILC2 analysis in $TSLPR^{-/-}$ mice.

ILC2, a population of lineage-negative (Lin^-) cells that express both Thy1.2 and IL-33R, in IL-1β-producing B16 tumors implanted in WT (left panel) and $TSLPR^{-/-}$ (right panel) mice. Presented dot-plots are representative of three independent experiments with similar results.

Figure S6:

Messenger RNA levels of *IL-4*, *IL-13*, *Arg2*, *MR*, *Fizz*, *Arg1*, and *YM1* at the IL-1β-producing B16 tumor site of vehicle- and anti-CD25 neutralizing antibody-treated $Rag1^{-/-}$ mice ($n = 10$). Presented data are representative of two independent experiments with similar results.

Figure S7: Illustration depicts how IL-1β promotes melanoma metastases

(A) IL-1β produced from the site of metastatic melanoma promotes TSLP production from melanoma-associated fibroblasts. (B) M2-macrophages and ILC2s are induced in Th2 microenvironment, which leads to tumor metastasis.

Supplemental Table 1

	+IL-1β		+M2		M2+IL-1β	
Symbol	Fold	*p*	Fold	*p*	Fold	*p*
Apc	1.3412	0.010316	1.084	0.639938	1.4763	0.000648
Brms1	1.1952	0.108206	-1.1095	0.900877	-1.3342	0.016292
Ccl7	1.2271	0.309036	26.7483	0.015404	52.3943	0
Cd44	1.0714	0.202497	-1.0945	0.899628	-1.184	0.017848
Cd82	1.0621	0.524264	-1.5644	0.136895	-2.8199	0.00131
Cdh1	1.1534	0.6369	-4.1582	0.024184	-1.4483	0.207373
Cdh11	1.2271	0.309036	3.3676	0.035687	3.38	0.150492
Cdh6	-1.4245	0.352949	-1.2587	0.557997	1.2047	0.93624
Cdh8	1.2271	0.309036	2.0898	0.180318	-1.2041	0.219783
Cdkn2a	1.2271	0.309036	2.0898	0.180318	-1.2041	0.219783
Chd4	1.1676	0.037773	-1.1116	0.761108	-1.4087	0.000664
Col4a2	-1.1393	0.654254	-2.3386	0.105962	-1.4109	0.013438
Csf1	1.2293	0.152753	1.0439	0.644729	1.4175	0.004931
Ctbp1	-1.1338	0.248706	-1.8703	0.106871	-2.0772	0.00124
Ctnna1	1.0036	0.926323	-1.1292	0.962193	1.2238	0.118803
Ctsk	-1.0768	0.677231	-1.1044	0.953359	-2.8712	0.062699
Ctsl	1.0962	0.292158	1.2778	0.03826	-1.3698	0.014648
Cxcl12	1.2271	0.309036	3.5678	0.002396	1.939	0.330781
Cxcr2	1.2271	0.309036	3.3746	0.332216	-1.2041	0.219783
Cxcr4	1.2271	0.309036	3.1683	0.323111	1.7626	0.40677
Denr	-1.144	0.081588	1.059	0.296686	-1.1096	0.104632
Elane	2.8551	0.021072	4.087	0.154713	-1.3189	0.857547
Ephb2	1.0917	0.536441	1.1712	0.470983	-2.0753	0.000733
Etv4	1.0073	0.946644	-1.5659	0.037307	-1.5451	0.142811
Ewsr1	-1.015	0.744821	-1.3685	0.544224	-2.1327	0.000029
Fat1	-1.1573	0.021433	-1.3161	0.097307	-1.3204	0.002472
Fgfr4	-2.0356	0.357302	1.0258	0.724825	1.1431	0.754905
Flt4	1.3246	0.86072	1.4784	0.583022	-1.49	0.569554
Fn1	1.2677	0.061661	1.0923	0.571852	1.0227	0.774761
Fxyd5	1.0945	0.281637	1.75	0.027599	1.7901	0.000208
Gpnmb	1.5086	0.000428	1.0588	0.646999	1.6483	0.018791
Hgf	1.2271	0.309036	2.0898	0.180318	-1.0752	0.762811
Hpse	1.0385	0.564399	1.0686	0.597861	-1.71	0.001576
Hras1	1.0419	0.22569	-1.1758	0.711592	-1.2366	0.000151
Htatip2	-1.0105	0.89717	1.1058	0.471299	1.0128	0.784851
Igf1	1.2271	0.309036	15.751	0.12218	19.4451	0.0145
Il18	1.1974	0.144545	1.0943	0.484805	-1.1815	0.112996
Il1b	1.2271	0.309036	3.8674	0.346585	-1.2041	0.219783
Itga7	1.2271	0.309036	2.0898	0.180318	-1.2041	0.219783
Itgb3	1.4421	0.00966	-1.1755	0.545299	-1.4113	0.008337
Kiss1	1.112	0.784689	2.1695	0.25962	-1.088	0.840452
Kiss1r	1.2271	0.309036	2.0898	0.180318	1.1024	0.65621

Kras	1.1286	0.299661	1.2415	0.304126	-1.3485	0.026844
Lpar6	-1.2502	0.146661	1.195	0.431696	-1.5185	0.028557
Mcam	-1.1356	0.033098	-1.508	0.155118	-1.5277	0.00133
Mdm2	1.0115	0.852952	-1.0772	0.888115	-1.4051	0.002357
Met	1.146	0.076822	-1.4436	0.00285	1.0984	0.236124
Mmp10	-1.2301	0.507566	2.4386	0.386383	-1.8175	0.220731
Mmp11	1.2359	0.615628	1.6189	0.277888	1.5703	0.23486
Mmp13	1.2271	0.309036	2.0898	0.180318	4.3731	0.005313
Mmp2	1.2718	0.007884	1.021	0.802314	-1.3128	0.052737
Mmp3	1.2271	0.309036	2.0898	0.180318	-1.2041	0.219783
Mmp7	1.2271	0.309036	2.0898	0.180318	-1.2041	0.219783
Mmp9	1.0426	0.873414	2.7076	0.321542	2.6342	0.035145
Mta1	1.0616	0.25466	-1.386	0.314831	-1.116	0.083763
Mtss1	1.1067	0.298133	-1.4879	0.044229	1.284	0.015158
Myc	1.0929	0.200044	1.0845	0.604489	1.3886	0.005245
Mycl	2.275	0.034129	4.2204	0.102198	-1.2041	0.219783
Nf2	1.2288	0.092355	-1.2695	0.72603	-1.6208	0.000582
Nme1	-1.0537	0.727892	1.4939	0.036814	-1.304	0.055
Nme2	1.4365	0.012021	1.7093	0.330755	2.0811	0.036304
Nme4	1.0448	0.284826	1.0666	0.672172	1.2187	0.108366
Nr4a3	2.3078	0.000283	-1.725	0.012461	1.2882	0.190928
Plaur	1.0008	0.996657	-1.4399	0.357886	-1.224	0.010044
Pnn	-1.0122	0.928874	1.1642	0.158301	-1.124	0.14695
Pten	1.0146	0.765932	-1.1714	0.676298	-1.255	0.008715
Rb1	1.0069	0.940209	-1.2122	0.911737	-1.7847	0.002827
Rorb	1.5781	0.131893	2.4635	0.084404	-1.2041	0.219783
Rpsa	-1.1343	0.090083	-1.089	0.882637	1.5826	0.028305
Set	1.0601	0.485228	1.1791	0.524397	1.7967	0.001919
Smad2	1.1679	0.144327	1.3491	0.145212	1.3296	0.002027
Smad4	1.1062	0.409828	-1.3161	0.63182	-1.848	0.005104
Src	1.1491	0.081223	-1.3957	0.423486	-1.6384	0.005651
Sstr2	1.3587	0.412662	1.2835	0.496637	-1.1452	0.901493
Syk	1.2271	0.309036	2.0898	0.180318	-1.2041	0.219783
Tcf20	1.2931	0.000469	-1.388	0.243152	-1.3155	0.002167
Tgfb1	-1.0045	0.951692	-1.3213	0.448863	-1.6343	0.001818
Timp2	-1.2129	0.014599	1.1661	0.326182	-1.017	0.751595
Timp3	-1.1554	0.042166	-1.23	0.821779	-1.3155	0.007756
Timp4	-3.7049	0.130359	2.5048	0.370105	1.0039	0.879569
Tnfsf10	-1.1554	0.57972	2.3983	0.383538	-1.6939	0.256885
Trp53	-1.4285	0.011541	-1.1604	0.4605	-1.5168	0.006379
Tshr	1.2271	0.309036	3.3381	0.073948	3.8942	0.087118
Vegfa	1.0796	0.244744	-1.2368	0.694335	-1.635	0.000427

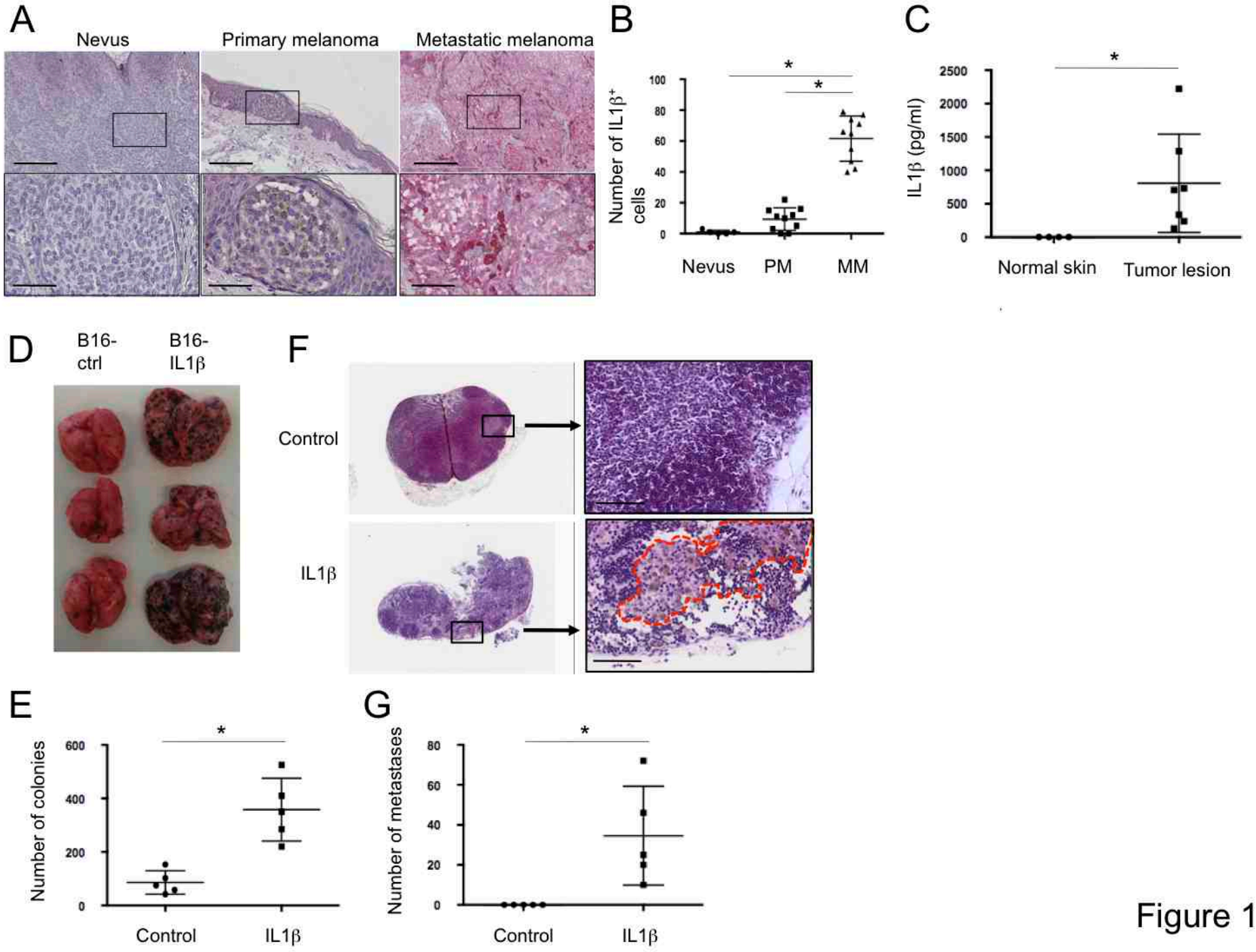
A
Nevus
Primary melanoma
Metastatic melanoma
B
Number of IL1β+ cells
100
80
60
40
20
0
*
*
Nevus
PM
MM
C
IL1β (pg/ml)
2500
2000
1500
1000
500
0
*
Normal skin
Tumor lesion
D
B16-ctrl
B16-IL1β
F
Control
IL1β
E
Number of colonies
600
400
200
0
*
Control
IL1β
G
Number of metastases
80
60
40
20
0
*
Control
IL1β

Figure 1

Figure 2

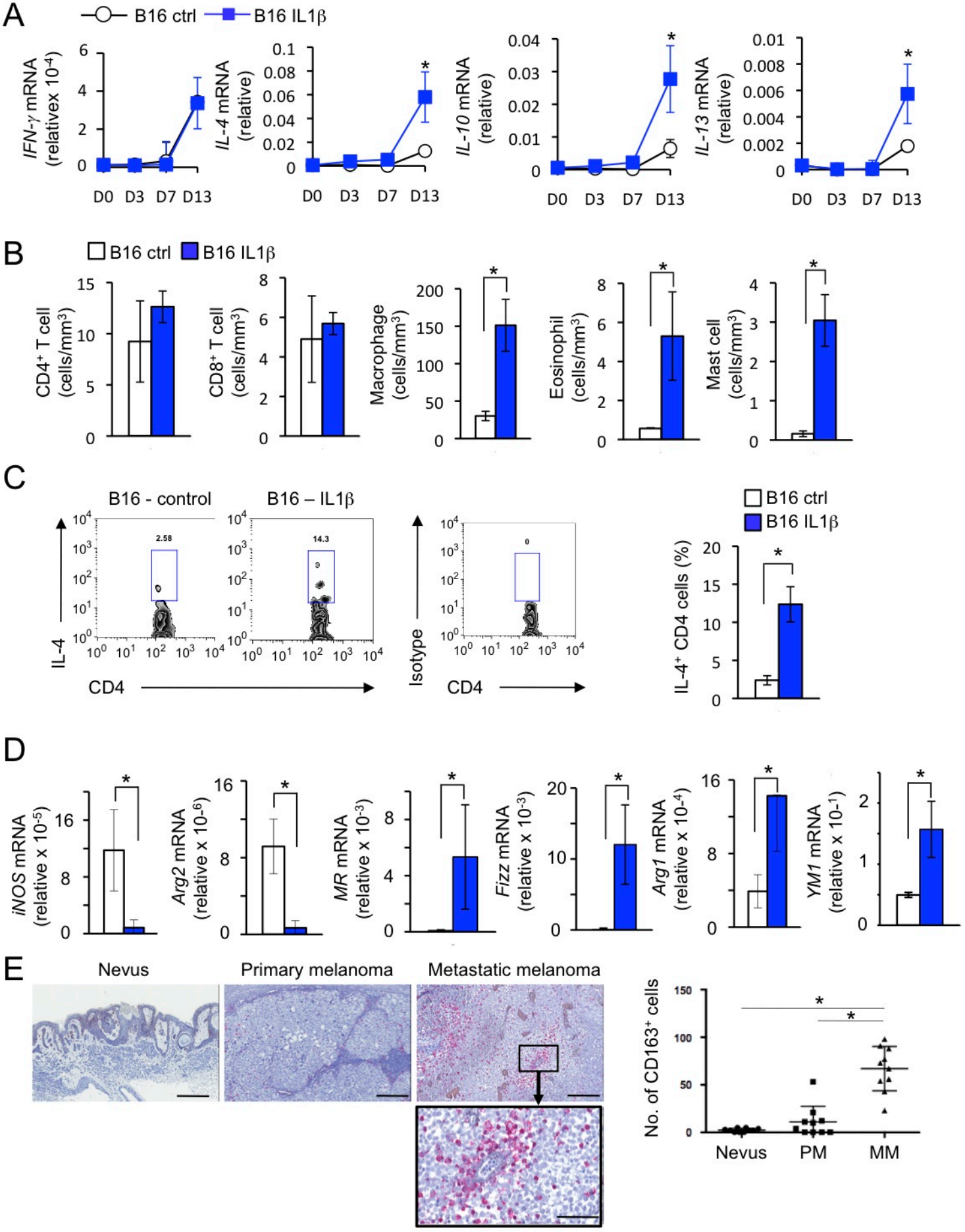
A
B16 ctrl
B16 IL1β
IFN-γ mRNA (relativex 10-4)
IL-4 mRNA (relative)
IL-10 mRNA (relative)
IL-13 mRNA (relative)
D0 D3 D7 D13
B
B16 ctrl
B16 IL1β
CD4+ T cell (cells/mm3)
CD8+ T cell (cells/mm3)
Macrophage (cells/mm3)
Eosinophil (cells/mm3)
Mast cell (cells/mm3)
C
B16 - control
B16 – IL1β
2.58
14.3
IL-4
CD4
Isotype
B16 ctrl
B16 IL1β
IL-4+ CD4 cells (%)
D
iNOS mRNA (relative x 10-5)
Arg2 mRNA (relative x 10-6)
MR mRNA (relative x 10-3)
Fizz mRNA (relative x 10-3)
Arg1 mRNA (relative x 10-4)
YM1 mRNA (relative x 10-1)
E
Nevus
Primary melanoma
Metastatic melanoma
No. of CD163+ cells
Nevus
PM
MM

Figure 3

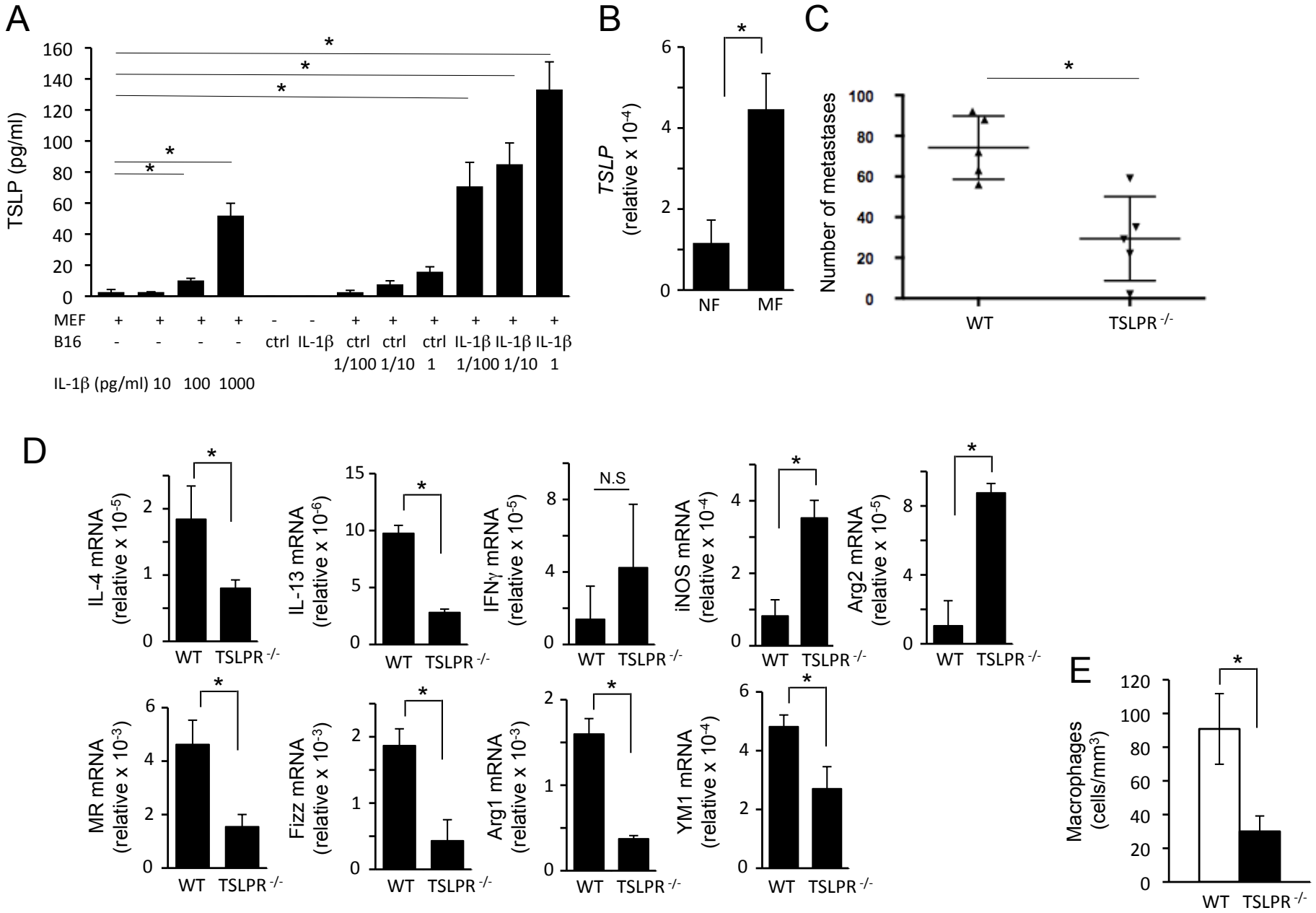
A
TSLP (pg/ml)
MEF
B16
ctrl
IL-1β
1/100
1/10
1
IL-1β (pg/ml) 10 100 1000
B
TSLP (relative x 10-4)
NF
MF
C
Number of metastases
WT
TSLPR -/-
D
IL-4 mRNA (relative x 10-5)
IL-13 mRNA (relative x 10-6)
IFNγ mRNA (relative x 10-5)
N.S
iNOS mRNA (relative x 10-4)
Arg2 mRNA (relative x 10-5)
MR mRNA (relative x 10-3)
Fizz mRNA (relative x 10-3)
Arg1 mRNA (relative x 10-3)
YM1 mRNA (relative x 10-4)
E
Macrophages (cells/mm3)

Figure S1

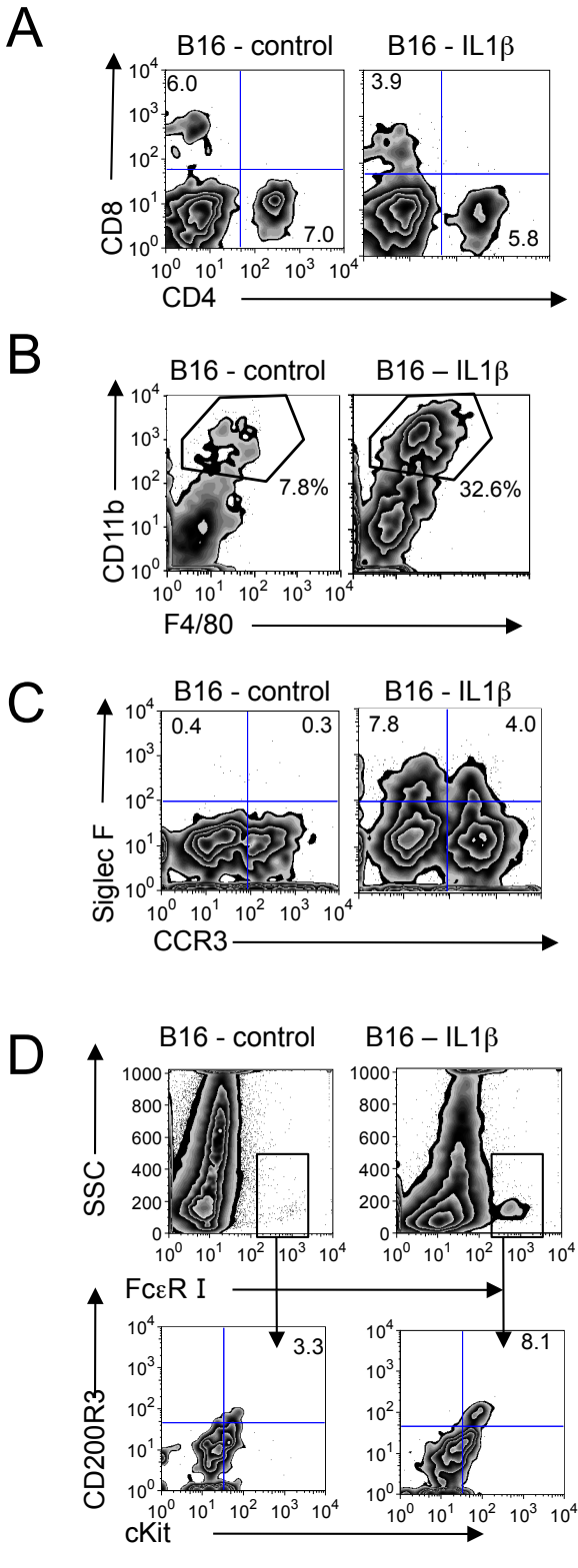
A
B16 - control
B16 - IL1β
6.0
7.0
3.9
5.8
CD8
CD4
B
B16 - control
B16 – IL1β
7.8%
32.6%
CD11b
F4/80
C
B16 - control
B16 - IL1β
0.4
0.3
7.8
4.0
Siglec F
CCR3
D
B16 - control
B16 – IL1β
SSC
FcεR I
3.3
8.1
CD200R3
cKit

Figure S2

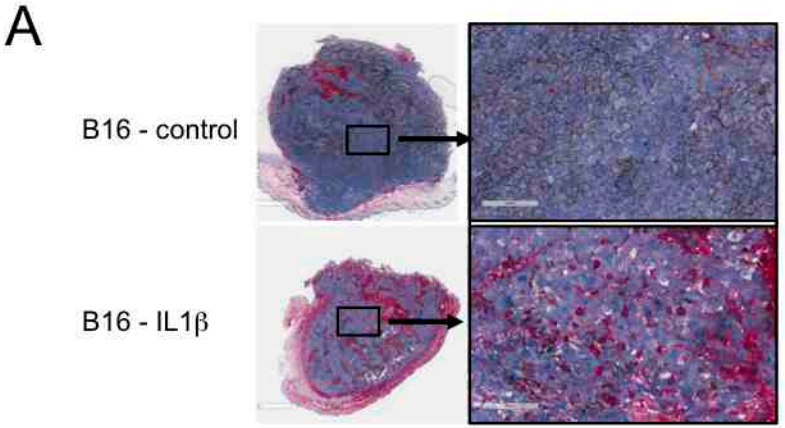

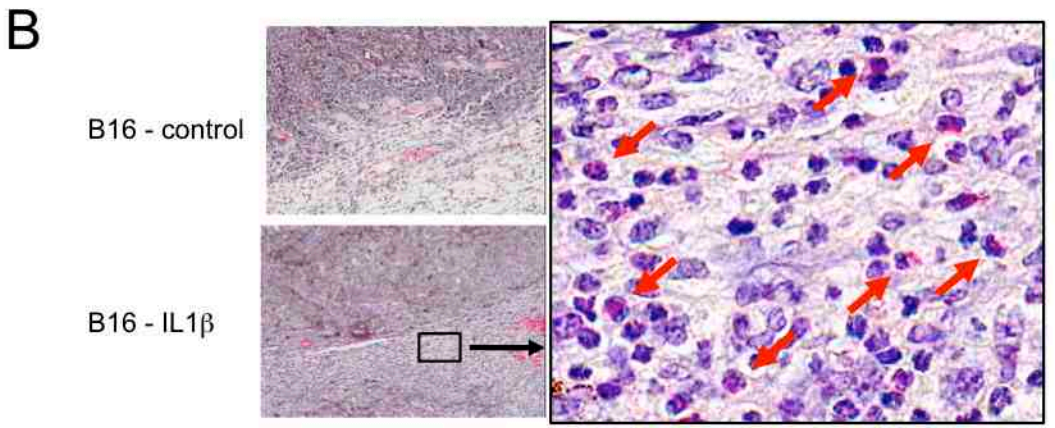

Figure S3

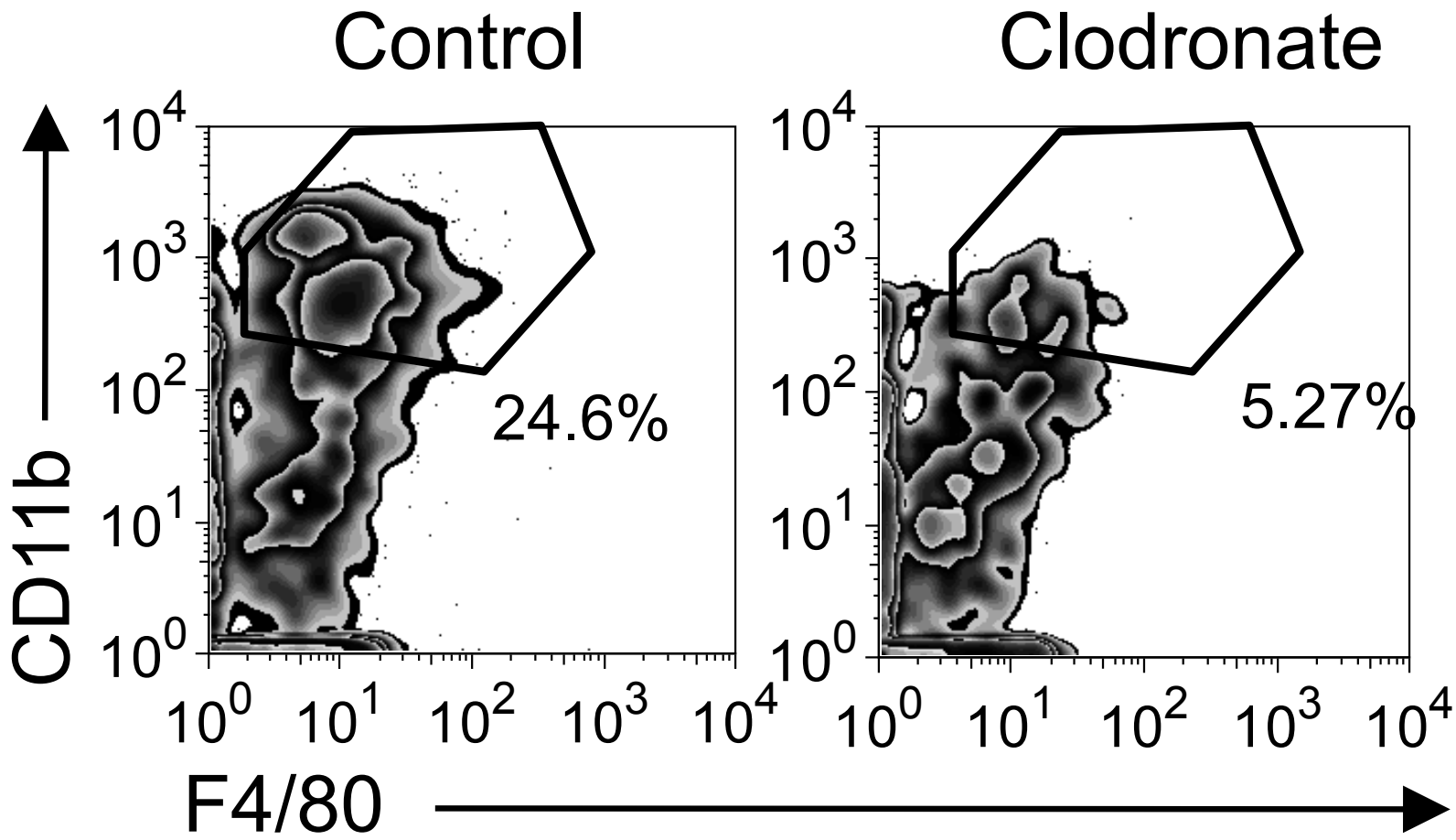

Figure S4

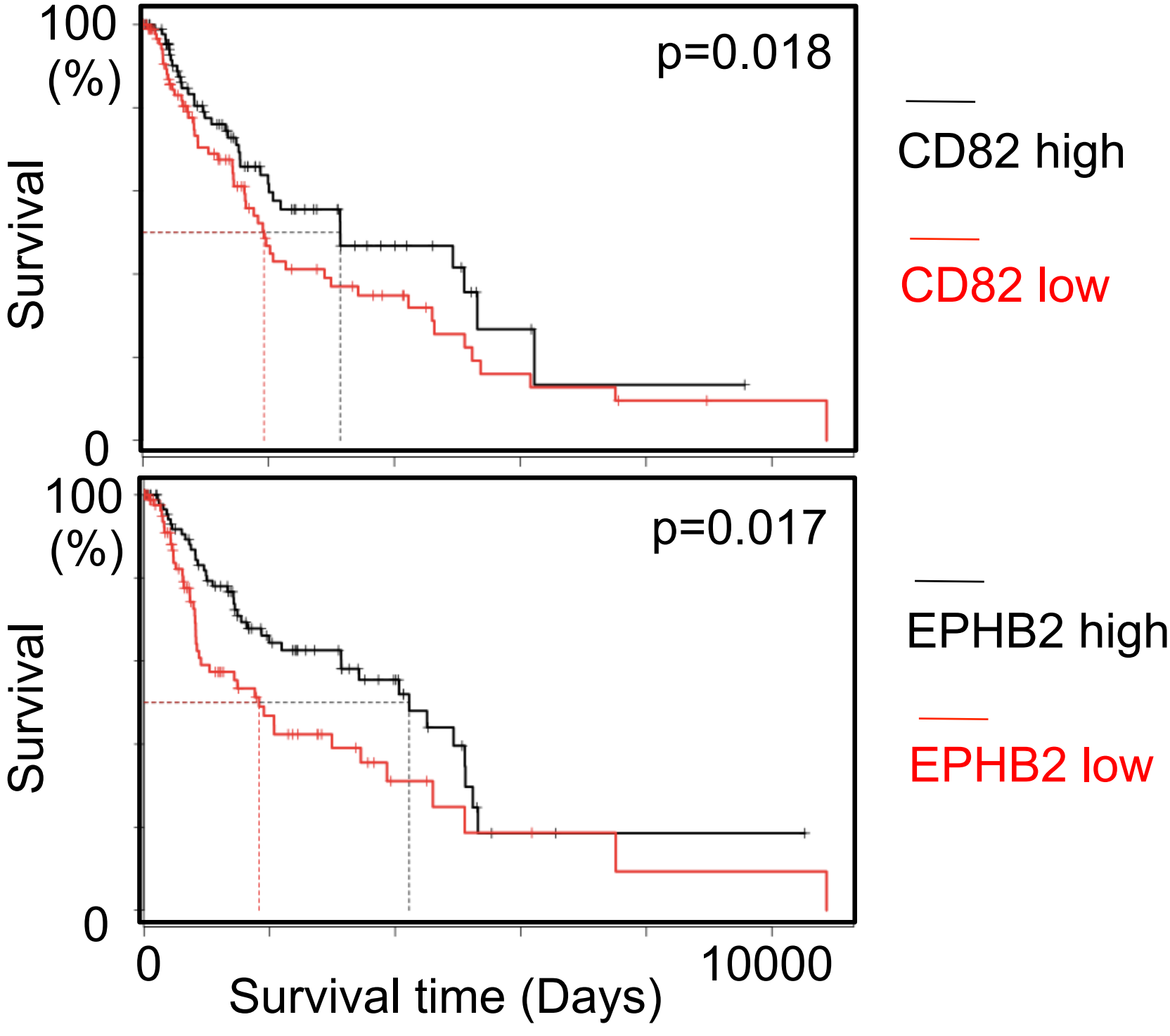
100
(%)
Survival
0
p=0.018
CD82 high
CD82 low
100
(%)
Survival
0
p=0.017
EPHB2 high
EPHB2 low
0
10000
Survival time (Days)

Figure S5

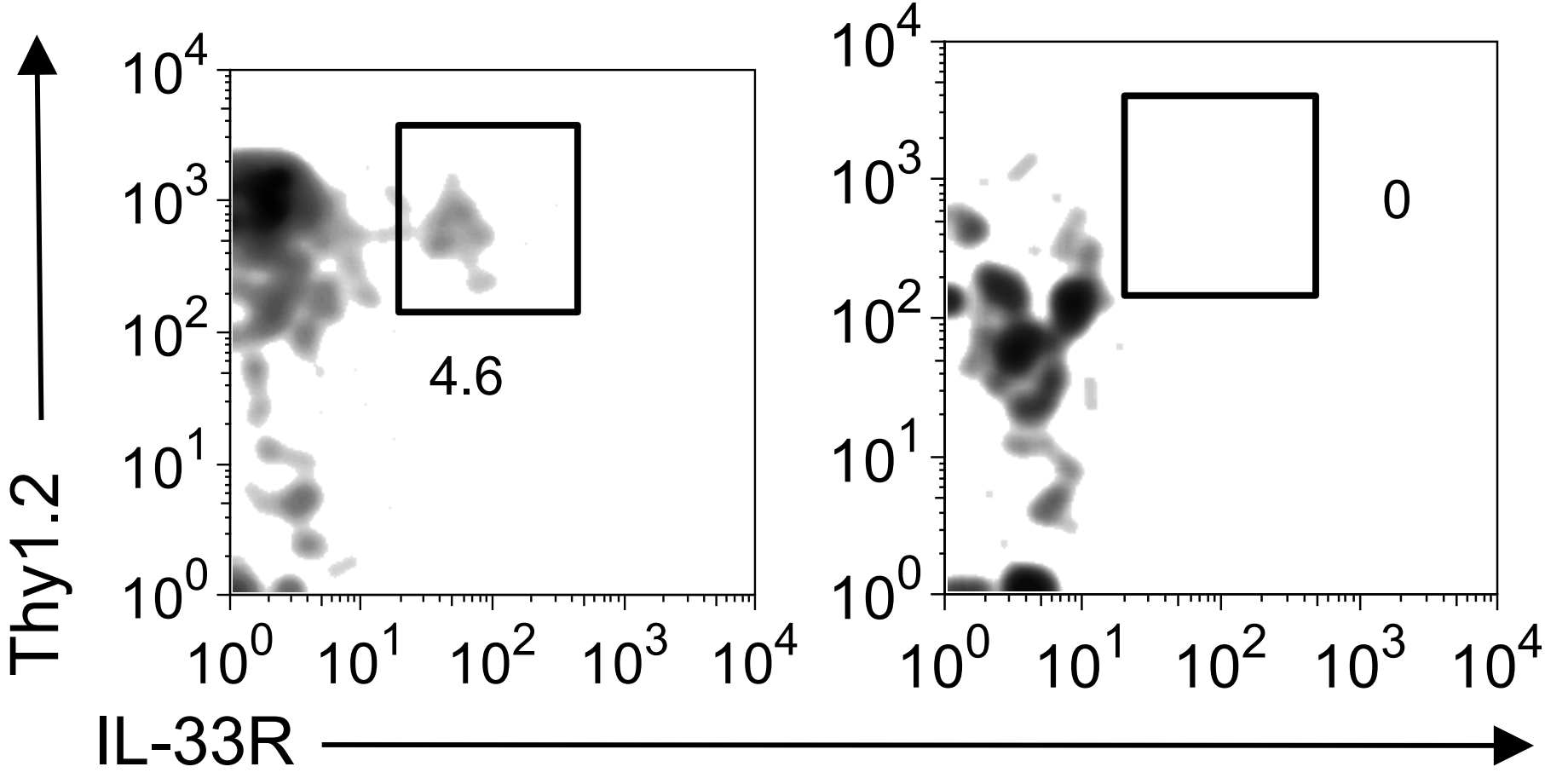

Figure S6

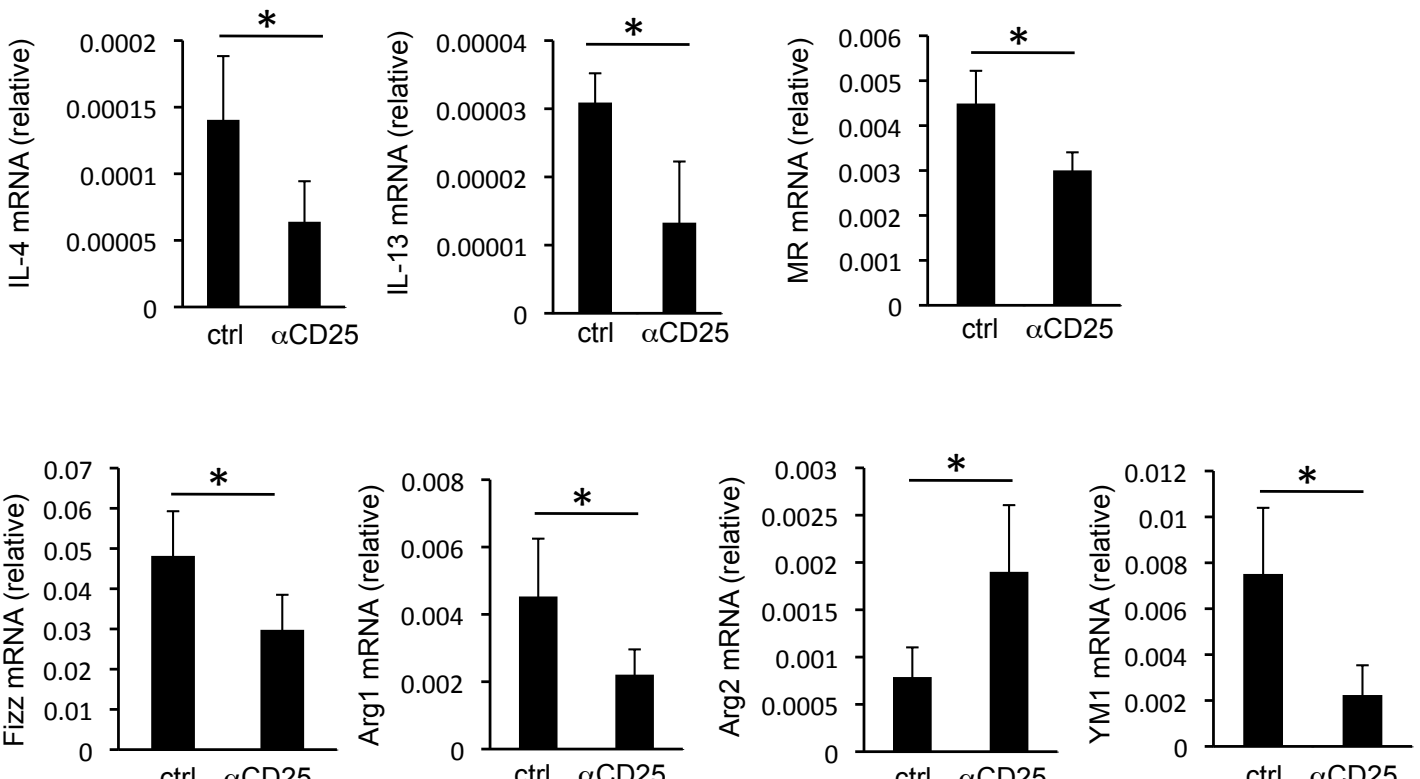
IL-4 mRNA (relative)
0.0002
0.00015
0.0001
0.00005
0
*
ctrl
αCD25
IL-13 mRNA (relative)
0.00004
0.00003
0.00002
0.00001
0
*
ctrl
αCD25
MR mRNA (relative)
0.006
0.005
0.004
0.003
0.002
0.001
0
*
ctrl
αCD25
Fizz mRNA (relative)
0.07
0.06
0.05
0.04
0.03
0.02
0.01
0
*
ctrl
αCD25
Arg1 mRNA (relative)
0.008
0.006
0.004
0.002
0
*
ctrl
αCD25
Arg2 mRNA (relative)
0.003
0.0025
0.002
0.0015
0.001
0.0005
0
*
ctrl
αCD25
YM1 mRNA (relative)
0.012
0.01
0.008
0.006
0.004
0.002
0
*
ctrl
αCD25

Figure S7

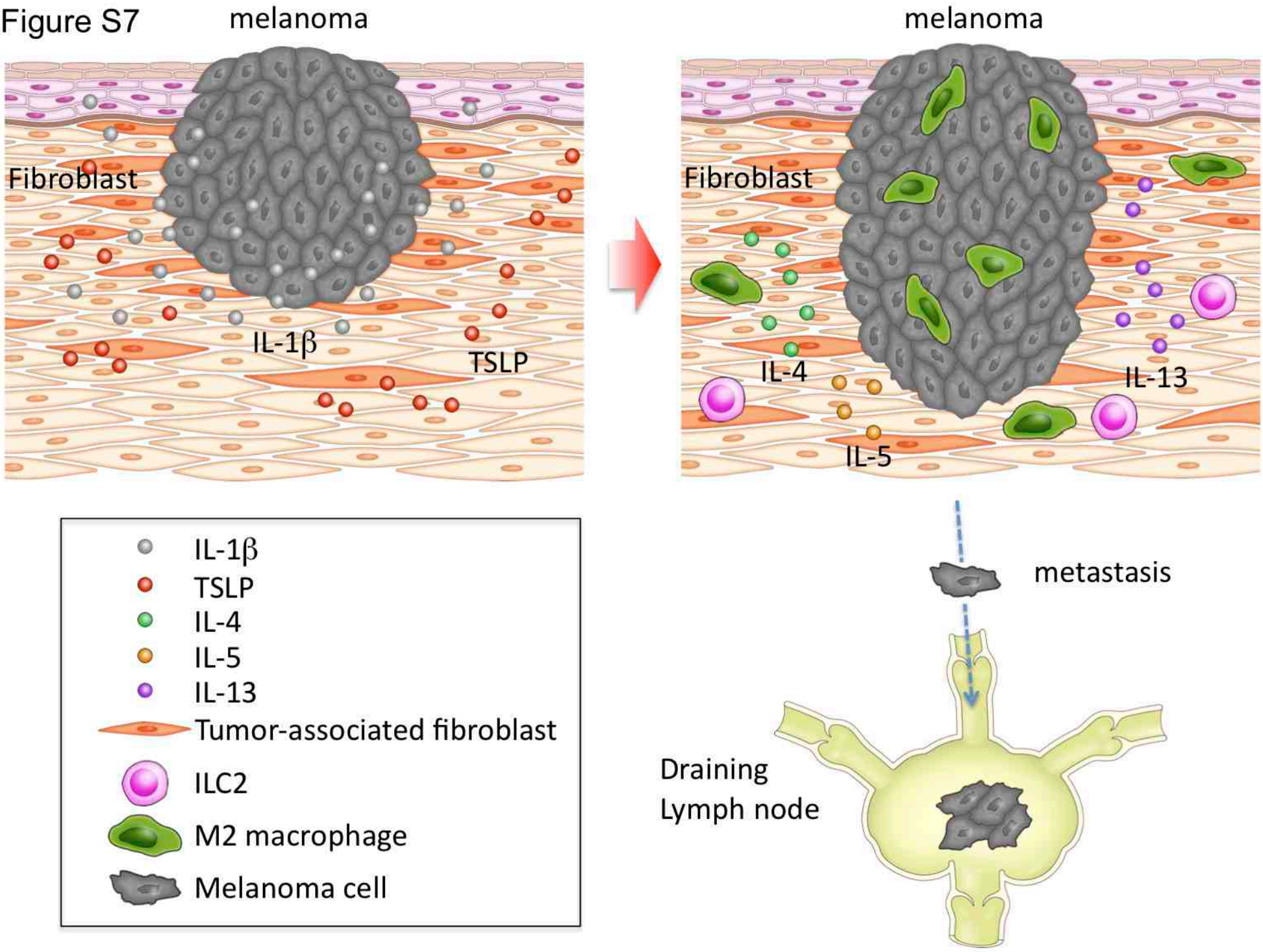
melanoma
Fibroblast
IL-1β
TSLP
melanoma
Fibroblast
IL-4
IL-5
IL-13
IL-1β
TSLP
IL-4
IL-5
IL-13
Tumor-associated fibroblast
ILC2
M2 macrophage
Melanoma cell
metastasis
Draining
Lymph node

Figure 4

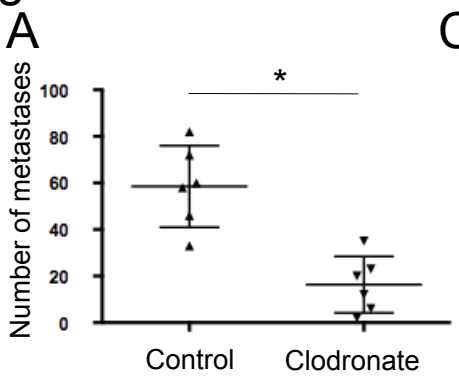

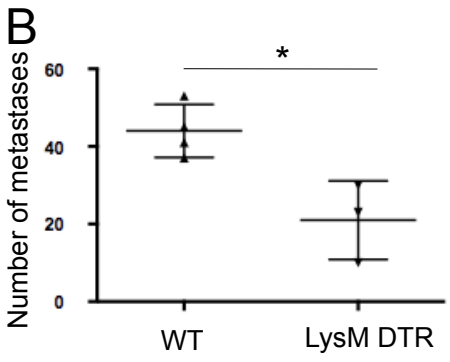

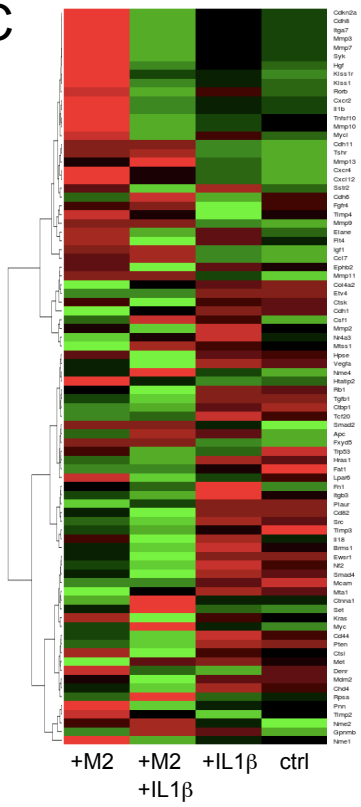

	+IL1β		+M2		+M2+IL1β	
	Fold	*p*	Fold	*p*	Fold	*p*
Cd82	1.062	0.524	-1.564	0.136	-2.819	<0.05
Ctbp1	-1.133	0.248	-1.870	0.106	-2.077	<0.05
Ephb2	1.091	0.536	1.171	0.470	-2.075	<0.001
Ewsr1	-1.015	0.744	-1.368	0.544	-2.132	<0.001
Igf1	1.227	0.309	15.751	0.122	19.445	<0.05
Mmp13	1.227	0.309	2.089	0.180	4.373	<0.05
Mmp9	1.042	0.873	2.707	0.321	2.634	<0.05
Nme2	1.436	<0.05	1.709	0.330	2.081	<0.05